Characterisation RyR1 variants linked to malignant hyperthermia

A thesis presented to Massey University in partial fulfilment of the requirements for a Masters of Science in Biochemistry.

Jeremy Stephens

2016

Acknowledgements

Firstly, and most formally, I would like to thank my supervisor Professor Kathryn Stowell for giving me the opportunity to work in your lab. Thank you for all the help and support you have been kind enough to provide over the past two years.

Secondly, I would like to thank my co supervisor Associate Professor Andrew Sutherland-Smith. Thank you for always making time to provide help and advice during this project.

I would like to thank the current and past members of the Twilite zone. Anja, thank you for all the time you have spent trouble shooting and providing advice. Lili, thank you for all the help you were kind enough to provide. Remai, thank you for all of your support and always being happy to help out with any problems I had. Sean, thanks for the support. Ruth, thanks for the support and encouragement. Bex, while you were not directly involved with my work thank you for helping out when possible.

I would like to thank Associate Professor Gill Noris and Dr Mark Patchett. Thank you for always making time to provide help and advice along with providing some reagents that may have not been directly available to myself.

Trevor Loo, thank you for always making time to provide help throughout the past two years. The expression of the ryanodine receptor will have been very difficult without your help. Thank you for performing mass spectrometry.

Thank you Niki Murray for your help performing microscopy.

Abstract

Malignant hyperthermia is a potentially fatal disorder of skeletal muscle manifesting as a rise in body temperature in response inhalational anaesthetics and muscle relaxants. Further clinical signs include muscle rigidity and increased oxygen consumption. The increased metabolism is induced by alterations to Ca^{2+} homeostasis resulting from the dysregulation of the sarcoplasmic reticulum protein the ryanodine receptor type 1 (RyR1). A large proportion of known malignant hyperthermia linked genetic variants reside within the gene encoding the type 1 ryanodine receptor, *RYR1*. Malignant hyperthermia can be diagnosed by *in vitro* contracture testing of biopsied muscle tissue. The use of DNA diagnostic testing is advantageous, however it is limited to only 35 of the proposed 400 *RYR1* linked variants known to be associated with malignant hyperthermia.

The research described in this thesis reports the functional characterisation of two *RYR1* variants linked to malignant hyperthermia, c.641C>T and c.7042_7044delCAG resulting in the amino acid changes p.T214M and p.ΔE2348. The ability of each variant to release Ca^{2+} in response to a stimulus was examined in a heterologous system. The variant p.ΔE2348 was shown to be hyperactive in response to agonists indicating the variant is the cause of malignant hyperthermia, while the p.T214M variant does not appear to have an effect ryanodine receptor function.

To understand the relationship between RyR1 function and any structural alterations induced by the p.T214M and p.ΔE2348 variants, the domain housing each variant was cloned for bacterial expression. Subsequent purification and structural characterisation could be used to explain the role each variant plays with respect to the onset of MH. The RyR1 N-terminal domain, amino acids 1-558, and helical domain, amino acids 2091-2525, were expressed in *E. coli* and partially purified. The domains were shown to be soluble and stable following expression.

Abbreviations

A280	Absorbance at 280 nm
ABC	Ammonium bicarbonate
ACN	Acetonitrile
AM	Acetoxymethyl
ADP	Adenosine di-phosphate
ATP	Adenosine tri-phosphate
Bp	Base pairs
Casq	Calsequestrin
CCD	Central core disease
cDNA	Complementry DNA
DAPI	4',6'-diamidino-2-phenylindole
DHPR	Dihydropyrudine receptor
DMEM	Dulbecco's modified eagle's medium
DMSO	Dimethyl sulphoxide
DNA	Deoxyribonucleic acid
DP4	Domain peptide 4
DTT	Dithiothreitol
Dyspedic	Lack of the ryanodine receptor type 1 gene
E. coli	*Escherichia coli*
EC	Excitation-contraction
EC_{50}	Half maximal effective concentration
EDTA	Ethlenediaminetetraacetic acid
EGTA	Ethylene glycol tetraacectic acid
EM	Electron microscopy
ER	Endoplasmic reticulum
FCS	Foetal calf serum
FITC	Fluorescein isothiocyanate
FKBP12	12-kDa FK506 binding protein
GST	Glutathione s transferase
HEK239T	Human embryonic kidney cells
HEPES	4-(2-hydroxethyl)-1-piperazineethanesulfonic acid

IP3R	Inositol tri phosphate receptor
IP3	Inositol tri phosphate
IPTG	Isopropyl-β-D-1-thiogalactopyranoside
IVCT	*In vitro* contracture test
kDa	Kilo Dalton
LB	lysogeny broth
MBP	Maltose binding protein
MH	Malignant hyperthermia
MHN	Malignant hyperthermia negative
MHS	Malignant hyperthermia susceptible
MS	Mass spectrometry
NTD	N-terminal domain
PBS	Phosphate buffered saline
PCR	Polymerase chain reaction
PDI	Protein disulphide isomerase
PVDF	Polyvinylidene fluoride
RIH	Ryanodine receptor, Inositol triphosphate receptor homology
RyR1	Ryanodine receptor protein
RYR1	Ryanodine receptor cDNA
SDS	Sodiumdodecysulfate
SDS-PAGE	Sodiumdodecysulfate-polyacrylamide gel electrophoresis
SEM	Standard error of the mean
SERCA	Sarco- and- endoplasmic reticulum ATP-ase
SR	Sarcoplasmic reticulum
TAE	Tris acetate EDTA buffer
TBST	Tris buffered saline Tween 20
TE	TE
TEMED	Tetramethylethylenediamine
Tris	Trisaminomethane
TRITC	Tetramethyl rhodamine isothiocyanate
T-tubule	Transverse tubule

Table of contents

List of figures

List of tables

Chapter 1 Introduction

1.1 Malignant hyperthermia

Malignant hyperthermia (MH) is a potentially fatal, pharmacogenetic autosomal dominant disorder of skeletal muscle (1). MH is triggered following exposure to commonly used volatile anaesthetics or depolarising muscle relaxants with patients exhibiting symptoms that include muscle rigidity, hypermetabolism, increased body temperature, acidosis, cellular degradation and tachycardia. There are normally no observable symptoms in susceptible patients during day to day life. MH is thought to effect roughly 1 in 40,000 people (2); this estimation is based on the small selection of the population who have been screened for the disease and is likely to be an underestimation. MH is particularly prevalent within the Manawatu region of New Zealand where 1:200 people who undergo anaesthesia at Palmerston North hospital must be treated as MH-susceptible (3).

Currently the gold standard for the diagnosis of MH is the *in vitro* contracture test (IVCT) (1). This first involves a muscle biopsy being taken from a patient's *quadriceps femoris* muscle. The biopsied muscle is dissected into bundles of muscle fibers and suspended in a buffer allowing the muscle to gently contract. Increasing concentrations of the agonists halothane or caffeine are added to the buffer. Should the patient be susceptible to MH (MHS) a significant increase in the strength of muscle contraction will be noted in the case of both agonists. A patient who displays no alteration in the strength of muscle contraction is not susceptible to MH (MHN). Should a person be diagnosed MHS following an IVCT, non triggering anaesthetics will need to be used in the future. The IVCT does not always return an unequivocal result; in some cases a muscle biopsy will display an abnormal contracture response to only halothane or caffeine and in this case the patient is classified as MHS_H or MHS_C respectively (1). The patient is still classified as being susceptible to MH and will be given non triggering anaesthesia if needed.

1.2 Skeletal muscle

Skeletal muscle is an excitable tissue tasked with the voluntary movement of one body part with respect to another. Actin and myosin within myofilaments are the proteins required for contraction of muscle tissue (figure 1.1). The contraction of skeletal muscle is a voluntary process under the control of the somatic nervous system. The neural stimulation of a muscle fiber will cause the cell membrane to depolarise, and an action potential will rapidly travel across the cell membrane and down invaginations within the membrane (T-tubules). T-tubules are in close proximity to the main Ca^{2+} storage site within the cell, the sarcoplasmic reticulum (SR). Neural stimulation will induce the mass release of Ca^{2+} from the SR. Within myofibrils are the proteins required for the contraction of skeletal muscle actin and myosin. In the presence of Ca^{2+}, myosin binding sites on actin open, at which time myosin will hydrolyse ATP inducing muscle contraction.

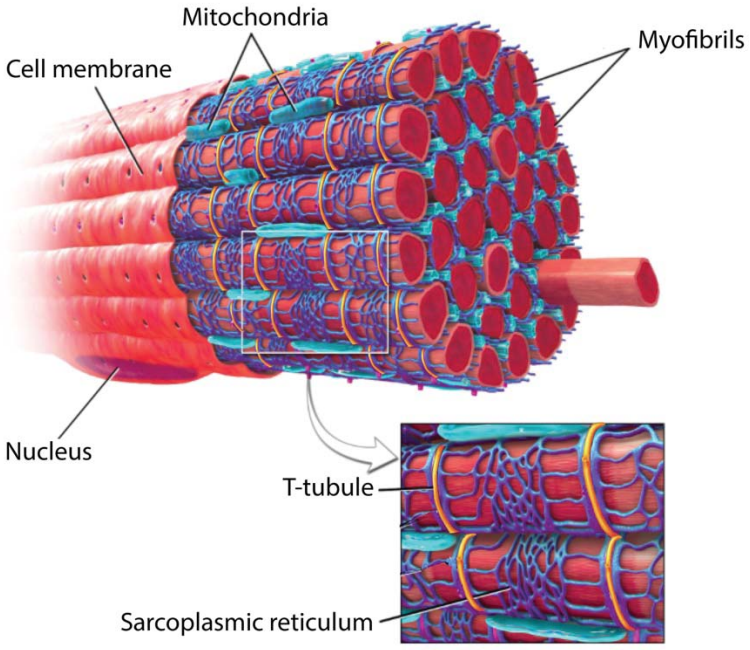

Figure 1.1 General architecture of a skeletal muscle fiber. Mitochondria have been highlighted in blue. Myofibrils have been highlighted in red. The sarcoplasmic reticulum has been highlighted in purple. The T-tubule in yellow. Figure adapted from (4) (no permission required to use figure).

The dihydropyridine receptor (DHPR) is an L-type voltage dependent Ca^{2+} channel located within T-tubules (5, 6). The DHPR forms a physical interaction with the Ca^{2+} channel ryanodine receptor type 1 (RyR1) (figure 1.2), which spans the SR membrane. In a process known as excitation-contraction (EC) coupling, the conformational change induced in the DHPR, following stimulation, forces a concomitant conformational change in RyR1 (7, 8) leading to the seemingly instant release of Ca^{2+} and associated muscle contraction. At rest, the cytosolic concentration of Ca^{2+} is ~ 100 nM but following RyR1 activation the concentration rapidly increases tenfold (9). Free cytosolic Ca^{2+} is transported back into the SR by the sarcoplasmic/endoplasmic reticulum ATPase (SERCA). This protein hydrolyses ATP to pump Ca^{2+} against its concentration gradient back into the SR. Once returned to the SR the ions are can again be released into the cytosol.

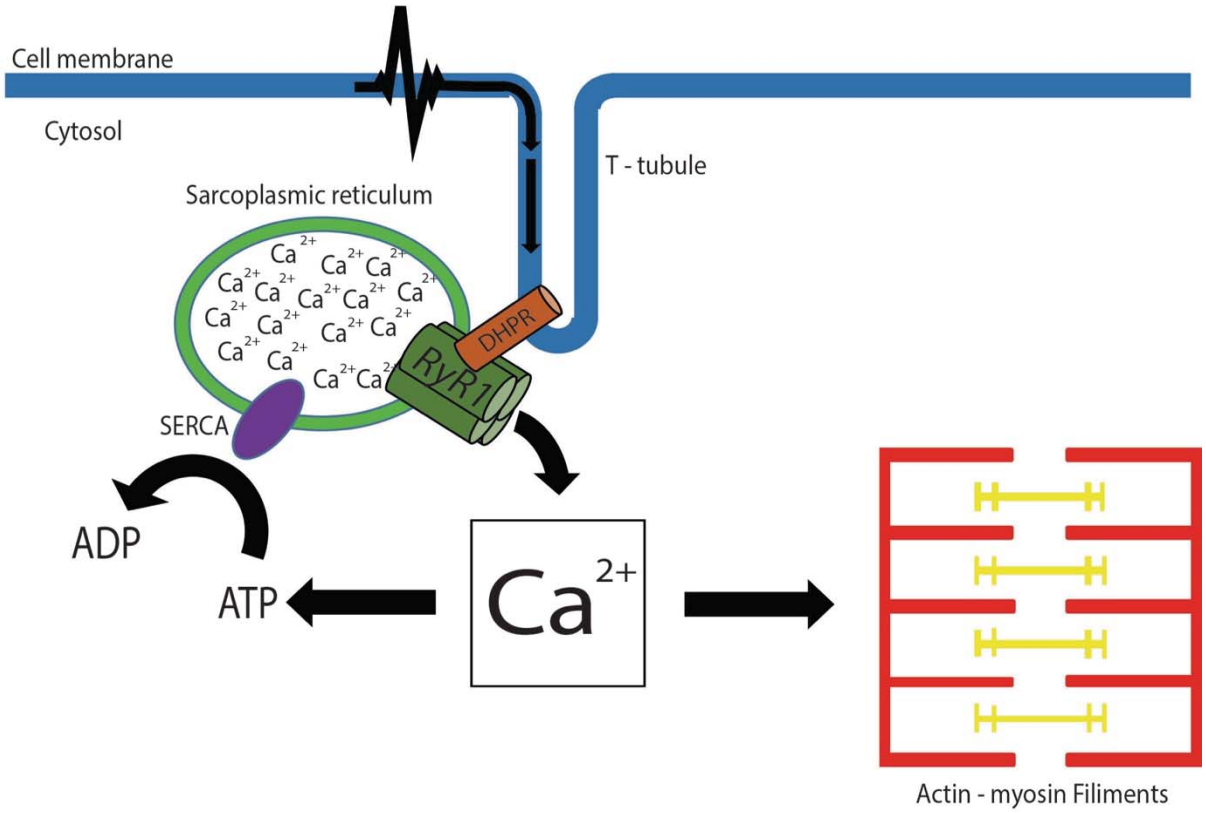

Figure 1.2 Schematic representation of the factors controlling calcium homeostasis in skeletal muscle cells. An action potential travels along across the cell membrane and down the T-tubule (blue) activating DHPR (orange). The DHPR stimulates the RyR1 (green) releasing Ca^{2+} from the sarcoplasmic reticulum. Once in the cytosol Ca^{2+} can initiate muscle contraction by opening myosin binding sites on actin. Ca^{2+} is transported back into the SR via the SERCA (purple) powered by ATP hydrolysis.

It is widely accepted that abnormal skeletal muscle calcium homeostasis is the cause of the MH phenotype. Between 50 - 70 % of the patients susceptible to MH have been shown to have nucleotide variations within the gene encoding the skeletal muscle ryanodine receptor, *RYR1*, located on chromosome 19q13.1 (10). More than 400 *RYR1* variants linked to MH have been identified, yet only 35 have been confirmed as being MH causative as of January 2016 (11).

MH was once a deadly disease with a mortality rate of about 70 % in patients displaying symptoms. Following the development and use of dantrolene, a Ca^{2+} blocking agent, the mortality rate has dropped significantly, however MH episodes still occur. Dantrolene acts to close the channel but exactly how it functions is not well defined (12).

1.3 The ryanodine receptor

The ryanodine receptor is an SR membrane spanning protein with an estimated mass of 2.3 MDa. There are three isoforms of the channel: type 1 expressed in skeletal muscle, type 2 expressed in cardiac muscle and type 3 expressed in a range of tissue types. All three isoforms share an amino acid identity of roughly 65 %. Type 1 is the only channel to be associated with MH and is the only channel to be activated by EC coupling; the other two isoforms rely on other mechanisms for activation (13).

RyR1 is a homotetramer where each subunit is approximately 5000 amino acids long with a molecular mass of approximately 565 kDa. RyR1 forms an overall mushroom-like structure, with the majority of the protein's mass being located on the cytosolic side of the membrane (figure 1.3). The N-terminal and central regions of RyR1 form the cytoplasmic cap while the C-terminal region forms the transmembrane stalk (14). The channel is comprised of a number of domains, each playing a significant role in channel function.

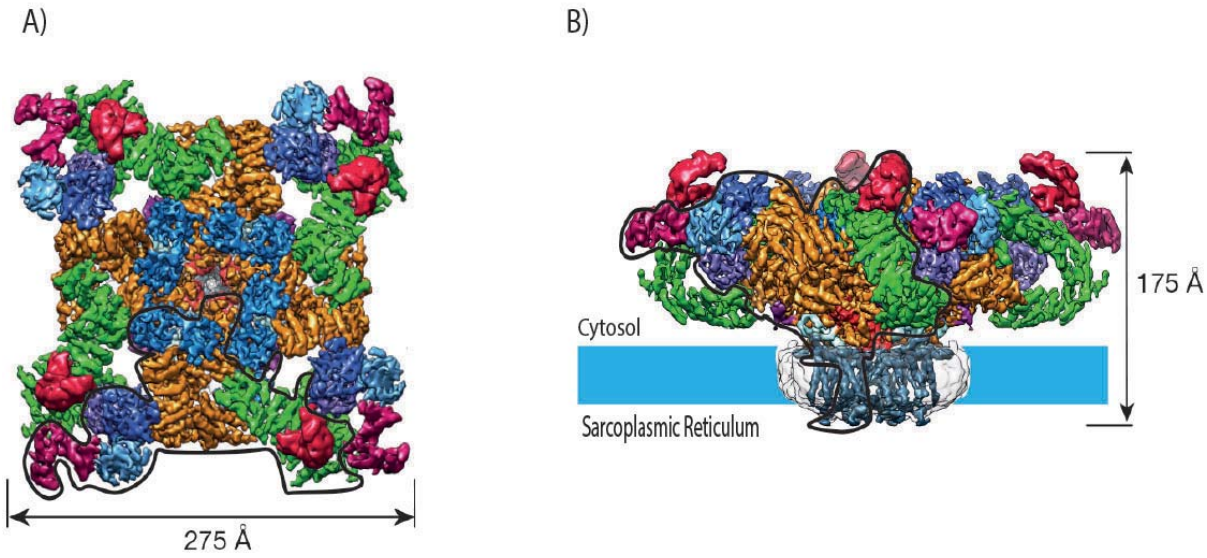

Figure 1.3 Cryo-electron microscopy structure of RyR1 in the closed state, imaged at 6.1 Å resolution. The figure indicates the general structure of RyR1 tetramer, differing regions of the channel have been represented by individual colours. Overall dimensions of the channel have been indicated. An individual subunit has been outlined in black. A) A view from the cytoplasm. B) A lateral view of the channel. The sarcoplasmic reticulum membrane has been highlighted in blue. (Figure was adapted from (15), permission was obtained through Rightslink)

1.4 Variant mapping

MH-linked variants were initially identified within two hotspot domains of RyR1, the N-terminal domain and specific areas of the central region (16). The high number of MH-linked variants found within these two specific regions lead to the hypothesis that the two regions form a network of specific interactions with each other and move relative to each other during channel opening (17). Should an amino acid variant occur within one of these regions there is potential for the domain interface, in the closed state, to be destabilised, causing the channel to open more easily under certain conditions. This hypothesis was later supported following the production of cryo-electron microscopy (EM) images of the channel (14, 18, 19). More MH-linked variants have been found outside of these regions however, indicating specific amino acid interactions in other regions of the channel are also required for proper channel function.

1.5 Other RyR1 associated diseases

Central core disease (CCD) is normally a dominantly inherited disease linked with variants in *RYR1*. In this case amino acid variants are generally linked to the C-terminal region of RyR1 corresponding to the transmembrane domain (20). RyR1 in this case can either be characterised as being a leaky channel, in which case a specific amino acid variation will cause RyR1 to favour the open state at rest allowing calcium ions to leak continually from the SR (21). In this situation a concentration gradient across the SR membrane cannot be maintained resulting in a decreased SR Ca^{2+} store. Following RyR1 stimulation, insufficient Ca^{2+} will be released from already diminished stores, resulting in a reduced cytosolic Ca^{2+} concentration rendering a decreased contracture response. Alternatively, a non responsive channel will result in a constitutively closed channel releasing significantly less Ca^{2+}. In this case the propagation of the electrical signal through the DHPR is not received by RyR1, with these channels being referred to as EC uncoupled. Both forms of defective RyR1 channels can explain the CCD phenotype of muscle weakness and reduced muscle tension (22). CCD is normally diagnosed by abnormal histology which shows regions in the muscle core that lack mitochondria and oxidative enzyme activity (23-25). The cytosolic overload of Ca^{2+} from leaky RyR1 channels has been implicated in mitochondrial damage resulting in decreased mitochondrial presence and sarcoplasmic disorganisation (23-25). HEK293T cells transfected with CCD linked *RYR1* variants and loaded with a fluorescent Ca^{2+} indicator can be used to analyse leaky channels characterised by an increased Ca^{2+}-induced fluorescence at rest coupled with a decreased response to agonists (26), or a decreased response to RyR1 agonists in the case of EC uncoupled channels.

Multi mini core disease (MmD) is a non-progressive myopathy characterised by distal joint laxity, muscle weakness and respiratory problems are common along with progressive scoliosis. When characterised histologically, MmD patients present with multiple small cores (which are variable in size and number) resulting from reduced oxidative activity in muscle tissue, mild fibrosis and the presence of internal nuclei (22). Similar to CCD, MmD patients have a decreased mitochondrial presence and display variable degrees of disruption to the sarcolemma (27). RyR1 is one of many proteins where amino acid variations have been associated with MmD. MmD caused

by RyR1 variations is recessive with the associated amino acid variants being distributed throughout the protein. Many patients displaying MmD symptoms are however, heterozygous for the disease-linked variant. Tissue-specific allele silencing has also been suggested as a disease mechanism, where the wild type allele is suppressed, with only the disease linked variation being expressed (28). The reduced expression of RyR1 is thought to result in decreased Ca^{2+} conductance (29). Compound herterozygosity, where a patient has two separate *RYR1* variants, one on each allele can also result in MmD (30).

1.6 Regulation of RyR1

As the release of Ca^{2+} from the SR dramatically alters muscle cell physiology, it is essential that cytosolic Ca^{2+} levels are tightly regulated. RyR1 responds to a number of cellular signals many of which are mediated through protein-protein interactions. Specific interactions are able to both up or down regulate channel function.

1.6.1 Protein-protein interactions

Under resting conditions calmodulin (CaM) binds to amino acids 3614–3643 of RyR1 acting as an RyR1 agonist (31). When cytosolic Ca^{2+} reaches roughly 1 μM, CaM will bind Ca^{2+} leading to a conformational change in the protein. This opens a second RyR1 binding site allowing CaM to interact with the amino acids 1975-1999 of an adjacent RyR1 subunit (32). In the Ca^{2+}-bound state CaM acts as an antagonist, causing the channel to favour the closed state, limiting further calcium release.

Calsequestrin (Casq) is a sarcoplasmic reticulum lumenal protein that sequesters calcium ions, effectively acting as a Ca^{2+} buffer. Casq drastically reduces the Ca^{2+} concentration gradient across the SR membrane allowing SERCA to efficiently return Ca^{2+} to the SR (33). When the luminal concentration of Ca^{2+} is diminished Casq has been shown to form an interaction with RyR1, mediated by the membrane spanning proteins triadin and junctin limiting further Ca^{2+} release through the channel (34). This allows the luminal store of Ca^{2+} ions to be replenished and thus repeated rounds of EC coupling. Knock out mice have been used to characterise the specific

function of Casq; these mice are particularly susceptible to death following exposure to halothane, displaying symptoms characteristic of an MH episode. When the mice were treated with dantrolene prior to being exposed to halothane symptoms were alleviated. During these experiments it was concluded that Casq plays a key role in the regulation of Ca^{2+} release. While total knock out of Casq has been implicated in MH, specific variants in the protein have also been indirectly linked to MH (35). When functionally characterised *in vitro*, specific Casq variants were shown to have decreased Ca^{2+} binding capacity. The same variants when structurally characterised displayed an altered tertiary structure. It was proposed the altered structure resulted in decreased Ca^{2+} binding capacity, potentially limiting Casq's ability to interact with and regulate RyR1.

FKBP12 is a protein known to interact with the ryanodine receptor and is thought to stabilise the closed state of the channel (36). Each RyR1 subunit will bind one FKBP12 molecule in a 1:1 ratio. Loss of FKBP12 binding will cause the channel to favour the open state leading to an increase in Ca^{2+} release. FKPB12 is a cytosolic protein and will only interact with regions of RyR1 that are exposed to the cytosol. Early studies proposed that RyR1 amino acids valine 2461 and proline 2462 play an important role in this interaction (37). More recent studies have indicated RyR1's SPRY1 domain (amino acids 639–833) is responsible for FKBP12 binding, particularly the amino acids phenylalanine 674 and leucine 675 (38). Loss of FKBP12 binding leads to loss of EC coupling such that RyR1 can no longer be activated via the DHPR (36). The DHPR interacts directly with RyR1's SPRY2 domain; the two SPRY domains are adjacent to each other in the three dimensional structure of the channel (14) (figure 1.4). It has been suggested that binding of FKBP12 may induce a conformational change within SPRY1 that propagates through to the SPRY2 domain and may have an effect on the binding of the DHPR.

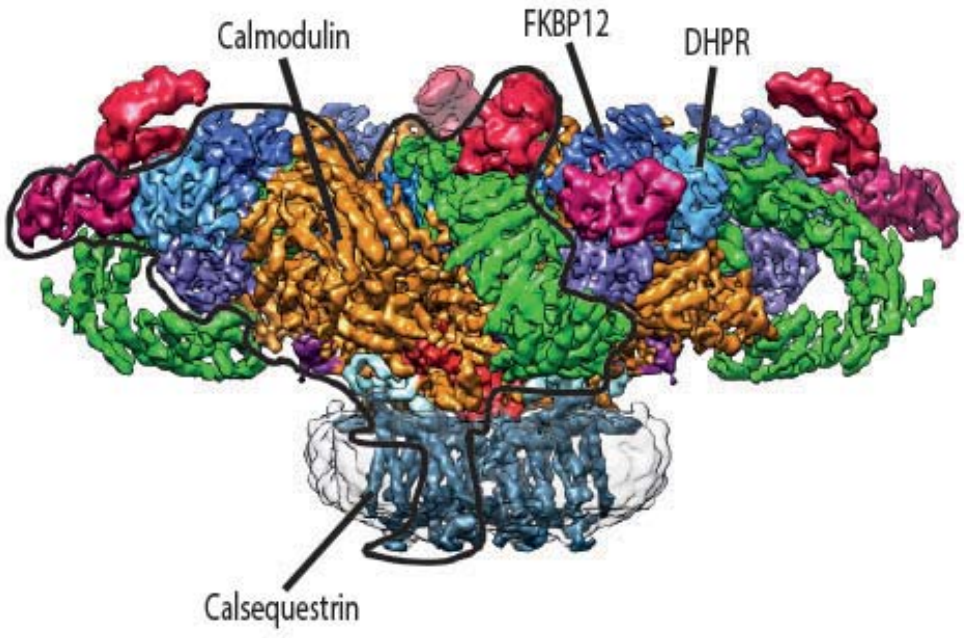

Figure 1.4 Schematic representation of protein interactions with RyR1. The three dimensional cryo-electron microscopy structure confirmed at 6.1 Å in the closed state has been represented with the site of protein interactions being indicated. A single RyR1 subunit has been outlined in black (figure adapted from (15), permission for publishing figure was obtained from RightsLink)

The cytoplasmic region of the α_{1S} subunit of the DHPR, loop II-III, interacts with RyR1 (7, 39) (figure 1.5). The conformational change induced in the α_{1s} subunit following electrical stimulation propagates through this loop and causes a conformational change in RyR1 opening the channel. The direct interaction of DHPR and RyR1 is essential for EC coupling and the seemingly instant release of Ca^{2+} leading to muscle contraction. An arginine to histidine variation at amino acid 1086 of the α_{1S} subunit of the DHPR has been reported to cause MH (40). The amino acid is located on the III-IV loop and is not in direct contact with RyR1. The functional analysis indicated the variation was able to lead to increased calcium release through RyR1 in both the case of electrical stimulation, a DHPR agonist, and caffeine, a RyR1 agonist. This led to the proposal of the hypothesis, that the III-IV loop is involved in the negative regulation of calcium release through RyR1.

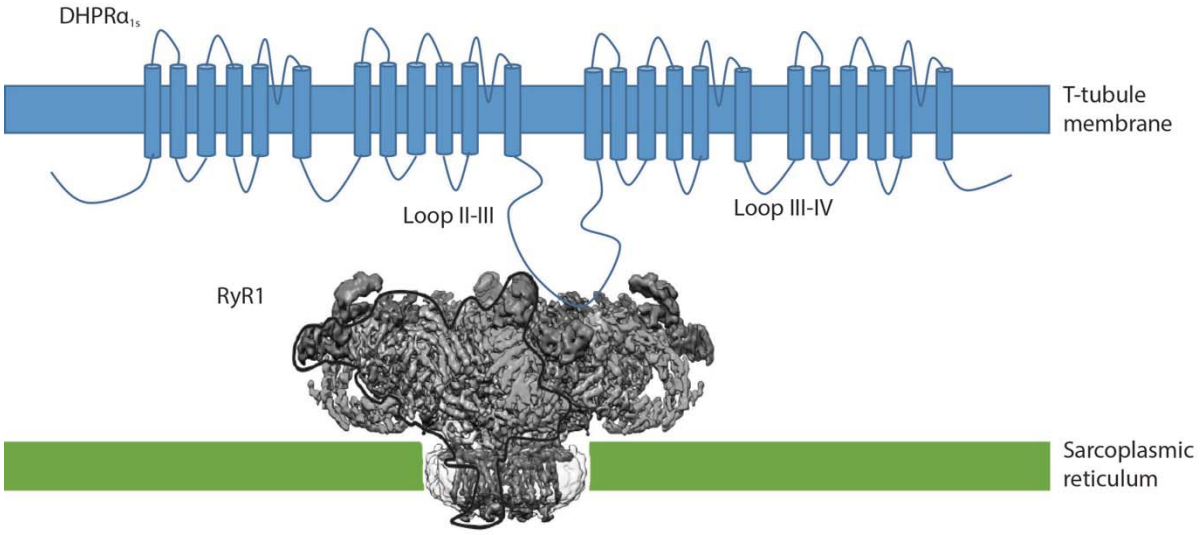

Figure 1.5 Interaction between RyR1 DHPR α_{1S} loop II-III. (figure adapted from (15), permission for publishing figure was obtained from RightsLink)

An ordered array of RyR1 forms on the SR membrane where every second RyR1 forms an interaction with DHPR (41). Ca^{2+} release through RyR1 is not solely induced by DHPR. RyR1 can be activated by a combination of protein and ligand interactions along with posttranslational modifications. The release of Ca^{2+} via these mechanisms is not instantaneous as the process relies strongly on the diffusion of stimulatory molecules within the cell. RyR1 channels in contact with DHPR will release Ca^{2+} quickly following the initial neuronal signal, while the non DHPR associated RyR1 channels will release Ca^{2+} with a delayed response, aiding in prolonging Ca^{2+} release and increasing the strength of the associated muscle contraction.

1.6.2 Ligand interactions

Ca^{2+} is able to interact with and allosterically regulate RyR1 (15). The increase in cytosolic Ca^{2+} concentration resulting from DHPR activation is not high enough to induce an intense and rapid muscle contraction. However, it is likely the increased Ca^{2+} presence surrounding the SR membrane is involved in the regulation of RyR1 (6). There are two Ca^{2+} binding sites on RyR1; one with a high affinity and one with a low affinity (42). The high affinity binding site, an EF hand motif (43), on the cytoplasmic face of the channel, when bound to Ca^{2+} induces a conformational

change in the transmembrane domain (15). This lowers the activation threshold of RyR1, allowing Ca^{2+} to be more easily released. This process is known as Ca^{2+} - induced Ca^{2+} - release. When cytosolic Ca^{2+} reaches millimolar concentrations, Ca^{2+} will bind to the low affinity binding site, stabilising the closed state of the channel (42). Thus high concentrations of cytosolic Ca^{2+} acts as a RyR1 antagonist directly, by binding to RyR1 and indirectly, mediated through CaM (32).

ATP is a strong metabolic signal. When the cytosolic concentration reaches millimolar levels ATP binds to RyR1 stabilising the open state of the channel. RyR1 with Ca^{2+} bound to the high affinity site coupled with ATP binding can cause the channel to remain in the open state without electrical stimulation (44). Sequence analysis of RyR1 suggests the presence of 16 ATP binding sites, although fewer were noted during ATP binding assays. The amino acids 699-706, 1081-1084, 1195-1200 (45), 2370-2375 (46), 2402-2795 (45) have been shown to play a key role in the binding of the nucleotide. There are no studies to suggest RyR1 is able to hydrolyse ATP; its interaction with RyR1 appears to be purely regulatory (47).

ADP is also able to bind to RyR1 (45), having the opposite effect on channel regulation. When ADP is present in high concentrations it is an indication the cell is in a metabolically deficient state. ADP binds to RyR1 stabilising the closed state of the channel limiting calcium release. Downstream ATP hydrolysis, normally induced by channel activity is also decreased, preserving what ATP is present for essential cellular functions. RyR1 is thought to have a higher affinity for ATP compared to ADP (48) and it is thought both nucleotides interact with the same binding pockets.

RyR1 has a higher affinity for Mg^{2+} than Ca^{2+}; the two ions are thought to compete for the same binding site. When bound, Mg^{2+} stabilises the closed state of the channel, limiting Ca^{2+} release. Before Ca^{2+} can bind, it has been suggested a conformational change must occur in RyR1 ejecting Mg^{2+} and opening the Ca^{2+} binding site. In a resting state it has been proposed that for every 1 Ca^{2+} bound to RyR1 there are 3 Mg^{2+} bound (49). In the presence of Mg^{2+} RyR1 displays decreased Ca^{2+} release even in the presence of ATP and the RyR1 agonist caffeine (50). These observations highlight the inhibitory function of Mg^{2+} and the importance of Ca^{2+} binding in the activation of RyR1.

1.7 Post translational modification of RyR1

RyR1 can be phosphorylated by protein kinase A and calmodulin-dependent protein kinase (51, 52). The phosphorylation of serine 2843 has been shown to cause the dissociation of the regulatory protein FKBP12, leading to an increased Ca^{2+} release (53). Protein phosphatase 1 acts to remove the covalently linked phosphate, allowing FKBP12 to bind to the channel stabilising the closed state (53, 54).

During metabolism, particularly in working muscle, reactive oxygen species are created, altering the redox state of the cell (55). The SR membrane protein NADPH oxidase 4, in the presence of cytosolic oxygen, will oxidise NADPH to $NADP^+$ within the SR. The liberated electron is passed on to cytosolic O_2 producing a superoxide ion. The increased concentration of superoxide ions surrounding the SR membrane has the potential to oxidise RyR1, thus altering channel function (56, 57). During oxidation, the thiol group of a cysteine residue has the potential to donate its hydrogen atom to the superoxide ion. Cysteine, in the oxidised state, has the potential to form covalent bonds with other oxidised molecules within the cell. The RyR1 cysteine residues 36, 2326, 2363, and 3635 (accession number NP_001095188.1), following oxidation, have been linked to disulphide bond formation with each other causing the channel to favour the open state, prolonging Ca^{2+} release (55, 58, 59). Nitric oxide, a product of amino acid metabolism, also has the potential to oxidise the same cysteine residues again leading to the formation of disulphide bonds. In the presence of nitric oxide RyR1, in the oxidised state, is also susceptible to *S*-nitrosylation. This modification has been shown to lead to an increased Ca^{2+} release from the SR by enhancing Ca^{2+}-induced activation (58). The antioxidant S-glutathione will readily donate a hydrogen atom from its thiol group to a reactive oxygen species. RyR1, in the oxidised state, is particularly susceptible to covalent modification by oxidised S-glutathione, where a disulphide bond forms between the two oxidised thiol groups. Once bound to RyR1, S-glutathione limits the inhibitory effect of Mg^{2+} ions leading to an increased Ca^{2+} release (58). The cysteine residues 36, 315, 811, 906, 1591, 2326, 2363, 3193, and 3635 have been shown to be endogenously modified by either S-nitrosylation or *S*-glutathionylation (59). Covalent modification of cysteine 3635 inhibits the binding of the regulatory protein calmodulin (60, 61). Conversely, calmodulin binding inhibits the covalent modification of this amino acid.

1.8 Pharmacology

Halothane is a volatile anaesthetic that was commonly used during surgery requiring general anaesthesia, from the mid 1950's until the 1980's when it was phased out, in favour of alternative anaesthetics. Halothane has been shown to induce an MH episode in MHS patients only; it has no effect on MHN patients. Halothane is commonly used in the IVCT test to diagnose MH susceptibility (1).

Caffeine is a known activator of the central nervous system; it is able to initiate contraction of skeletal muscle and relax smooth muscle. At concentrations lower than 1 mM caffeine is able to stimulate Ca^{2+} release from the SR and is used during the IVCT to diagnose MH susceptibility (1). Caffeine has been shown to enhance calcium-induced calcium-release. This may be the reason it is able to induce an MH episode *in vitro*, as a binding site has yet to be confirmed on RyR1 (62). Mutational analysis suggests the amino acids Gly 2370, Gly 2373 and Gly 2375 are involved in the binding of caffeine or receiving the resulting stimuli. Functional analysis following mutation of these glycine residues individually lead to a loss of caffeine sensitivity (46).

4-chloro-*m*-cresol, 4-C*m*C, has been shown to alter the permeability of Ca^{2+} from the SR (63). It is a significant activator of Ca^{2+} release, being able to induce release at concentrations roughly 100 times lower than caffeine (64). 4-C*m*C is able to activate calcium release in both MHS and MHN patients, although the sensitivity in an MHS patient is significantly higher. Some RyR1 variants have been shown to have a limited response to electrical stimulation. These channels also display no response to 4-C*m*C indicating that 4-C*m*C may activate RyR1 by exploiting the mechanism used to receive the neural stimulation (65). Caffeine was able to stimulate Ca^{2+} release in these channels so is likely to activate calcium release via a different mechanism. 4-C*m*C has been shown to be a useful tool for the diagnosis of MH. It causes the release of Ca^{2+} in a well-defined dose-dependent manner.

1.9 Functional characterisation of MH-linked RyR1 variants

1.9.1 The *in vitro* contracture test

The *in vitro* contracture test, IVCT, is currently the gold standard for the diagnosis of MH (1). The procedure is morbidly invasive as a large muscle biopsy must be extracted for analysis. While DNA-based diagnostic tests have been established, they are limited in that only an MHS diagnosis can be made with respect to known causative variants (66, 67). The establishment of a comprehensive library of known causative variants is the current trend in MH-based research, in order to provide an alternative to the IVCT to families with a known MH causative variant. One key criterion for the acceptance of a DNA test for diagnostic purposes is that the specific variant must be functionally characterised. A range of cell based assays are currently being used to determine the effect that specific amino acid variations may have on RyR1 function.

1.9.2 Myotubes

Myoblasts are non-differentiated muscle cells that can be extracted from a muscle tissue sample. The cells are easily cultured and following the removal of serum from the media, the myoblasts will differentiate into myotubes (68). Myotubes replicate the phenotype of intact muscle cells and express all proteins present within muscle cells, particularly those involved in EC coupling. Exposing the cells to RyR1 specific agonists allows for the analysis of RyR1 variants in a state closely resembling physiological conditions (69). Problems can arise when examining functional RyR1 variants in myotubes isolated from a patient. The results of the functional analysis can be affected by the unique genetic background of the individual. Any alteration seen in Ca^{2+} regulation can be confirmation of the patient being susceptible to MH, but may not be a direct indication of altered RyR1 function as amino acid variations in other proteins may affect the results.

1.9.2 Lymphocytes

Lymphocytes express RyR1 making them a convenient and easily available source for the characterisation of MH as they can be extracted from a blood sample (70, 71). The cells do not have a contractile phenotype and it is thought they exploit the function of RyR1 for Ca^{2+}-related signal transduction. While endogenous RyR1 is expressed, other proteins involved in the EC coupling process are not. Many of these have the potential to form interactions with and regulate RyR1 function. The onset of MH in RyR1 variants resulting in the loss of specific protein-protein interactions cannot be effectively characterised in this system and will likely return a result comparable to wild type. Alternative splicing of RyR1 also occurs in lymphocytes (72), exon 70 is deleted from *RYR1* mRNA (73). The ryanodine receptor is still functional but the onset of MH resulting from functional variants within this region cannot be characterised in this system. The use of these cells in the characterisation of a specific RyR1 variant can again be effected by the genetic background of the patient.

1.9.3 Human embryonic kidney cells

Human Embryonic Kidney, HEK293T, cells have been widely used to characterise RyR1 variants (74-76). The cells are commercially available and hence are not affected by genetic variation between host sources. Specific *RYR1* variants must first be identified in a patient susceptible to MH and introduced into *RYR1* cDNA within a mammalian expression vector. Followed by introduction into HEK293T cells by transfection. As HEK293T cells do not express a functional RyR1 any alteration to Ca^{2+} regulation can be attributed to the expressed RyR1 variant. These cells do not express any of the proteins involved in EC coupling. So while these cells are a useful system, an MH phenotype resulting from the loss of protein/protein interactions *in vivo* cannot be analysed in this system. Therefore, caution must be exercised when characterising an RyR1 variant that shows no functional difference to wild type RyR1.

1.9.4 COS-7

Similar to HEK 293T cells COS-7 cells can also be transfected with *RYR1* cDNA (77). Again the cells do not express an endogenous functional ryanodine receptor. Like HEK 293T cells COS-7 cells do not express a number of the proteins involved in the EC coupling process, so a true implication for a functional RyR1 variant may not be detected following functional analysis.

1.9.5 Dyspedic myotubes

Dyspedic myotubes are myotubes that do not express RyR1. The cells are differentiated from 1B5 cells, myoblasts extracted from *RYR1* knock out mice (78). Following transfection with *RYR1* cDNA, a variant can be specifically analysed to see its effect on Ca^{2+} homeostasis (79). The expressed RyR1 variants will be exposed to an environment resembling an intact muscle cell allowing for the formation of the desired protein-protein interactions required for proper RyR1 function (80). The advantage of using dyspedic myotubes over patient isolated myotubes is that the genetic background is the same differing only in the expressed RyR1 variant. This makes the characterisation of an isolated RyR1 variant more specific.

To examine alterations to calcium homeostasis in all cell based assays; cells are loaded with a Ca^{2+}-sensitive fluorescent indicator e.g. fura 2-AM and exposed to RyR1 agonists. The release of calcium from the SR/ER causes an alteration in the fluorescence intensity from the fluorophore which can be measured using a fluorescence microscope or a spectrofluorometer. MHS variants display an increased fluorescence intensity in the presence of RyR1 agonists compared to a wild type control, representing an increased cytosolic Ca^{2+} concentration indicative of the MH phenotype.

1.9.6 Knock-in mice

RyR1 variants can also be characterised at the organism level. Mice are commonly used in this context. To characterise a specific RyR1 variant mouse embryonic stem cells are transfected with variant containing *RYR1* cDNA. Once the cDNA has entered the nucleus the variant will incorporate into the host genome by specific recombination. Functional characterisation the RyR1 variant can be performed on the mice by exposing them to halothane and monitoring the onset of characteristic MH symptoms (81). Alternatively functional characterisation can be performed on myotubes extracted from the knock-in mice (82).

1.9.7 Electrophysiology

Single channel electrophysiology has been used to characterise RyR1 variants (83). RyR1 must be extracted from the sarcoplasmic reticulum before being incorporated into a planar lipid bilayer. The conditions on each side of the membrane can be maintained to resemble physiological conditions. RyR1 can then be exposed to a specific agonist where any changes in the membrane potential resulting from channel opening can be measured. Any changes to the membrane potential in RyR1 variants compared to wild type RyR1 can be attributed to altered channel function.

Patch clamp electrophysiology in the whole cell configuration has been used to characterise RyR1 variants with respect to MH (84, 85). Myoblasts were extracted and differentiated into myotubes. The cell membranes were depolarised under controlled conditions activating the DHPR and as a consequence activating RyR1. RyR1 function was indirectly measured by measuring changes in cytosolic Ca^{2+} levels using a Ca^{2+}-sensitive fluorescent indicator. In this system RyR1 is characterised in a state representing physiological conditions where the channel is activated in much the same way it would under *in vivo* conditions.

1.10 Previously determined ryanodine receptor structures

Limited high resolution structural analysis has been performed on RyR1, making it difficult to determine how specific amino acid interactions are likely to affect the function of the channel with respect to the tertiary structure.

Recently a cryo-EM structure of the entire channel at a resolution of 3.4 Å was reported (14). This work provided a strong insight into the overall structure of the channel, highlighting domain boundaries, the distribution of secondary structure and in some cases the positioning of specific amino acids (figure 1.6).

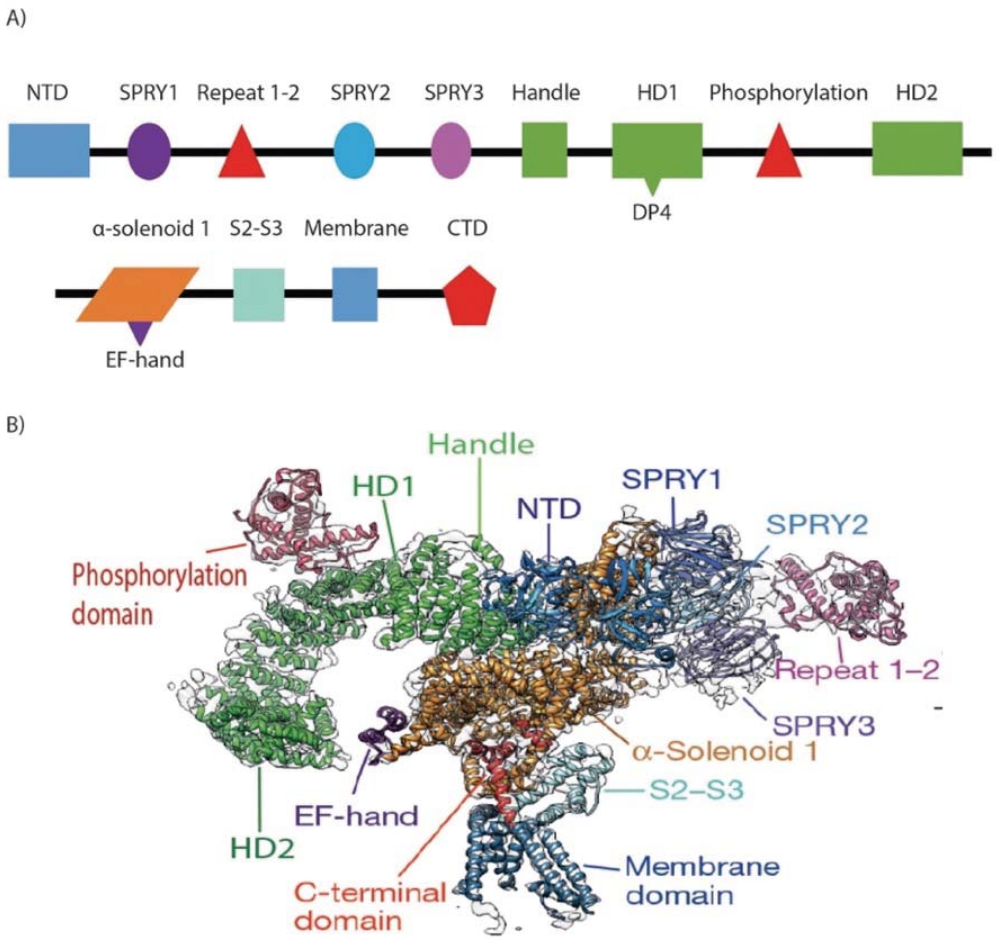

Figure 1.6 Domain distribution of RyR1. A) Schematic representation of the proposed domain distribution of RyR1. B) An individual subunit of RyR1 has been represented with individual domains highlighted in differing colours. (figure adapted from (15) permission for publishing figure was obtained through RightsLink).

Prior to this work lower resolution cryo-EM structures had been reported (18, 86); these studies were able to examine the overall structure of the channel including

domain distribution and some secondary structure formation. The main highlight of the studies was to examine the structural differences between the three ryanodine receptor isoforms in both the open and closed states. RyR1 undergoes a significant conformational change during channel opening; the transmembrane domain rotates with respect to the cytoplasmic assembly, while the cytoplasmic domains undergo a substantial conformational shift (19). It was noted all domains move in a very structured manner with the cytoplasmic domains moving upward and outward, pulling the more centrally located domains with them opening the ion channel. The structure of RyR1 in its entirety has yet to be determined by X-ray crystallography, however the crystal structures of specific domains have been determined.

The crystal structure of the rabbit RyR1 N-terminal domain has been determined using X-Ray diffraction analysis (87, 88). The structure reported comprised amino acids 1-210 followed by the greater N-terminal region, amino acids 1-559. The amino acids 1-559 were shown to form three sub domains: A, B and C. Domains A and B are predominantly comprised of beta strands while domain C is rich in alpha helices. The crystal structure of the N-terminal domain was mapped to the cryo-EM structure of the channel, locating it at the peak of the mushroom structure at the subunit interface (14) (figure 1.7). Domains A and B are thought to be involved in the tetramerisation process of RyR1 (89) while domain C was implicated in the formation of interdomain interactions with the adjacent handle and HD1 domains (14).

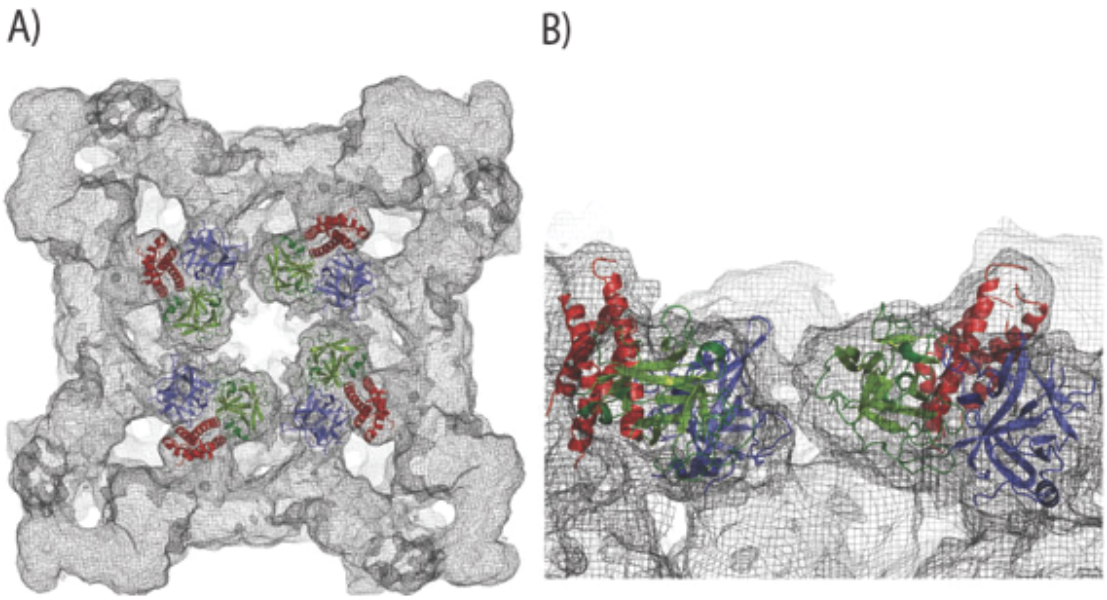

Figure 1.7 Location of the N-terminal domain with respect to the RyR1 tetramer. Domain A is represented in blue, domain B is represented in green, Domain C is represented in red. A) The cytoplasmic view of the RyR1 tetramer, the N-terminal domain of each subunit has been highlighted. B) A lateral view of RyR1. The domain interface has been highlighted and the position of the N-terminal domain from each domain has been highlighted (figure taken from (88) permission to publish figure was obtained through RightsLink).

The N-terminal domain of RyR1, was originally considered to be a “hotspot” domain with respect to MH-linked variants. A large proportion of MH-linked variants were located in this region. Many of have been structurally characterised, with a number of variants located at the extremities of the domain shown to have a limited structural impact on the domain. It was proposed these MH-linked variants may interfere with formation of interdomain interactions leading to the onset of MH under certain conditions.

Structures of two SPRY domains comprising amino acids 650-844 and 1070-1246 have been determined by X ray crystallography (38, 39). The two SPRY domains within RyR1 are separated by a region of tandem repeats, amino acids 862-1054 referred to as repeat 1-2. This region was also crystallised separately and structurally analysed in the same study. The two domains were mapped to the extremities of the mushroom structure. Both the SPRY 1 and 2 domains have been implicated in the binding of regulatory proteins; SPRY 1 has been shown to interact with FKBP12, stabilising the closed state of the channel (38). SPRY 2 has been

implicated with the interaction of DHPR, with the domain playing a key role in receiving the stimulatory signal leading to channel opening (39). The domains are named due to the sequence homology shared between a fungal tyrosine kinase, spore lysis A, and the ryanodine receptor (90). SPRY domains have been identified in a number of different protein families involved in a myriad of cellular process and are characterised by a β sandwich structure.

The DP4 domain comprising amino acids 2442-2477 has been structurally analysed by NMR (91). This domain is formed from two alpha helices, and is located within a greater alpha helical rich HD1 domain. The DP4 domain was proposed to play a key role in the stabilisation of RyR1 in the closed state as a number of MH-linked amino acid variants have been identified within this small region. Protein binding assays have been used to show the domain is likely to be involved in interdomain interactions (92). The domain is also thought to be involved in the binding of ryanodine as specific MH-linked variants within the region were shown to reduce ryanodine binding capacity (93).

The phosphorylation domain, comprising amino acids 2734–2940, has also been structurally analysed by X-ray crystallography (94, 95). The region was shown to be post-translationally modified by the enzymes protein kinase A and calmodulin-dependent protein kinase II β at Ser 2843 (53). A number of MH-linked variants surround the phosphorylation site and are thought to limit the regions ability to be modified. While other variants have been linked to the disruption of interdomain interactions. MH-linked variants were located in the local area surrounding the phosphorylation site and were thought to affect the potential for the domain to be post translationally modified. Other MH linked variants were located at the external reaches of the domain and are thought to limit the transmission of the regulatory signal to the rest of the channel.

1.11 Motivation for research described in this thesis

Two nucleotide variants within *RYR1* have been linked to malignant hyperthermia in a small number of families world wide, c.641C>T and c.7042_7044delCAG. The nucleotide variants result in the amino acid variations p.T214M and p.ΔE2348

respectively (96, 97). In New Zealand a proband had been shown to contain both variants, one inherited maternally and one inherited paternally. The mother, known to have the c.641C>T variant, was diagnosed MHN by the IVCT (1). The proband was diagnosed MHS by IVCT. The father having the c.7042_7044delCAG variant to date has declined testing by IVCT. The c.614C>T variant segregates with MHS in three families in the United Kingdom all of whom have been classified MHS by IVCT (96).

1.12 Hypothesis of study

The ryanodine receptor amino acid variants, p.T214M and p.ΔE2348 (GenBank accession NP_000531.2) linked to malignant hyperthermia will alter Ca^{2+} release from the sarcoplasmic reticulum in response to RyR1 agonists 4-C*m*C and caffeine.

1.13 Aims of study

1) To functionally characterise the RyR1 variants p.T214M and p.ΔE2348.

- Each nucleotide variant was introduced into the full-length human RyR1 cDNA (NM_000540.2).
- Each variant was expressed in a mammalian cell line.
- Confirmation of expression of *RYR1* cDNA using immunoblotting and immunofluorescence microscopy.
- Ca^{2+} release was measured for each variant and compared to wild type RyR1 expressing cells.

2) To structurally characterise each each variant.

- The cDNA of the domains housing each variant was amplified by PCR and cloned into a range of bacterial expression vectors.

- *E. coli* was transformed with each vector and expression was induced with IPTG.
- The RyR1 domains were partially purified and shown to be soluble.

Chapter 2 Materials and methods

2.1 Materials

Commercially purchased kits or products are listed below. All laboratory chemicals used were research grade or equivalent.

- 2X HiFi hotstart ready mix, Kapa Biosystems, Wilmington, MA, USA
- 1 KB plus DNA ladder, Invitrogen, Auckland, New Zealand
- Various restriction endonuclease enzymes, New England Biolabs Inc, Ipswich, MA, USA
- Antarctic phosphatase, New England Biolabs, New England Biolabs Inc, Ipswich, MA, USA
- Zymoclean™ Gel DNA Recovery Kit, ZymoResearch, Irvine, CA, USA
- T4 DNA ligase, Roche, Mannheim, Germany
- HiPure plasmid isolation kit, Roche, Mannheim, Germany
- HiPure plasmid midiprep Kit, Roche, Mannheim, Germany
- T25 flasks, Nunc, Rokilde, Denmark
- Poly-D-lysine, Sigma Aldrich, Steinheim, Germany
- Dulbecco's Modified Eagle's Medium, Sigma Aldrich
- Fetal bovine serum, Gibco, Auckland, New Zealand
- Penicillin/Streptomycin, Gibco, Auckland, New Zealand
- cOmplete mini EDTA free protease inhibitor, Roche, Mannheim, Germany
- Primary and secondary antibodies for western blotting, Sigma Aldrich, Steinheim, Germany or Santa Cruz Biotechnology, Dallas, TX, U.S.A.
- BM Chemoiluminesence Blotting substrate, Roche, Mannheim, Germany
- 4 well plates, Thermofisher, Eugene, OR, USA
- FITC and TRITC conjugated secondary antibodies for immunostaining, Jackson Immuno Research, PA, USA
- ProLong Gold AntiFade mounting solution containing DAPI, Thermofisher, Eugene, OR, USA
- 96 well plates, Greiner Bio one, Frieckenhausen, Germany
- Pluronic acid, Sigma Aldrich, Steinheim, Germany

- 4-Chrolo-*m*-cresol, BDH Chemicals, Lutherworth, England
- Caffeine, Sigma Aldrich, Steinheim, Germany
- PWO polymerase, Roche, Steinheim, Germany
- OneStep™ PCR Inhibitor Removal Kit, ZymoResearch, Irvine, CA, USA
- Dialysis bags, scientific instrument center, Columbus, OH, USA
- Viva spin protein concentrators, GE Healthcare, Stockholm, Sweden
- Glutathione sepharose 4B, GE Healthcare, Stockholm, Sweden
- PreScission protease, GE Healthcare Life Science, Stockholm, Sweden
- Amylose conjugated magnetic resin, New England Biolabs, Ipswich, MA, USA
- Genenase, New England Biolabs, Ipswich, MA, USA
- Tyrpsin, Sigma Aldrich, Steinheim, Germany

2.2 Methods

2.2.1 Construction of *RYR1* variants and bacterial expression vectors

2.2.1.1 Site directed mutagenesis

Mutagenesis was carried out by PCR-amplification of ~70 ng of plasmid DNA containing approximately 2.7 kb of the relevant subclones of human *RYR1* cDNA (accession number NM_000540.2) using the 2x Kapa HiFi HotStart Readymix diluted 4 times. Complementary mutagenic primer pairs sourced from Integrated DNA Technologies (appendix I) were used for method based on the Stratagene QuikChange™ kit. Temperature cycling conditions were 95 °C for 5 min; 98 °C for two minutes; 57 °C for 30 seconds; 72 °C at 1 min/kb; 72 °C for five minutes; steps 2-3 were repeated 18 times. The PCR products were digested with 20 units of restriction endonuclease *Dpn*I according to the manufacturer's instructions.

2.2.1.2 Polymerase chain reaction (PCR)

PWO polymerase was used in conjunction with specific primers (appendix I) to amplify *RYR1* cDNA according to the manufacturer's instructions. Restriction

endonuclease sites were included in the primer sequence allowing for the amplified cDNA to be directionally cloned into bacterial expression vectors. Annealing temperatures were altered for specific primers. The temperature cycling conditions were as follows: 95 °C for five minutes; 95 °C for thirty seconds; 57-72 °C for fifteen seconds; 72 °C for one minute per 1000 base pairs; 72 °C for seven minutes. The denaturation, annealing and amplification steps were repeated 35 times. PCR products were analysed for size and purity by agarose gel electrophoresis using 1 x TAE buffer (4.84 g Tris, 1.14 mL glacial acetic acid, 2 mL 0.5 M EDTA, pH 8, final volume 1 L in purified water), a 2 % (w/v) gel was used to analyse PCR products expected to be smaller then 1000 bp a 1 % (w/v) gel was used to analyse PCR products expected to be larger then 1000 bp. Ethidium bromide (0.5 µg/mL) staining was used to visualise DNA using the Image Lab 5.1 software.

2.2.1.3 PCR product purification

The ZymoResearch, OneStep™ PCR Inhibitor Removal Kit was used to purify the PCR product according to the manufacturer's instructions. DNA was eluted into a final volume of 50 µL and stored at -20 °C.

2.2.1.4 DNA sequencing

Sanger sequencing using a capillary ABI3730 Genetic Analyzer with BigDye™ Terminator Version 3.1 chemistry was carried out at the Massey Genome Service, Palmerston North, New Zealand confirming the correct nucleotide sequence of plasmid DNA, or the introduction of specific nucleotide variations by site directed mutagenesis.

2.2.1.5 Restriction endonuclease digest

Restriction endonuclease digestion was used to prepare PCR products and vectors for cloning and the characterisation of plasmids. Reactions were prepared according to manufacturer's instructions in a final volume of 20 µL. The progression of each digestion was analysed by agarose gel electrophoresis using 1 X TAE the

percentage of agarose varied depending on the size of expected DNA fragments, 1 % (w/v) was used to analyse fragments larger then 1000 bp, 2 % (w/v) was used to analyse fragments smaller then 1000 bp. Ethidium bromide, 0.5 µg/mL, was used to visualise DNA using the Image Lab 5.1 software.

2.2.1.6 Antarctic phosphatase treatment of digested vectors

Digested vectors were treated with antarctic phosphatase according to manufacturer's instructions for one hour at 37 °C. The enzyme was heat inactivated at 75 °C for fifteen minutes.

2.2.1.7 Digestion product purification

The Zymoclean™ Gel DNA Recovery Kit was used following the manufacturer's protocol to purify vector and insert DNA after restriction endonuclease digestion and separation by agarose gel electrophoresis. The purified DNA was eluted into a final volume of 12 µL.

2.2.1.8 Ligation

T4 DNA ligase was used to ligate digested *RYR1* cDNA and PCR products into digested vectors following manufacturer's instructions. A vector to insert molar ratio of 1:3 was used. The reaction mixes were incubated 18 °C for 3 hours or over night at 16 °C in a final volume of 10 µL.

2.2.1.9 Competent *E. coli* cells

Single DH5α, BL21(DE3), BL21(DE3) Gro ES/EL and Rosetta (DE3) colonies were picked from LB plates and used to inoculate 5 mL LB broths and grown over night at 37 °C with constant shaking. In the case of BL21(DE3) Gro ES/EL and Rosetta (DE3) broths contained 33 µg/mL chloramphenicol. One mL of this culture was used as a starting culture to inoculate a 100 mL LB broth; again broths used to grow BL21(DE3) Gro ES/EL and Rosetta (DE3) contained 33 µg/mL chloramphenicol. The

culture was incubated at 37 °C with constant shaking until reaching an $O.D_{600}$ of 0.8. Cells were harvested by centrifugation at 6000 x g at 4 °C for ten minutes and suspended in 5 mL 0.1 M $CaCl_2$ at 4 °C. Cells were centrifuged at 6000 x g for ten minutes and suspended in 3.4 mL 0.1 M $CaCl_2$ at 4 °C and incubated over night at 4 °C. Fifty percent glycerol (0.6 mL) was added to the cells, mixed well and the resulting mix was divided into 50 µL aliquots and stored at -80 °C.

2.2.1.10 Transformation of competent *E. coli* strains

Competent cells were thawed on ice prior to the addition of a ligation mixture or 10 ng of plasmid DNA; the cells were then incubated on ice for twenty minutes. Cells were heat shocked at 42 °C for ninety seconds and incubated on ice for five minutes. DH5α cells were diluted with 900 µL LB broth and incubated at 37 °C for ninety minutes cells were then plated onto LB plates containing 100 µg/mL ampicillin. BL21 (DE3) were plated directly onto LB plates supplemented with ampicillin at 100 µg/mL. BL21 (DE3) Gro ES/EL Rosetta (DE3) cells were plated directly onto LB plates containing 100 µg/mL ampicillin and 7 µg/mL chloramphenicol. The genetic modification of *E.coli*, was approved by the Environmental Risk Management Authority, under the approval code GMO11/MU003.

2.2.1.11 Alkaline lysis plasmid isolation

Single DH5α colonies were picked from LB plates and used to inoculate LB broths containing 100 µg/mL ampicillin. Broths were incubated over night at 37 °C with constant shaking. Two mL of the resulting culture was harvested by centrifugation at 13,000 x g and resuspended in 100 µL suspension buffer (25 mM Tris HCl pH 8 50 mM glucose, 10 mM EDTA). Two hundred µL lysis buffer (0.2 M NaOH, 1% SDS) was added and incubated at room temperature for three minutes before the addition of 150 µL precipitation buffer (5 M potassium acetate 60 mL, 11.5 mL glacial acetic acid, sterile water to a final volume of 100 mL). Soluble and insoluble fractions were separated by centrifugation at 13,000 x g for ten minutes. Nine hundred µL 100 % ethanol was added to the resulting liquid phase and centrifuged at 13,000 x g for 10 minutes. The soluble and insoluble fractions were separated the resulting insoluble

fraction was washed in 1 mL 70 % ethanol and centrifuged at 13,000 x g for ten minutes. The supernatant was removed and the insoluble DNA containing fraction was allowed to air dry at room temperature. DNA was then suspended in 50 µL TE (10 mM Tris HCl, 1 mM EDTA).

2.2.1.12 Isolation of plasmid DNA: small scale

The Invitrogen HiPure plasmid isolation kit, based on the alkaline lysis method, was used to purify high quality DNA from DH5α cells. The kit was used following manufacturer's instructions. DNA was eluted into a final volume of 50 µL.

2.2.1.13 Isolation of plasmid DNA: medium scale

For the purification of larger quantities of plasmid DNA the Invitrogen Pure link HiPure plasmid midiprep Kit based was used. The protocol was followed per the manufacturer's instructions. *E. coli* cultures were grown in 50 mL LB and harvested by centrifugation at 7000 x g at 4 °C for ten minutes. Purified DNA was dissolved in 150 µL TE.

2.2.2 HEK293T cells

2.2.2.1 Cryo storage of HEK293T cells

HEK293T cells grown to 90 % confluence in a T25 flask were washed off the bottom of the flask using foetal bovine serum and collected by centrifugation at 200 x g for 5 minutes. The pellet was resuspended in 1 mL FBS containing 10 % DMSO and was then dispensed into cryo tubes which were slowly cooled down to - 80 °C.

2.2.2.2 Reanimation of HEK293T cells

HEK293T cells stored at -80 °C were quickly thawed to 37 °C, and resuspended in 5 mL complete DMEM (Dulbecco's Modified Eagle's Medium, 10 % fetal bovine serum, 0.5% penicillin/streptomycin). Cells were harvested by centrifugation at 200 x g and

were resuspended in 5 mL complete DMEM, cells were grown at 37 °C, 5 % CO_2 in a humidified atmosphere in a T25 flask placed horizontally.

2.2.2.3 Passaging of HEK293T cells

Upon reaching 90 % confluence, measured by an inverted optical microscope, HEK293T cells were washed from the bottom of the T25 flask. Half a mL of the resulting cell suspension was used to seed a new T25 flask, 7.5 mL of fresh complete DMEM was added to the flask and was incubated, placed horizontally, at 37 °C, 5 % CO_2 in a humidified atmosphere.

2.2.2.4 Coating of tissue culture plastic

Poly-D-lysine was suspended in water to a final concentration of 0.01 % (w/v). Tissue culture plastic ware used for Ca^{2+} release assays and immunofluorescence were coated by the addition of 0.01 % poly-D-lysine and incubated for one hour under the exposure of UV light to sterilise the plates. Poly-D-Lysine was removed and the plates were stored at 4 °C in plastic wrap until use.

2.2.2.5 Cell culture and transfection

HEK293T cells for all applications were grown in complete DMEM at 37 °C, 5 % CO_2 in a humidified atmosphere. For immunoblotting cell were grown to 90 % confluence in a T25 flask in 8 mL of media. For immunofluorescence cells were grown to 50 % confluence in a four chamber slide in 1 mL media. For Ca^{2+} release assays cells were grown to 80 % confluence in UV transparent 96 well plates in 200 µL media. Media was replaced one hour prior to transfection once the correct level of confluence was achieved. The genetic modification of HEK293t cells was approved by the Environmental Risk Management Authority under the approval number GMO11/MU003.

For immunoblotting HEK293T cells were transiently transfected with *RYR1* cDNA or empty pcDNA3.1+ plasmids using 6 µg DNA, 24 µL fugene HD, non supplemented DMEM to final volume of 300 µL. Which was added directly to the 8 mL medium in

T25 flasks. After forty-eight hours the medium was replaced and growth was continued for a further twenty-four hours. Protein was extracted from transiently transfected HEK293T cells after washing the cells in PBS (0.14 M NaCl, 2.7 mM KCl, 10 mM Na_2HPO_4, 1.8 mM KH_2PO_4 pH 7.2) and resuspending the cells in 150 µL of lysis buffer (0.1M Tris HCl, pH 7.8, 0.5% triton X-100, 20 µL 7x cOmplete Mini EDTA-free protease inhibitor). Insoluble proteins were separated via centrifugation at 13,000 x g at 4 °C. Supernatant was stored at -80 ^oC with limited freeze-thaw cycles.

For immunofluorescence HEK293T cells were transiently transfected with *RYR1* cDNA or empty pcDNA3.1+ plasmids using 1 µg DNA, 3 µL Fugene 6 and non supplemented DMEM to a final volume of 50 µL. Fresh medium was replaced after forty-eighty hours and cells were incubated for a further twenty-four hours prior to processing.

For Ca^{2+} release assays, HEK293T, in 100 µL complete DMEM per well, were transiently transfected with *RYR1* cDNA or empty pcDNA3.1+ plasmids using 100 ng DNA, 1.2 µL Fugene HD in non supplemented DMEM to a final volume of 14 µL. cells were incubated for twenty-four hours before the addition of 100 µL complete DMEM to each well. Cells were incubated for a further twenty-four hours before the medium was replaced with 200 µL fresh complete DMEM. After a further twenty-four hour incubation the transfected cells were used in calcium release assays.

2.2.2.6 SDS-PAGE

Protein extracts were resolved using either 7 % or 12.5 % polyacrylamide gels, depending on the size of the protein of interest. Seven % resolving gels were used for proteins greater then 90 kDa, 12.5 % resolving gels were used for proteins less then 90 kDa. Gels were prepared using BioRad mini protein gel casting system using the following components

	7 % resolving gel	4 % stacking gel	12.5 % resolving gel	6 % stacking gel
Water	5.5 mL	3.15 mL	3.3 mL	2.9 mL
Tris (1.5 M pH, 8.8)	2.5 mL		3.5 mL	
Tris (0.5 M, pH 6.8		1.2 mL		1.2 mL
10 % SDS	100 µL	50 µL	80 µL	50 µL
10 % APS	100 µL	50 µL	50 µL	50 µL
TEMED	10 µL	5 µL	5 µL	5 µL

Table 1.1 List of components used for either 7 % or 12.5 % SDS-PAGE.

After electrophoresis gels were either subjected to immunoblotting or stained for fifteen minutes with Coomassie-blue (0.1 % (w/v) Coomassie blue-R250, 45 % methanol, 10 % glacial acetic acid) and destained in 10 % methanol, 10 % glacial acetic acid.

2.2.2.7 Immunoblotting

Protein extracts from transiently transfected HEK293T cells (~270 µg), *E. coli* cell extracts (~30 µg) or purified RyR1 recombinant RyR1 protein (~0.1 µg) were incubated with 5 x protein loading dye (60 mM Tris HCl, pH 6.8, 25 % glycerol (v/v), 2% SDS (w/v), 14.4 mM β-mercapoethanol, 0.1 % bromophenol blue (w/v)) for ten minutes. Protein concentrations were measured using the Bradford dye binding method (98). Protein samples were loaded onto an SDS-PAGE gel and electrophoresis was carried out at 120 mV for either two hours (7.5 % gel) or one hour thirty minutes (12 % gel). The gel was soaked in transfer buffer (15.6 mM Tris HCl, 0.12 M glycine containing 10 % methanol) and was transferred to a PVDF membrane, pre charged by soaking in methanol, at 70 mA for twenty hours at 4 °C for full-length RyR1 or one hour thirty minutes at room temperature for other proteins. The membrane was blocked with 5 mL 5 % skim milk (w/v) in TBST (0.05 M Tris HCl, 0.15 mM NaCl, 0.1 % tween 20) for three hours with gentle agitation at room temperature. The membrane was then incubated in 5 mL primary antibody diluted in 2.5 % skim milk in TBST (34C (Sigma, R129) diluted 1:1000, anti-tubulin

(Sigma, T8203) diluted 1:5000, anti GST (Sigma, G7781) diluted 1:5000 or H21 (Santa Cruz biotechnology, Sc-34019) diluted 1:20,000) with constant gentle shaking either overnight at 4 °C for 34C, anti-tubulin and H21 antibodies, or at room temperature for one hour for anti GST. The membrane was washed in 10 mL TBST three times for ten minutes each. The membrane was incubated in 5 mL horse radish peroxidase conjugated secondary antibody diluted in 2.5 % skim milk in TBST (anti mouse 1:5000 (Sigma, A9044), anti goat (Sigma, A5420) or anti rabbit 1:5000 (Sigma, A0545) at room temperature for one hour before three ten minute washes in 10 mL TBST. Chemiluminescence blotting substrate was prepared by mixing 3 mL Luminescence substrate solution A with 30 µL starting solution B. The substrate was applied to the membranes prior to visualisation of the proteins by the exposure to X-ray film.

2.2.2.8 Immunofluorescence

After a seventy-two hour transfection cells were washed with 500 µL PBS (0.14 M NaCl, 2.7 mM KCl, 10 mM Na_2HPO_4, 1.8 mM KH_2PO_4 pH 7.2); fixed in 500 µL 2 % paraformaldehyde in PBS for fifteen minutes at room temperature and washed three times in PBS then permeabilised in 0.1 % triton X-100 in PBS for five minutes. After three washes in PBS, the cells were blocked in 1 mL 5 % bovine serum albumin, 0.5 % Tween-20 in PBS with gentle shaking at room temperature for five minutes then incubated overnight at 4 °C with gentle shaking in 1 mL primary anti body solution (mouse 34C diluted 1:1000 and rabbit anti protein disulphide isomerase (Sigma, p7496) diluted 1:1000 in PBS). The cells were then incubated at room temperature for twenty minutes, and washed three times in 1 mL PBS. The cells were then incubated at room temperature in 500 µL secondary antibody solution (fluorescein isothiocyanate, FITC conjugated goat anti mouse secondary antibody diluted 1:200 (Jackson immuno research, 15095003), tetramethylrhodamine, TRITC, conjugated goat anti rabbit secondary antibody (Jackson immuno research, 11025003) diluted 1:200 in PBS), followed by three washes in 1 mL PBS. A cover slip was mounted using 7 µL ProLong Gold AntiFade mounting solution containing DAPI to stain the nucleus. The cells were incubated over night before being visualised using a Leica

SP5 DM6000B Scanning Confocal Microscope at 1260 X magnification at the Manawatu Microscopy and Imaging Centre.

2.2.2.9 Measurement of Ca^{2+} release

Following the seventy-two hour transfection, cells were washed once in 100 µL balanced salt solution, BSS, containing 2 mM Ca^{2+} buffer (140 mM NaCl, 2.8 mM KCl, 1 mM $MgCl_2$, 10 mM glucose, 10 mM HEPES, pH 7.25). One hundred µL BSS containing 2 mM Ca^{2+} and 2 µM fura 2-AM and 0.01 % pluronic acid was added to each well and incubated for one hour at 37 °C in darkness. The cells were washed once in 100 µL BSS containing 2 mM $CaCl_2$ and once in BSS containing 2 mM EGTA. One hundred µL BSS containing 2 mM EGTA was added to each well. All fluorescence measurements were made using an Olympus IX81 fluorescence microscope measuring emission 510 nm with excitation at 340 nm and 380 nm using a wavelength switch. A fluorescence ratio baseline was established before the addition of 100 µL ryanodine receptor agonist, either 4-C*m*C or caffeine dissolved in BSS containing 2 mM EGTA. The final concentrations used were 4-C*m*C: 200, 300, 400, 600, 800 and 1000 µM, caffeine: 0.5, 2, 4, 6, 8, 10 and 15 mM.

2.2.2.10 Statistical analysis

The amount of Ca^{2+} released for each agonist concentration was normalised to account for differences in cell density between each assay and represented as a percentage of the total Ca^{2+} released from either 1000 µM 4-C*m*C or 15 mM caffeine. A minimum of 8 biological replicates were carried out for each ryanodine receptor construct, the results were pooled and were represented as mean ± standard error of the mean (SEM) for each concentration of agonist used. Sigmoidal curves were plotted using OriginLab Origin 8 software. The agonist concentration required for half maximal fluorescence change, EC_{50}, was calculated for individual curves from each assay and represented as mean ± SEM. The Student's unpaired T-test with Bonferoni correction was used to determine the statistical significance of each EC_{50} value in the form of a p-value with each variant being compared to wild type.

2.2.3 Protein expression and purification from *E. coli*

2.2.3.1 Protein expression in *E. coli*

A single colony of either BL21(DE3), BL21 (DE3) GroES/EL or Rosetta (DE3) transformed with an expression vector was picked from an LB plate containing 100 µg/mL ampicillin; in addition, LB plates used to grow BL21 (DE3) GroES/EL or Rosetta (DE3) also contained 7 µg/mL chloramphenicol. Cells were grown in LB broths containing appropriate antibiotics, 100 µg/mL ampicillin, BL21(DE3), 100 µg/mL ampicillin, 33 µg/mL chloramphenicol, BL21(DE3) GroES/EL and Rosetta (DE3). Cells were incubated at 37 °C with shaking until reaching an $O.D_{600}$ of 0.6. Cell cultures were placed on ice for fifteen minutes and ethanol was added to the culture to a final concentration of 2 %. Cells were incubated at 18 °C with shaking for twenty minutes prior to the induction of expression by the addition of 0.1 mM IPTG. Cells were incubated with shaking for 3 hours at 18 °C and then harvested by centrifugation at 6000 x g at 4 °C for ten minutes. Cell pellets were frozen at -20 °C for further use.

2.2.3.2 Protein extraction from BL21(DE3)

A BL21(DE3) pellet (50 mL culture volume) was suspended in 1 mL sonication buffer (140 mM NaCl, 2.8 mM KCl, 1 mM $MgCl_2$, 2 mM EGTA, 10 mM glucose, 10 mM HEPES, pH 7.25, 1 mM DTT, 1 mM EDTA, 1X cOmplete Mini EDTA-free protease inhibitor). Sonication was carried out at 10 kHz three times for ten seconds. Insoluble proteins were separated by centrifugation at 13,000 x g for fifteen minutes at 4 °C. Soluble and insoluble fractions were resolved by SDS-PAGE and visualised with Coomassie blue stain

2.2.3.3 *In vitro* refolding

Single BL21(DE3) colonies, transformed with an expression vector, were picked from an LB plate and grown over night at 37 °C with shaking in a 5 mL LB broth containing with 100 µg/mL ampicillin. Two mL of the resulting culture was used as a starter culture to initiate growth in 1 L LB broths containing 100 µg/mL ampicillin.

Cells were grown at 37 °C with shaking to an $O.D_{600}$ of 0.6 and expression was induced by the addition of 0.1 mM IPTG, followed by incubation with shaking for sixteen hours at 30 °C. Cells were harvested by centrifugation at 6000 x g for ten minutes at 4 °C and suspended in 40 mL lysis buffer (50 mM tris HCl pH 8, 150 mM NaCl, 5 mM tris (2-carboxyethyl)phosphine hydrochloride)). Cells were lysed by being passed through a French press three times at 5000psi. Insoluble proteins were separated by centrifugation at 13,000 x g for fifteen minutes at 4 °C. Insoluble proteins were washed in the following buffers: wash buffer 1 (50 mM Tris HCl pH 8.5, 150 mM NaCl, 2 % Triton X-100), wash buffer 2 (50 mM Tris HCl pH 8.5, 150 mM NaCl, 2 mM 3-((3-cholamidopropyl) dimethylammonio)-1-propanesulfonate)), wash buffer 3 (50 mM Tris HCl pH 8.5, 2 M NaCl). Following each wash step insoluble proteins were separated via centrifugation at 16,000 x g, the pellet was then resuspended in the subsequent buffer. Insoluble proteins following wash in buffer 3 were suspended in solublisation buffer, (50 mM Tris HCl pH 9, 150 mM NaCl, 10 mM β mercapoethanol and 6 M guanidine hydrochloride). Refolding was performed using dialysis at room temperature for five hours in refolding buffer (50 mM Tris HCl pH 8.5, 50 mM KCl, 5 mM β mercapoethanol). Soluble protein was then concentrated using viva spin 2 protein concentrator with a molecular weight cut off of 15,000 kDa as per manufacturer's instructions.

2.2.3.4 Batch purification of protein expressed from the pGEX6p3 vector using glutathione sepharose 4B

After the expression of the pGEX6p3 vector containing *RYR1* cDNA in a 50 mL culture volume, BL21(DE3) cells were lysed by sonication at 10 kHz for ten seconds. Soluble proteins were incubated with 50 µL glutathione sepharose 4B at room temperature for thirty minutes according to manufacturer's instructions. Glutathione sepharose 4B was separated from non bound proteins by centrifugation at 2,500 x g for five minutes at 4 °C. The resin was then washed with 1 mL column buffer (0.14 M NaCl, 2.7 mM KCl, 10 mM Na_2HPO_4, 1.8 mM KH_2PO_4 pH 7.2). Protein was eluted from the glutathione sepharose by three washes of 25 µL elution buffer (50 mM Tris HCl, 10 mM reduced glutathione, pH 8.0). Each wash was kept for further analysis by SDS-PAGE.

2.2.3.5 PreScission protease digestion

Following the expression of the pGEX 6p3 vector in 50 mL culture volumes. BL21(DE3) cells were lysed by sonication at 10 kHz for ten seconds and soluble protein was incubated with 50 µL glutathione sepharose 4B for thirty minutes per the manufacturer's instructions. Glutathione sepharose 4B was separated from non bound proteins by centrifugation at 2,500 x g for five minutes at 4 °C. The glutathione sepharose 4B was washed with 1 mL column buffer, followed by 1 mL high ionic strength buffer (50 mM Tris HCl, 500 mM NaCl, 1 mM EDTA, 1 mM DTT, pH 7.0), then washed in 1 mL PreScission protease buffer (50 mM Tris HCl, 150 mM NaCl, 1 mM EDTA, 1 mM DTT, pH 7.0). The glutathione sepharose 4B was suspended in 50 µL PreScission protease buffer containing 2 units PreScission protease and incubated at 4 °C for sixteen hours with constant end over end rotation. The glutathione sepharose 4B was separated from the buffer solution by centrifugation at 2,500 x g for five minutes, the supernatant was centrifuged at 70,000 x g for fifteen minutes and kept for further analysis by SDS-PAGE. The glutathione sepharose 4B was washed with 1 mL protease buffer then suspended in 50 µL 5 x protein loading dye and centrifuged at 2,500 x g for five minutes, the resulting liquid phase was kept for analysis by SDS-PAGE.

2.2.3.6 Batch purification of protein expressed from the pMALp2g vector using an amylose conjugated magnetic resin

Following expression of the pMALp2g vector containing *RYR1* cDNA in 50 mL culture volumes, BL21(DE3) cells were lysed by sonication at 10 kHz for ten seconds. Soluble proteins were incubated at 4 °C with 200 µL amylose magnetic resin following the manufacturer's instructions for thirty minutes. A magnet was used to separate the resin from the supernatant. The resin was washed in 4 mL column buffer (20 mM Tris HCl pH 7.4 200 mM NaCl, 1 mM EDTA, 1 mM DTT), then washed in 4 mL high ionic strength buffer (20 mM Tris HCl pH 7.4, 500 mM NaCl, 1mM EDTA, 1 mM DTT), then washed in 4 mL column buffer. Proteins bound to the resin were eluted by three, 200 µL, washes in elution buffer (20 mM Tris HCl pH 7.4, 200

mM NaCl, 1 mM EDTA, 1 mM DTT). The resulting washes were kept for further analysis by SDS-PAGE.

2.2.3.7 Genenase digestion of protein expressed from the pMALp2g vector after elution from the amylose resin

The pMALp2g containing *RYR1* cDNA was expressed in a 50 mL culture volume. BL21(DE3) cells were lysed by sonication at 10 % for ten seconds and soluble proteins were incubated with 200 µL amylose resin for thirty minutes at 4 °C. A magnet was used to separate the resin from the supernatant. The resin was washed in 4 mL column buffer, then washed in 4 mL in high ionic strength buffer, followed by a wash in 4 mL Genenase digestion buffer (20 mM Tris HCl pH 8.0, 200 mM NaCl). Protein was eluted from the resin by three washes with 100 µL of a modified elution buffer (20 mM Tris HCl pH 8.0, 200 mM NaCl, 10 mM maltose). Genenase was added to the resulting eluates in a ratio of 1 unit per 20 µL and incubated at 25 °C for eight hours. Following digestion, the reaction mix was centrifuged at 70,000 x g for fifteen minutes the resulting supernatant was analysed by SDS-PAGE.

2.2.3.8 Genenase digestion of protein expressed from the pMALp2g vector bound to the amylose resin

Following expression of the pMALp2g vector in a 50 mL culture volume, BL21 (DE3) cells were lysed by sonication at 10 kHz for ten seconds. Soluble protein was incubated with 200 µL amylose resin at 4 °C for thirty minutes according to the manufacturer's instructions. A magnet was used to separate the resin from the supernatant. The resin was washed in 4 mL column buffer, followed by a wash in 4 mL high ionic strength buffer, then washed in 4 mL genenase digestion buffer. The resin was suspended in 100 µL genenase digestion buffer containing 2.5 units of genenase and incubated at 25 °C at room temperature for 8 hours with gentle end over end rotation. The resin was separated from the supernatant using a magnet. The supernatant was centrifuged 70,000 x g and kept for analysis by SDS-PAGE. The resin was washed in 4 mL genenase digestion buffer and suspended in 200 µL

protein loading dye the resin was separated from the supernatant using a magnet, the resulting liquid phase was kept for analysis for by SDS-PAGE.

2.2.3.9 Mass spectrometry

Protein samples were separated by SDS-PAGE. The gel was incubated in fixative solution (10 % acetic acid, 40 % methanol) for one hour at room temperature then washed three times in milli Q water. The gel was stained overnight in colloidal Coomassie blue (75.6 mM ammonium sulphate, 2 mL 5 % Coomassie G250, 1.2 mL phosphoric acid, water to a final volume 100 mL) diluted in methanol in a 4:1 ratio and destained in water at 60 °C. Bands thought to correspond to the ryanodine receptor were excised from the gel. All stain was removed by three, twenty minute washes in 50 mM ammonium bicarbonate (ABC) at 37 °C with a final wash in 80 % acetonitrile (ACN). The supernatant was removed and the gel pieces were dried in centrifugal evaporator. The protein in the gel pieces was reduced by incubation in 10 mM DTT in 50 mM ABC for 1 hour at 37 °C. The gel pieces were washed three times in 50 mM ABC and once in 80 % ACN and dried in a centrifugal evaporator. The protein in the gel pieces was alkylated by incubation in 0.5 mM iodoacetamide in 50 mM ABC for one hour in the dark. The gel pieces were washed three times in 50 mM ABC and once in 80 % ACN and dried in a centrifugal evaporator. The gel pieces were rehydrated in trypsin solution (15 ng/µL trypsin in 50mM ABC) and incubated over night at 37 °C in the dark. The supernatant was removed and protein was eluted from the gel by the addition of 60 µL 60 % ACN, 0.1 % formic acid. The gel pieces were sonicated in a water bath for one minute. The supernatant was removed and kept. The gel pieces were suspended in the 100 % ACN then sonicated in a water bath eluting all protein remaining in the gel. The two eluted fractions were pooled and reduced to a final volume of 20 µL in a centrifugal evaporator samples were stored at -80 °C until analysis could be performed.

The mass spectroscopic analysis was performed by Trevor Loo, IFS Massey University or Dianna Carne, Centre for Protein Research Otago University.

Chapter 3 Functional characterisation of the RyR1 MH-linked variants p.T214M and p.ΔE2348

3.1 Introduction

Two nucleotide variants of *RYR1* have been linked to malignant hyperthermia; c.641C>T and c.7042_7044delCAG. Both variants have been found in families in New Zealand and around the world known to display MH symptoms (96, 97). In one case a proband was shown to have both variants, one inherited from their mother and the other inherited from their father.

As MH is a life threatening disorder, it is advantageous to determine a patient's susceptibility prior to undergoing general anaesthesia, particularly in individuals with a known family history, allowing non triggering agents to be used if need be. In New Zealand the *in vitro* contracture test is the gold standard to diagnose MH (1). DNA based diagnostic tests have been established for some disease-linked variants and are becoming more accepted as an alternative to the IVCT (66, 67). An MH diagnosis by DNA testing is limited, in that only an MHS diagnosis can be made with respect to known MH-causing nucleotide variants and a true MHN diagnosis can only be made by undergoing an IVCT. The current objective in MH based research is to establish a comprehensive library of known MH causing nucleotide variants, adding breadth to the DNA based diagnostic tests limiting the need for the invasive IVCT test. One key criterion for the acceptance of a DNA test for diagnostic purposes is that the specific variant must be functionally characterised. To do so variants are expressed in controlled cellular environments where alterations to calcium release from the SR can be analysed.

HEK 293T cells do not express a functional ryanodine receptor to any measurable level; making them a useful cell line for the expression and functional analysis of *RYR1* variants. A well defined system for the transfection and expression of *RYR1* variants in HEK293T has been previously established (99). Following expression of RyR1 cells are loaded with the Ca^{2+}-sensitive fluorescent indicator, fura 2-AM, and exposed incremental doses of the RyR1 agonist 4-C*m*C. Any alterations to the release of Ca^{2+} compared to a wild type control can be attributed to the RyR1 variant

and by extrapolation the variant can be classed as being MH-causative. HEK293T cells are a non-excitable, non-contractile cell line and as a result do not express a number of proteins involved in the EC coupling process. The onset of MH resulting from the loss of regulatory protein interactions with RyR1 or alteration of response to excitation cannot be explored in this system and as a result the variant may display a similar phenotype to wild type expressing cells.

3.2 Preparation of *RYR1* variant cDNA

The aim of this study was to compare the activity of RyR1 variants in response to the RyR1 agonists 4-C*m*C and caffeine to wild type RyR1 under the same conditions. To do so the MH-linked *RYR1* variants c.641C>T and c.7042_7044delCAG were introduced into the full-length *RYR1* cDNA which was then used to express the RyR1 variants p.T214M and p.ΔE2348 respectively in HEK293T cells. The *RYR1* cDNA and amino acid sequences in this chapter refer to the gene bank accession numbers NM_000540.2 and NP_000531.2 respectively.

3.2.1 Site directed mutagenesis

As the cDNA of *RYR1* is over 15 kb in length site directed mutagenesis cannot be accurately performed on the cDNA in its entirety. A subclone of *RYR1*, corresponding to nucleotides 1-2700 cloned into the pBluescipt II KS+ vector, pBSXC+ (appendix II), was used as a template for mutagenesis. Specific primers were used to introduce the c.641C>T variant. Following propagation of the vector in *E. coli* DH5α, the vector was purified and the presence of the variant was confirmed by Sanger sequencing (figure 3.1). The MH-linked *RYR1* variant c.7042_7044delCAG was been previously introduced into full-length *RYR1* by Cornelia Roesl (100).

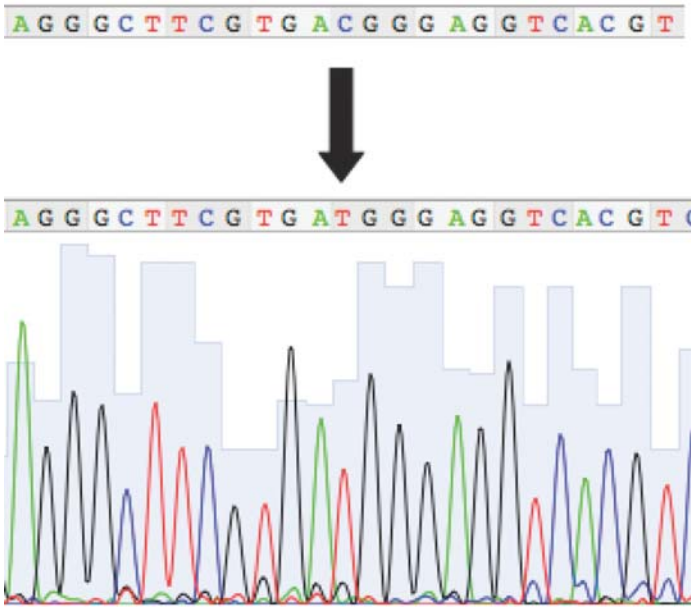

Figure 3.1 Sanger sequencing confirming the introduction of c.641C>T into the pBSXC+ vector. The wild type sequence has been represented at the top of the figure. The induced c.641C>T variant is highlighted by the arrow.

A three step cloning strategy was followed to introduce the c.641C>T variant into full-length *RYR1*. The cloning process utilised has been represented in figure 3.2. Firstly, the *RYR1* nucleotides 1-2502 containing the c.641C>T variant were introduced into the vector pBSXK, containing the *RYR1* nucleotides 1-6952. The resulting pBSXK c.641C>T vector was digested with the restriction endonucleases *Xba*I and *Kpn*I, liberating the *RYR1* cDNA. The mammalian expression vector pcDNA3.1+ was digested with *Nhe*I and *Kpn*I and the complementary overhang created following digestion with both *Xba*I and *Nhe*I was exploited to introduce the *RYR1* cDNA into the pcDNA3.1+ vector producing the vector pcNK c.641C>T. The *RYR1* C-terminal nucleotides 6953-15,261 corresponding to either wild type or the c.7042_7044delCAG variant were introduced into the the pcNK c.641C>T vector, producing pc*RYR1* c.641C>T or c.641C>T/7042_7044delCAG vectors.

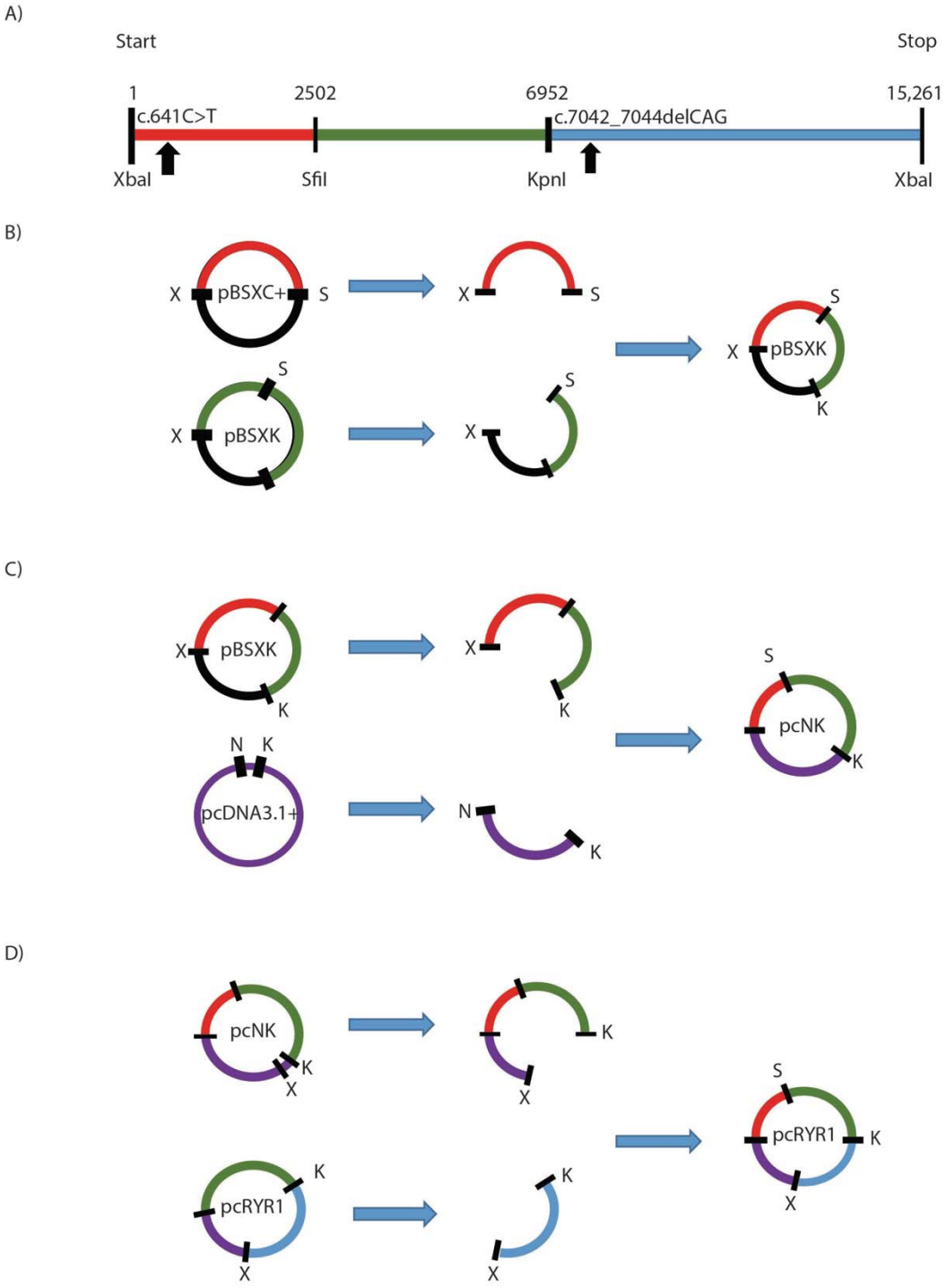

Figure 3.2 Representation of the cloning strategy used to construct the pc*RYR1* c.641C>T and pc*RYR1* c.641C>T/7042_7044delCAG vectors. A) *RYR1* cDNA, the position of the specific restriction endonuclease recognition sites within the *RYR1* cDNA exploited during the cloning process have been indicated by nucleotide number. The position of the 641C>T and 7042_7044delCAG variants have been highlighted by the black arrows. The *RYR1* cDNA corresponding to each vector used during the sub-cloning process is indicated by colour: pBSXC+ red, pBSXK red and green, pc*RYR1* red, green and blue. B) The cloning process used to construct the pBSXK c.641C>T vector.

The pBluescript II KS+ vector DNA has been represented in black. The restriction endonucleases *Xba*I, *Sfi*I and *Kpn*I have been represented by the letter X, S and K respectively. C) The cloning process used to construct the pcNK c.641C>T vector, the pcDNA3.1+ vector has been represented in purple, the restriction endonuclease *Nhe*I has been represented by the letter N. D) The cloning process used to produce the c.641C>T and c.641C>T/7042_7044delCAG pc*RYR1* vectors.

3.2.2 Confirming the identity of pBSXK 641C>T vector

The construction of the the vector pBSXK 641C>T was confirmed by restriction endonuclease digestion with the enzymes *Xho*I, *Kpn*I and *Sfi*I (figure 3.3).

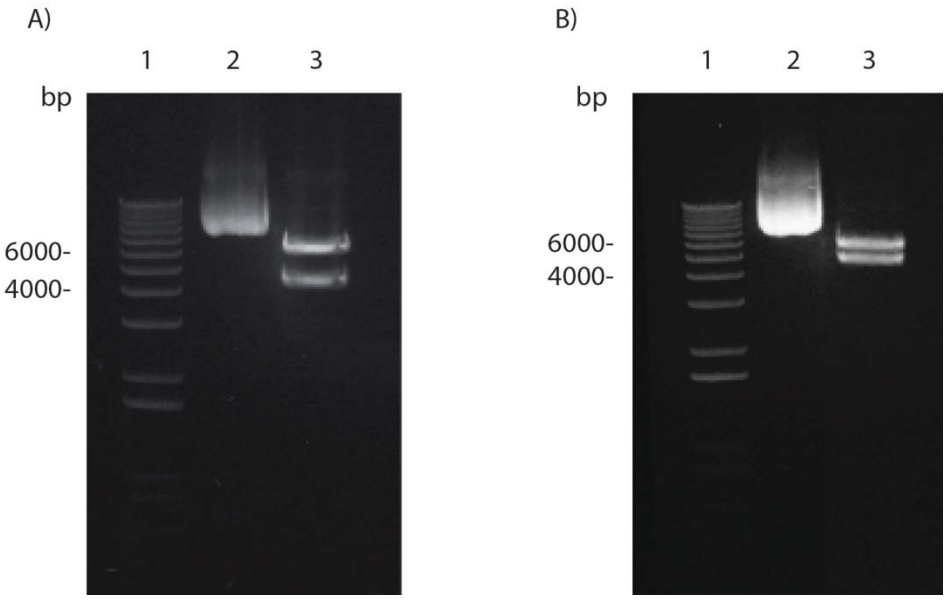

Figure 3.3 Restriction endonuclease digestion to confirm the identity of the pBSXK 641C>T vector. A) digest with the *Xho*I enzyme. Lane 1, 1 kb plus size marker. Lane 2, undigested pBSXK 641C>T vector. Lane 3 pBSXK 641C>T digested with *Xho*I. B) Lane 1, 1 kb plus size marker. Lane 2, undigested pBSXK 641C>T vector. Lane 3 pBSXK 641C>T digested with *Kpn*I and *Sfi*I. DNA was resolved by 1 % (w/v) agarose gel electrophoresis using 1 X TAE at 90 mV for one hour and visualised by 0.5 µg/mL ethidium bromide staining using the Image Lab 5.1 software.

Following digestion with the restriction endonuclease Xho I two fragments of the expected lengths, 4,019 and 5,816 base pairs were detected (figure 3.3). A second digest with the restriction endonucleases *Sfi*I and *Kpn*I rendered two bands of the expected sizes of 4,452 and 5,383. Sanger sequencing was used to confirm the presence of the 641C>T variant.

3.2.3 Confirming the identity of pcNK 641C<T

The identity of the pcNK 641C<T vector was confirmed by restriction endonuclease digestion by the enzymes *Nhe*I, *Kpn*I and *Xho*I.

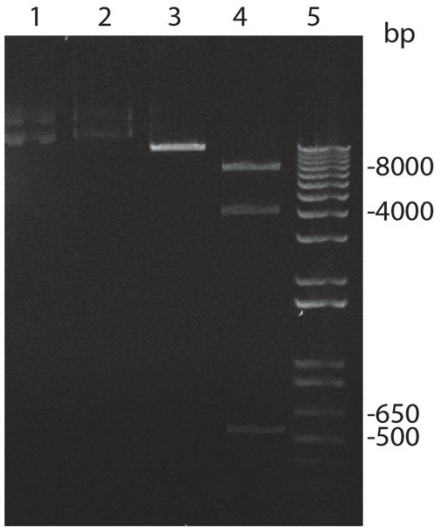

Figure 3.4 Restriction endonuclease digestion to confirm the identity of the pcNK c.641C>T vector. A) Lane 1, undigested pcNK c.642C>T. lane 2, pcNK c.641C>T digested with *Nhe*I. Lane 3, pcNK c.641C>T digested with *Kpn*I. Lane 4, pcNK digested with *Xho*I. Lane 5, 1 kb plus size marker. DNA was resolved by 1 % (w/v) agarose gel electrophoresis in 1 X TAE at 90 mV for one hour and visualised by 0.5 µg/mL ethidium bromide staining using the Image Lab 5.1 software.

The digestion of the pcNK c.641C>T with the restriction enzyme *Xho*I rendered three fragments of the expected sizes 552, 4019 and 7790 base pairs (figure 3.4). When digested with *Kpn*I a single band of 12,000 was noted. No digestion was detected when the digest was performed with *Nhe*I. During the construction of the pcNK vector the *Nhe*I restriction site within the pcDNA3.1+ was abolished so no digestion was expected. Sanger sequencing was used to confirm the presence of the 641C>T variant.

3.2.4 Confirming the identity of the pc*RYR1* 641C<T, pc*RYR1* 641C<T/7042_7044delCAG and pc*RYR1* 7042_7044delCAG

The identity of the pc*RYR1* variants was confirmed by digestion with the restriction endonuclease *Eco*RV (figure 3.5).

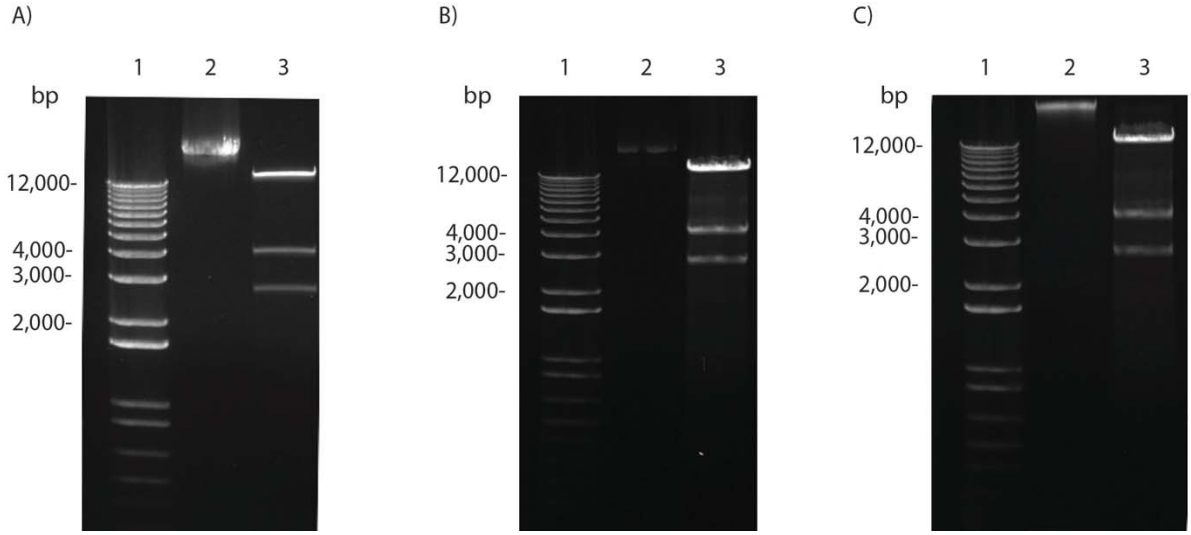

Figure 3.5 Restriction endonuclease digestion to confirming the identity of pc*RYR1* vectors. Lane 1, 1 kb plus size marker. Lane 2) non digested pc*RYR1* vector. Lane 3, pc*RYR1* digested with *Eco*RV. A) Confirming the identity of pc*RYR1* c.641C>T. B) Confirming the identity of pc*RYR1* c.641C>T / 7042_7044delCAG. C) Confirming the identity of pc*RYR1* 7042_7044delCAG. DNA was resolved by 1 % (w/v) agarose gel electrophoresis in 1 X TAE at 90 mV for one hour and visualised by 0.5 µg/mL ethidium bromide staining using the Image Lab 5.1 software.

Following digestion of the pc*RYR1* vectors with *Eco*RV DNA fragments of the expected sizes 2,656, 4,081 and 13,862 base pairs were detected for all vectors (figure 3.5). Sanger sequencing was used to confirm the presence of the c.642C>T and c.7042_7044delCAG variants.

3.3 Confirming the expression of RyR1 variants in HEK293T cells

To compare the functional alterations of RyR1 variants to wild type RyR1 each variant must be expressed in equal quantities. Western blot analysis was used to confirm the expression of RyR1 variants. Total protein was extracted from transiently transfected HEK293T cells, protein samples were separated by SDS-PAGE and transferred to a PVDF membrane. RyR1 expression was analysed by

immunodetection where the intensity of the protein signal indicated the level of protein expression (figure 3.6). The previously characterised RyR1 variants p.wild type, p.G248R (26) and p.R2452W (99) were used as controls for the expression of RyR1. The cytoskeletal protein tubulin was also detected during western blot analysis ensuring a relatively consistent amount of protein was loaded into the gel in each sample.

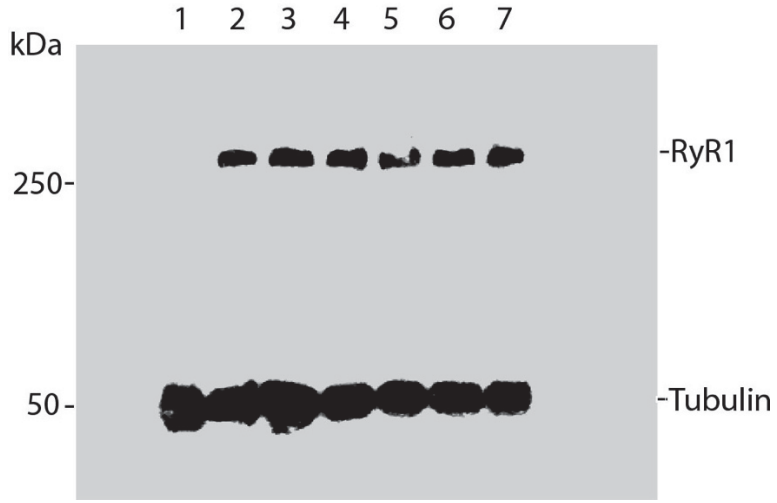

Figure 3.6 Immunoblot confirming the expression of RyR1 variants in HEK293T cells. Total protein (270 µg) extracts were separated on a 7.5% SDS-PAGE gel and transferred onto a PVDF membrane at 70 mA. RyR1, >250 kDa, and α-tubulin, 50 kDa, were detected using anti-RyR1 (34C) and anti-α-tubulin antibodies respectively. Lane 1, pcDNA3.1+ vector only. lane 2, pc*RYR1* p.wild type. lane 3, pc*RYR1* p.G248R. lane 4, pc*RYR1* p.R2452W. lane 5, pc*RYR1* p.T214M. lane 6, pc*RYR1* p.T214M/ΔE2348. lane 7, pc*RYR1* p. ΔE2348.

No RyR1 was detected in cells transfected with the pcDNA3.1+ empty vector, indicating there is no detectable endogenous expression of the channel in HEK293T cells (figure 3.6). Tubulin content across all protein extracts was not consistent, a larger tubulin content was detected in cells expressing the RyR1 wild type and RyR1 p.G248R compared to the protein extracts containing the other RyR1 variants. In all cases the amount of RyR1 was consistent indicating a somewhat decreased RyR1 expression in cells transfected with the pc*RYR1* p.wild type and p.G248R with respect to total protein content.

3.4 Confirmation of RyR1 location within HEK293T cells

Co-localisation studies using confocal microscopy were performed to ensure the expressed RyR1 was located on the ER. After a seventy-two hour transfection cells were fixed to a microscope slide and labelled with antibodies specific for RyR1, and the ER protein, protein disulphide isomerase, PDI. A FITC conjugated secondary antibody was used to detect the RyR1 specific primary antibody, a TRITC conjugated secondary antibody was used to detect the PDI primary antibody. DAPI was used to stain the nuclei. HEK293T cells transiently transfected with the pcDNA3.1+, pc*RYR1* p.wild type, pc*RYR1* p.G248R and pc*RYR1* p.R2452W vectors were used as controls, to compare the expression of pc*RYR1* p.T214M, pc*RYR1* p.T214M/ΔE2348 and pc*RYR1* p.ΔE2348.

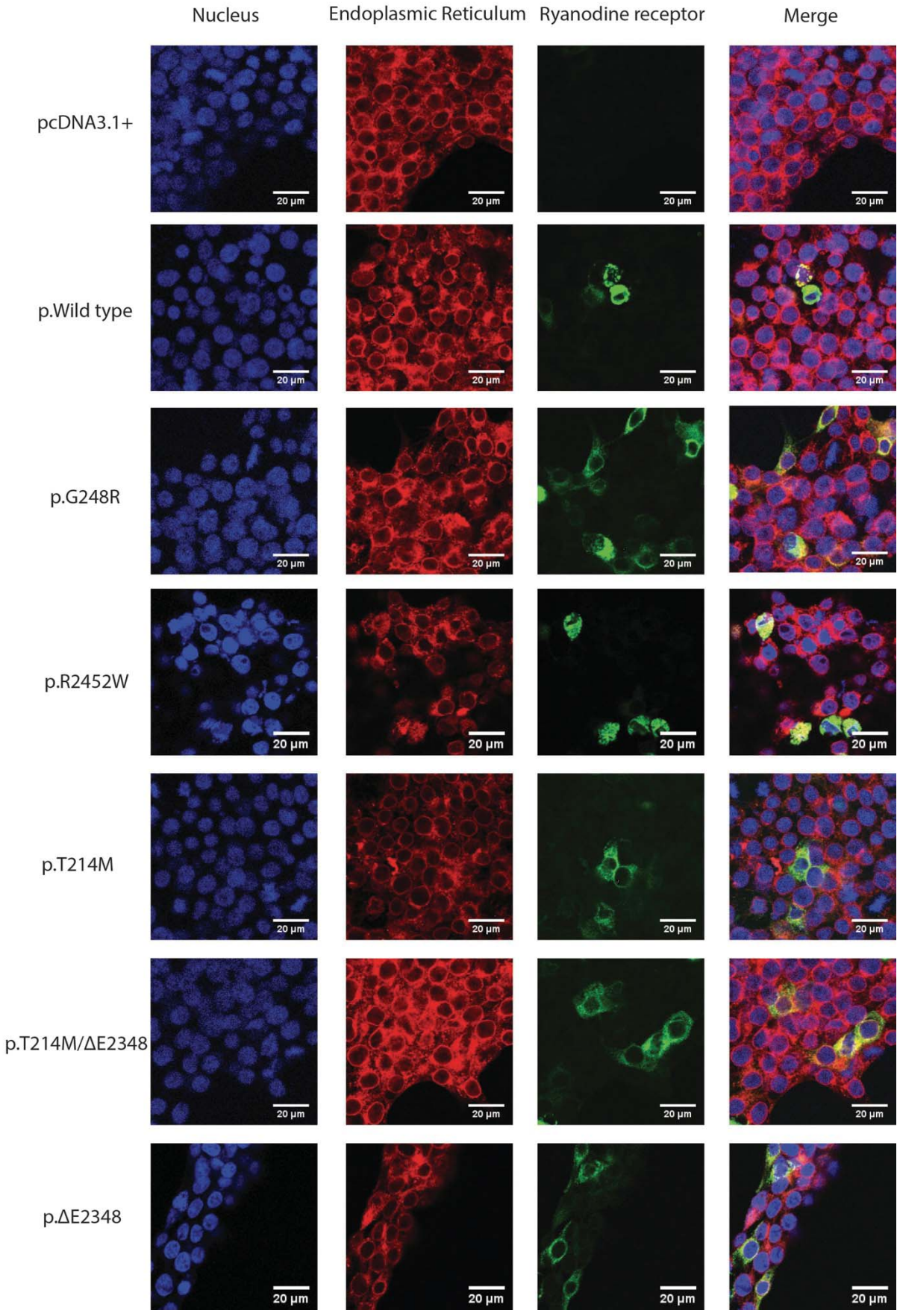
Nucleus
Endoplasmic Reticulum
Ryanodine receptor
Merge
pcDNA3.1+
p.Wild type
p.G248R
p.R2452W
p.T214M
p.T214M/ΔE2348
p.ΔE2348
20 µm

Figure 3.7 Immunofluorescent staining of transiently transfected HEK293T cells with *RYR1* cDNA. Variants are indicated by their amino acid change. Primary antibodies that specifically recognise RyR1 (34C) and PDI as well as fluorescently-labelled secondary antibodies FITC (green) and TRITC (red) were used to visualise RyR1 and PDI respectively, while nuclei were visualised by staining the cells with DAPI (blue). Cells were examined by confocal fluorescence microscopy at a magnification of 1260 X; the scale bar in each image represents a length of 20 microns.

All HEK293T cells transiently transfected with *RYR1* cDNA expressed RyR1 while no RyR1 was detected in cells transfected with the empty pcDNA3.1+ (figure 3.7). Merged images, in cells transfected with *RYR1* cDNA, confirm the localisation of RyR1 to the ER. Immunostaining indicated a small percentage of cells expressed RyR1, likely due to the size of the *RYR1* cDNA adding limitations to the transfection efficiency. In all cases a consistent number of cells expressed RyR1. The expression of RyR1 in this case is a representation of the number of cells expressing RyR1 during the previous immunoblot and the following functional analysis.

3.5 Analysis of RyR1 variant activity in HEK293T cells

RyR1 variants were functionally characterised by exposing transiently transfected cells to incremental doses of the RyR1 agonists 4-C*m*C and caffeine. The sensitivity of each variant to the agonist was determined by indirectly measuring cytosolic levels of Ca^{2+} after loading cells with the Ca^{2+}-sensitive fluorescent indicator fura 2-AM. Once fura 2-AM enters the cytosol the acetoxymethyl (AM) group is removed by cellular esterases, the deesterified Fura-2 is able bind Ca^{2+}. Fura-2 can be excited by the wavelengths 340 nm and 380 nm with an emission wavelength of 510 nm in both cases. In the Ca^{2+} bound state the emission intensity at 510 nm increases when excited by 340 nm. Alternatively, the emission intensity at 510 nm decreases when excited by 380 nm (appendix III). The 340 nm / 380 nm fluorescence ratio is an accurate way to measure increases in cytosolic Ca^{2+} concentration as an equal increase in the fluorescence intensity following excitation with 340 nm will be detected compared to the decrease in fluorescence following excitation at 380 nm.

3.5.1 Functional characterisation of RyR1 variants using 4-C*m*C

RyR1 variants were functionally characterised by exposing transiently transfected HEK293T cells to incremental doses of the RyR1 specific agonist 4-C*m*C. The change in fluorescence ratio induced at each 4-C*m*C concentration was represented as a percentage of the Ca^{2+} released at 1000 µM, the 4-C*m*C concentration previously characterised to induce maximal Ca^{2+} release (99). The previously characterised RyR1 variants (p.wild type, p.G248R and p.R2452W) were used as controls, to compare the sensitivity of the cells expressing the RyR1 variants p.T214M, p.T214M/ΔE2348 and p.ΔE2348 to the agonist.

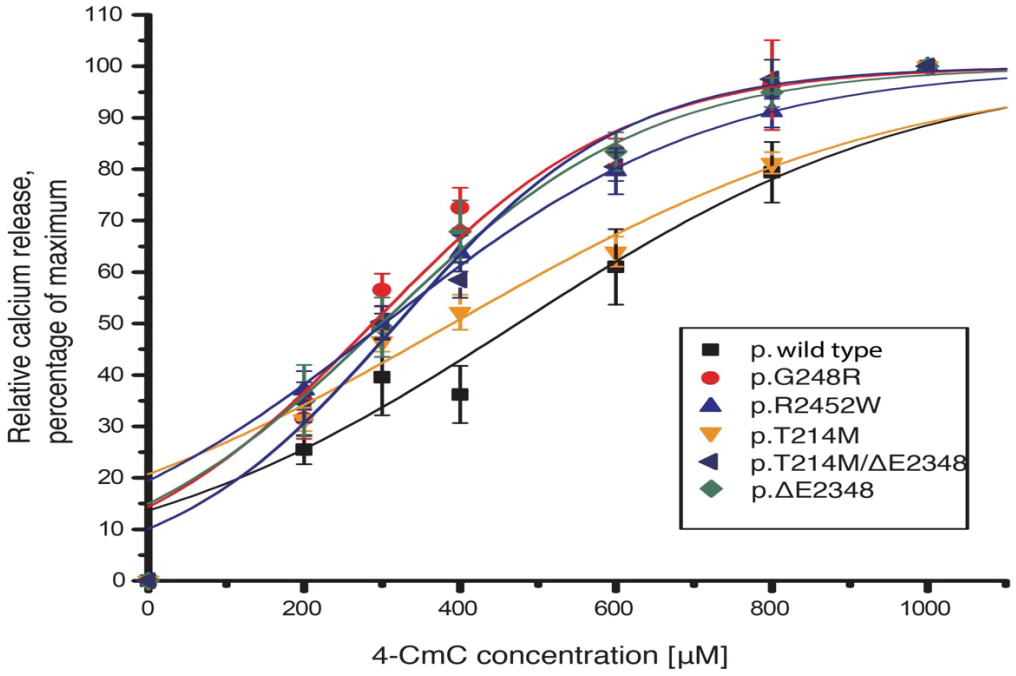

Figure 3.8 Ca^{2+}-release illustrated in 4-CmC concentration-response curves for transiently transfected HEK293T cells. Ca^{2+} released was measured for 4-C*m*C concentrations between 0 and 1000 µM. Values were normalised to Ca^{2+} released at 1000 µM 4-C*m*C and represented as mean ± SEM (n≥8). Sigmoidal curves were plotted using OriginLab Origin 8 software.

The concentration of 4-C*m*C required to half maximally activate each RyR1 variant (EC_{50}) was determined. EC_{50} values were determined for individual assays and represented as mean ± SEM. The unpaired students T-test was used to determine the statistical significance of the difference between RyR1 variants and wild type

(table 3.1). Applying the Bonferoni correction a P-value smaller then 0.00833 was considered significantly different.

RyR1 variant	EC_{50} μM	SEM	P-value
p.wild type	481	15.00	
p.G248R	270	6	$8.21511x10^{-4}$
p.R2452W	341	7.7	$6.6x10^{-4}$
p.T214M	403	15	.250
p.T214M/ΔE2348	319	15.22	$2.08303x10^{-5}$
p.ΔE2348	261	20.7	$1.45294x10^{-4}$

Table 3.1 EC_{50} for RyR1 variants following activation by 4-CmC. Results are represented as mean ± SEM. The Student's unpaired T-test was used to determine the statistical difference between the EC_{50} value for cells transfected with wild type *RYR1* cDNA and each variant. P < 0.00833 was considered to be statistically significant.

As expected the calcium response curves for the MHS controls p.G248R and p.R2452W RyR1 variants were significantly different compared to the wild type control, highlighted by the decreased EC_{50} values of 270 and 341 μM compared to 481 μM for wild type (table 3.1). The EC_{50} value for the p.T214M variant was not statistically different from the cells expressing the wild type vector. Although the shape the calcium response curve was somewhat different (figure 3.8). At low concentrations of 4-C*m*C, 200-400 μM, the p.T214M variation shows a higher relative calcium release compared to the MHN control. Between concentrations 4-C*m*C 600-1000 μM the relative calcium release was similar to wild type, this suggests that the variant may have some effect on channel function. Cells expressing the p.T214M/ΔE2348 and p.ΔE2348 variants displayed similar Ca^{2+} response curves to the MHS positive controls. The decreased EC_{50} values of 319 and 269 μM respectively were deemed to be significantly different from wild type indicating the p.ΔE2348 variant is likely to cause the onset of MH symptoms.

3.5.2 Optimisation of the caffeine induced Ca^{2+} release

Caffeine is commonly used to characterise RyR1 variants with respect to MH. Each study previously characterising MH-linked RyR1 variants with respect to caffeine

sensitivity has used a different system to transiently transfect, express and induce Ca^{2+} release in HEK293T cells. As a result each study reports differing caffeine concentration response curves suggesting unique EC_{50} values for both wild type and RyR1 variants (64, 75, 101). Caffeine has yet to be used to characterise RyR1 variants in the system described in sections 2.2.2.5 and 2.2.2.9. Therefore, an incremental concentration gradient of the agonist needed to be optimised to differentiate wild type and MHS variants. Previous studies have indicated caffeine concentrations ranging from 8 – 30 mM will induce maximal Ca^{2+} release from the ER (46, 101). To establish the concentration of caffeine to induce maximal release of Ca^{2+} from the ER, cells transiently transfected with pc*RYR1* p.wild type, pc*RYR1* p.G248R or pc*RYR1* p.R2452W loaded with fura-2AM were exposed to caffeine concentrations ranging from 5 mM to 30 mM (figure 3.9). A wide range of caffeine concentrations was selected to ensure the concentration to induce maximal Ca^{2+} release was detected.

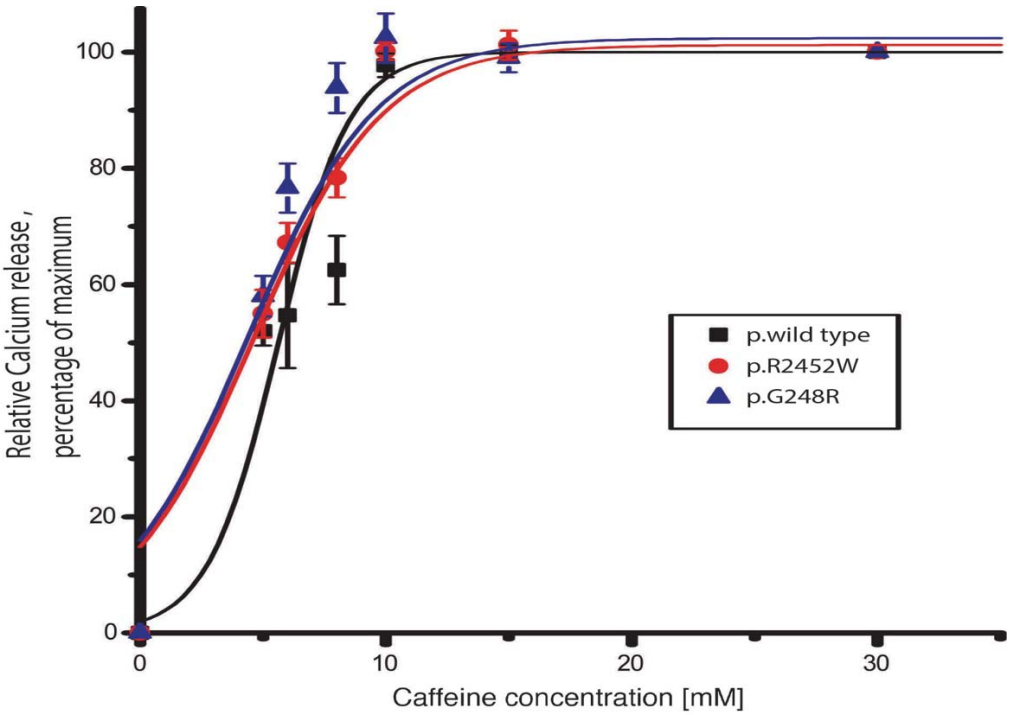

Figure 3.9 Ca^{2+}-release illustrated in caffeine concentration-response curves for transiently transfected HEK293T cells. Ca^{2+} release is illustrated in concentration-response curves for transiently transfected HEK293T cells. Ca^{2+} release was measured for caffeine concentrations between 0 and 30 mM, values were normalised to Ca^{2+} released at 30 mM and represented as mean ± SEM (n≥5). Sigmoidal curves were plotted using OriginLab Origin 8 software.

The results of this experiment show that 15 mM caffeine will induce maximal Ca^{2+} release in this system. Differences in the relative Ca^{2+} release between cells expressing wild type RyR1 and the two previously characterised RyR1 variants can be seen at concentrations between 5 and 8 mM. A decreased response to caffeine was detected in this study compared to others. This is particularly noticeable at 6 mM caffeine. HEK293T cells expressing wild type RyR1 displayed a relative Ca^{2+} release of 55 %, compared to other systems where a relative release of 60 - 100 % was noted (46, 64, 101). When MH-linked variants were exposed to 8 mM caffeine in this set of experiments a relative response of 88 – 93 % was detected. However, in other studies a relative response of 100 % is more commonly observed. HEK 293T cells transfected the empty pcDNA3.1+ vector did not display any noticeable response to caffeine indicating the expressed RyR1 variants are responsible for the released Ca^{2+} in response to the RyR1 agonist.

Previous studies have indicated a caffeine concentration ranging from 0.25 - 1 mM will induce minimal Ca^{2+} release in transiently transfected HEK293T cells (46, 75, 101). As an altered caffeine response compared to previous studies has been established in this system, transiently transfected HEK293T cells were exposed to a wide range of caffeine concentrations (0.25 - 4 mM) (figure 3.10) ensuring the caffeine concentration to induce minimal Ca^{2+} release was detected.

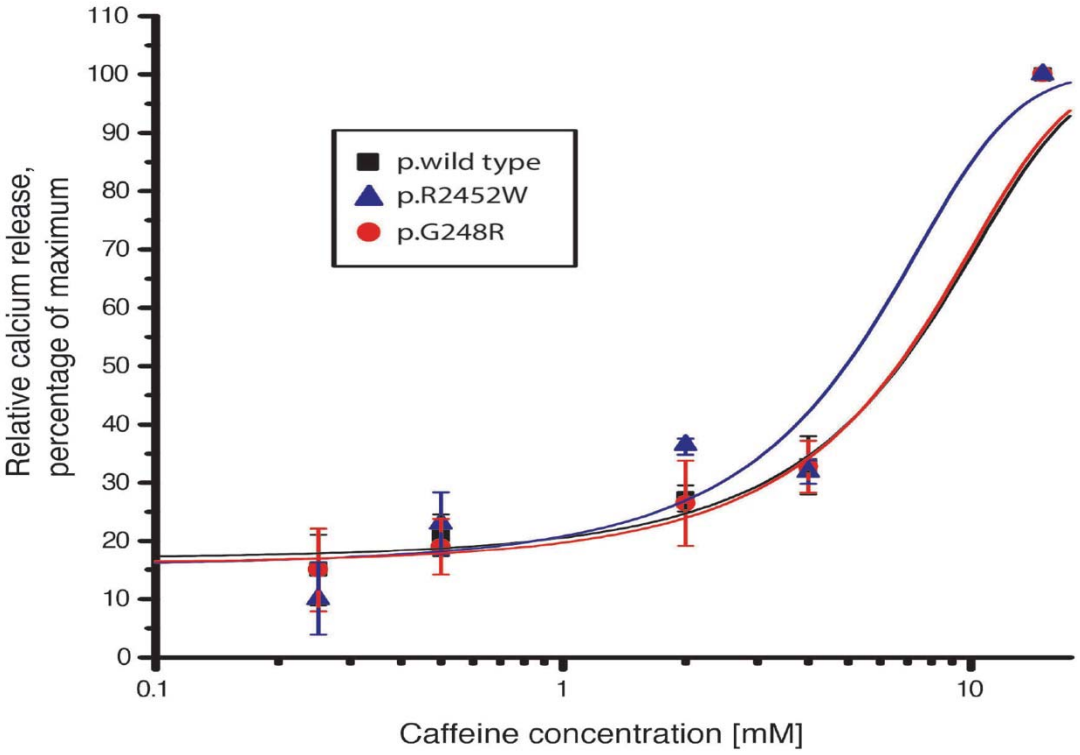

Figure 3.10 Ca^{2+}-release illustrated in caffeine concentration-response curves for transiently transfected HEK293T cells. Ca^{2+} release was measured for caffeine concentrations between 0 and 15 mM, values were normalised to Ca^{2+} released at 15 mM caffeine and represented as mean ± SEM (n≥4). Sigmoidal curves were plotted using OriginLab Origin 8 software.

HEK293T cells expressing wild type RyR1 had an almost identical calcium response to cells expressing the p.G248R variant when exposed to caffeine concentrations ranging from 0.25 - 15 mM. The p.R2452W variant, however displayed somewhat different characteristics. Again a decreased relative Ca^{2+} release was detected with respect to both wild type RyR1 and MH-linked variants compared to other studies. This was particularly noticeable at 2 mM caffeine, where cells expressing MH-linked variants in this study displayed a relative Ca^{2+} release of 26 %, while previous reports indicate approximately 80 % Ca^{2+} release is expected (75, 101).

This set of experiments suggests exposing transiently transfected HEK293T cells to incremental doses of caffeine ranging from 0.5 - 15 mM would induce Ca^{2+} release concentration response curves that can differentiate MHS and MHN RyR1 variants. Functional differences between wild type RyR1 and MH-linked variants were expected to be seen between the caffeine concentration 4 mM and 10 mM as this was the range where the most differentiation occurred.

3.5.3 Functional characterisation RyR1 variants using caffeine

Transiently transfected HEK293T cells expressing the p.T214M, p.ΔE2348 and p.T214M/ΔE2348 RyR1 variants were exposed to the incremental caffeine concentrations ranging from 0.5 - 15 mM. The relative Ca^{2+} release was compared to HEK293T cells expressing the p.wild type, p.G248R and p.R2452W RyR1 variants (figure 3.11).

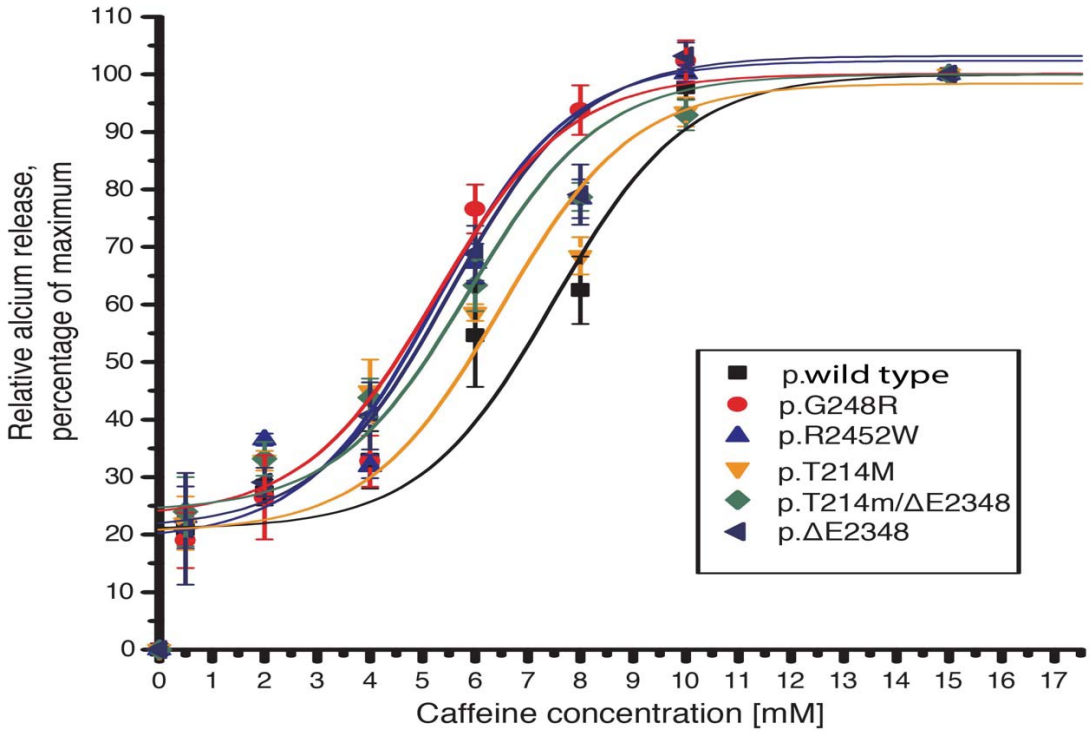

Figure 3.11 Ca^{2+}-release illustrated in caffeine concentration-response curves for transiently transfected HEK293T cells. Ca^{2+}-release is illustrated in concentration-response curves for transiently transfected HEK293T cells. Ca^{2+} released was measured for caffeine concentrations between 0 and 15 mM, values were normalised to Ca^{2+} released at 15 mM caffeine and represented as mean ± SEM (n≥8). Sigmoidal curves were plotted using OriginLab Origin 8 software.

The concentration of caffeine required to half maximally activate each RyR1 variant was determined for individual assays and represented as mean ± SEM. The unpaired students T-test was used to determine the statistical significance of the difference of each RyR1 variant compared to wild type. Applying the Bonferoni

correction a P-value smaller then 0.00833 was considered significantly different (table 3.2).

RyR1 variant	EC_{50}	SEM	P-value
p.wild type	6.49	0.232649	
p.G248R	4.60	0.180278	$4.02E^{-5}$
p.R2452W	5.18	0.074967	0.00148
p.T214M	6.25	0.167743	0.250
p.T214M/ΔE2348	5.20	0.164638	0.00154
p.ΔE2348	5.20	0.061237	0.00172

Table 3.2 EC_{50} for RyR1 variants following activation by caffeine. EC_{50} values for individual assays were determined and represented as mean ± SEM. The Student's unpaired T test with Bonferoni correction was used to determine the statistical difference between the EC_{50} value for cells transfected with wild type *RYR1* cDNA and each variant. P<0.00833 was considered to be statistically significant.

As expected HEK293T cells expressing the p.G248R and p.R2452W RyR1 variants displayed increased Ca^{2+} release compared to wild type. This is indicated by the decreased EC_{50} values of 4.60 and 5.18 mM respectively compared to 6.49 mM for wild type (table 3.2). Cells expressing the p.T214M variant again displayed an EC_{50} value similar to wild type of 6.25 mM. However, the concentration response curve was again altered compared to wild type (figure 3.11). At concentrations ranging from 0.5 – 4 mM the agonist response was comparable to the MHS variants, while at higher concentrations (6 – 10 mM) the relative calcium release was similar to wild type. These observations indicate the variant may have some effect on channel function. Cells expressing the p.ΔE2348 and p.T214M/ΔE2348 RyR1 variants both displayed an increased relative calcium release compared to wild type cells. The EC_{50} values in both cases of 5.20 mM was comparable to the MHS controls, indicating the ΔE2348 variant is likely to have a significant effect on channel function.

3.6 Measurement of resting cytosolic calcium levels

In some cases, specific RyR1 variants have been shown to cause leakage of Ca^{2+} from the SR under resting conditions. While many of these variants are linked to

other muscular diseases (102) many MH-linked variants also display similar characteristics (26, 103). Prior to the addition of RyR1 agonists 4-C*m*C or caffeine, the resting fluorescence emission ratio at 510 nm was measured. The average fluorescence emission of cells transfected with each pc*RYR1* vector was compared to cells transfected with the empty pcDNA3.1+ vector (table 3.3). The students unpaired t-test with Bonferoni correction was used to determine the statistical significance of each value. Applying the Bonferoni correction a P-value smaller then 0.007142 was considered to be statistically significant.

RyR1 varinat	Mean Fluorescence	SEM	P-value
pcDNA3.1+	1.03035	0.00616	
p.wild type	1.03835	0.00281	0.22291
p.G248R	1.03057	0.00444	0.13118
p.R2452W	1.06179	0.00508	2.99E-05
p.T214M	1.03832	0.00341	0.99381
p.T214M/ΔE2348	1.04986	0.00573	0.05691
p.ΔE2348	1.08895	0.00504	7.98E-16

Table 3.3 resting Ca^{2+} of RyR1 variants in HEK293T cells. Represented is the mean ± SEM fluorescence emission ratio at 510 nm following excitation at 340 nm and 380 nm for individual assays. The Student's unpaired T test applying the Bonferoni correction was used to determine the statistical difference between cells transfected with the pcDNA3.1+ vector only, and each RyR1 construct. P<0.007142 was considered to be statistically significant.

The p.R2452W and p.ΔE2348 variants had a statistically significant increase in resting fluorescence compared to cells expressing other variants (table 3.3). The increased fluorescence is an indication the individual amino acid variants could have destabilised the channel in the closed state under non stimulatory conditions allowing Ca^{2+} to leak across the SR membrane. It is interesting to note the resting Ca^{2+} level of the p.T214M/ΔE2348 variant was more comparable to cells expressing wild type RyR1. This suggests that the p.T214M variant may counter the destabilisation caused by the p.ΔE2348 variant when the variants are expressed on the same subunit.

3.7 Discussion

The p.T214M RyR1 variant has been shown to segregate with MH in three U.K families known to be susceptible to the disease either by IVCT or displaying MH symptoms (96). The variant has also been found in one New Zealand based family, in this case the patient was shown to be borderline MHN by IVCT (1). In this case a contracture strength of 0.4 g and 0.2 g was measured for 2 % halothane and 2 mM caffeine respectively. Should the contraction strength exceed 0.2 g for both halothane and caffeine the patient is classed being MHS. It has been suggested that a small percentage of IVCT experiments will result in a false negative describing the muscle donor as being MHN when in fact they are susceptible to MH (104). This may be the case for this patient. In comparison the proband known to have both the p.T214M and p.ΔE2348 variants displayed strong contractures of 5.2 g and 3.0 g for 2 % halothane and 2 mM caffeine respectively.

HEK293T cells expressing the MH-linked RyR1 variant p.T214M were exposed to the RyR1 agonists 4-C*m*C and caffeine but could not be functionally distinguished from the wild-type RyR1 channel via EC_{50} values (tables 3.1 and 3.2) . However a different shaped response curve suggests some altered function of the channel (figures 3.8 and 3.11). While transiently transfected HEK293T cells express exogenous RyR1, they do not express any other proteins involved in EC coupling. Therefore, a functional implication of the p.T214M variant cannot be ruled out. The variant may limit the formation of specific protein-protein interactions, leading to the onset of MH in skeletal muscle cells, a process which cannot be investigated in this system.

Threonine 214 is located in the N-terminal domain of RyR1. This region of the rabbit RyR1 channel has been structurally characterised by X-Ray crystallography (88). The region consists of three subdomains, A, B and C linked together by a hydrophilic interface. The threonine residue is located within the linker region between domains A and B, the side chain of the amino acid is directed towards the core of the protein. The amino acid substitution from a small hydrophilic threonine residue to the larger aliphatic methionine appears to have not significantly altered channel function in this set of experiments.

HEK293T cells expressing the MH-linked RyR1 variant p.ΔE2348 were exposed to the RyR1 agonists 4-C*m*C and caffeine, and displayed similar characteristics to the MHS controls. This indicates the p.ΔE2348 variant is likely the cause the MH symptoms. Cells expressing the double, p.T214M/ΔE2348, variant also displayed an increased Ca^{2+} release in response to both agonists. The near atomic resolution Cryo-electron microscopy structure of RyR1 predicts glutamic acid 2348 resides within the alpha helix rich HD1 domain (105). Only the back bone amino acid sequence was traced for this domain where it was thought the amino acid resides within an alpha helix. The amino acid is highly conserved (97) and its deletion may induce structural alterations destabilising the channel resulting in the MH phenotype.

Previous studies have used caffeine to characterise RyR1 variants with respect to MH. Each study has reported a different EC_{50} value for wild type RyR1 ranging from 0.6 - 4 mM (64, 106) compared to 6.49 mM in this study. The tenfold difference in EC_{50} values indicates a significant difference in RyR1 function in each system. In each study, different conditions were used for the growth, transfection and Ca^{2+} release. All variables have the potential to alter Ca^{2+} release characteristics. While being soluble in water, caffeine is thought to easily drop out of solution. The differences in RyR1 response to caffeine may result from the agonist's limited solubility, should caffeine drop out of solution it will not be able to enter the cell and as a consequence will not be able to induce Ca^{2+} release. This may explain the decreased Ca^{2+} release noted in this study. In some studies, Ca^{2+} release was also induced by 4-C*m*C. EC_{50} values for wild type RyR1 ranged from 60 – 200 μM compared to 481 μM in this study (26, 64), highlighting the difference in RyR1 function in this system compared to others.

While different concentration response curves for RyR1 variants were detected in each study, the relative difference in EC_{50} values between wild type RyR1 and MH-linked variants remains relatively consistent. In many cases HEK293T cells expressing wild type RyR1 have an EC_{50} value 1.5-2 fold larger then an MH-linked variant (64, 75, 106). However, in this set of experiments a smaller relative difference was noted. Wild type RyR1 displayed an EC_{50} with a 1.25 fold increase compared to the p.R2452W variant. The relative difference between wild type RyR1 and the p.G248R variant on the other hand was more consistent with other studies with a

1.49 fold increase in EC_{50} value. Again highlighting how different systems used to characterise RyR1 variants can have an effect on RyR1 function.

No alteration in the resting cytosolic Ca^{2+} level was detected from cells expressing the p.G248R variant compared to wild type RyR1 expressing cells, consistent with the previous characterisation of the variant (26, 107). No difference in resting Ca^{2+} levels were also noted for the p.T214M variant in this set of experiments. However, both the p.R2452W and p.ΔE2348 variants displayed an increased cytosolic Ca^{2+} level under resting conditions. Indicating the variants may destabilise the closed state of the channel, causing it to favour the open state at rest. This suggests a "leaky" RyR1 channel may be a cause for the onset of MH as well as the characteristic hypersensitive phenotype (21, 26, 107). HEK293T cells expressing the p.T214M/ΔE2348 variant did not display an increase in the cytosolic Ca^{2+} level at rest, potentially indicating the p.T214M variant is able to compensate for the destabilisation caused by the p.ΔE2348 variant.

Arginine 2452 is located within the previously characterised DP4 domain (91), consisting of the amino acids 2442-2477. A number of MH-linked variants have been found within this domain, indicating the domain is likely to play an important role in the function of the channel. Protein binding assays have implicated the DP4 domain in interdomain interactions (92). The substitution from the positively charged arginine to a large hydrophobic residue, tryptophan, may limit the formation of specific amino acid interactions, causing the channel to favour the open state under resting conditions, and inducing the MH phenotype under stimulatory conditions.

To analyse the effect of both the p.T214M and the p.ΔE2348 RyR1 variants in the same cell line both variants were cloned into the same expression vector. In this case transfected cells are homozygous for the two variants. Cells expressing this construct displayed a similar Ca^{2+} response curve after being exposed to 4-C*m*C and caffeine to the MHS controls. As the proband known to have both variants has inherited one variant from each parent he cannot express an RyR1 subunit containing both variants as is the case for RyR1 expression in this recombinant system. Further analysis will need to be performed to characterise RyR1 expressing both variants on separate subunits.

3.8 Conclusion

Following the functional characterisation of the c.641C>T, p.T214M RyR1 variant in transiently transfected HEK293T cells no significant alteration to channel function was detected. The functional characterisation of the variant performed in the above study does not rule out the potential for the variant to cause MH, however further analysis will need to performed to characterise the variant. Functional analysis of the c.7042_7044delCAG, p.ΔE2348 suggests the RyR1 variant is the cause of the MH symptoms, and as a result all patients known to have the variant should be treated as being being MHS.

Chapter 4 Overexpression and purification of the RyR1 N-terminal domain

4.1 Introduction

During the opening of RyR1, the channel undergoes a significant conformational change. Low resolution structural analysis of RyR1 in both the open and closed states suggests the N-terminal domain moves relative to the central regions of the channel while one subunit moves relative to another (108, 109). A number of MH-linked amino acid variants have been found within the N-terminal domain of RyR1 each of which is thought to destabilise the highly specific interactions formed with adjacent domains, forcing the channel to favour the open state under certain conditions (88, 110).

The structure of the rabbit RyR1 N-terminal domain (accession number NP_001095188.1) has been previously characterised by X-ray crystallography (87, 88, 110). Firstly, the amino acids 1-210 were characterised followed by the amino acids 1-559. The structural characterisation of the amino acids 1-559 suggested the region of RyR1 is comprised of three sub domains; A, B and C (88). Domains A and B are rich in beta strand secondary structure while domain C is rich in alpha helices (figure 4.1).

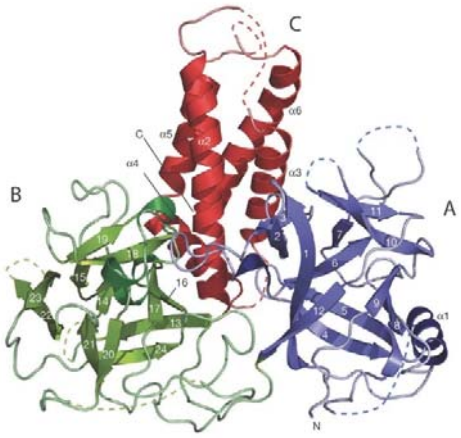

Figure 4.1 A representation of the crystal structure of the N-terminal domain of the rabbit RyR1. Domain A has been represented in blue. Domain B in green and domain C in red. Figure has been taken from (88), permission to use the figure was obtained through RightsLink.

The crystal structure of the rabbit RyR1 N-terminal domain was mapped to the cryo-EM structure of full-length RyR1. The region was thought to be located at the peak of the mushroom structure at the subunit interface (88) (figure 4.2). Where domains A and B have been implicated in the tetramerisation process of full-length RyR1. *In vitro* analysis of the region suggests that the domain forms tetramers when expressed in isolation from the rest of the channel (89).

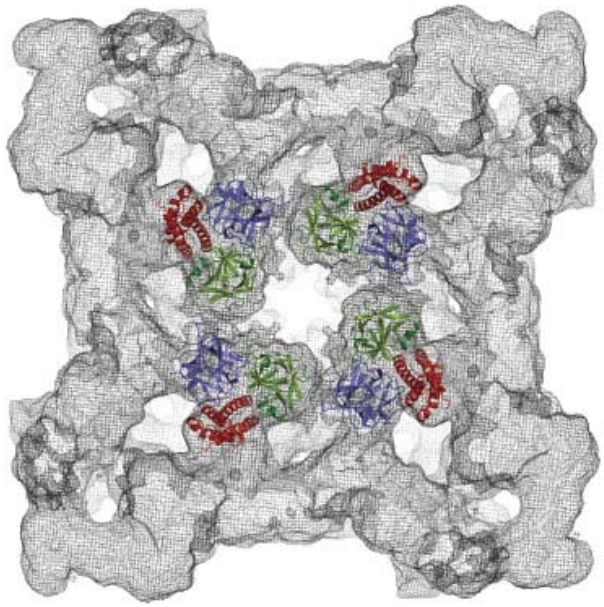

Figure 4.2 Location of the N-terminal domain with respect to the RyR1 tetramer. Represented is a cytoplasmic view of RyR1 (grey surface) following the characterisation of RyR1 by cryo-EM at 9.6 Å. The crystal structure of the rabbit RyR1 N-terminal domain has been mapped to cyro EM structure domain A has been represented in blue, domain B has been represented in green and domain C has been represented in red. Figure has been taken from (88), permission to use the figure was obtained through RightsLink.

The inositol tri phosphate receptor (IP3R) is a Ca^{2+} release channel more commonly expressed in non-contractile cells. Ca^{2+} release through the IP3R is mediated by increased cytosolic concentrations of the molecule inositol tri phosphate (IP3) produced in response to an extra cellular stimulus. Though Ca^{2+} release is mediated by a differing stimulus to RyR1, IP3R is regulated by very similar cellular signals, including ATP, Ca^{2+} and FKBP12 (111). The RyR1 and the IP3R share two regions of amino acid identity, commonly referred to as the RyR, IP3R homology (RIH) domains. The first RIH domain is housed within the N-terminal domain of each protein, with respect to RyR1 the RIH domain is located within domain C and

corresponds to amino acids 466-643 (GenBank accession number NP_000531.2) (112) (figure 4.3). The shared amino acid identity between the two Ca^{2+} channels suggests the region may be responsible for the common regulation of each channel or may be involved in common allosteric mechanisms during channel opening.

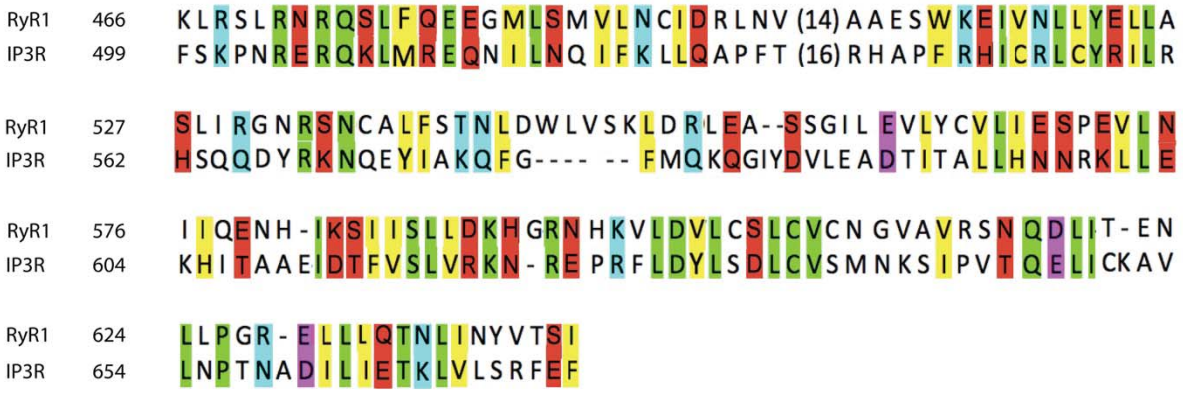

Figure 4.3 Sequence alignment of the RIH domain from human RyR1 and human IP3R. Amino acids highlighted in green indicate a conserved amino acid. Blue highlights a conserved positive charge. Pink highlights a conserved a negative charge. Yellow highlights conserved hydrophobic properties. Red highlights conserved polar properties. The amino acid number of each protein has been indicated.

The N-terminal domain of the IP3R has also been structurally characterised by X-ray crystallography and was also shown to be comprised of three subdomains A, B and C (113, 114). Following the structural characterisation of the rabbit RyR1 amino acids 1-559 it was noted the region contains a significant amount of structural similarity with the IP3R N-terminal domain (88) (figure 4.4). However the RIH domain was not expressed in its entirety in either study.

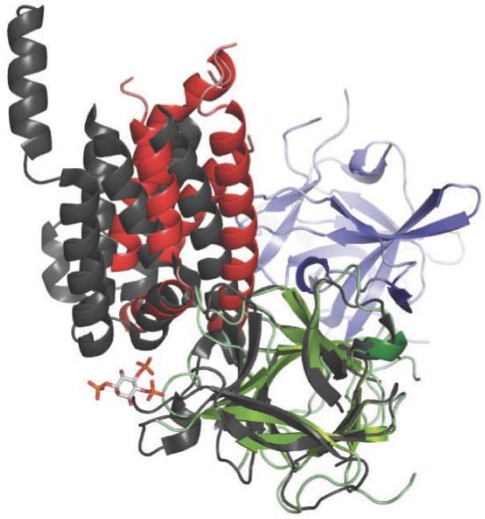

Figure 4.4 Super position of the rabbit RyR1 N-terminal domain ABC structure with the IP3R BC structure in the IP3 bound state (Protein Data Bank ID:1N4K). RyR1 domains A, B and C have been coloured in blue, green and red respectively, IP3R is coloured in grey. The super position was based on domain B of each structure. Figure taken from (88) permission to use the figure was obtained through RightsLink.

To date only the BC domain of IP3R, in the IP3 bound sate, has been structurally characterised by high resolution X-ray crystallography (113). It is worth noting the relative positions of domains B and C differ with respect to RyR1 and the IP3R in the IP3 bound state. It is known the N-terminal domain of IP3R undergoes a conformational change during the binding of IP3 where it has been suggested domain C moves relative to domain B (115). It is currently unknown if the N-terminal domain of RyR1 undergoes a similar conformational change during channel opening. The conserved structural similarity between the N-terminal domain of both proteins suggests the two regions may play a similar role with respect to the function of their respective protein.

When the structure of RyR1 was determined by cryo-EM at 3.8 Å domain C, particularly the RIH domain, was implicated in the formation of inter domain interactions with the adjacent central regions of the channel (14). It has been proposed specific MH-linked variants within this region were implicated in the disruption of these interactions destabilising the channel and leading to the onset of MH under certain conditions.

Many MH-linked variants within the N-terminal domain have been structurally characterised by X-ray crystallography and are located at the extremities of the sub domains A, B or C (88, 89). The structural characterisation of these variants indicated the amino acid change had minimal effect on the tertiary structure of the domain. However, they are proposed to effect the formation of interdomain interactions effecting global folding of the channel. This was particularly prevalent when MH-linked variants located at the interface of the A, B or C domains were structurally characterised for example. A drastic shift in tertiary structure of the region was detected.

Threonine 214 is located within the N-terminal domain of human RyR1. The corresponding residue of rabbit RyR1 is located within the linker region between domains A and B. The side chain of the residue is directed towards the centre of the region. The substitution of this amino acid to the larger, aliphatic, residue methionine has been linked to the onset of MH symptoms (96). It is unknown if the variant has a structural consequence on the N-terminal domain potentially causing MH as the variant has yet to be structurally characterised. To date no high resolution structural analysis has been performed on the human RyR1 N-terminal domain. All structural work has been performed on the rabbit RyR1, with human MH-linked variants being mapped to the domain. Due to the rabbit and human RyR1 having a high amino acid sequence identity this work can be considered meaningful. However, the best way to examine the structural implications of specific human MH-linked amino acid variants is to structurally characterise the human RyR1 N-terminal domain.

4.2 Results

4.2.1 Bioinformatics

The overall amino acid identity of RyR1 is very high across a range of organisms (13). To understand how well the N-terminal amino acids are maintained, potentially suggesting a conserved tertiary structure and regulatory mechanisms, the RyR1 amino acid sequences from a range of organisms and RyR isoforms were aligned (figure 4.5).

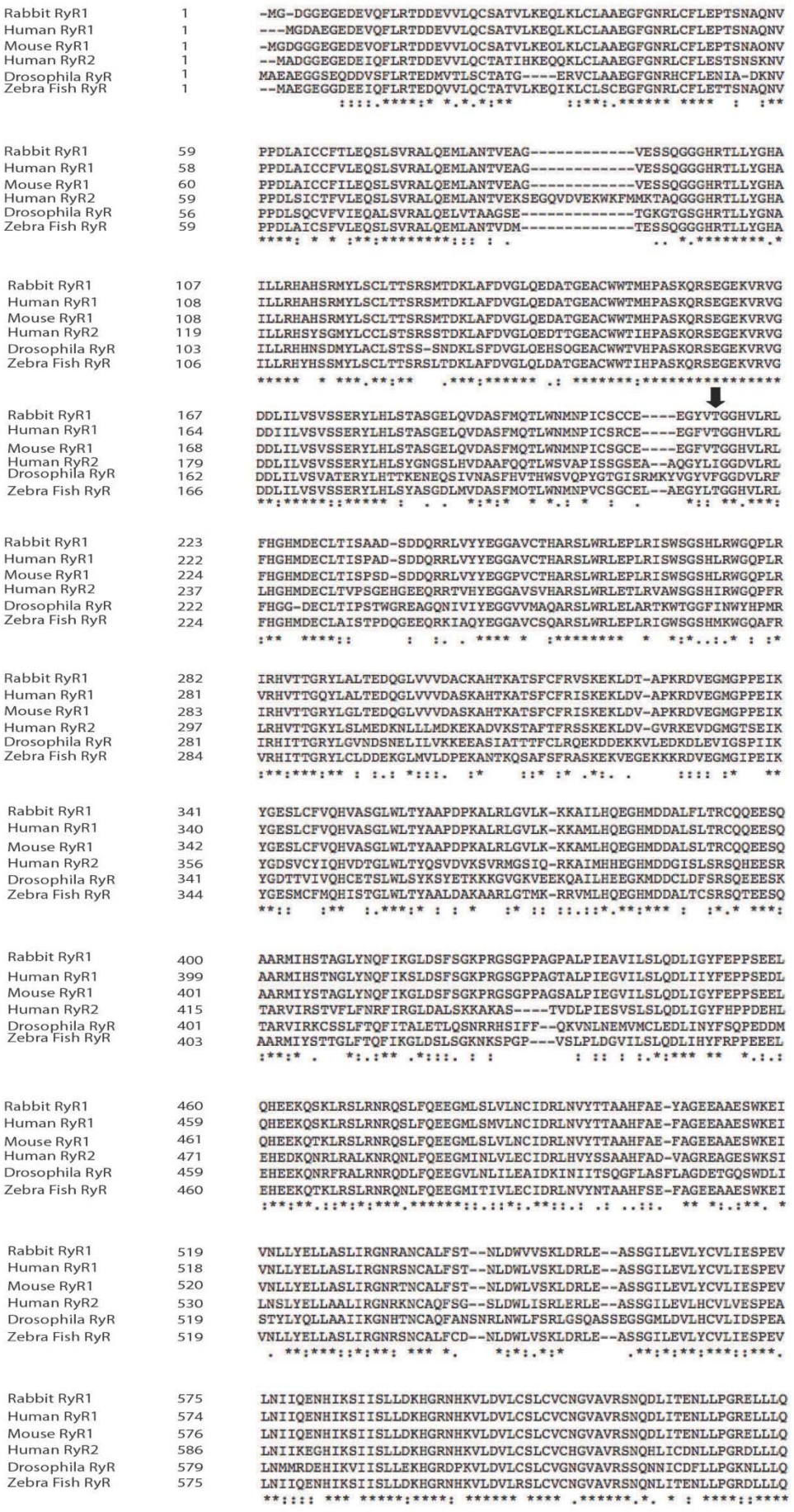
Rabbit RyR1 1 -MG-DGGEGEDEVQFLRTDDEVVLQCSATVLKEQLKLCLAAEGFGNRLCFLEPTSNAQNV
Human RyR1 1 ---MGDAEGEDEVQFLRTDDEVVLQCSATVLKEQLKLCLAAEGFGNRLCFLEPTSNAQNV
Mouse RyR1 1 -MGDGGGEGEDEVQFLRTDDEVVLQCSATVLKEQLKLCLAAEGFGNRLCFLEPTSNAQNV
Human RyR2 1 --MADGGEGEDEIQFLRTDDEVVLQCTATIHKEQQKLCLAAEGFGNRLCFLESTSNSKNV
Drosophila RyR 1 MAEAEGGSEQDDVSFLRTEDMVTLSCTATG----ERVCLAAEGFGNRHCFLENIA-DKNV
Zebra Fish RyR 1 --MAEGEGGDEEIQFLRTEDQVVLQCTATVLKEQIKLCLSCEGFGNRLCFLETTSNAQNV
Rabbit RyR1 59 PPDLAICCFTLEQSLSVRALQEMLANTVEAG----------VESSQGGGHRTLLYGHA
Human RyR1 58 PPDLAICCFVLEQSLSVRALQEMLANTVEAG----------VESSQGGGHRTLLYGHA
Mouse RyR1 60 PPDLAICCFILEQSLSVRALQEMLANTVEAG----------VESSQGGGHRTLLYGHA
Human RyR2 59 PPDLSICTFVLEQSLSVRALQEMLANTVEKSEGQVDVEKWKFMMKTAQGGGHRTLLYGHA
Drosophila RyR 56 PPDLSQCVFVIEQALSVRALQELVTAAGSE----------TGKGTGSGHRTLLYGNA
Zebra Fish RyR 59 PPDLAICSFVLEQSLSVRALQEMLANTVDM----------TESSQGGGHRTLLYGHA
Rabbit RyR1 107 ILLRHAHSRMYLSCLTTSRSMTDKLAFDVGLQEDATGEACWWTMHPASKQRSEGEKVRVG
Human RyR1 108 ILLRHAHSRMYLSCLTTSRSMTDKLAFDVGLQEDATGEACWWTMHPASKQRSEGEKVRVG
Mouse RyR1 108 ILLRHAHSRMYLSCLTTSRSMTDKLAFDVGLQEDATGEACWWTMHPASKQRSEGEKVRVG
Human RyR2 119 ILLRHSYSGMYLCCLSTSRSSTDKLAFDVGLQEDTTGEACWWTIHPASKQRSEGEKVRVG
Drosophila RyR 103 ILLRHHNSDMYLACLSTSS-SNDKLSFDVGLQEHSQGEACWWTVHPASKQRSEGEKVRVG
Zebra Fish RyR 106 ILLRHYHSSMYLSCLTTSRSLTDKLAFDVGLQLDATGEACWWTIHPASKQRSEGEKVRVG
Rabbit RyR1 167 DDLILVSVSSERYLHLSTASGELQVDASFMQTLWNMNPICSCCE----EGYVTGGHVLRL
Human RyR1 164 DDIILVSVSSERYLHLSTASGELQVDASFMQTLWNMNPICSRCE----EGFVTGGHVLRL
Mouse RyR1 168 DDLILVSVSSERYLHLSTASGELQVDASFMQTLWNMNPICSGCE----EGFVTGGHVLRL
Human RyR2 179 DDLILVSVSSERYLHLSYGNGSLHVDAAFQQTLWSVAPISSGSEA--AQGYLIGGDVLRL
Drosophila RyR 162 DDLILVSVATERYLHTTKENEQSIVNASFHVTHWSVQPYGTGISRMKYVGYVFGGDVLRF
Zebra Fish RyR 166 DDLILVSVSSERYLHLSYASGDLMVDASFMQTLWNMNPVCSGCEL--AEGYLTGGHVLRL
Rabbit RyR1 223 FHGHMDECLTISAAD-SDDQRRLVYYEGGAVCTHARSLWRLEPLRISWSGSHLRWGQPLR
Human RyR1 222 FHGHMDECLTISPAD-SDDQRRLVYYEGGAVCTHARSLWRLEPLRISWSGSHLRWGQPLR
Mouse RyR1 224 FHGHMDECLTISPSD-SDDQRRLVYYEGGPVCTHARSLWRLEPLRISWSGSHLRWGQPLR
Human RyR2 237 LHGHMDECLTVPSGEHGEEQRRTVHYEGGAVSVHARSLWRLETLRVAWSGSHIRWGQPFR
Drosophila RyR 222 FHGG-DECLTIPSTWGREAGQNIVIYEGGVVMAQARSLWRLELARTKWTGGFINWYHPMR
Zebra Fish RyR 224 FHGHMDECLAISTPDQGEEQRKIAQYEGGAVCSQARSLWRLEPLRIGWSGSHMKWGQAFR
Rabbit RyR1 282 IRHVTTGRYLALTEDQGLVVVDACKAHTKATSFCFRVSKEKLDT-APKRDVEGMGPPEIK
Human RyR1 281 VRHVTTGQYLALTEDQGLVVVDASKAHTKATSFCFRISKEKLDV-APKRDVEGMGPPEIK
Mouse RyR1 283 IRHVTTGRYLGLTEDQGLVVVDASKAHTKATSFCFRISKEKLDV-APKRDVEGMGPPEIK
Human RyR2 297 LRHVTTGKYLSLMEDKNLLLMDKEKADVKSTAFTFRSSKEKLDV-GVRKEVDGMGTSEIK
Drosophila RyR 281 IRHITTGRYLGVNDSNELILVKKEEASIATTTFCLRQEKDDEKKVLEDKDLEVIGSPIIK
Zebra Fish RyR 284 VRHITTGRYLCLDDEKGLMVLDPEKANTKQSAFSFRASKEKVEGEKKKRDVEGMGIPEIK
Rabbit RyR1 341 YGESLCFVQHVASGLWLTYAAPDPKALRLGVLK-KKAILHQEGHMDDALFLTRCQQEESQ
Human RyR1 340 YGESLCFVQHVASGLWLTYAAPDPKALRLGVLK-KKAMLHQEGHMDDALSLTRCQQEESQ
Mouse RyR1 342 YGESLCFVQHVASGLWLTYAAPDPKALRLGVLK-KKAMLHQEGHMDDALSLTRCQQEESQ
Human RyR2 356 YGDSVCYIQHVDTGLWLTYQSVDVKSVRMGSIQ-RKAIMHHEGHMDDGISLSRSQHEESR
Drosophila RyR 341 YGDTTVIVQHCETSLWLSYKSYETKKKGVGKVEEKQAILHEEGKMDDCLDFSRSQEEESK
Zebra Fish RyR 344 YGESMCFMQHISTGLWLTYAALDAKAARLGTMK-RRVMLHQEGHMDDALTCSRSQTEESQ
Rabbit RyR1 400 AARMIHSTAGLYNQFIKGLDSFSGKPRGSGPPAGPALPIEAVILSLQDLIGYFEPPSEEL
Human RyR1 399 AARMIHSTNGLYNQFIKSLDSFSGKPRGSGPPAGTALPIEGVILSLQDLIIYFEPPSEDL
Mouse RyR1 401 AARMIYSTAGLYNQFIKGLDSFSGKPRGSGPPAGSALPIEGVILSLQDLIGYFEPPSEEL
Human RyR2 415 TARVIRSTVFLFNRFIRGLDALSKKAKAS----TVDLPIESVSLSLQDLIGYFHPPDEHL
Drosophila RyR 401 TARVIRKCSSLFTQFITALETLQSNRRHSIFF--QKVNLNEMVMCLEDLINYFSQPEDDM
Zebra Fish RyR 403 AARMIYSTTGLFTQFIKGLDSLSGKNKSPGP---VSLPLDGVILSLQDLIHYFRPPEEEL
Rabbit RyR1 460 QHEEKQSKLRSLRNRQSLFQEEGMLSLVLNCIDRLNVYTTAAHFAE-YAGEEAAESWKEI
Human RyR1 459 QHEEKQSKLRSLRNRQSLFQEEGMLSMVLNCIDRLNVYTTAAHFAE-FAGEEAAESWKEI
Mouse RyR1 461 QHEEKQTKLRSLRNRQSLFQEEGMLSLVLNCIDRLNVYTTAAHFAE-FAGEEAAESWKEI
Human RyR2 471 EHEDKQNRLRALKNRQNLFQEEGMINLVLECIDRLHVYSSAAHFAD-VAGREAGESWKSI
Drosophila RyR 459 EHEEKQNRFRALRNRQDLFQEEGVLNLILEAIDKINIITSQGFLASFLAGDETGQSWDLI
Zebra Fish RyR 460 EHEEKQTKLRSLRNRQNLFQEEGMITIVLECIDRLNVYNTAAHFSE-FAGEEAAESWKEI
Rabbit RyR1 519 VNLLYELLASLIRGNRANCALFST--NLDWVVSKLDRLE--ASSGILEVLYCVLIESPEV
Human RyR1 518 VNLLYELLASLIRGNRSNCALFST--NLDWLVSKLDRLE--ASSGILEVLYCVLIESPEV
Mouse RyR1 520 VNLLYELLASLIRGNRTNCALFST--NLDWLVSKLDRLE--ASSGILEVLYCVLIESPEV
Human RyR2 530 LNSLYELLAALIRGNRKNCAQFSG--SLDWLISRLERLE--ASSGILEVLHCVLVESPEA
Drosophila RyR 519 STYLYQLLAAIIKGNHTNCAQFANSNRLNWLFSRLGSQASSEGSGMLDVLHCVLIDSPEA
Zebra Fish RyR 519 VNLLYELLASLIRGNRSNCALFCD--NLDWLVSKLDRLE--ASSGILEVLYCVLIESPEV
Rabbit RyR1 575 LNIIQENHIKSIISLLDKHGRNHKVLDVLCSLCVCNGVAVRSNQDLITENLLPGRELLLQ
Human RyR1 574 LNIIQENHIKSIISLLDKHGRNHKVLDVLCSLCVCNGVAVRSNQDLITENLLPGRELLLQ
Mouse RyR1 576 LNIIQENHIKSIISLLDKHGRNHKVLDVLCSLCVCNGVAVRSNQDLITENLLPGRELLLQ
Human RyR2 586 LNIIKEGHIKSIISLLDKHGRNHKVLDVLCSLCVCHGVAVRSNQHLICDNLLPGRDLLLQ
Drosophila RyR 579 LNMMRDEHIKVIISLLEKHGRDPKVLDVLCSLCVGNGVAVRSSQNNICDFLLPGKNLLLQ
Zebra Fish RyR 575 LNIIQENHIKSIISLLDKHGRNHKVLDVLRSLCVCNGVAVRSNQNLITENLLPGRDLLLQ

Figure 4.5 Sequence alignment of the N-terminal domain of ryanodine receptor isoforms from a range of organisms. The sequence alignment was performed using the Clustal omega software (116). The N-terminal amino acids from rabbit, human and mouse RyR1 were aligned with human RyR2 and the ryanodine receptor from drosophila and zebra fish, the respective amino acid numbers have been represented. * represents an identical amino acid. . represents a somewhat conserved amino acid. : represents a conservation of amino acid chemistry as defined by Clustal. The amino acid threonine 214 has been indicated by the black arrow.

The amino acid identity conservation is high across the mammalian organisms examined, while the amino acid sequence is slightly more divergent in more distantly related organisms, drosophila and zebra fish (figure 4.5). A number of amino acids are conserved however. The high amino acid identity was maintained in the cardiac muscle RyR isoform, RyR2, though some amino acids were divergent. The N-terminal domain of RyR2 has been implicated in the binding of anions, resulting in altered channel regulation (117), this has yet to be confirmed for RyR1. The differing amino acid sequence is likely involved in the isoform specific regulation of each channel. The amino acid threonine 214 is conserved across RyR1 of the mammalian organisms examined, however the amino acid is not well maintained across human RyR2 and drosophila RyR, potentially indicating the amino acid is not specifically required for the function of the channel.

PHYRE (Protein Homology/analogY Recognition Engine) V 2.0 (118) software was used to predict the secondary structure of the human RyR1 N-terminal domain. The software aligns a desired amino acid sequence with proteins of known structure to make an estimation of the secondary structure based off amino acid identity (figure 4.6).

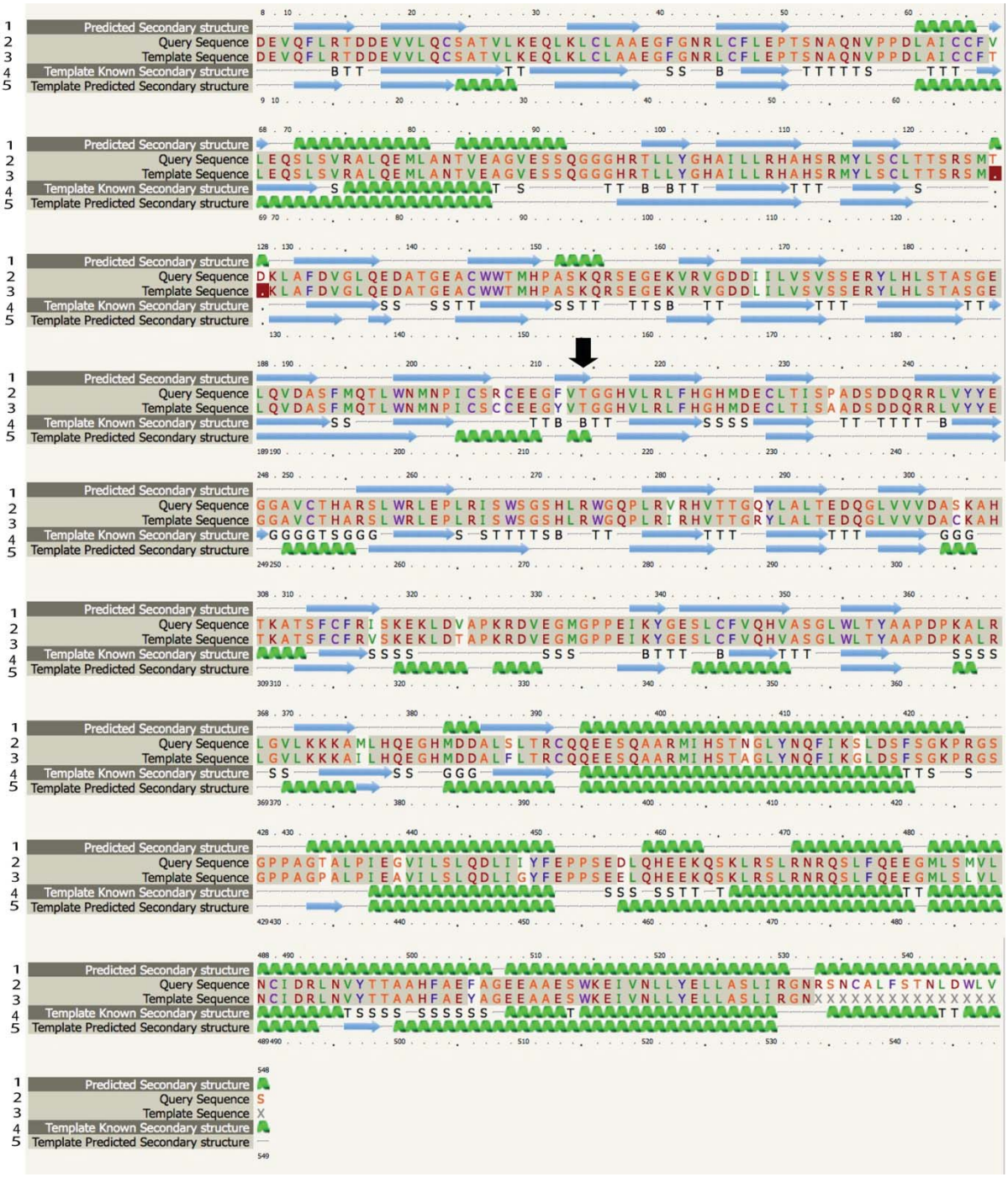

Figure 4.6 Sequence alignment of human and rabbit RyR1 N-terminal domain and secondary structure prediction of the human RyR1. The secondary structure prediction was performed by the PHYRE 2.0 software. Lane 1, predicted secondary structure of human RyR1. Lane 2, the sequence of human RyR1. Lane 3, the sequence of rabbit RyR1. Lane 4, the known structure of rabbit RyR1. Lane 5, the predicted structure of rabbit RyR1 using software algorithms. The blue arrows indicate predicted beta strand, green helices indicate predicted alpha helical structure, B indicates the residue is in an isolated β-turn, T indicates a hydrogen bonded turn. S indicates a bend in structure. The amino acid threonine 214 has been indicated by the black arrow.

With 96% sequence identity compared to the previously characterised rabbit RyR1 N-terminal domain, the PHYRE 2.0 software was able to make a prediction of the distribution of secondary structure of human RyR1 with 100% confidence. The software predicted human RyR1 N-terminal domain will adopt an almost identical distribution of secondary structure to rabbit RyR1 N-terminal domain. Threonine 214 was predicted to reside in a beta strand however the corresponding threonine residue of Rabbit RyR1 was shown to reside within a β-turn (88). Potentially suggesting there are some limitations in the algorithms used by the PHRYE 2.0 software to predict secondary structure or the RyR1 N-terminal domain may adopt a somewhat unexpected structure.

4.2.2 Cloning strategy

PCR primers were designed to amplify the human *RYR1* cDNA nucleotides 1-1674 (accession number NM_000540.2) corresponding to amino acids 1-558. The region of RyR1 corresponded to the previously characterised rabbit RyR1 N-terminal domain. The region was comprised of the three domains; A, B and C and threonine 214, although the RIH domain was not included in its entirety. The RIH domain was truncated to the same extent during the expression and characterisation of the rabbit RyR1 N-terminal domain, where the region was soluble and was thought to adopt its native structure (88, 89). Indicating the expression of the entire homology domain was not essential for the region to adopt a soluble and stable structure. A range of bacterial expression vectors (pET32a, pProEXHtb, pGEX6p3 and pMALp2g) were chosen to express the RyR1 region as each contains a specific tag with the potential to aid in solubility and purification of the expressed protein. As each vector has a different reading frame and different restriction endonuclease recognition sites present in the multiple cloning site, two specific primer pairs were designed to amplify the *RYR1* cDNA for the directional cloning into each vector. A sub clone of the ryanodine receptor cDNA, pBSXC+, corresponding to *RYR1* nucleotides 1-2,700, was used as a template for PCR amplification.

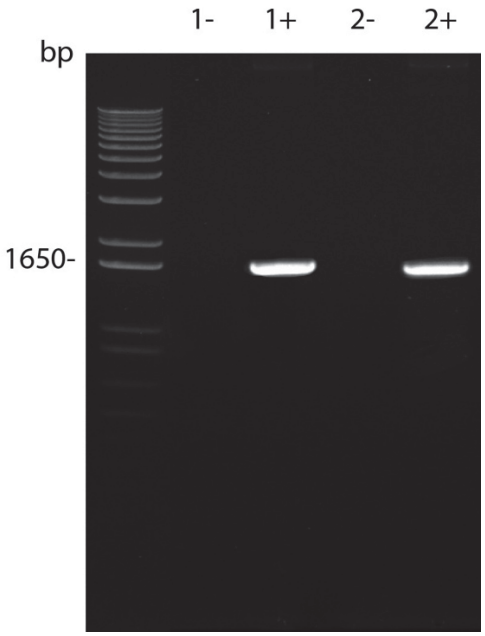

Figure 4.7 PCR amplification of the *RYR1* cDNA nucleotides 1-1674. 1 represents primer pairs amplifying cDNA for cloning into the pET32a and pGEX6p3 vectors. 2 represents primer pairs for cloning into the pProEXHtb and pMALp2g vectors. – represents control amplification containing no template DNA. + represents PCR amplification containing template DNA. DNA was resolved by 1 % (w/v) agarose gel electrophoresis at 90 mV for one hour and visualised by 0.5 µg/mL ethidium bromide staining using the Image Lab 5.1 software.

Following PCR amplification a single band of 1674 base pairs was detected using both primer pairs (figure 4.7). No contamination was detected in the no template controls. Each PCR product along with the bacterial expression vectors were digested with specific restriction endonucleases. The digested PCR product was ligated into the corresponding vector (appendix IV). Sanger sequencing was used to confirm the presence of *RYR1* cDNA within each vector, along with confirming the correct reading frame and the absence of PCR induced nucleotide variants resulting in an altered amino acid sequence.

The Expasy ProtParam software (119) was used to predict the properties of the proposed RyR1 N-terminal domain expressed from each vector. The tag added to the RyR1 N-terminal domain has the potential to alter the physical properties of the expressed protein. The software will predict the molecular mass, theoretical pI, extinction coefficients and aliphatic index of a protein based off the amino acid sequence (table 4.1).

	pET321	pProEXHTb	pGEX6p3	pMALp2g
Amino acid number	740	592	791	977
Molecular weight (Da)	81649.4	65929.7	89020.7	107640.1
Theoretical pI	5.59	5.67	5.56	5.46
Extinction coefficients are in units of M^{-1} cm^{-1}, at 280 nm, assuming all cysteine residues are reduced	81360	73340	110240	135220
Aliphatic index	85.46	84.86	88.04	85.23

Table 4.1 The predicted physical properties of the RyR1 N-terminal domain in conjunction with the N-terminal tag expressed from a range of vectors. The physical properties of the protein expressed from each vector was predicted using the ExPASy ProtParam software.

The molecular weight of each protein differs due to the size of the tag added to the N-terminal domain when expressed from each vector. The pI of each fusion protein is around 5.5, the use of a sonication buffer above pH 6.5 should help prevent precipitation. The extinction coefficient is used to calculate the protein concentration using absorbance at 280 nm. The aliphatic index is an indication of the hydrophobicity of a protein. Should the aliphatic index for a given protein be above 80 it is an indication the protein has a high number of hydrophobic amino acids, which is the case for the proposed RyR1 N-terminal domain expressed from all vectors. The corresponding region of rabbit RyR1 contained a comparable number of hydrophobic amino acids. The region was soluble and stable in solution indicating the high hydrophobicity of the region has no effect on solubility. Due to the high amino acid identity shared between the rabbit and human RyR1 regions it was thought the human RyR1 N-terminal domain will adopt a soluble structure despite the seemingly high hydrophobic amino acid content.

4.2.3 Initial expression tests

BL21 (DE3) a strain of *E. coli* cells specialised in the expression of recombinant proteins were transformed with each vector individually. The cells are deficient in specific proteases (120, 121) limiting the risk of proteolysis of the expressed RyR1

domain. The cells were grown at 37 °C until reaching an $O.D_{(600)}$ of 0.6 at which time expression was induced by the addition 0.1 mM IPTG. The cells were incubated at 37 °C for 3 hours. The cells were harvested and suspended in sonication buffer (250 mM KCl and 10 mM HEPES, pH 7.4 with 25 μg ml^{-1} DNase I, 25 μg ml^{-1} lysozyme, 14 mM β-mercaptoethanol and 1 mM phenylmethylsulphonyl fluoride) and lysed by sonication. Soluble and insoluble fractions were separated by centrifugation at 13,000 x g for ten minutes. SDS-PAGE was used to separate proteins within each fraction (figure 4.8), the RyR1 N-terminal domain was insoluble following expression of each vector.

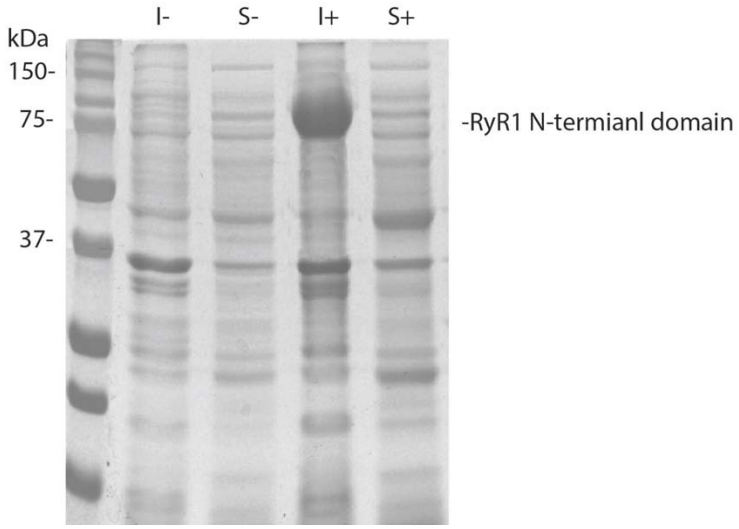

Figure 4.8 An example the expression of the RyR1 N-terminal domain in BL21(DE3) cells. The RyR1 N-terminal domain was expressed from the pET32a vector. I represents insoluble proteins, S represents soluble proteins, - represents non-induced cells, + represents induced cells.

4.2.4 Optimisation of expression

In an attempt to improve the solubility of the proposed RyR1 N-terminal domain the conditions with which expression was induced were altered. BL21 (DE3) cells were grown at 37 °C to an $O.D_{600}$ of 0.6 then expression was induced by the addition of 0.1 mM IPTG, the cells were incubated at 18 °C for a further 3 hours. Again no soluble protein was expressed. In another approach, the cells were placed under a range of stresses prior to the addition of IPTG, the culture was either placed on ice for fifteen minutes, or ethanol was added to a final concentration of 2 %, then the

culture was incubated at 18 °C for twenty minutes encouraging the expression of host chaperonin proteins, before expression was induced by 0.1 mM IPTG. However, no soluble protein was detected. The sonication buffer used to lyse the cells was identical to that used in the previous study to crystallise the rabbit N-terminal domain (88). The buffer has a relatively high ionic strength of 250 mM KCl and may denature or alter the solubility of the RyR1 N-terminal domain. The components of the sonication buffer were altered to resemble more physiological conditions to prevent protein precipitation. A summary of the solubility of the RyR1 N-terminal domain has been represented in table 4.2.

	pGEX6p3	pET32a	pProEXHTb	pMALp2g
Expressed at 37 °C	Insoluble	Insoluble	Insoluble	Insoluble
Expressed at 18 °C	Insoluble	Insoluble	Insoluble	Insoluble
Heat stress	Insoluble	Insoluble	Insoluble	Insoluble
Ethanol induced stress	Insoluble	Insoluble	Insoluble	Insoluble
Physiological sonication buffer	Insoluble	Insoluble	Insoluble	Insoluble

Table 4.2 Summary of the solubility of the amino acids 1-558 expressed from a range of expression vectors in BL21 (DE3).

Rosetta (DE3), a derivative of BL21(DE3) cells specialised in the expression of eukaryotic proteins, were transformed with each expression vector. Rosetta (DE3) cells carry a second expression vector leading to the expression of tRNA corresponding to codons heavily used in eukaryotic genomes (AGG, AGA, ATA, CTA, CCC and GGA) (122). These codons are rarely used in *E. coli* and as a result cells would normally have a decreased pool of the corresponding tRNA. The increased concentration of specific tRNA in Rosetta (DE3) has been shown to increase the translation efficiency of eukaryotic RNA preventing protein misfolding. Rosetta (DE3) cells have been successfully used to express various regions of RyR1 leading to the structural characterisation of the region (88, 94, 123). Expression of the RyR1 N-terminal domain was induced in Rosetta (DE3) cells as described for BL21(DE3) cells (section 4.2.5). A summary of the solubility of the proposed RyR1 N-terminal domain expressed from each vector has been represented in table 4.3.

	pGEX6p3	pET32a	pProEXHTb	pMALp2g
Expressed at 37 °C	Insoluble	Insoluble	Insoluble	Insoluble
Expressed at 18 °C	Insoluble	Insoluble	Insoluble	Insoluble
Heat stress	Insoluble	Insoluble	Insoluble	Insoluble
Ethanol induced stress	Insoluble	Insoluble	Insoluble	Insoluble
Physiological sonication buffer	Insoluble	Insoluble	Insoluble	Insoluble

Table 4.3 Summary of the solubility of the amino acids 1-558 expressed from a range of expression vectors in Rosetta (DE3).

No soluble protein was detected following the expression of each vector in Rosetta (DE3) cells. Some codons rarely utilised by *E. coli* do not have the overexpression of their specific tRNA supplemented by the second expression vector within Rosetta (DE3) cells, potentially indicating misfolding of the RyR1 N-terminal domain could still occur resulting from a decrease in translation efficiency. The nucleotide sequence of the *RYR1* N-terminal domain was closely analysed where codons considered to be rare with respect to the *E. coli* genome were detected (figure 4.9).

ATG GGT GAC GCA GAA GGC GAA GAC GAG GTC CAG TTC CTG CGG ACG GAC GAT GAG GTG
GTC CTG CAG TGC AGC GCT ACC GTG CTC AAG GAG CAG CTC AAG CTC TGC CTG GCC GCC GAG
GGC TTC GGC AAC CGC CTG TGC TTC CTG GAG CCC ACT AGC AAC GCG CAG AAT GTG CCC CCC
GAT CTG GCC ATC TGT TGC TTC GTC CTG GAG CAG TCC CTG TCT GTG CGA GCC CTG CAG GAG
ATG CTG GCT AAC ACG GTG GAG GCT GGC GTG GAG TCA TCC CAG GGC GGG GGA CAC AGG
ACG CTC CTG TAT GGC CAT GCC ATC CTG CTC CGG CAT GCA CAC AGC CGC ATG TAT CTG AGC
TGC CTC ACC ACC TCC CGC TCC ATG ACT GAC AAG CTG GCC TTC GAT GTG GGA CTG CAG GAG
GAC GCA ACA GGA GAG GCT TGC TGG TGG ACC ATG CAC CCA GCC TCC AAG CAG AGG TCT
GAA GGA GAA AAG GTC CGC GTT GGG GAT GAC ATC ATC CTT GTC AGT GTC TCC TCC GAG CGC
TAC CTG CAC CTG TCG ACC GCC AGT GGG GAG CTC CAG GTT GAC GCT TCC TTC ATG CAG ACA
CTA TGG AAC ATG AAC CCC ATC TGC TCC CGC TGC GAA GAG GGC TTC GTG ACG GGA GGT CAC
GTC CTC CGC CTC TTT CAT GGA CAT ATG GAT GAG TGT CTG ACC ATT TCC CCT GCT GAC AGT
GAT GAC CAG CGC AGA CTT GTC TAC TAT GAG GGG GGA GCT GTG TGC ACT CAT GCC CGC TCC
CTC TGG AGG CTG GAG CCA CTG AGA ATC AGC TGG AGT GGG AGC CAC CTG CGC TGG GGC
CAG CCA CTC CGA GTC CGG CAT GTC ACT ACC GGG CAG TAC CTA GCG CTC ACC GAG GAC CAG
GGC CTG GTG GTG GTT GAC GCC AGC AAG GCT CAC ACC AAG GCT ACC TCC TTC TGC TTC CGC
ATC TCC AAG GAG AAG CTG GAT GTG GCC CCC AAG CGG GAT GTG GAG GGC ATG GGC CCC
CCT GAG ATC AAG TAC GGG GAG TCA CTG TGC TTC GTG CAG CAT GTG GCC TCA GGA CTG TGG
CTC ACC TAT GCT GCT CCA GAC CCC AAG GCC CTG CGG CTC GGC GTG CTC AAG AAG AAG GCC
ATG CTG CAC CAG GAG GGC CAC ATG GAC GAC GCA CTG TCG CTG ACC CGC TGC CAG CAG
GAG GAG TCC CAG GCC GCC CGC ATG ATC CAC AGC ACC AAT GGC CTA TAC AAC CAG TTC ATC
AAG AGC CTG GAC AGC TTC AGC GGG AAG CCA CGG GGC TCG GGG CCA CCC GCT GGC ACG
GCG CTG CCC ATC GAG GGC GTT ATC CTG AGC CTG CAG GAC CTC ATC ATC TAC TTC GAG CCT
CCC TCC GAG GAC TTG CAG CAC GAG GAG AAG CAG AGC AAG CTG CGA AGC CTG CGC AAC
CGC CAG AGC CTC TTC CAG GAG GAG GGG ATG CTC TCC ATG GTC CTG AAT TGC ATA GAC CGC
CTA AAT GTC TAC ACC ACT GCT GCC CAC TTT GCT GAG TTT GCA GGG GAG GAG GCA GCC GAG
TCC TGG AAA GAG ATT GTG AAT CTT CTC TAT GAA CTC CTA GCT TCT CTA ATC CGT GGC AAT
CGT AGC AAC TGT GCC CTC TTC TCC ACA AAC TTG GAC TGG CTG GTC AGC AAG CTG GAT CGG
CTG GAG GCC TCG TCT GGC ATC

Figure 4.9 Rare codons within the *RYR1* nucleotides 1-1674 with respect the *E. coli* genome. Codons considered to be rare with respect to the *E. coli* genome have been highlighted in red. A cut off 0.85 % usage within the *E. coli* genome was used as a threshold to consider a codon rare.

Not only were the codons supplemented by the Rosetta (DE3) cells commonly used in the *RYR1* cDNA, but other codons considered to be rare with respect to *E. coli* including CGG, TGC, CGA, CCT, TGT, AGT, TCG, TGC (124) were also heavily used (figure 4.9). In many cases the codons occurring in the *RYR1* N-terminal domain cDNA four times as frequently as compared to the *E. coli* genome. Following over expression of the RyR1 N-terminal domain, the tRNA in the amino acid bound state corresponding to these codons may have been quickly depleted potentially adding limitations to the translation efficiency and resulting in protein misfolding.

When the *RYR1* cDNA from the human and the previously characterised rabbit N-terminal domain were compared it was noted that there was little difference between the organisms. However, human *RYR1* had slight tendency towards the use of rare

E. coli codons compared to the rabbit *RYR1* (appendix V). This may explain the lack of solubility noted in this study. However, the use of a different expression vector may also be a factor (88).

4.2.5 Codon optimisation of *RYR1* nucleotides 1-1674

Codon optimisation of the *RYR1* cDNA for optimal translation within *E. coli* was performed by GenScript. During the process codons considered to be rare with respect to the *E. coli* genome were replaced with codons more commonly used. For example, the arginine codons, AGG and AGA were altered to codons with a twenty-fold increase in usage with respect to the *E. coli* genome, CTG and CGC. While codons that may not necessarily be uncommon with respect to *E. coli* but are drastically over used in the *RYR1* cDNA were also altered spreading out the load across a range of codons across the sequence (appendix VI).

The codon optimised cDNA was then cloned into the expression vectors previously used. BL21(DE3) cells were transformed with each vector and expression was carried out as previously described.

	pGEX6p3	pET32a	pProEXHTb	pMALp2g
Expressed at 37 °C	Insoluble	Insoluble	Insoluble	Soluble
Expressed at 18 °C	Soluble	Insoluble	Insoluble	Soluble
Heat stress	soluble	Insoluble	Insoluble	Soluble
Ethanol induced stress	soluble	Insoluble	Insoluble	Soluble
Physiological sonication buffer	soluble	Insoluble	Insoluble	Soluble

Table 4.4. Expression summary of codon optimised *RYR1* N-terminal domain expressed from a range of vectors in BL21(DE3) cells.

Soluble RyR1 N-terminal domain was expressed from both the pGEX6p3 and pMALp2g vectors (table 4.4). As no soluble protein was expressed from either of these vectors using the original *RYR1* cDNA. It is an indication the codon optimised cDNA has improved the expression process.

4.2.6 Characterisation of the RyR1 N-terminal domain expressed from the pGEX6p3 vector

A soluble protein with a molecular mass of 90 kDa, the theoretical molecular mass of the GST-tagged RyR1 N-terminal domain (table 4.1) was detected following expression of the codon optimised *RYR1* cDNA from the pGEX6p3 vector (figure 4.10 A)).

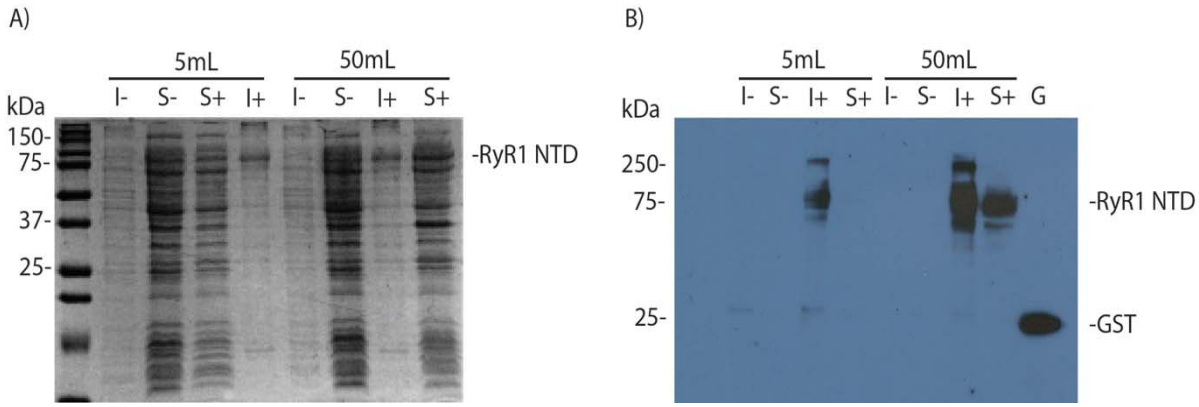

Figure 4.10 Expression of the *RYR1* codon optimised cDNA from the pGEX6p3 vector. The RyR1 N-terminal domain was expressed from either 5 mL or 50 mL *E. coli* cultures. I represents insoluble proteins. S represents soluble proteins. – represents cells not induced by IPTG. + cells exposed to IPTG. Protein was separated by 12.5 % SDS-PAGE at 120 mV for one hour thirty minutes, A) SDS-PAGE analysis of RyR1 N-terminal domain expression, proteins were visualised by Coomassie blue staining. B) Western blot analysis confirming the identity of the protein expressed from the pGEX6p3 vector. Proteins were transferred onto a PVDF membrane at 70 mV for one hour. A GST specific primary antibody was used to detect the GST tag of the RyR1 N-terminal domain. G represent BL21(DE3) cells expressing GST.

Western blot analysis using a GST specific antibody confirmed the solubility of the protein thought to correspond to the GST-tagged RyR1 N-terminal domain (figure 4.10 B)). The protein was only soluble when expressed from a 50 mL *E. coli* culture. The 50 mL culture was housed within a 250 mL conical flask compared to a 5 mL culture which was housed within a culture tube. The use of a conical flask increases the aeration of the cells, placing them under less anaerobic stress and is likely the cause for the increased solubility. The GST specific primary antibody was also able to interact with three other proteins. The first, a protein with a molecular mass of roughly 30 kDa, the protein was noted in the insoluble fraction of both non-induced

and induced cells indicating the protein is an *E. coli* host protein. The second, a protein with a molecular mass of roughly 70 kDa, this protein was detected in both the soluble and insoluble fractions following expression. As this protein was only detected in induced cells it is likely to be a degradation product of the RyR1 domain, potentially resulting from protease digestion by *E. coli* host proteases. The third protein has a molecular mass higher then the precision plus size marker, the protein was only detected in the insoluble fraction following expression, it is likely the RyR1 N-terminal domain has formed an aggregate and was unable to enter the resolving gel.

4.2.7 Batch purification of the GST-tagged RyR1 N-terminal domain using glutathione sepharose 4B

Following expression of the pGEX6p3 vector cells were lysed and soluble proteins were incubated with glutathione sepharose 4B. The resin was washed removing all non-specifically bound proteins. The GST-tagged RyR1 N-terminal domain was then eluted from the resin (figure 4.11).

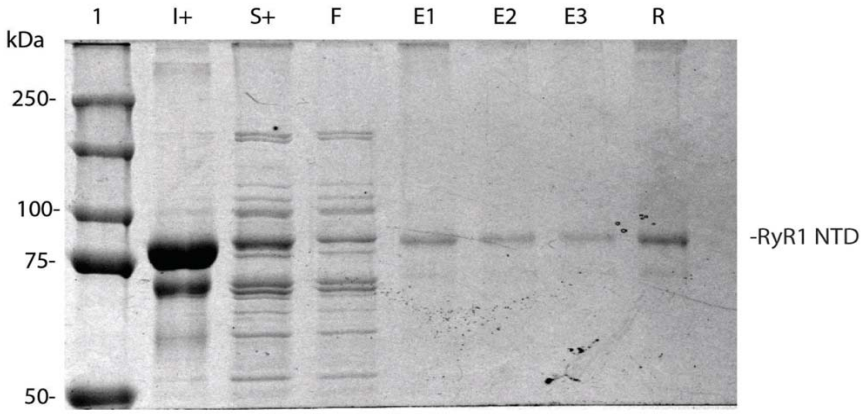

Figure 4.11 Batch purification of RyR N-terminal domain using glutathione sepharose 4B. Lane 1, precision plus size marker. I+, indicates insoluble proteins following induction with IPTG. S+ indicates soluble proteins following induction with IPTG. F, represents the flow through following incubation with glutathione sepharose 4B. E 1-3 represent individual washes in elution buffer. R represents the glutathione sepharose 4B following elution. Protein was separated by 7 % SDS-PAGE at 120 mV for one hour thirty minutes and were visualised by Coomassie blue staining.

Following batch purification two proteins were noted following elution from the resin (figure 4.11) one with a molecular mass of roughly 90 kDa likely corresponding to the GST-tagged RyR1 N-terminal domain, and one with a molecular mass of roughly 70 kDa this protein is likely a degradation product of the RyR1 region. A protein with this molecular mass was also detected during western blot analysis following initial expression (figure 4.10 B)) strongly indicating the protein has a GST tag.

4.2.8 PreScission protease digestion of the GST-tagged N-terminal domain

The protein expressed from the pGEX6p3 vector contains the specific recognition site for the protease, human rhinovirus 3C. The protease site is located between the GST tag and the RyR1 N-terminal domain corresponding to the amino acids Leu Glu Val Leu Phe Gln Gly Pro with cleavage occurring between Gln and Gly. The region surrounding the protease site has been designed to be unstructured open and accessible aiding in protease digestion. The GST tag was specifically cleaved from the RyR1 N-terminal domain to continue the characterisation of the RyR1 domain with out interference from the tag. The physical properties of the RyR1 N-terminal domain following the removal of the tag were predicted using the ExPASy ProtParam software (119) (table 4.5).

	GST -tagged RyR1 N-terminal domain	GST	RyR1 N-terminal domain
Amino acid number	791	238	564
Molecular weight (Da)	89020.7	27716	62491
Theoretical pI	5.56	6.0	5.55
Extinction coefficients in units of M^{-1} cm^{-1}, at 280 nm, assuming all cysteine residues are reduced	110240	42860	67380
Aliphatic index	88.04	89.71	88.21

Table 4.5 Proposed physical properties of the GST-tagged RyR1 N-terminal domain. The parameters were predicted using the ExPASy ProtParam software. The GST-tagged RyR1 N-terminal domain has been compared to the GST tag and the RyR1 N-terminal domain following digestion.

Commonly referred to as the PreScission protease, a recombinantly expressed GST-tagged human rhinovirus 3C protease, was used to cleave the GST tag from the RyR1 N-terminal domain. To aid in the purification of the cleaved N-terminal domain the digestion was performed with the tagged RyR1 N-terminal domain bound to glutathione sepharose 4B (figure 4.12).

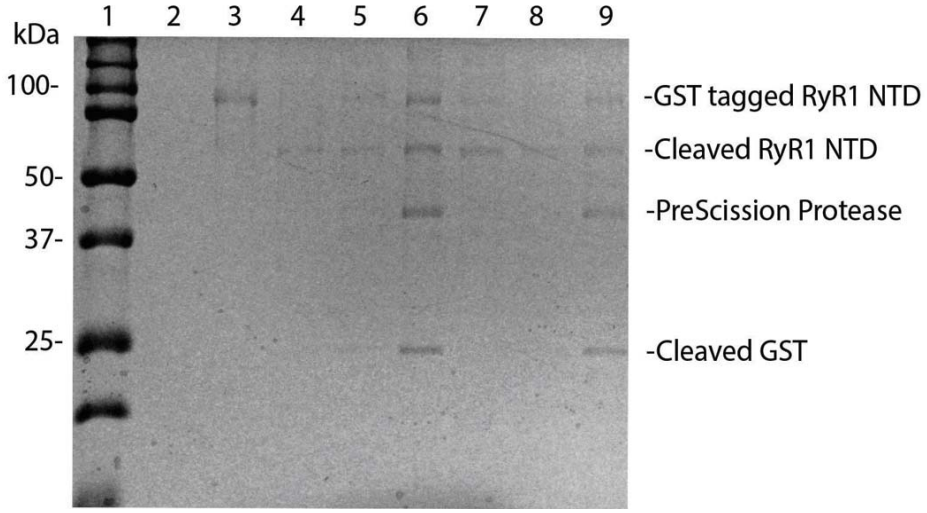

Figure 4.12 PreScission protease digestion of the GST-tagged RyR1 N-terminal domain. The GST-tagged N-terminal domain, bound to glutathione sepharose 4B, was digested by PreScission protease. Following digestion, the glutathione sepharose 4B was separated from the digestion buffer. Lane 1, precision plus size marker. Lane 2, empty. Lane 3, Non digested GST-tagged N-terminal domain. Lane 4, supernatant following an eight hour digestion at 4 °C. lane 5, supernatant following the wash of the glutathione sepharose 4B. lane 6, glutathione sepharose 4B after an eight hour digestion at 4 °C. lane 7, supernatant following an eight hour digestion at 25 °C. lane 8, supernatant following the wash of the glutathione sepharose 4B. lane 9, glutathione sepharose 4B after an eight hour digestion at 4 °C. Proteins were separated by 12.5 % SDS-PAGE at 120 mV for one hour thirty minutes and visualised by Coomassie blue staining.

The PreScission protease digestion was initially performed at 4 °C according to the manufacturer's instructions (figure 4.12. lanes 4-6). An incomplete digestion was detected with a large amount of the non digested RyR1 N-terminal domain remaining associated with the resin. A protein of approximately 60 kDa, the theoretical size of the cleaved N-terminal domain (table 4.5) was released into the digestion buffer. It is interesting to note this protein also remained associated to the glutathione sepharose 4B following digestion. In an attempt to improve the efficiency of the digestion, the incubation temperature was increased to 25 °C (figure 4.12, lanes 7-

9). The increase in temperature did not alter the efficiency of the digest and again an incomplete digestion as detected. The protein thought to correspond to the cleaved RyR1 N-terminal domain was again associated with the resin.

Western blot analysis was used to confirm the identity of each protein following the digestion. Primary antibodies specific for the GST tag and the RyR1 N-terminal domain, H21, were used to confirm the identity of each protein (figure. 4.13).

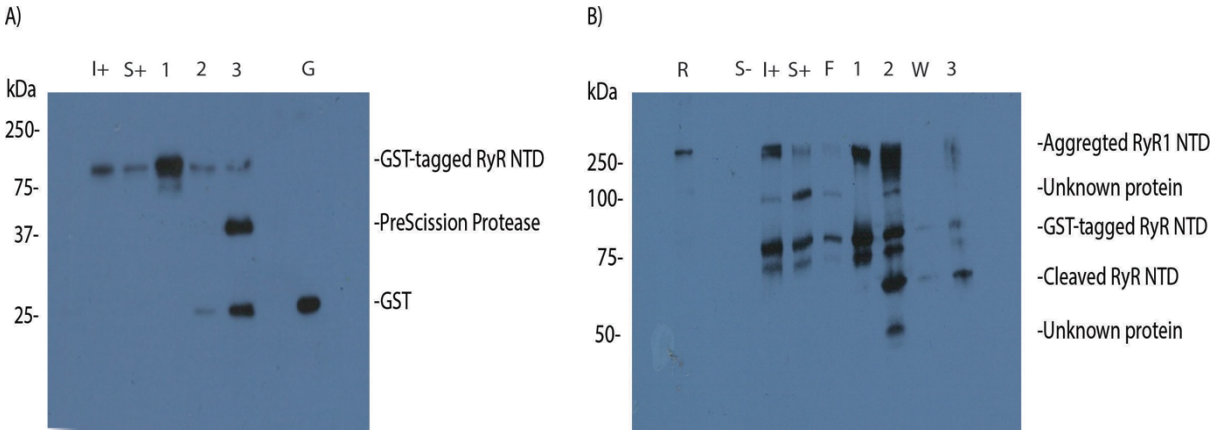

Figure 4.13 Imunodetection confirming the identity of proteins following PreScission protease digestion. PreScission protease digestion was performed with both the tagged RyR1 N-terminal domain and the PreScission protease bound to glutathione sepharose 4B. Proteins were separated by 12.5 % SDS-PAGE for one hour thirty minutes at 120 mV and transferred to a PVDF membrane. Proteins were detected using specific antibodies. I represents insoluble proteins. S represents soluble proteins. – represent non induced cells. + represent induced cells. 1, glutathione sepharose 4B before digestion. 2, soluble proteins following digestion. 3, glutathione sepharose 4B following digestion. A) immunodetection using a GST specific antibody. G, BL21(DE3) expressing GST. B) immunodetection using the H21 antibody. R, HEK293T cells expressing wild type RyR1. F, flow through following purification. W, soluble proteins following the resin wash.

Both the GST and H21 antibodies confirmed the digestion did not proceed to completion. The GST specific antibody was able to confirm the identity of the tagged RyR1 domain, the PreScission protease and the cleaved GST, though was unable to interact with the cleaved RyR1 domain (figure 4.13 A)). The H21 antibody was able to detect the presence of a protein with the molecular mass of the roughly 60 kDa, the protein thought to correspond to the RyR1 N-terminal domain (figure 4.13 B)). Some non-specific bands were also noted in this case. A high molecular weight band was detected the band likely represents the GST-tagged RyR1 N-terminal domain

that has aggregated and has not entered the resolving gel. This protein was previously detected by the GST specific antibody antibody (figure 4.10). A protein with a molecular mass of approximately 100 kDa was also detected. The protein is likely a stress response protein expressed by the *E. coli* cells in response to the induction of the vector as the protein was not detected prior to expression of the RyR1 N-terminal domain. This protein was detected in the supernatant following protease digestion potentially indicating the protein is forming an interaction with the RyR1 N-terminal domain allowing it to be released from the resin. A protein of roughly 70 kDa was detected following expression and was able to interact with the resin. A protein of this molecular mass was previously shown to interact with the resin (figure 4.11) and can be detected during western blot analysis by the GST specific antibody (figure 4.10) strongly suggesting the protein is GST-tagged. The protein was not detected by the H21 antibody in non-induced cells indicating the protein is not an *E. coli* host protein. Suggesting the RyR1 N-terminal domain may be subjected to protease digestion by *E. coli* host proteases resulting in a polypeptide with a decreased molecular mass. A protein with a molecular mass of roughly 50 kDa was detected following PreScission protease digestion, this protein was not detected in other lanes suggesting it is likely a product of the specific PreScission protease digestion of the already truncated N-terminal domain.

The domains A and B, within the expressed RyR1 region, have been implicated in the tetramerisation process of full-length RyR1 (89). In the case of the RyR1 N-terminal domain expressed from the pGEX6p3 vector the GST tag is an extension of the A domain. Should the N-terminal domain form oligomers, the B domain of an adjacent subunit may shield the PreScission protease recognition site limiting digestion efficiency. The formation of oligomers between the digested RyR1 N-terminal domain and the non-digested RyR1 domain may also explain why the cleaved RyR1 N-terminal domain has remained associated with the resin following digestion.

Both the PreScission protease and the GST-tagged N-terminal domain were bound to glutathione sepharose 4B during digestion. The large sepharose beads may limit the ability of each protein to easily move throughout the digestion solution limiting potential interactions and potentially causing the incomplete digestion. A combination

of an inaccessible protease site coupled with a decreased motility may result in an incomplete digestion.

To explore the idea of oligomerisation between the GST-tagged N-terminal domain and the cleaved RyR1 N-terminal domain, the sepharose resin following digestion was washed in elution buffer. The cleaved N-terminal domain was eluted from the resin (figure 4.14). Indicating the cleaved N-terminal domain is forming an interaction with a GST-tagged protein.

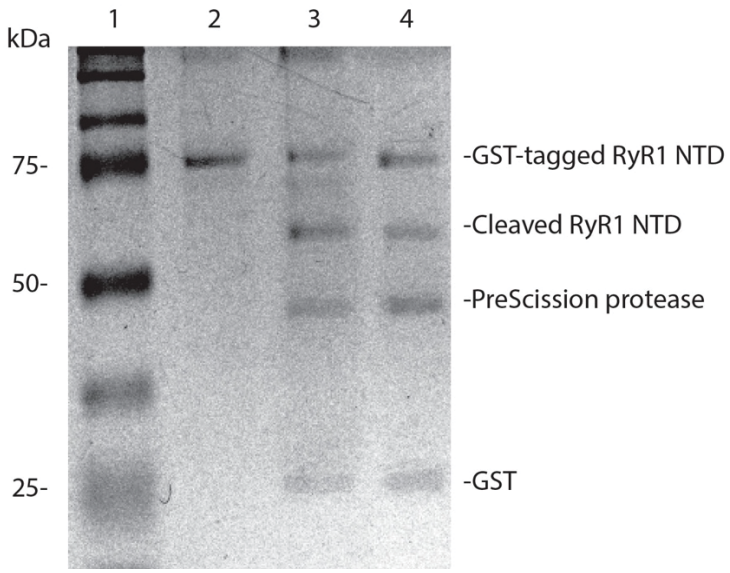

Figure 4.14 Confirming the specificity of interaction between cleaved RyR1 N-terminal domain and the glutathione sepharose 4B. Following digestion of the GST-tagged N-terminal domain the glutathione sepharose 4B was washed in a high ionic strength wash buffer then elution buffer. Lane 1, precision plus size marker. Lane 2, GST-tagged RyR1 N-terminal domain, before digestion. Lane 3, glutathione sepharose 4B following digestion. Lane 4, supernatant following wash in elution buffer. Proteins were separated using a 12.5 % resolving gel and run at 120 mV for one hour 40 minutes and visualised by Coomassie blue staining.

4.2.9 Confirmation of solubility of the cleaved N-terminal domain

To ensure the cleaved N-terminal domain was soluble, the supernatant following PreScission protease digestion was centrifuged at 70,000 x g (figure 4.15).

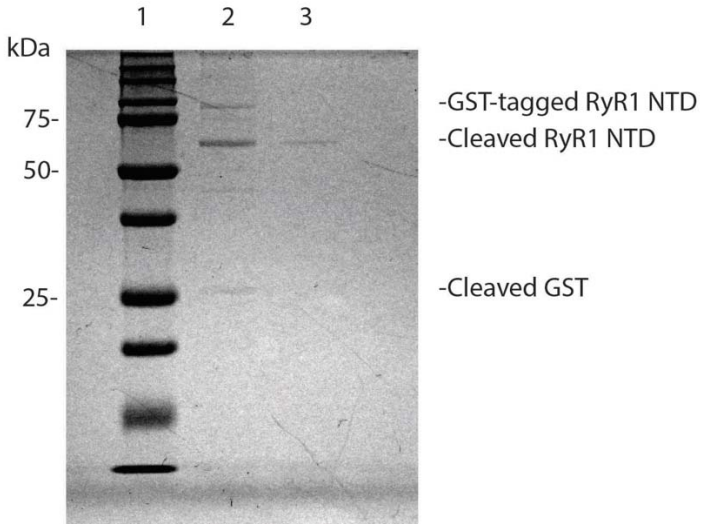

Figure 4.15 Ultra centrifugation of the cleaved RyR1 N-terminal domain. Following PreScission protease digestion the cleaved N-terminal domain was centrifuged at 70,000 x g at 4 °C for ten minutes. Following the centrifugation, the supernatant was resolved by 12.5 % SDS-PAGE for one hour thirty minutes and protein was visualised by Coomassie blue staining. Lane 1, precision plus size marker. Lane 2, digestion product pre centrifugation. Lane 3, digestion product post centrifugation.

The cleaved RyR1 N-terminal domain remained in solution during the centrifugation process, indicating the domain is both soluble and stable without the GST tag. However, some protein has been removed from solution.

4.2.10 Confirming the identity of the cleaved RyR1 N-terminal domain using mass spectrometry

MALDI MS/MS was used to confirm the identity of the cleaved RyR1 N-terminal domain. Following PreScission protease digest, proteins were separated according to their molecular mass by SDS-PAGE, the band thought to correspond to the cleaved N-terminal domain was excised from the gel and subjected to in gel digestion by the protease trypsin. The resulting fragments were then separated and subjected to MS/MS.

Matched peptides shown in ***bold red***.

```
  1 MGDAEGEDEV QFLRTDDEVV LQCSATVLKE QLKLCLAAEG FGNRLCFLEP
 51 TSNAQNVPPD LAICCFVLEQ SLSVRALQEM LANTVEAGVE SSQGGGHRTL
101 LYGHAILLRH AHSRMYLSCL TTSRSMTDKL AFDVGLQEDA TGEACWWTMH
151 PASKQRSEGE KVRVGDDIIL VSVSSERYLH LSTASGELQV DASFMQTLWN
201 MNPICSRCEE GFVTGGHVLR LFHGHMDECL TISPADSDDQ RRLVYYEGGA
251 VCTHARSLWR LEPLRISWSG SHLRWGQPLR VRHVTTGQYL ALTEDQGLVV
301 VDASKAHTKA TSFCFRISKE KLDVAPKRDV EGMGPPEIKY GESLCFVQHV
351 ASGLWLTYAA PDPKALRLGV LKKKAMLHQE GHMDDALSLT RCQQEESQAA
401 RMIHSTNGLY NQFIKSLDSF SGKPRGSGPP AGTALPIEGV ILSLQDLIIY
451 FEPPSEDLQH EEKQSKLRSL RNRQSLFQEE GMLSMVLNCI DRLNVYTTAA
501 HFAEFAGEEA AESWKEIVNL LYELLASLIR GNRSNCALFS TNLDWLVSKL
551 DRLEASSGIL EVLYCVLIES PEVLNIIQEN HIKSIISLLD KHGRNHKVLD
```

Figure 4.16 MS/MS results for the gel purified RyR1 N-terminal domain. Sequenced fragments have been highlighted in red.

Only 38% of the N-terminal domain sequence was detected during the mass spectrometry process confirming the identity of the domain (figure 4.16). A number of fragments were detected from both the N and C terminal regions of the domain, indicating that little or no nonspecific degradation is occurring.

Each of the sequenced fragments detected during the MS/MS process were fed into the Basic Local Alignment Search Tool, BLAST. The software aligns an input sequence with all known proteins and will return a confidence rating of all alignments. In most cases each fragment corresponded to the N-terminal domain of RyR1 with a confidence rating of 100 %, some fragments did align to other proteins with a decreased confidence. Some fragments did not align to RyR1 at all, many of these fragments corresponded to keratin, a protein commonly found in dust and a likely contaminant of the digestion process. No fragments were detected that correspond with any notable confidence to an *E. coli* protein indicating no host contamination.

4.2.11 Characterisation of the RyR1 N-terminal domain expressed from the pMALp2g vector

A soluble protein 105 kDa in size, the theoretical mass of maltose binding protein (MBP) tagged RyR1 N-terminal domain (table 4.1), was detected following expression of the pMALp2g vector (figure 4.17 A)).

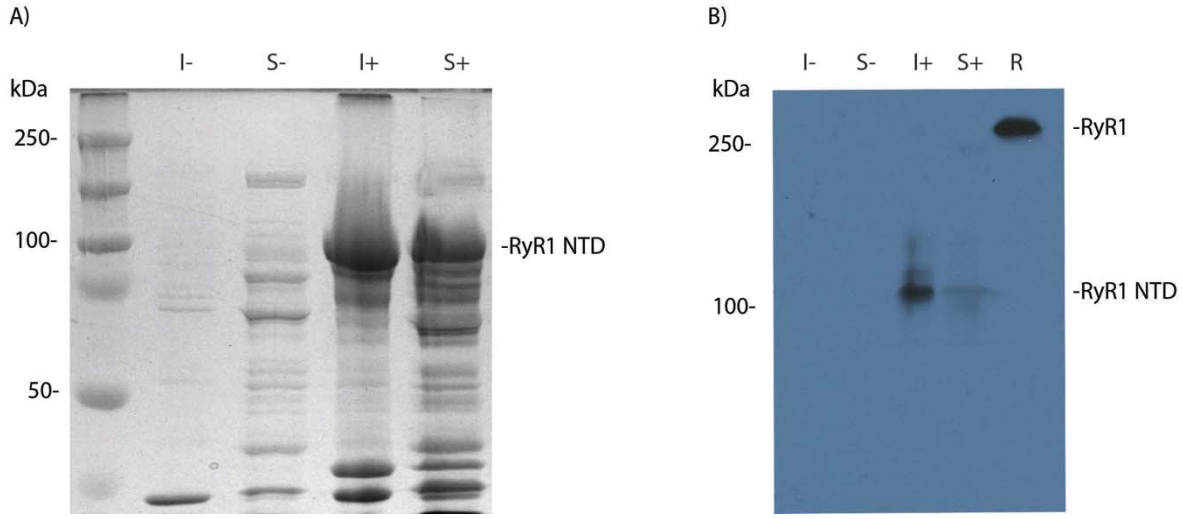

Figure 4.17 Expression of codon optimised RYR1 cDNA from the pMALp2g vector. I represents insoluble proteins and S represents soluble proteins. A – symbol indicates cells that have not been exposed to IPTG. A + symbol represents cells where expression was induced by IPTG. Proteins were separated by 7 % SDS-PAGE and resolved at 120 mV for 2 hours. A) SDS-PAGE gel showing the expression of the RyR1 N-terminal domain from the pMALp2g vector proteins were visualised by Cooassie blue staining. B) Western blot analysis confirming the identity of the protein expressed from the pMALp2g vector. Proteins were transferred to a PVDF membrane at 70 mA for twenty hours. The RyR1 domain was detected using the H21 primary antibody. R, HEK293T cells expressing full-length RyR1 wild type

Western blot analysis using the H21 antibody confirmed the solubility of the RyR1 N-terminal domain (figure 4.17 B)). The antibody was able to interact with the protein thought to correspond to the RyR1 N-terminal domain. Though it was also able to interact with an insoluble protein following expression with a mass of roughly 120 kDa. This may indicate the antibody is non-specifically binding to another protein. This protein was not detected in non induced cells so may be a stress response protein *E. coli* has expressed following the onset of expression. The full-length wild type RyR1 expressed in HEK 293T cells was used as a positive control.

4.2.12 Batch purification of the pMALp2g expressed RyR1 N-terminal domain

The carbohydrate binding properties of the MBP tag was used to purify the tagged N-terminal domain. Following protein expression, the cell lysate was incubated with an amylose conjugated resin. Proteins not associated to the resin were washed from the resin. A buffer containing maltose was then used to elute the MBP-tagged ryanodine receptor (figure 4.18).

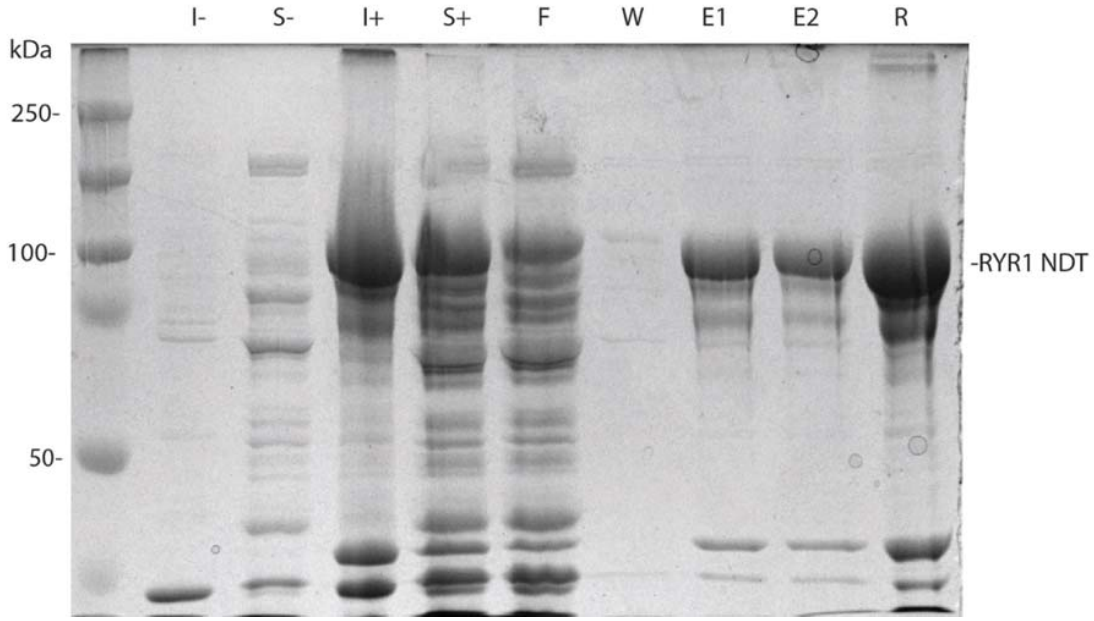

Figure 4.18 Batch purification of MBP-tagged N-terminal domain. Soluble proteins following expression of the pMALp2g vector were incubated with an amylose conjugated resin. The resin was washed removing all non bound proteins. The MBP-tagged RyR1 was then eluted from the resin. Protein samples were resolved by 7 % SDS-PAGE at 120 mV for one hour thirty minutes and visualised by Coomassie blue staining. I represents insoluble proteins. S represents soluble proteins. – represents non induced cells. + represents induced cells. F represents flow thorough following incubation with the amylose resin. W represents supernatant following a wash in non denaturing buffer. E 1-2, represent individual washes in elution buffer. R represents the resin following elution.

The protein thought to correspond to the MBP-tagged RyR1 N-terminal domain was able to interact with and be eluted from the amylose conjugated resin (figure 4.18). A number of proteins other then the tagged N-terminal domain were able to bind to the amylose resin and remained bound through the wash stages, the proteins were also able to be eluted from the resin. It is likely these proteins have specific carbohydrate

binding activities and are specifically interacting with the amylose conjugated resin. As a result, the tagged N-terminal domain could only be partially purified using this method.

4.2.13 Genenase digestion of the MBP-tagged N-terminal domain

Similar to the protein expressed from the pGEX6p3 vector, the MBP-tagged RyR1 N-terminal domain has an unstructured region between the MBP tag and RyR1 though in this case the region contains the recognition site for the protease genenase. The predicted physical properties of the RyR1 N-terminal domain and the cleaved MBP tag have been represented in table 4.6.

	MBP-tagged RyR1 N-terminal domain	MBP	RyR1 N-terminal domain
Amino acid number	977	413	564
Molecular weight (Da)	107640.1	45009.0	62599
Theoretical pI	5.46	5.39	5.49
Extinction coefficients are in units of M^{-1} cm^{-1}, at 280 nm, assuming all cysteine residues are reduced	135220	66350	67280
Aliphatic index	85.23	82.35	88.03

Table 4.6 Proposed physical properties of the MBP-tagged RyR1 N-terminal domain. The parameters were predicted using the ExPASy ProtParam software (119). The MBP-tagged RyR1 N-terminal domain has been compared to the MBP tag and the RyR1 N-terminal domain following digestion.

Initially the genenase digestion was performed on the RyR1 N-terminal domain following elution from the amylose resin (figure 4.19).

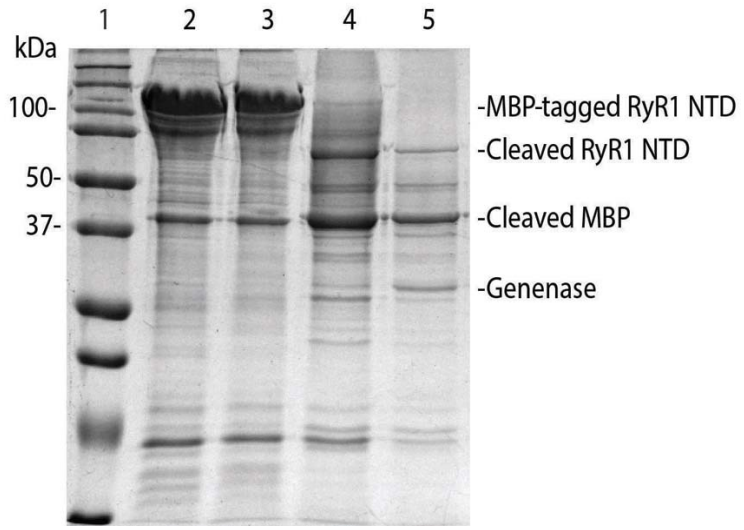

Figure 4.19 Genenase digestion of the MBP-tagged RyR1 N-terminal domain. The N-terminal domain was partially purified using amylose resin and subjected to genenase digestion. Proteins were separted by 12.5 % SDS-PAGE at 120 mV for one hour thirty minutes proteins were visualised by Coomassie blue staining. Lane 1, precision plus size marker. Lane 2, amylose resin before elution. Lane 3, proteins eluted from the amylose resin. Lane 4, eluted fraction following digestion with Genenase. Lane 5, digested fraction following centrifugation at 70,000 x g.

The digestion proceeded to completion with a protein with molecular weight of roughly 60 kDA, the theoretical molecular mass of the cleaved N-terminal domain (table 4.6), being noted. After centrifugation at 70,000 x g the protein thought to correspond to the cleaved N-terminal domain was still soluble although some protein has been removed from the solution (figure 4.19).

4.2.14 Confirming the identity of the RyR1 N-terminal domain

The protein thought to correspond to the cleaved N-terminal was excised from the gel and subjected to in gel digestion by trypsin. Following MALDI MS/MS no peptide fragments corresponding to RyR1 were detected. A number of fragments corresponding to either *E. coli* host proteins or keratin were identified indicating contamination from of lack of purity of the sample and / or contamination during the digestion process.

In an attempt gain a pure RyR1 N-terminal domain following genenase digestion, the digestion was repeated with the MBP-tagged RyR1 N-terminal domain bound to the amylose resin (figure 4.20).

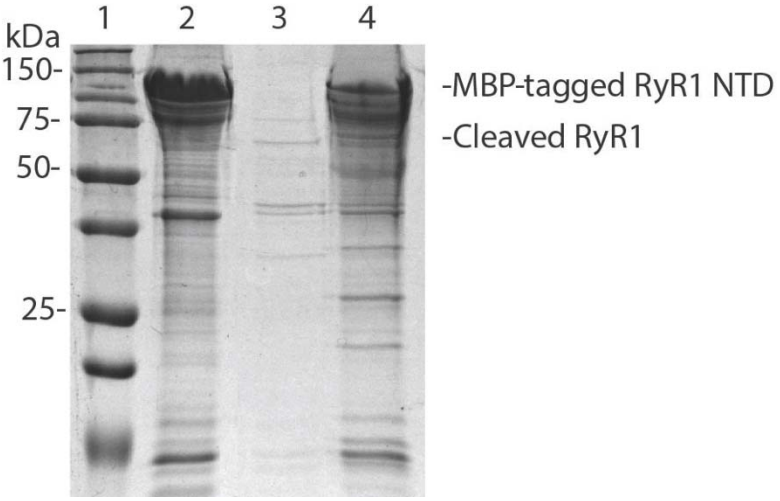

Figure 4.20 Genenase digestion of the MBP-tagged N-terminal domain bound to the amylose resin. Lane 1, precision plus molecular size marker. Lane 2, amylose resin before digestion. Lane 3 supernatant following digestion. Lane 4, resin following digestion. Proteins were separated by 12.5 % SDS-PAGE at 120 mV for one hour thirty minutes and visualised by Coomassie blue staining.

Limited protease digestion was detected in this case. It seems having the N-terminal domain bound to the resin adds limitations to the digestion process. The genenase recognition site may be shielded by the amylose conjugated resin. The potential formation of oligomers may also add further restraints to the digestion process. MALDI MS/MS was attempted to confirm the identity of the protein thought to correspond to the cleaved N-terminal domain however no fragments corresponding to RyR1 were detected. Many of the proteins detected corresponded to keratin, likely indicating the digestion process was subject to contamination.

4.3 Chapter summary

The N-terminal domain of the skeletal muscle ryanodine receptor, expressed from codon optimised cDNA from the pGEX6p3 and pMALp2g vectors is soluble. Each protein has been partially purified and protease digestion to remove the respective tag has been performed. The identity of the RyR1 N-terminal domain expressed from

the pGEX6p3 vector was confirmed by MALDI MS/MS. However, the identity of the N-terminal domain expressed from the pMALp2g vector has yet to be confirmed.

Chapter 5 Over expression and purification of the RyR1 helical domain

5.1 Introduction

The central region of RyR1 is comprised of a number of putative domains, each playing a significant role in the regulation of the channel (14). Following the production of the near atomic resolution cryo-EM structure of rabbit RyR1, two domains within the central region were shown to form extensive interdomain interactions with the N-terminal domain (the handle domain and the helical domain) (14) (figure 5.1). During the opening of the channel, the handle and helical domains have been shown to move relative to the N-terminal domain in a very structured manner (18, 108, 125). It is thought specific MH-linked variants within these regions have the potential to disrupt specific interactions between the domains leading to the dysregulation of the channel and the onset of MH symptoms (17).

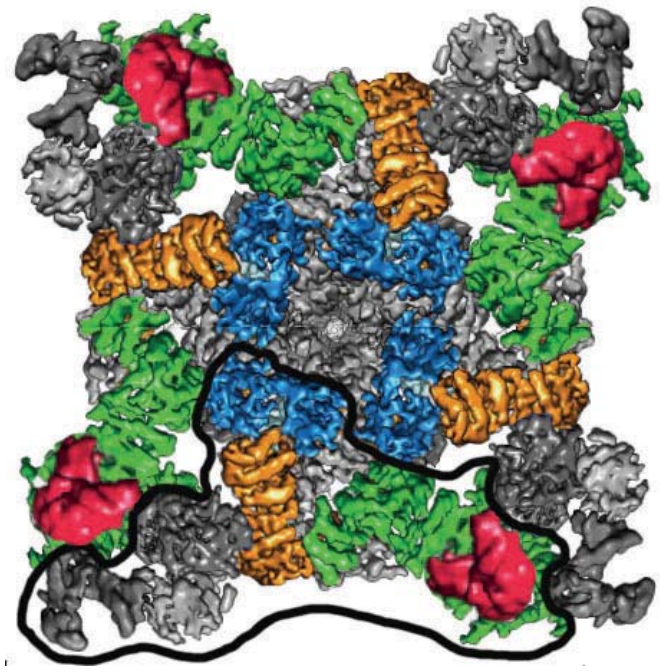

Figure 5.1 Location of the central region with respect to the RyR1 channel tetramer. Represented is a cytoplasmic view of the RyR1 tetramer. The N-terminal domains A and B have been represented in blue. Domain C along with the handle domain are represented in orange. The helical domain is represented in green and red. A single subunit is outlined in black. Figure adapted from (15), permission to use figure was obtained through RightsLink.

The greater helical domain is thought to contain three sub domains, the HD1 domain, the previously structurally characterised phosphorylation domain (126), and the HD2 domain. Following the generation of the of the cryo-EM structure of the full-length rabbit RyR1 the greater helical domain was not well resolved (14). The structural resolution of the HD1 and HD2 domains, comprising amino acids 2146–2712 and 3016–3572 respectively, was high enough to trace the amino acid back bone leading to an interpretation of secondary structure formation where both regions were shown to be rich in alpha helices. The phosphorylation domain, amino acids 2734–2940, located at the periphery of the channel, was not well resolved and only domain distribution was detected (figure 5.2).

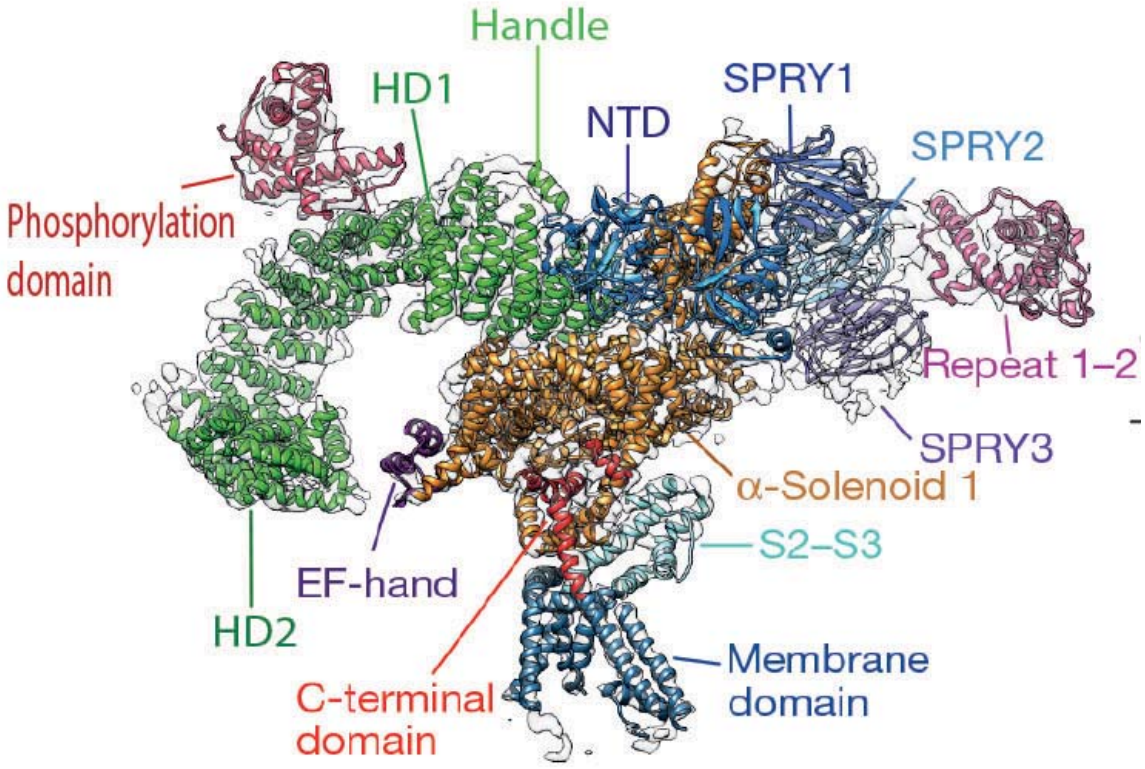

Figure 5.2 Domain distribution of the RyR1 monomer. Proposed domains of RyR1 have been represented in individual colours. Figure adapted from (15) permission to use figure was obtained through RightsLink.

No high resolution structural analysis has been performed on the HD1 domain in its entirety to date. The DP4 domain, comprising amino acids 2442-2477, has been characterised by NMR (91). The domain may only be 35 amino acids long but it contains a significant number of MH-linked variants, indicating the region plays a significant role in the channel, where it is likely involved in the regulation of the

channel in the closed state. It has also been implicated in the formation of interdomain interactions (17, 92).

The HD1 domain also houses the second region of high amino acid identity shared with the IP3R. In this case the RIH domain corresponds to RyR1 amino acids 2186-2365 (GenBank accession number NP_000531.2) (112) (figure 5.3). The RIH domain in this case was implicated in the formation of interdomain interactions with the adjacent N-terminal and handle domains (14). The amino acid identity shared between the two Ca^{2+} channels may suggest the region plays a key regulatory role within both channels or is involved in common conformational changes during the opening of each channel.

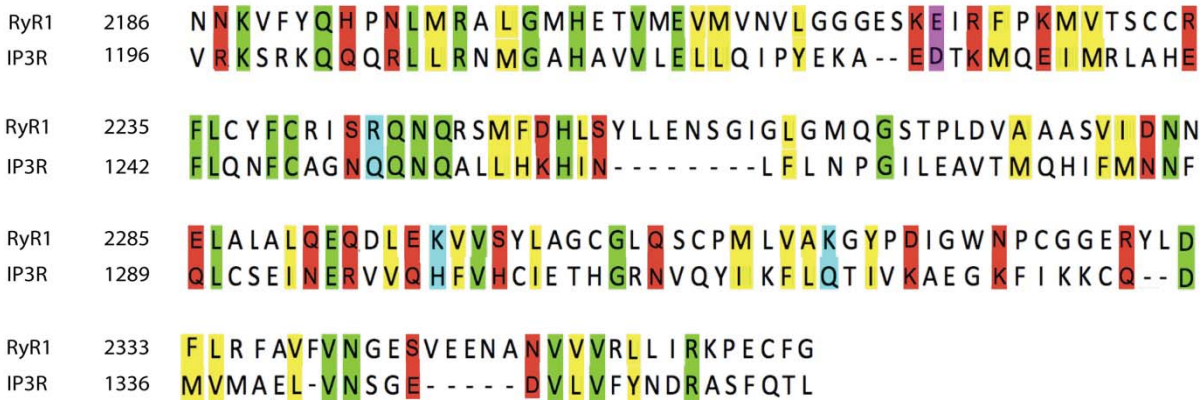

Figure 5.3 Sequence alignment of the RIH domain from RyR1 and IP3R. The amino acid numbers have been indicated. Amino acids highlighted in green indicate a conserved amino acid. Blue highlights a conserved positive charge. Pink highlights a conserved negative charge. Yellow highlights conserved hydrophobic properties. Red highlights conserved polar properties.

Glutamic acid 2348 is thought to reside within an alpha helix within the HD1 domain (14). The deletion of this amino acid has been linked to the onset of MH symptoms under certain conditions (97). The deletion of this amino acid may inhibit the formation of secondary and / or tertiary structure potentially limiting the formation of interdomain interactions or may limit the binding of regulatory signals leading to the onset of MH symptoms.

5.2 Results

5.2.1 Bioinformatic analysis

A truncated region of the HD1 domain of the pig cardiac ryanodine receptor, RyR2, amino acids 2326-2432 (accession number X98330) has been functionally characterised (127). This region was shown to interact with both ATP and caffeine, and while originally implicated in the binding of FKBP12 (36, 128, 129) no interaction between these two proteins was detected. The region was structurally characterised by circular dichroism though to date no high resolution structural analysis has been performed. The human RyR1 shares a region of high amino acid identity with the characterised region of pig RyR2 (figure 5.4). The high amino acid identity suggests the region is likely involved in the common regulation of both channels.

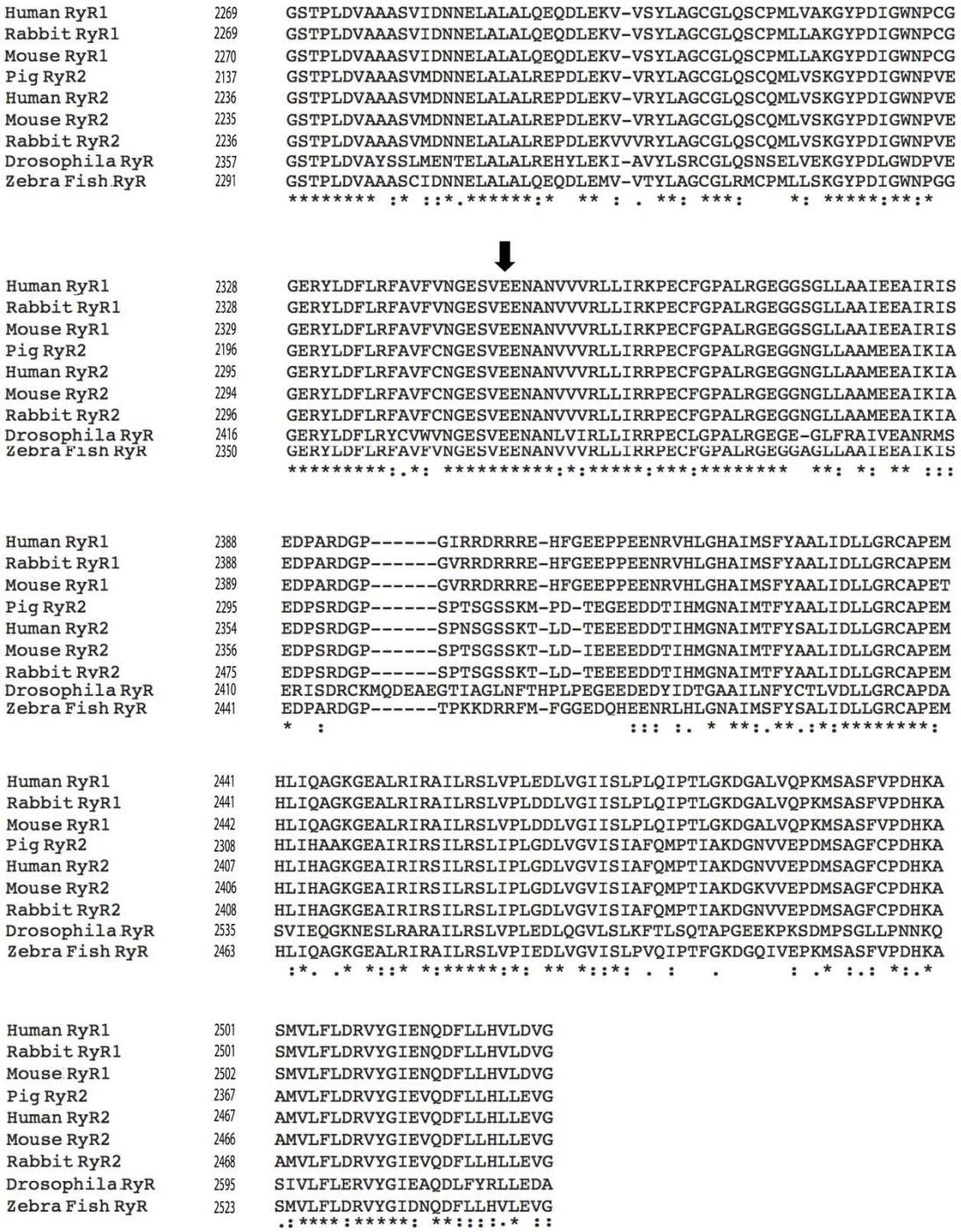

Figure 5.4 Sequence alignment of RyR1 and RyR2 HD1 regions from a range of organisms. The Clustal omega software (116) was used to align the amino acid sequence of RyR1 and 2 from a range of organisms. The amino acid numbers have been indicated. * indicates an identical amino acid, . indicates a somewhat conserved amino acid. : indicates a conserved amino acid chemistry as defined by Clustal. Glutamic acid 2348 has been indicated by the black arrow.

The amino acid sequence identity of the previously characterised pig RyR2 region is maintained across RyR isoforms from a range of organisms. Drosophila has the most divergent RyR sequence though much of the amino acid identity is maintained (figure 5.4). In some cases, an amino acid's identity will be maintained with respect to RyR1 though the corresponding amino acid of RyR2 is different. This is particularly prevalent between amino acids 2388-2410 of human RyR1. This may indicate these amino acids are involved in the isoform-specific regulation of each channel, or may have little or no role in structural formation of the channel. Glutamic acid 2348 is conserved across all organisms and RyR isoforms, indicating that this amino acid may have some importance in domain structure and function.

The human RyR1 amino amino acid 2269-2525 sequence, the region of RyR1 corresponding to the previously characterised region of pig RyR2, was submitted to the PHYRE 2.0 software (118) for secondary structure prediction. The amino acid sequence was aligned with the full-length rabbit RyR1, structurally characterised by cryo-EM at 9.6 Å. With 99 % sequence identity the known rabbit RyR1 structure was used as a reference to predict the distribution of secondary structure of the human RyR1 region with 100 % confidence (figure 5.5).

Figure 5.5 Secondary structure prediction of the RyR1 amino acids 2269-2525. The PHYRE 2.0 software was used to predict the secondary structure of the RyR1 region. lane 1, the predicted secondary structure of human RyR1. Lane 2, the amino acid sequence of human RyR1. Lane 3, the amino acid sequence of rabbit RyR1. Lane 4, the known structure of rabbit RyR1 determined by cryo EM at 9.6 Å. Lane 5, the predicted structure of rabbit RyR1 using software algorithms. The blue arrows indicate predicated beta stand, green helices indicate predicted alpha helical structure, T indicates a hydrogen bonded turn. S indicates a bend in structure. Glutamic acid 2348 has been indicated by the black arrow.

The RyR1 region was predicted to be comprised of a number of alpha helices (figure 5.5). The amino acids 2388-2410 were predicted to be unstructured, it is interesting to note these amino acids correspond the region of RyR1 that has very little sequence identity with RyR2 (figure 5.4). The PHRYE 2.0 software predicts glutamic acid 2348 to be located within an unstructured region. The RyR1 region had some sequence similarity with other proteins submitted to the protein data bank though the sequence identity was significantly lower, resulting in a lower confidence score for the structure prediction.

The RyR1 amino acids 2370-2375 (46) and 2402-2795 (45) have been linked to the binding of ATP leading to an up regulation of channel function. Both ADP and AMP have also been shown to interact with RyR1, having an opposite effect on regulation and are thought to interact with the same nucleotide binding motif with a lower

affinity (45). Caffeine's interaction with RyR1 has also been linked with the amino acids 2370-2375 (46), it has been suggested ATP and caffeine interact with the same binding pocket.

Functional characterisation of the pig RyR2 amino acids 2326-2432 indicated that the region could interact with ATP, ADP, AMP and caffeine (127). The high amino acid identity shared between RyR isoforms suggests the corresponding region of RyR1 may contain a common ATP binding motif. Bioinformatic analysis of RyR2 suggested the region contains an ATP binding motif commonly found in P-loop kinases which are a diverse family of proteins with the potential to transfer the γ phosphate of ATP onto other proteins, nucleotides and other small molecules within the cell (130). P-loop kinases contain a glycine rich loop region commonly referred to as the Walker A motif, which has been linked to hydrolysis of ATP. Two other highly conserved regions, Walker B and lid motifs, aid in the binding of ATP leading to hydrolysis (130). While RyR2 has been suggested to house the characteristic ATP binding motifs, the channel has yet to be shown to hydrolyse the nucleotide. The corresponding region of RyR1 was aligned with the characterised region of RyR2 and a number of other previously characterised P-loop kinases to analyse the ATP binding potential of the region (figure 5.6).

Figure 5.6 Sequence alignment of the proposed ATP binding motif of RyR1, RyR2 and three examples of P-loop kinases. The Walker A, Walker B and lid motifs have been highlighted. Human RyR1 was compared to the previously characterised pig RyR2, along with previously characterised P-loop kinases; adenylate kinase, *Solfolobus acidocaldarius* (131); thymidylate kinase, *E. coli* (132); guanylate kinase, *Saccharomyces cerevisiae* (133)

Both RyR1 and 2 contain the characteristic motifs for ATP binding including the Walker A (GXXXGKT/S), Walker B (hhhD) and Lid motifs (RXXXR). It is interesting to note both RyR isoforms lack the amino acids required for ATP hydrolysis, K and T/S in the Walker A motif (134). The substitution of these two amino acids for two

leucine residues is likely to explain the lack of ATP hydrolysis. The proposed Walker A motif corresponds to the RyR1 amino acids 2370-2378, housing the glycine residues 2370, 2373 and 2375 previously implicated in the binding of both ATP and caffeine (46).

5.2.2 Cloning strategy

PCR primers were designed to amplify the *RYR1* cDNA nucleotides 6,807-7,575 (accession number NM_000540.2) corresponding to amino acids 2269-2525. The region included the previously characterised DP4 domain, the proposed ATP binding motif and glutamic acid 2348, in this case only part of the RIH domain. The RIH domain was truncated to the same extent during the functional characterisation of the corresponding region of pig RyR2 indicating the homology domain is not essential for the region to adopt a soluble and stable tertiary structure. Specific restriction endonuclease sites were included in the primers for directional cloning into a range of bacterial expression vectors (pET32a, pProEXHtb and pGEX6p3). Each adds a specific tag to the proposed RyR1 domain with the potential to aid in solubility and purification. As each vector has a different reading frame and different restriction endonuclease recognition sites present in the multiple cloning site, specific primers were used to amplify the *RYR1* cDNA for cloning into each vector. The plasmid pc*RYR1* wild type was used as the template for PCR amplification

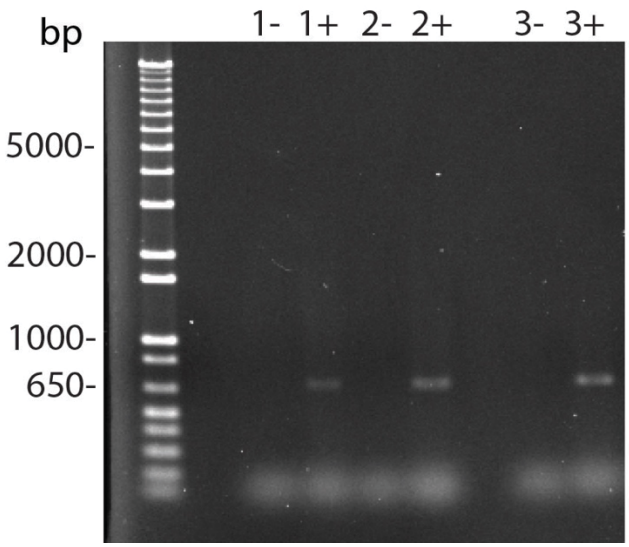

Figure 5.7 PCR amplification of *RYR1* nucleotides 6,807-7,575. PCR products, 20 % of the reaction volume, were loaded into a 2 % (w/v) agarose gel and separated at 80 volts for one hour. DNA was visualised by 0.5 µg/mL ethidium bromide staining using the Image Lab 5.1 software. 1, Amplification using primers specific for the pET32a vector. 2, Amplification using primers specific for the pProEXHTb vector. 3, Amplification using primers specific for the pGEX6p3 vector. – represents a negative control, with no template DNA added. + represents reactions amplifying pc*RYR1*.

PCR products showed a single band of the expected size and no contamination was detected in the no template controls (figure 5.7). The PCR products were digested with specific restriction endonucleases and ligated into their respective expression vectors (appendix VII). Sanger sequencing confirmed the correct reading frame was maintained in all three vectors along with the absence of PCR induced nucleotide variants.

The expression of each vector will add a different N-terminal tag to the proposed RyR1 helical domain. Each tag has the potential to aid in the expression and purification of the expressed protein and may alter the properties of the RyR1 region. The ExPASy ProtParam software (119) was used to predict the parameters of the proposed RyR1 helical domain expressed from each vector (table 5.1).

Physical property	pET32a	pPROEXHTb	pGEX6p3
Amino acid number	395	288	456
Size (kDa)	42614.5	31399.7	51031.9
Theoretical pI	5.53	4.76	5.39
Extinction Coefficient M^{-1} cm^{-1}, at 280 nm. assuming all cysteine residues are reduced	25440	18910	54320
Aliphatic index	95.41	94.15	97.54

Table 5.1 Predicted physical properties of the RyR1 amino acids 2269-2525 expressed from a range of expression vectors. Properties of each protein were determined using the ExPASy ProtParam software.

The size, in kDa, of the proposed helical domain expressed from each vector is different in each case due to the different tag added by each vector (table 5.1). The theoretical pI does not differ significantly; buffers used to solubilise each polypeptide will need to have a pH above 6.5 to ensure the RyR1 region has a net negative charge preventing precipitation. The proposed helical domain expressed from each vector has an aliphatic index above 80, indicating the region has a high content of hydrophobic amino acids. The corresponding region of pig RyR2 contained a comparable number of hydrophobic amino acids, the expressed polypeptide was soluble indicating the high content of hydrophobic amino acids has no effect on solubility. As the RyR1 region has a high amino acid identity it was thought the seemingly high hydrophobic amino acid content would not effect solubility.

5.2.3 Initial expression

E. coli, BL21(DE3), were transformed with each expression vector individually. The cells were grown in LB broths at 37 °C and upon reaching an $O.D_{600}$ of 0.6 expression was induced by the addition of IPTG to a final concentration of 0.1 mM. The cells were incubated at 37 °C for a further three hours before being harvested by centrifugation. The cells were suspended in sonication buffer (20 mM Tris HCl pH 8.0, 500 mM NaCl, 3% glycerol, 2 mM DTT, 1 mM EDTA, 1X cOmplete Mini EDTA-free protease inhibitor) and lysed by sonication. Soluble and insoluble fractions were separated by centrifugation at 13,000 x g for ten minutes and analysed by SDS-

PAGE (figure 5.8). The induction of expression of each vector in transformed BL21(DE3) cells lead to insoluble protein.

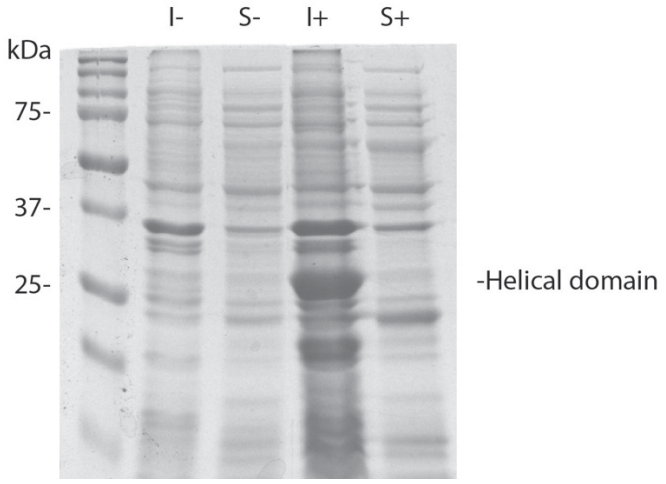

Figure 5.8 the RyR1 helical domain expressed from the pProEXHTb vector. I represents insoluble proteins, S represents soluble proteins. – represents non induced cells, + represents induced cells.

5.2.4 Optimisation of expression

Expression conditions were altered in an attempt to improve solubility. Cells were grown to an $O.D_{600}$ of 0.6 at 37 °C. Following the addition of 0.1 mM ITPG the cells were incubated at the temperatures 18, 25 or 30 °C, but no soluble protein was detected. In another approach the cells were placed under stress, encouraging the expression of chaperonin proteins, prior to induction either by being placed on ice for ten minutes or by adding ethanol to the culture to a final concentration of 2 %. Cells were incubated at 18 °C for thirty minutes before expression was induced by 0.1 mM IPTG, but no soluble protein was expressed.

The sonication buffer was identical to the one used by Blayney *et al* during the characterisation of pig RyR2. The high NaCl concentration of 500 mM and pH of 8.0 may be denaturing the expressed protein following cell lysis. Components of the sonication buffer were altered to resemble physiological conditions. The alteration of the ionic strength and pH did not increase the solubility of the expressed RyR1 helical domain. The cysteine residues 2326 and 2363 have been implicated in the formation of disulphide bonds in full-length RyR1 with adjacent domains (55, 58).

When the proposed helical domain was expressed in isolation from the rest of the channel there was potential for disulphide bond formation to occur within the domain limiting protein folding if the surrounding environment was too oxidising. The concentration of the the reducing agent, DTT, was increased to 5 mM though this did not improve solubility, neither did the use of a second stronger reducing agent 5 mM tris(2-carboxyethyl)phosphine. A summary of the expression conditions and protein solubility is represented in table 5.2

Cell line	Condition	pET32a	pProEXHTb	pGEX6p3
BL21(DE3)	Expressed at 37 °C	Insoluble	Insoluble	Insoluble
	Expressed at 18, 25 and 30 °C	Insoluble	Insoluble	Insoluble
	Heat stress	Insoluble	Insoluble	Insoluble
	Ethanol induced stress	Insoluble	Insoluble	Insoluble
	Physiological sonication buffer	Insoluble	Insoluble	Insoluble

Table 5.2 Summary of the solubility of RyR1 amino acids 2269-2525 expressed from a range of expression vectors in BL21 (DE3) cells.

Rosetta (DE3) cells were transformed with each vector. Expression was induced as described for BL21(DE3) cells (section 5.2.4) with all conditions being taken into account, but again no soluble protein was expressed (table 5.3)

Cell line	Condition	pET32a	pProEXHTb	pGEX6p3
Rosetta (DE3)	Expressed at 37 °C	Insoluble	Insoluble	Insoluble
	Expressed at 18, 25 and 30 °C	Insoluble	Insoluble	Insoluble
	Heat stress	Insoluble	Insoluble	Insoluble
	Ethanol induced stress	Insoluble	Insoluble	Insoluble
	Physiological sonication buffer	Insoluble	Insoluble	Insoluble

Table 5.3 Summary of the solubility of RyR1 amino acids 2269-2525 expressed from a range of expression vectors in Rosetta (DE3) cells.

To aid in the folding of the proposed helical domain, BL21(DE3) cells were co transformed with a second expression vector coding for the chaperonin protein Gro

ES/EL. Expression of Gro ES/EL is under the control of an IPTG inducible promoter, and was expressed along side the helical domain. Gro ES/EL hydrolyses ATP to aid in the folding of globular proteins causing the protein to adopt its native structure (135).

Cell line	Condition	pET32a	pProEXHTb	pGEX6p3
BL21(DE3) Gro ES/EL	Expressed at 37 °C	Insoluble	Insoluble	Insoluble
	Expressed at 18, 25 and 30 °C	Insoluble	Insoluble	Insoluble
	Heat stress	Insoluble	Insoluble	Insoluble
	Ethanol induced stress	Insoluble	Insoluble	Insoluble
	Physiological sonication buffer	Insoluble	Insoluble	Insoluble

Table 5.4 Summary of the solubility of RyR1 amino acids 2269-2525 expressed from a range vectors in BL21(DE3) Gro ES/EL.

The expression of the chaperone did not result in expression of soluble protein (table 5.4), likely indicating the RyR1 helical domain is forming insoluble aggregates within the *E. coli* expression hosts.

5.2.5 *In vitro* re folding

In vitro refolding is a method designed to denature and solubilise insoluble protein aggregates. The removal of denaturant has been shown in some cases to cause the protein to renature into a soluble and stable protein (136).

Expression of each vector was induced in BL21(DE3) cells with 0.1 mM IPTG. Following lysis, the insoluble fraction was washed in a range of buffers to remove phospholipids and insoluble membrane proteins, leaving behind insoluble protein aggregates. The insoluble fraction following the final wash was suspended in solubilisation buffer (50 mM tris HCl pH 9.0, 150 mM NaCl, 10 mM β mercapoethanol, 6 M urea). The polypeptides expressed from the pGEX6p3 and pProEXHTb vectors dissolved into the buffer. However, the polypeptide expressed from the pET32a vector remained insoluble. Dialysis was performed on the pGEX6p3 and pProEXHTb expressed protein into refolding buffer (50 mM tris pH

9.0, 150 mM NaCl, 10 mM β mercapoethanol) but both polypeptides quickly dropped out of solution. Following separation of soluble and insoluble fractions no soluble protein was detected. To improve the solubility of the polypeptide expressed from the pET32a vector the concentration of the urea in the solubilisation buffer was increased to 8 M but the protein remained insoluble. A second solubilisation buffer was used (50 mM Tris HCl pH 9, 300 mM NaCl, 10 mM β mercapoethanol, 6 M guanidine hydrochloride) which was able to dissolve all three polypeptides. Again during dialysis all protein dropped out of solution quickly and no soluble protein was detected. Alterations were made to the refolding buffer: The NaCl concentration was increased to 300 mM and 500 mM, glycerol was added to a final concentration of 5 % and the pH was decreased to 7.5, but no soluble protein was detected.

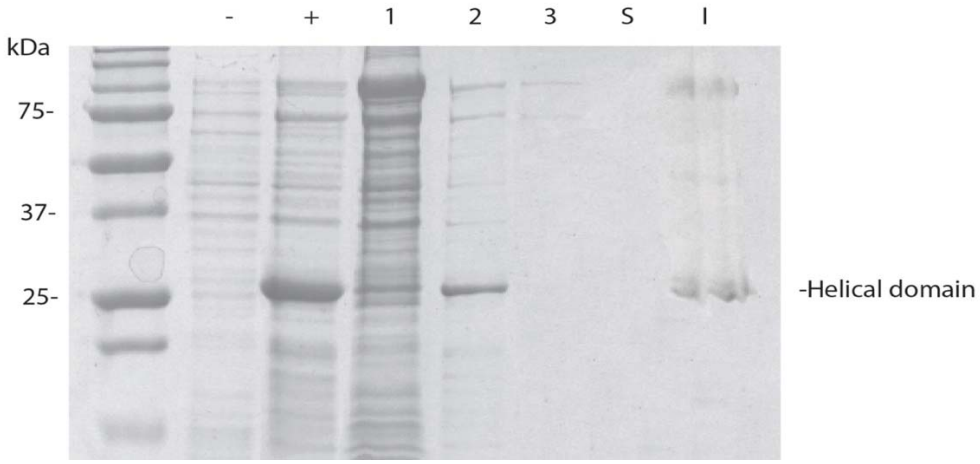

Figure 5.9 *In vitro* re folding of the RyR1 amino acids 2269-2525 expressed from the pProEXHTb vector. Insoluble proteins were separated from soluble proteins following cell lysis, protein aggregates were purified and subjected to denaturation and re folding. – indicates insoluble proteins from non induced cells. + indicates insoluble proteins from induced cells. The numbers 1-3 represent soluble proteins following each wash step. S represents soluble proteins following refolding. I represents insoluble proteins following refolding. Protein fractions were separated by SDS-PAGE resolved at 120 mV for one hour thirty minutes, proteins were visualised by Coomassie blue staining.

A small amount of the proposed RyR1 helical domain was soluble in wash buffers 1 and 2 (figure 5.9). Buffer 1 contained triton x100, a non ionic detergent used to solubilise membrane proteins and phospholipids during the purification of insoluble protein aggregates (136). When the insoluble protein fraction was washed in this buffer, proteins with an exposed hydrophobic surface area and phospholipids were likely solubilised by incorporation into triton x100-derived micelles. A significant

number of proteins were solubilised in this buffer. Buffer 2 contains 3-((3-cholamidopropyl) dimethylammonio)-1-propanesulfonate, a zwitterionic detergent commonly used in the solubilisation of membrane proteins and phospholipids under nondenaturing conditions. Similar to triton x100, 3-((3-cholamidopropyl) dimethylammonio)-1-propanesulfonate was likely to solubilise proteins with an exposed hydrophobic surface area by micelle formation. The RyR1 helical domain is to some extent soluble in both buffers suggesting the protein may have some exposed hydrophobic surface area causing it to be insoluble following expression. As the helical domain is predominantly insoluble in both buffers it is a strong indication the expressed protein is insoluble due to protein aggregation. No RyR1 helical domain is soluble in wash buffer 3 the buffer contains 2 M NaCl. A concentration of NaCl this high was used to disrupt any non specific ionic interactions that may have formed between *E. coli* host proteins and the aggregated helical domain. In theory purifying the aggregated RyR1 helical domain. While no soluble protein was noted in this study following *in vitro* refolding, an optimised combination of denaturing and refolding buffers may result in the refolding of the helical domain.

The induction of expression of the RyR1 amino acids 2269-2525 from a range of expression vectors all resulted in insoluble protein. As a result, further analysis of the RyR1 region could not be performed. The slightly divergent amino acid sequence of RyR1 compared to the previously characterised region of pig RyR2 region may have had an effect on the solubility of the region, however, the use a different expression vector may also have been a factor. The expressed region of RyR1 is thought to reside on the cytoplasmic face of the channel. However, the region is rich in hydrophobic amino acids which may have been the cause of the insolubility of the region when expressed in isolation from the rest of the channel.

5.2.6 Bioinformatic analysis

It was thought increasing the boundaries of the proposed helical domain to include the RIH domain in its entirety may aid in improving the solubility of the expressed polypeptide. The RyR1 amino acid 2091-2525 sequence housing the RIH domain, the DP4 domain, the proposed ATP binding motif and glutamic acid 2348 was

submitted to the PHYE 2.0 software (118) for secondary structure analysis (figure 5.10).

Figure 5.10 Secondary structure prediction of the human RyR1 amino acids 2091-2525. The secondary structure prediction was performed by the PHYRE 2.0 software with the human RyR1 amino acid sequence being compared to the previously characterised full-length rabbit RyR1. Lane 1, the predicted secondary structure of human RyR1. Lane 2, the sequence of human RyR1. Lane 3, the sequence of rabbit RyR1. Lane 4, the known structure for rabbit RyR1. Lane 5, the predicted structure of rabbit RyR1 using software algorithms. The blue arrows indicate predicted beta strand, green helices indicate predicted alpha helical structure, T indicates a hydrogen bonded turn. S indicates a bend in the structure. Glutamic acid 2348 has been indicated by the black arrow.

The PHYRE 2.0 software was able to predict the secondary structure of the human RyR1 amino acids 2091-2525 with 100 % confidence using the full-length rabbit RyR1, previously characterised by cryo-EM at 9.6 Å, as a reference. The two proteins have 99 % sequence identity, and are predicted to adopt a similar structure, rich in alpha helices.

5.2.7 Cloning strategy

PCR primers were designed to amplify *RYR1* cDNA nucleotides 6,271-7,575, corresponding the RyR1 amino acids 2091-2525. The resulting PCR products were cloned into the expression vectors pProEXHTb vector and the previously unused pMALp2g vector (appendix VIII). Sanger sequencing confirmed the cloning of *RYR1* cDNA into both expression vectors, sequencing also confirmed the reading frame was maintained along with no introduction of PCR induced nucleotide variants leading to an alteration in amino acid sequence.

The ExPASy ProtParm software (119) was used to predict the physical properties of the protein expressed from each vector (table 5.5).

Physical property	pProEXHTb	pMALp2g
Amino acid number	463	854
Size (Da)	51622.5	94000.7
Theoretical pI	5.59	5.40
Extinction Coefficient M^{-1} cm^{-1}, at 280 nm. assuming all cysteine residues are reduced	30370	94365
Aliphatic index	97.90	92.21

Table 5.5 Predicted physical properties of the RyR1 amino acids 2091-2525 expressed from the pProEXHTb and pMALp2g vectors. Properties of each protein were determined using the ExPASy ProtParam software.

5.2.8 Optimisation of the expression of the proposed helical domain

BL21(DE3) cells were transformed with each expression vector individually and expression was induced by IPTG. The expression conditions used during the initial optimisation of the proposed helical domain (section 5.2.4) were replicated. A summary of protein solubility following expression of each vector is presented in table 5.6.

Cell line	Condition	pProEXHTb	pMALp2g
BL21(DE3)	Expressed at 37 °C	Insoluble	Soluble
	Expressed at 18 °C	Insoluble	Soluble
	Heat stress	Insoluble	Soluble
	Ethanol induced stress	Insoluble	Soluble
	Physiological sonication buffer	Insoluble	Soluble

Table 5.6 Summary of the solubility of RyR1 amino acids 2091-2525 expressed from the pProEXHTb and pMALp2g vectors in BL21(DE3) cells.

The proposed helical domain was insoluble when expressed from the pProEXHTb vector (table 5.6). The proposed domain was soluble when expressed from the pMALp2g vector (figure 5.11). The inclusion of the RIH domain may have aided in improving the solubility of the domain, however the use of a different expression vector adding a different N-terminal tag to the domain may also have aided in improving the solubility.

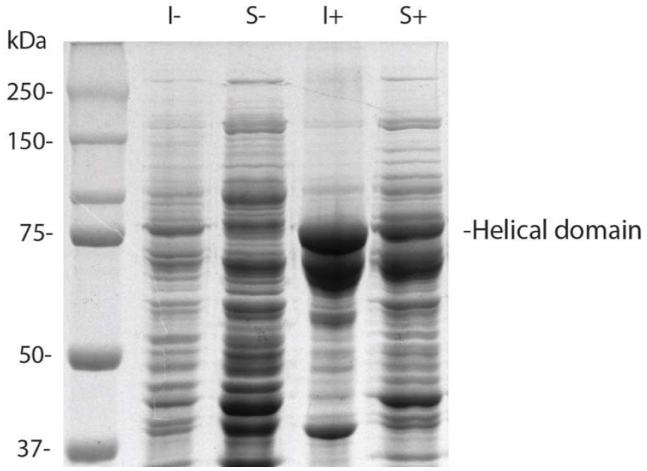

Figure 5.11 Expression of the RyR1 helical domain from pMALp2g vector. Following expression, soluble and insoluble fractions were separated by 7 % SDS-PAGE at 120 mV for one hour thirty minutes, proteins were visualised by Coomassie blue staining. I represents insoluble protein. S represents insoluble proteins. – represents cells that have not been induced by IPTG. + represents cells where expression has been induced by IPTG.

Two proteins approximately 70 and 80 kDa in size were noted in both the insoluble and soluble fractions following expression of the pMALp2g vector (figure 5.11).

When compared to the non-induced controls no protein of these molecular weights were visible. The theoretical molecular mass of the RyR1 helical domain expressed from the pMALp2g vector is predicted to be 94 kDa (table 5.5). Potentially suggesting the helical domain may have been subjected to protease digestion by *E. coli* host proteases or the protein may migrate through the gel with an increased motility then its predicted molecular mass may indicate. Mass spectrometry was used to confirm the identity of the protein thought to correspond to the MBP-tagged RyR1 helical domain expressed from the pMALp2g vector. Following expression, cells were lysed and the resulting cell lysate was resolved by SDS-PAGE. The band thought to correspond to the tagged RyR1 helical domain was excised from the gel, and subjected to in-gel digestion by trypsin at the Centre for Protein Research, Otago University, New Zealand. Following digestion protein fragments were eluted from the gel, the sequence of each resulting fragment was determined by MALDI MS/MS.

1	MKIKTGARIL	ALSALTTMMF	SASALAKIEE	GKLVIWINGD	KGYNGLAEVG
51	KKFEKDTGIK	VTVEHPDKLE	EKFPQVAATG	DGPDIIFWAH	DRFGGYAQSG
101	LLAEITPDKA	FQDKLYPFTW	DAVRYNGKLI	AYPIAVEALS	LIYNKDLLPN
151	PPKTWEEIPA	LDKELKAKGK	SALMFNLQEP	YFTWPLIAAD	GGYAFKYENG
201	KYDIKDVGVD	NAGAKAGLTF	LVDLIKNKHM	NADTDYSIAE	AAFNKGETAM
251	TINGPWAWSN	IDTSKVNYGV	TVLPTFKGQP	SKPFVGVLSA	GINAASPNKE
301	LAKEFLENYL	LTDEGLEAVN	KDKPLGAVAL	KSYEEELAKD	PRIAATMENA
351	QKGEIMPNIP	QMSAFWYAVR	TAVINAASGR	QTVDEALKDA	QTNSSSNNNN
401	NNNNNNLGPG	AAHYVEFGSP	RSLQELVSHM	VVRWAQEDFV	QSPELVRAMF
451	SLLHRQYDGL	GELLRALPRA	YTISPSSVED	TMSLLECLGQ	IRSLLIVQMG
501	PQEENLMIQS	IGNIMNNKVF	YQHPNLMRAL	GMHETVMEVM	VNVLGGGESK
551	EIRFPKMVTS	CCRFLCYFCR	ISRQNQRSMF	DHLSYLLENS	GIGLGMQGST
601	PLDVAAASVI	DNNELALALQ	EQDLEKVVSY	LAGCGLQSCP	MLVAKGYPDI
651	GWNPCGGERY	LDFLRFAVFV	NGESVEENAN	VVVRLLIRKP	ECFGPALRGE
701	GGSGLLAAIE	EAIRISEDPA	RDGPGIRRDR	RREHFGEEPP	EENRVHLGHA
751	IMSFYAALID	LLGRCAPEMH	LIQAGKGEAL	RIRAILRSLV	PLEDLVGIIS
801	LPLQIPTLGK	DGALVQPKMS	ASFVPDHKAS	MVLFLDRVYG	IENQDFLLHV
851	LDVG				

Figure 5.12 MS/MS results for the gel purified MBP-tagged RyR1 helical domain. Peptides identified are highlighted in red.

Twenty-three fragments were detected leading to a total amino acid coverage of 39% of the expressed protein. The fragments were spread over the maltose binding protein tag and the ryanodine receptor confirming the identity of the expressed protein (figure 5.12). There were no sequence reads covering the last 150 amino acids of the helical domain. The region of RyR1 contains a number of arginine residues so trypsin should be able to digest this region of the polypeptide (137). However, the resulting fragments may not have been efficiently eluted from the gel

and as a result could not be analysed by MS/MS. Following expression, proteolysis of the RyR1 helical domain may have occurred by *E. coli* host proteases digesting the C-terminal region of the RyR1 domain. Protease digestion may explain the decreased molecular mass of 80 kDa compared to the predicted molecular mass of 95 kDa (table 5.5) and the lack of sequence reads during MS/MS in this region.

5.2.9 Purification of the RyR1 helical domain using an amylose conjugated magnetic resin

An amylose conjugated magnetic resin was used to purify the MBP-tagged helical domain. After induction of expression and cell lysis, soluble proteins were incubated with the resin. The resin was washed removing all non-specifically bound proteins. The tagged RyR1 helical domain was eluted from the resin (figure 5.13).

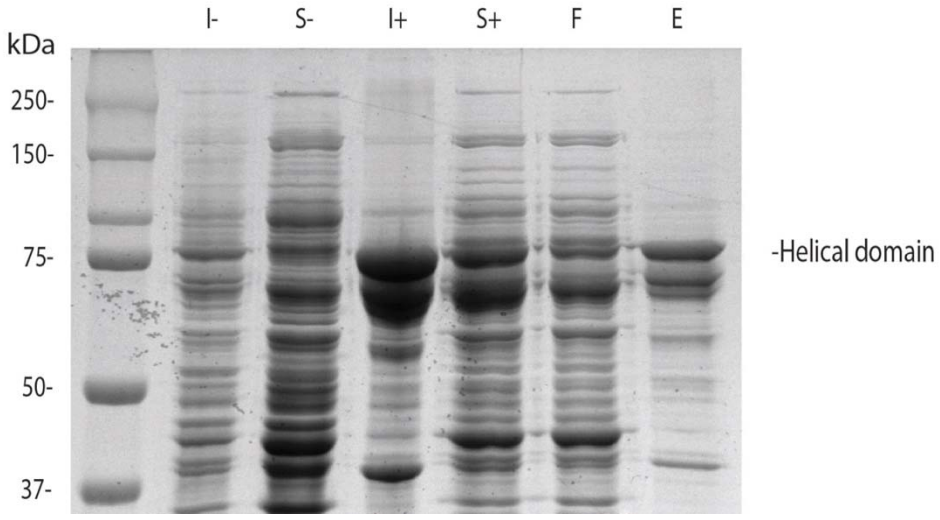

Figure 5.13 Purification of the MBP-tagged RyR1 helical domain using an amylose conjugated resin. Protein was expressed in BL21(DE3) cells. Following cell lysis, the helical domain was bound using an amylose conjugated resin. Following the removal of all non-specifically bound proteins the MBP-tagged helical domain was eluted from the resin. All fractions were resolved by 7.5 % SDS-PAGE at 120 mV for 1.5 hours proteins were visualised by Coomassie blue staining. I represents insoluble proteins, S represents soluble protein. – represents cells non induced by IPTG. + represents cells induced by IPTG. F is the flow through following incubation of protein with the amylose resin. E, all protein eluted from the resin.

The maltose binding protein tag was able to bind to and be eluted from the amylose resin (Figure 5.13). A number of other proteins were also able to interact with the amylose resin. These proteins were also able to be eluted from the resin indicating their interaction with the amylose is specific. As a result, the tagged helical domain could only be partially purified.

5.2.10 Genenase digestion of the MBP-tagged RyR1 helical domain

The protein expressed from the pMALp2g vector contains the recognition site for the protease genenase between the MBP tag and the RyR1 helical domain. The enzyme has a specific recognition sequence of Tyr, His and will only cleave proteins at this site. The MBP tag was specifically removed from the helical domain to continue the characterisation of the domain without interference from the tag. The physical properties of the RyR1 helical domain following the removal of the tag were predicted using the ExPASy ProtParam software (119) (table 5.7).

Physical property	Maltose binding protein	RyR1 helical domain
Amino acid number	413	441
Size (Da)	45009.0	49009.7
Theoretical pI	5.39	5.40
Extinction Coefficient, M^{-1} cm^{-1}, at 280 nm. assuming all cysteine residues are reduced	66350	28015
Aliphatic index	82.35	101.45

Table 5.7 Predicted physical properties of the RyR1 helical domain following genenase digestion. The ExPASy ProtParm software was used to predict the physical properties of the maltose binding protein tag and the helical domain following genenase digestion.

Initial genenase digestion was performed on the helical domain after elution from the resin. The progression of the digest was analysed by SDS-PAGE (figure 5.14).

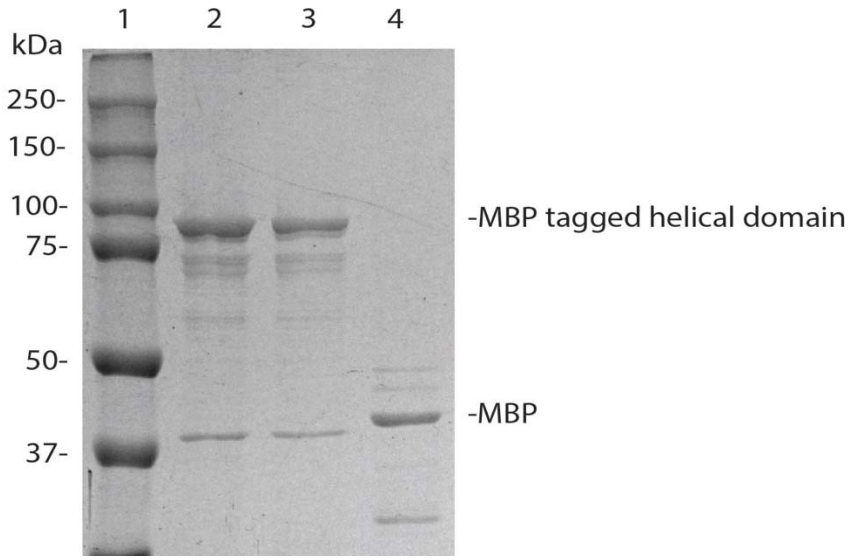

Figure 5.14 Genenase digestion of the MBP-tagged RyR1 helical domain. Genenase digestion was performed on the tagged helical region following partial purification all fractions were resolved using 12.5 % SDS-PAGE at 120 mV for 1.5 hours and visualised by Coomassie blue staining. Lane 1, precision plus size marker. Lane 2, amylose conjugated resin prior to elution. Lane 3, all proteins following elution from resin. Lane 4, elution product following genenase digestion.

The digestion proceeded to completion although only one prominent band with a molecular mass of 42 kDa was detected (figure 5.14). This band likely corresponds to the MBP tag, as the helical domain has a predicted mass of 49 kDa (table 5.7) and only a faint band of this molecular mass can be seen. The helical domain does not contain the recognition site for the protease genenase it is unlikely specific digestion occurred within the RyR1 domain. The cleaved helical domain may migrate through the gel with an increased mobility than predicted and may be shielded by the MBP tag. There are proteins detected following digestion that are not present prior to digestion, which may be the product of digestion of proteins other then the helical domain

In an attempt to characterise each protein fragment following digestion, the digestion was repeated with the tagged helical domain bound to the amylose resin. Following digestion, the RyR1 helical domain was released from the resin while the cleaved MBP tag remained associated to the resin (figure 5.15).

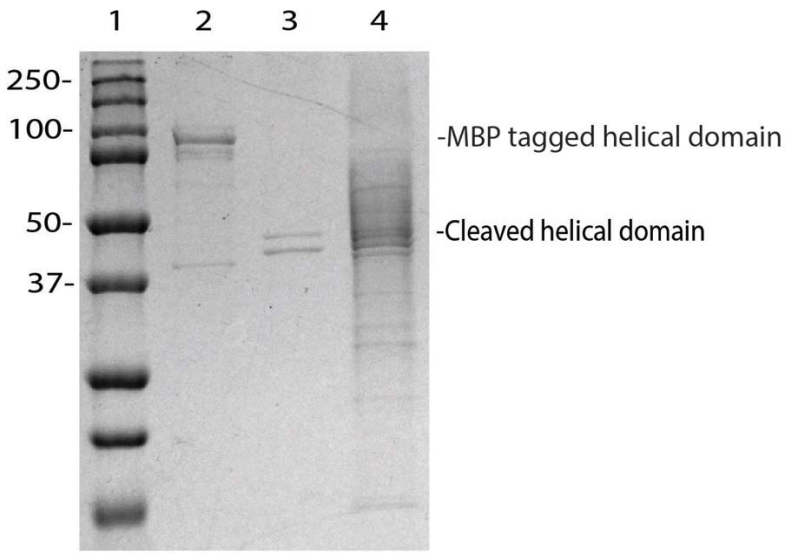

Figure 5.15 On resin genenase digestion of the MBP-tagged RyR1 helical domain. The MBP-tagged RyR1 helical domain was bound to an amylose conjugated magnetic resin following partial purification the RyR1 region was subjected to digestion by genenase. Following digestion, the supernatant was removed from the resin and centrifuged at 70,000 x g. Fractions were resolved by 12.5 % SDS-PAGE at 120 mV for 1.5 hours proteins were visualised by Coomassie blue staining. Lane 1, precision plus size marker. Lane 2, Amylose resin prior to digestion. Lane 3, supernatant following digestion and centrifugation. Lane 4, amylose resin following digestion.

The digest proceeded to completion. Two bands were detected in the supernatant following the digest, one of roughly 47 kDa and one of 42 kDa (figure 5.15). The higher molecular weight band likely corresponds to the cleaved helical domain. While the other is an unknown protein potentially a product of digestion of another protein bound to the resin. The helical domain remained in solution following centrifugation at 70,000 x g indicating the RyR1 domain is soluble and stable following the removal of the MBP tag. A band of 44 kDa can be seen bound to the amylose resin. This band most likely represents MBP, indicating the helical domain and the MBP tag can be separated by on resin digest.

5.2.11 Mass spectrometry to confirm the identity of the cleaved helical domain

The protein thought to correspond to the cleaved RyR1 helical domain was subjected to in-gel digestion by the enzyme trypsin at the Centre for Protein Research, Otago University, Dunedin, New Zealand. MALDI MS/MS was performed on the resulting fragments to confirm the identity of the cleaved RyR1 (figure 5.16)

1	PR**SLQELVSH**	**MVVRWAQEDF**	**VQSPELVR**AM	FSLLHR**QYDG**	**LGELLR**ALPR
51	**AYTISPSSVE**	**DTMSLLECLG**	**QIRSLLIVQM**	**GPQEENLMIQ**	**SIGNIMNNKV**
101	**FYQHPNLMR**A	LGMHETVMEV	MVNVLGGGES	K**EIRFPK**MVT	SCCRFLCYFC
151	RISRQNQRSM	FDHLSYLLEN	SGIGLGMQGS	TPLDVAAASV	IDNNELALAL
201	QEQDLEKVVS	YLAGCGLQSC	PMLVAK**GYPD**	**IGWNPCGGER**	**YLDFLRFAVF**
251	**VNGESVEENA**	**NVVVR**LLIR**K**	**PECFGPALRG**	**EGGSGLLAAI**	**EEAIR**ISEDP
301	ARDGPGIRRD	RRREHFGEEP	PEENRVHLGH	AIMSFYAALI	DLLGRCAPEM
351	HLIQAGKGEA	LRIRAILRSL	VPLEDLVGII	SLPLQIPTLG	KDGALVQPKM
401	SASFVPDHKA	SMVLFLDRVY	GIENQDFLLH	VLDVG	

Figure 5.16 MS/MS results for the gel purified RyR1 helical domain. Sequenced amino acids are highlighted in red.

Roughly 40% sequence coverage of the RyR1 region was detected following analysis, confirming the identity of the protein. Much of the sequence is located in the N-terminal and central regions of the domain. Again no polypeptides were detected corresponding to the last 150 amino acids (figure 5.16). Again suggesting the resulting digestion fragments may not have been efficiently eluted from the gel.

5.3 Chapter summary

The proposed RyR1 helical domain, amino acids 2091-2525, is soluble when expressed from the pMALp2g vector. The domain remained soluble following protease digestion to remove the maltose binding protein tag.

Chapter 6 Final summary and future directions

6.1 Functional characterisation of the RyR1 variants p.T214M and p.ΔE2348

Transiently transfected HEK 293T cells were used to functionally characterise two MH-linked *RYR1* variants; c.641C>T, p.T214M and c.7042_7044delCAG, p.ΔE2348. Ca^{2+} release from the SR was induced by the RyR1 agonists 4-C*m*C and caffeine and monitored using the fluorescent Ca^{2+} indicator fura 2-AM. The p.T214M variant was not functionally different from wild type RyR1 in this system. However, an altered Ca^{2+} response curve was detected in the case of both agonists compared to wild type RyR1. Suggesting the variant has some functional consequence. The p.ΔE2348 variant displayed an altered Ca^{2+} release compared to wild type RyR1 resulting in a significantly hypersensitive channel. This indicates the variant is likely to be the cause of MH.

A proband has been shown to contain both the c.641C>T, p.T214M and c.7042_7044delCAG, p.ΔE2348 RyR1 variants. One expressed from each allele. In an attempt to functionally characterise both RyR1 variants in the same cell line both variants were cloned into the same *RYR1* cDNA. In this case the cells were homozygous for both variants, which is not the case for the patient. The expressed RyR1 displayed similar characteristics to a hypersensitive channel. However, further work will need to be performed to characterise both variants in a heterozygous state.

6.2 Over Expression and purification of the N-terminal and helical domains of RyR1

The RyR1 N-terminal domain, expressed from codon optimised cDNA, was soluble following expression from the pGEX6p3 and pMALp2g vectors. The RyR1 N-terminal domain has, in both cases, been partially purified on a small scale. The N-terminal tags, GST and MBP respectively, were specifically removed by protease digestion. The helical domain was soluble when expressed from the pMALp2g vector. This

domain has been partially purified and the MBP tag has been removed by protease digestion. Further characterisation of the cleaved polypeptides is required.

6.3 Future directions

6.3.1 Functional characterisation of the RyR1 variants p.T214M and p.ΔE2348

HEK293T cells could be used to further characterise the RyR1 variants p.T214M and p.ΔE2348 expressed in a heterozygous state. In this case the cells could be transfected with two expression vectors each containing *RYR1* cDNA containing either the c.641C>T or the c.7042_7044delCAG variants. To ensure the cells are expressing both RyR1 variants each could be tagged with a different fluorescent marker for example green fluorescent protein or cherry red. Cells expressing both RyR1 variants would have to be selected over cells expressing either one or no RyR1 at all. Each RyR1 variant would have to be tagged in such a way to ensure there is no functional consequence resulting from the tag (138).

1B5 cells, *RYR1* knock out myoblasts, could be used to characterise RyR1 variants. The cells could be transduced with *RYR1* cDNA using a lenti viral system and then differentiated into myotubes (139). RyR1 could be expressed in an environment resembling an intact muscle cell, allowing for the characterisation of the RyR1 variants in an environment more closely resembling *in vivo* conditions. 1B5 cells provide a controlled environment for the functional characterisation of RyR1 variants, with the only genetic difference between cells being the expressed *RYR1* cDNA. This system would allow for the direct functional comparison of RyR1 variants. *RYR1*-null myoblasts could also be used to express RyR1 following micro injection with *RYR1* cDNA. In this case the cells can be injected with multiple expression vectors ensuring the cells are heterozygous for two different *RYR1* variants (140). Following microinjection the cells could be used in the functional characterisation the both the p.T214M and p.ΔE2348 variants in a heterozygous state.

For an animal model of MH, *RYR1* knock-in mice could be used to characterise RyR1. In this case mouse embryonic stem cells could be transfected with variant

containing *RYR1* cDNA; the variant containing DNA is specifically incorporated into the host genome by homologous recombination. The stem cells are then used to impregnate female mice. The resulting offspring express the RyR1 variant in an environment that truly represents *in vivo* conditions. To characterise variants in this case knock-in mice could be exposed to halothane and monitored for signs of MH including, an increase in body temperature and muscle rigidity (81). Alternatively, myoblasts could be extracted from the mouse muscle and following differentiation into myotubes functional analysis could be performed (82).

Single channel electrophysiology could also be used to characterise RyR1 variants. RyR1 channels could be extracted from the sarcoplasmic reticulum of knock-in mice and incorporated into a planar lipid bilayer. The membrane potential across the bilayer is measured and following RyR1 stimulation alterations to the membrane potential can be recorded. RyR1 variant function including the duration of channel opening and the concentration of agonist required to open the channel could be measured and compared to a wild type control. This approach could provide insights into how amino acid variants can alter channel function under a range of different conditions.

The FLP-In^{TM} recombination system has been used to create stable RyR1 variant expressing cell lines (141). MH-linked *RYR1* variants could be introduced into full-length *RYR1* cDNA cloned into a FLP recombinase target vector, where *RYR1* is flanked by FLP recombinase target sites. Cells can be transfected with the *RYR1* containing vector and a second expression vector coding for the FLP recombinase. The FLP recombinase is used insert *RYR1* into the host genome by specifically recombining the FLP recombinase target sites on the *RYR1* vector and complementary regions of the host genome. The establishment of stable cell lines eliminates the need for continual transfection of cells prior to performing functional analysis adopting this system could be advantageous in saving time and resources. The system could also be used to introduce protein binding partners of RyR1 by co-transfection with the relevant cDNAs.

The creation of *RYR1* variants currently requires site directed mutagenesis of *RYR1* cDNA which is fifteen kilobases in length. While the use of high fidelity polymerases should prevent the introduction of non desired nucleotide variants the problem still

persists. Because of this, mutagenesis is normally performed on small regions of *RYR1* and progressively introduced into the full-length cDNA. A process which is time consuming and often challenging. Therefore, the establishment of a system which eliminates the need for the subcloning process is advantageous. A technique has been developed for the introduction of specific variants directly into the genome of a cultured cell line and could be used for the generation stable cell lines containing *RYR1* variants. Referred to as CRISPR (Clustered Regularly Interspaced Short Palindromic Repeats) Cas the process involves the specific nuclease digestion of the host cell genomic DNA using a specific guide RNA to target a specific locus. The associated repair mechanism could be exploited to introduce a specific *RYR1* variant into the host genome using repair templates (142, 143). Cas9 is a nuclease commonly used by bacteria to defend against viral infection. Cas9 will interact with the specific guide RNA, targeting the nuclease to the viral genomic DNA, once bound Cas9 will digest the viral DNA. When expressed in mammalian cells, following transfection, Cas9 could be targeted to the host cell genomic DNA particularly the region coding for *RYR1*, by the use of specific guide RNA targeting *RYR1* segments. Following digestion, the host cell will attempt to repair the DNA break, a process which can be error prone. To ensure a specific *RYR1* variant is introduced into the host genome, specific variant-containing DNA complementary to the genomic DNA surrounding the digestion site, could be expressed from a second expression vector. The variant containing DNA will be incorporated into the host genome by the DNA repair mechanism aiding in the repair process. Establishing a cell line that expresses a specific RyR1 variant would eliminate the need for individual transfection prior to performing functional analysis. The use of myoblasts in this system would allow for the differentiation into myobtubes providing a physiologically relevant system for the characterisation RyR1 variants.

The functional characterisation of RyR1 variants, in the currently used system, is also time consuming. Several biological replicates must be tested to obtain sufficient results for analysis. Adopting a high throughput system for the characterisation of a number of samples at once would be an efficient alternative to the currently used systems. An example of such a system has been established (144). The system has the potential to measure extra cellular acidosis in 96 samples simultaneously. The increased secretion of protons is an indirect way of measuring the increased

metabolism induced by the increased cytosolic Ca^{2+} resulting from RyR1 activation. Both adherent and non-adherent cells can be assayed by this method making it an effective way to characterise a number of samples at once. However, the plate readers required to perform the analysis are expensive and as of yet have been not been shown to measure intracellular Ca^{2+} levels. Until an affordable high throughput system can be established progress in terms of functionally characterising RyR1 variants will continue to be slow.

6.3.2 Structural characterisation of the RyR1 N-terminal domain and helical domain

PreScission protease digestion to remove the GST tag from the RyR1 N-terminal domain polypeptide was incomplete. To improve the digestion efficiency, the domain could be eluted from the resin, as the glutathione sepharose 4B may be inhibiting the digestion process.

Genenase, the protease used to cleave the MBP tag from the pMALp2g expressed RyR1 domains is no longer commercially produced. The limited enzyme stocks still available for purchase have past their expiration date. To efficiently characterise each RyR1 domain using a MBP tag, the corresponding cDNA could be cloned into a new vector, for example pMALp5x. The protein expressed from this vector would contain the protease recognition site for the enzyme factor X, a well characterised and commercially available protease.

To further characterise each RyR1 domain, all experiments previously performed on a small scale need to be repeated and optimised on a larger scale. Expression of each RyR1 domain could be induced in *E. coli* cultures upwards of 1 L in volume. The purification of both the GST and MBP-tagged domains could be performed initially using an automated affinity purification system specific for the tag. The small scale tag-specific purification carried out thus far resulted in an impure protein sample and this may persist on a larger scale. Other purification methods, for example ion exchange chromatography, may need to be used to further purify the respective RyR1 domain. During the purification process the tag associated with the

RyR1 domain will need to be removed allowing for the specific analysis of the RyR1 domain without potential interference from the tag.

The purification of the N-terminal domain presents a final problem. This domain has been suggested to have a role in tetramer formation of full-length RyR1 (88, 89). Monomers and oligomers will need to be separated from each other during the purification process, which could be performed by size exclusion chromatography.

Once sufficiently pure, the secondary structure of each domain could be assessed by circular dichroism and the thermal stability assessed by tryptophan fluorescence. Should these results match those noted in previous studies performed on rabbit RyR1 (14, 87) it would indicate the human RyR1 domain has adopted the expected tertiary structure. X-ray crystallography could be used to structurally characterise each domain at high resolution. Each protein is likely to crystallise under different conditions. During initial crystallisation, the exact conditions required for a protein to form crystals is unknown so this must be interoperated experimentally. To increase the chances of crystal formation a range of conditions could be tested; different buffers could be used to solubilise the protein, different methods of crystal formation including hanging or sitting drop vapour diffusion could be used and different incubation temperatures could be tested. During the structural characterisation of rabbit RyR1 N-terminal domain, crystals were formed using the hanging drop vapour diffusion method (88). These conditions could be initially replicated to characterise the human RyR1 N-terminal domain. However, other conditions could also be tested to increase the chances of crystal formation. As no high resolution structural analysis has been performed on the helical domain of RyR1 a range of different conditions could be tested to increase the chances of crystal formation. Exposing crystals to X-rays and interpreting the resulting diffraction pattern could render the three dimensional structure of each domain. The high resolution structure of each domain could then be docked to the lower resolution cryo-EM structure of the RyR1 tetramer. This approach would be useful in predicting where each domain resides within the full-length channel and the potential role each domain plays with respect to RyR1 function (38, 89, 126).

To date only the wild type N-terminal and helical domains have been expressed. To understand how the MH-linked RyR1 variants p.T214M and p.ΔE2348 affect the

structure of the their respective domain, the *RYR1* variants c.641C>T and c.7042_7044delCAG could be introduced into the respective cDNA clones. Following purification and structural characterisation of each variant, any alterations in tertiary structure could be determined.

6.3.3 Functional characterisation of the RyR1 N-terminal domain

The sub domains A and B of the N-terminal domain have been implicated in the tetramerisation process of full-length RyR1 (88, 89). Domain A is thought to interact with domain B of an adjacent subunit. To further understand if this interaction is occurring the two domains could be expressed in isolation from each other, each with a different tag. The interaction between each domain could be analysed in the form of a pull down assay. The ability of specific MH-linked variants to hinder the tetramerisation process could be analysed by Förster resonance energy transfer. To do so each domain would need to be tagged with a different fluorescent marker. When the domains are in close contact fluorescence energy will be transferred from one marker onto the next which can be measured by a fluorescence microscope or spectrofluorometer. An MH-linked variant destabilising the domain interface should cause the domains to dissociate under lesser denaturing conditions compared to a wild type control. The dissociation of domains will be detected by a decrease in fluorescence intensity. Chemical cross-linking could also be performed to analyse the interaction between the domains. A fixative such as glutaraldehyde or formaldehyde will form a Schiff base with an exposed amine group, for example the side chains of lysine and glutamine. Both glutaraldehyde or formaldehyde have the potential to form two Schiff bases and could link amine groups of adjacent subunits. The increased molecular mass of the crosslinked protein could be assessed using SDS-PAGE.

6.3.4 Functional characterisation of the RyR1 helical domain

The helical domain of RyR1 has been implicated in the binding of ATP, caffeine (46) and FKBP12 (129). Once purification to homogeneity has been achieved binding assays could be performed to understand the interactions formed between RyR1

and these regulatory molecules, providing an insight into the role the domain plays with respect to the regulation of full-length channel. The helical domain's interaction with ATP could be monitored by exposing the purified domain to radiolabelled ATP. Following non-denaturing PAGE the ability of the domain to interact with the nucleotide could be analysed by interpreting radioactivity intensity. Any conformational change induced by the binding of ATP could be monitored by both circular dichroism and tryptophan fluorescence. A crystal structure of the domain in the ATP bound state could also be determined. Alterations in the ATP binding affinity induced by specific MH-linked variants could be determined. The ability of the domain to form interactions with caffeine could also be examined in the same manner. Pull down assays, Förster resonance energy transfer and cross linking studies could be used to analyse the proposed interaction between the RyR1 helical domain and FKPB12. The helical domain has been linked to the interaction with the adjacent N-terminal and handle domains (14). The interaction between these three domains could again be characterised by pull down assays, Förster resonance energy transfer and cross-linking assays. The effect of specific RyR1 variants have on these interactions could also be examined using the same experimental system.

6.5 Final summary

Performing functional analysis on RyR1 variants is important in understanding the link between specific RyR1 variants and MH. Currently the gold standard for the diagnosis of MH is the morbidly invasive IVCT. The establishment of a comprehensive DNA based diagnostic test is the current objective in MH research providing an alternative to the IVCT for families with a known causative *RYR1* variant. With more and more *RYR1* variants being functionally characterised an MHS diagnosis by DNA testing becomes an option for more and more families, limiting the need for the IVCT. While many MH-linked variants have been identified in RyR1, a number of other proteins also involved in EC coupling have been implicated in MH. Further functional characterisation of these proteins along with their associated variants will aid in the establishment of a truly comprehensive library of MH-associated variants. This would make the DNA diagnostic testing a realistic option for more families susceptible to MH. The RyR1 variant p.ΔE2348, has been identified

in families around the world (97), was functionally characterised in this study and displayed Ca^{2+} release characteristic of a hypersensitive channel. Therefore, the variant could be classed as being MH causative, and added to the diagnostic list established by the European malignant hyperthermia group.

While it is accepted that MH-linked RyR1 amino acid variants have the potential to alter channel function, little is known about how the variants alter the tertiary structure of the channel. It is thought that certain MH-linked RyR1 variants have the potential to interfere with the binding of regulatory proteins altering Ca^{2+} release from the SR. Other variants are thought to destabilise interdomain interactions within RyR1 altering the function of the channel. This study resulted in the preliminary purification schemes for two RyR1 domains which need to be optimised for further structural experimentation. The cloned cDNA fragments also represent a starting point for more extensive site directed mutagenesis. Many MH-linked variants that have not been functionally characterised occur in these regions. Structural studies on selected variants would provide further insight into the structure function relationship of RyR1 variants with respect to MH.

Reference list

1. Hopkins PM*, et al.* (2015) European malignant hyperthermia group guidelines for investigation of malignant hyperthermia susceptibility. *British Journal of Anaesthesia* 115(4):531-539.
2. Britt BA & Kalow W (1970) Malignant hyperthermia: a statistical review. *Can. Anaesth. Soc. J.* 17(4):293-315.
3. Pollock N, Langton E, Stowell K, Simpson C, & McDonnell N (2004) Safe duration of postoperative monitoring for malignant hyperthermia susceptible patients. *Anaesthesia and Intensive Care* 32(4):502-509.
4. Blausen.com (2014) "Blausen gallery 2014". *Wikiversity Journal of Medicine*.
5. Rebbeck RT*, et al.* (2014) Skeletal muscle excitation–contraction coupling: Who are the dancing partners? *The International Journal of Biochemistry & Cell Biology* 48:28-38.
6. Poláková E, Zahradníková AJ, Pavelková J, Zahradník I, & Zahradníková A (2008) Local calcium release activation by DHPR calcium channel openings in rat cardiac myocytes. *Journal of Physiology* 586(16):3839-3854.
7. Cui Y*, et al.* (2009) A dihydropyridine receptor α1s loop region critical for skeletal muscle contraction is intrinsically unstructured and binds to a SPRY domain of the type 1 ryanodine receptor. *The International Journal of Biochemistry & Cell Biology* 41(3):677-686.
8. Dirkson RT (2002) Bi-directional coupling between dihydropyridine receptors and ryanodine receptors. *Frontiers in Bioscience* 7:659-670.
9. Paolini C, Fessenden JD, Pessah IN, & Franzini-Armstrong C (2004) Evidence for conformational coupling between two calcium channels. *Proceedings of the National Academy of Sciences of the United States of America* 101:12748–12752.
10. JURKAT-ROTT K, McCarthy T, & LEHMANN-HORN F (2000) Genetics and pathogenesis of malignant hyperthermia. *Muscle and Nerve* 23:4-17.
11. Anonymous (2016[accessed January 2016]) EMHG list of causitive MH mitations
12. Zhao F, Li P, Chen W, Louis CF, & Fruen BR (2001) Dantrolene inhibition of ryanodine receptor Ca2+ release channels molecular mechanisms and isoform selectivity. *Journal of Biological Chemistry* 276:13810-12816.
13. Sorrentino V & Volpe P (1993) Ryanodine receptors: how many, where and why? *Trends in Pharmacological Sciences* 14(3):98-103.
14. Yan Z*, et al.* (2015) Structure of the rabbit ryanodine receptor RyR1 at near-atomic resolution. *Nature* 517(7532):50-55.
15. Efremov RG, Leitner A, Aebersold R, & Raunser S (2015) Architecture and conformational switch mechanism of the ryanodine receptor. *Nature* 517:39-43.
16. Treves S*, et al.* (2005) Ryanodine receptor 1 mutations, dysregulation of calcium homeostasis and neuromuscular disorders. *Neuromuscular Disorders* 15(9–10):577-587.
17. Ikemoto N & Yamamoto T (2000) Postulated role of inter-domain interaction within the ryanodine receptor in Ca2+ channel regulation. *Trends in Cardiovascular Medicine* 10(7):310-316.
18. Sharma MR, Jeyakumar LH, Fleischer S, & Wagenknecht T (2000) Three-dimensional structure of ryanodine receptor isoform three in two conformational states as visualized by cryo-electron microscopy. *Journal of Biological Chemistry* 275:9485-9491.
19. Samsó M, Feng W, Pessah IN, & Allen PD (2009) Coordinated movement of cytoplasmic and transmembrane domains of RyR1 upon gating. *Public Library of Science* 7(4):980-995.
20. Robinson R, Carpenter D, Shaw M-A, Halsall J, & Hopkins P (2006) Mutations in RYR1 in malignant hyperthermia and central core disease. *Human Mutation* 27(10):977-989.

21. Dirksen RT & Avila G (2004) Distinct effects on Ca2+ handling caused by malignant hyperthermia and central core disease mutations in RyR1. *Biophysical Journal* 87(5):3193-3204.
22. Brislin RP & Theroux MC (2013) Core myopathies and malignant hyperthermia susceptibility: a review. *Paediatric Anaesthsia* 23(9):834-841.
23. Brookes PS, Yoon Y, Robotham JL, Anders MW, & Shey-Shing S (2004) Calcium, ATP, and ROS: a mitochondrial love-hate triangle. *American Journal of Physiology* 287(4).
24. Klingler W, Rueffert H, Lehmann-Horn F, Girard T, & Hopkins P (2009) Core myopathies and risk of malignant hyperthermia. *Anesthesia & Analgesia* 109(4):1167-1173.
25. North KN*, et al.* (2014) Approach to the diagnosis of congenital myopathies. *Neuromuscular Disorders* 24(2):97-116.
26. Tong J, McCarthy TV, & MacLennan DH (1999) Measurement of resting cytosolic Ca2+ concentrations and Ca2+ store size in HEK-293 Cells transfected with malignant hyperthermia or central core disease mutant Ca2+ release channels. *Journal of Biological Chemistry* 274(2):693-702.
27. Jungbluth H (2007) Multi-minicore disease. *Orphanet Journal of Rare Diseases* 2(31).
28. Zhou H*, et al.* (2006) Epigenetic allele silencing unveils recessive RYR1 mutations in core myopathies. *The American Journal of Human Genetics* 79(5):859-868.
29. Zhou H*, et al.* (2007) Molecular mechanisms and phenotypic variation in RYR1-related congenital myopathies. *Brain* 130(Pt 8):2024-2036.
30. Monnier N*, et al.* (2008) Null mutations causing depletion of the type 1 ryanodine receptor (RYR1) are commonly associated with recessive structural congenital myopathies with cores. *Human Mutation* 29(5):670-678.
31. Moore CP*, et al.* (1999) A role for cysteine 3635 of RYR1 in redox modulation and calmodulin binding. *Biochemistry* 38(26):8532–8537.
32. Newman RA, Sorensen BR, Kilpatrick AM, & Shea MA (2014) Calcium-dependent energetics of calmodulin domain interactions with regulatory regions of the Ryanodine Receptor Type 1 (RyR1). *Biophysical Chemistry* 193–194:35-49.
33. NOVÁK P & SOUKUP T (2011) CalsequestrindDistribution, structure and function, its role in normal and pathological situations and the effect of thyroid hormones. *Physiolgical Research* 60(439-452).
34. Wei L, Gallant EM, Dulhunty AF, & Beard NA (2009) Junctin and triadin each activate skeletal ryanodine receptors but junctin alone mediates functional interactions with calsequestrin. *The International Journal of Biochemistry & Cell Biology* 41(11):2214-2224.
35. Lewis KM, Ronish LA, Rios E, & Kang C (2015) Characterization of two human skeletal calsequestrin mutants implicated in malignant hyperthermia and vacuolar aggregate myopathy. *Journal of Biological Chemistry* 290(48):28665-28674.
36. Avila G, Hui Lee E, Perez CF, Allen PD, & Dirksen RT (2003) FKBP12 binding to RyR1 modulates excitation-contraction coupling in mouse skeletal myotubes. *Journal of Biological Chemistry* 278:22600-22608.
37. Cameron AM*, et al.* (1997) FKBP12 binds the inositol 1,4,5-trisphosphate receptor at leucine-proline (1400–1401) and anchors calcineurin to this FK506-like domain. *Journal of Biological Chemistry* 272:27582-27588.
38. Yuchi Z*, et al.* (2015) Crystal structures of ryanodine receptor SPRY1 and tandem-repeat domains reveal a critical FKBP12 binding determinant. *Nature Communications* 6.
39. Lau K & Van Petegem F (2015) Crystal structures of the ryanodine receptor SPRY2 domain. *Biophysical Journal* 108(2):341a.
40. Weiss RG*, et al.* (2004) Functional analysis of the R1086H malignant hyperthermia mutation in the DHPR reveals an unexpected influence of the III-IV loop on skeletal muscle EC coupling. *American Journal of Physiology* 287(4):1094-1102.

41. Franzini-Armstrong C & Kish JW (1995) Alternate disposition of tetrads in peripheral couplings of skeletal muscle. *Journal of Muscle Research & Cell Motility* 6:319-324.
42. Laver DR (2007) Ca2+ stores regulate ryanodine receptor Ca2+ release channels via luminal and cytosolic Ca2+ sites. *Biophysical Journal* 92(10):3541-3555.
43. Lewit-Bentley A & Réty S (2000) EF-hand calcium-binding proteins. *Current Opinion in Structural Biology* 10(6):637-643.
44. Serysheva II, Schatz M, van Heel M, Chiu W, & Hamilton SL (1999) Structure of the skeletal muscle calcium release channel activated with Ca2+ and AMP-PCP. *Biophysical Journal* 77(4):1936-1944.
45. Popova OB, Baker MR, Tran TP, Le T, & Serysheva II (2012) Identification of ATP-binding regions in the RyR1 Ca2+ release channel. *Public Library of Science* 7:48725.
46. Du GG, Oyamada H, Khanna VK, & Maclennn DH (2001) Mutations to gly2370, gly2373 or gly2375 in malignant hyperthermia domain 2 decrease caffeine and cresol sensitivity of the rabbit skeletal-muscle Ca2„- release channel (ryanodine receptor isoform 1). *Biochemical Journal* 360:97-105.
47. Dias JM, Szegedi C, Jóna I, & Vogel PD (2006) Insights into the regulation of the ryanodine receptor: differential effects of Mg2+ and Ca2+ on ATP Binding. *Biochemistry* 45(31):9408-9415.
48. Kakuta Y (1984) Effects of ATP and related compounds on the Ca-induced Ca release mechanism of the Xenopus SR. *Pflügers Archiv* 400(1):72-79.
49. Gillespie D, Chen H, & Fill M (2012) Is ryanodine receptor a calcium or magnesium channel? Roles of K+ and Mg2+ during Ca2+ release. *Cell Calcium* 51(6):427-433.
50. Copello JA*, et al.* (2002) Differential activation by Ca2+, ATP and caffeine of cardiac and skeletal muscle ryanodine receptors after block by Mg2+. *The Journal of Membrane Biology* 187(1):51-64.
51. Ruehr ML*, et al.* (2003) Targeting of protein kinase A by muscle A kinase-anchoring protein (mAKAP) regulates phosphorylation and function of the skeletal muscle ryanodine receptor. *Journal of Biological Chemistry* 278:24831-24836.
52. Suko J*, et al.* (1993) Phosphorylation of serine 2843 in ryanodine receptor-calcium release channel of skeletal muscle by cAMP-, cGMP- and CaM-dependent protein kinase. *Biochimica et Biophysica Acta- Molecular Cell Research* 1175(2):193-206.
53. Reiken S*, et al.* (2003) PKA phosphorylation activates the calcium release channel (ryanodine receptor) in skeletal muscle. *Journal of Cell Biology* 160(6):919-928.
54. Ruehr ML*, et al.* (2003) Targeting of protein kinase A by muscle A kinase-anchoring protein (mAKAP) regulates phosphorylation and function of the skeletal muscle ryanodine receptor. *Journal of Biological Chemistry* 278:24831-24836.
55. Reid MB (2001) Invited review: redox modulation of skeletal muscle contraction: what we know and what we don't. *Journal of Applied Physiology* 90(2):724-731.
56. Sun Q-A, Wang B, Miyagi M, Hess DT, & Stamler JS (2013) Oxygen-coupled redox regulation of the skeletal muscle ryanodine receptor/Ca2+ release channel (RyR1). *Journal of Biological Chemistry* 288(32):22962-22971.
57. Sun Q-A*, et al.* (2011) Oxygen-coupled redox regulation of the skeletal muscle ryanodine receptor-Ca2+ release channel by NADPH oxidase 4. *Proceedings of the National Academy of Sciences* 108(38):16098-161103.
58. Aracena P, Sánchez G, Donoso P, Hamilton SL, & Hidalgo C (2003) S-glutathionylation decreases Mg2+ inhibition and S-nitrosylation enhances Ca2+ activation of RyR1 channels. *Journal of Biological Chemistry* 278:42927-42935.
59. Aracena-Parks P*, et al.* (2006) Identification of cysteines involved in S-nitrosylation, S-glutathionylation, and oxidation to disulfides in ryanodine receptor type 1. *Journal of Biological Chemistry* 281:40354-40368.

60. Moore CP, Zhang J-Z, & Hamilton SL (1999) A Role for cysteine 3635 of RYR1 in redox modulation and calmodulin binding. *Journal of Biological Chemistry* 274:36831-36834. .
61. Zhang J-Z*, et al.* (1999) Oxidation of the skeletal muscle Ca2+ release channel alters calmodulin binding. *American Journal of Physiology* 276(1):46-53.
62. M E (1975) Mechanism of action of caffeine on the sarcoplasmic reticulum of skeletal muscle. *Proceedings of the Japan Academy* 51(6):479-484.
63. Annegret H-F, Michael R, & Lehmann-Horn F (1996) 4-chloro-m-cresol: a specific tool to distinguish between malignant hyperthermia-susceptible and normal muscle. *Biochemical Pharmacology* 52(1):149-156.
64. Migita T*, et al.* (2009) Functional analysis of ryanodine receptor type 1 p.R2508C mutation in exon 47. *Journal of Anesthesia* 23(3):341-346.
65. Avila G, O'Connell KMS, & Dirksen RT (2003) The pore region of the skeletal muscle ryanodine receptor ss a primary locus for excitation-contraction uncoupling in central core disease. *Journal of Cell Biology* 121(4):277-286.
66. Litman RS & Rosenberg H (2005) Malignant hyperthermia update on susceptibility testing. *Journal of the American Medical Association* 293(23):2918-2924.
67. Stowell K, M. Pollock, N. (2008) DNA analysis and malignant hyperthermia susceptibility. *Anaesthesia and Intensive Care* 36(3).
68. Neville C, Rossenthal N, McGrew M, Bogdanova N, & Hauschka S (1998) Skeletal muscel cultures. *Metods in Muscle Biology* 52:85–116.
69. Wehner H, Rueffert H, Koenig F, J N, & Olthoff D (2002) Increased sensitivity to 4-chloro-m-cresol and caffeine in primary myotubes from malignant hyperthermia susceptible individuals carrying the ryanodine receptor 1 Thr2206Met (C6617T) mutation. *Clinical Genetics* 62(2):135-146.
70. Sei Y, Gallagher KL, & Basile AS (1999) Skeletal muscle type1 ryanodine receptor Is involved in calcium signaling in human B lymphocytes. *Journal of Biological Chemistry* 274:5995-6002.
71. Girard T*, et al.* (2001) B-lymphocytes from malignant hyperthermia-susceptible patients have an increased sensitivity to skeletal muscle ryanodine Receptor activators. *Journal of Biological Chemistry* 276:48077-48082.
72. Kraev N, Loke JCP, Kraev A, & MacLennan DH (2003) Protocol for the sequence analysis of ryanodine receptor subtype 1 gene transcripts from human leukocytes. *Anesthesiology* 99:289-296.
73. Broman m*, et al.* (2009) Mutation screening of the RYR1-cDNA from peripheral B-lymphocytes in 15 Swedish malignant hyperthermia index cases. *British Journal of Anaesthesia* 102(5):642-649.
74. Murayama T*, et al.* (2015) Divergent activity profiles of type 1 ryanodine receptor channels carrying malignant hyperthermia and central core disease mutations in the amino-terminal region. *Public Library of Science* 10(6):e0130606.
75. Tong J*, et al.* (1997) Caffeine and halothane sensitivity of intracellular Ca2+ release is altered by 15 calcium release channel (ryanodine receptor) mutations associated with malignant hyperthermia and/or central core disease. *Journal of Biological Chemistry* 272:26332-26339.
76. Sato K, Pollock N, & Stowell KM (2010) Functional studies of RYR1 mutations in the skeletal muscle ryanodine receptor using human RYR1 complementary DNA. *Anesthesiology* 112:1350-1354.
77. Treves S*, et al.* (1994) Alteration of intracelular Ca2+ transients in COS-7 cels transfected with the cDNA encoding skeletal-muscle ryanodine receptor carrying a mutation associated with malignant hyperthermia. *Biochemical Journal* 301(3):661-665.
78. Eltit JM*, et al.* (2010) RyR1-mediated Ca2+ leak and Ca2+ entry determine resting intracellular Ca2+ in skeletal myotubes. *Journal of Biological Chemistry* 285:13781-13787.

79. Yang T, Ta TA, Pessah IN, & Allen PD (2003) Functional defects in six ryanodine receptor isoform-1 (RyR1) mutations associated with malignant hyperthermia and their impact on skeletal excitation-contraction coupling. *Journal of Biological Chemistry* 278:25722-25730.
80. Buck ED, Nguyen HT, Pessah IN, & Allen PD (1997) Dyspedic mouse skeletal muscle expresses major elements of the triadic junction but lacks detectable ryanodine receptor protein and function. *Journal of Biological Chemistry* 272:7360-7367.
81. Chelu MG*, et al.* (2005) Heat- and anesthesia-induced malignant hyperthermia in an RyR1 knock-in mouse. *Journal of the Federation of American Societies for Experimental Biology* 20(2):329-330.
82. Yang T*, et al.* (2006) Pharmacologic and functional characterization of malignant hyperthermia in the R163C RyR1 knock-in mouse. *Anesthesiiology* 105:1164-1175.
83. O'Brien JJ*, et al.* (2002) Ca2+ activation of RyR1 ss not necessary for the initiation of skeletal-type excitation-contraction coupling. *Biophysical Journal* 82(5):2428-2435.
84. Rokach O*, et al.* (2013) Establishment of a human skeletal muscle-derived cell line: biochemical, cellular and electrophysiological characterization. *Biochemical Journal* 455(2):169-177.
85. Loy RE*, et al.* (2010) Muscle weakness in Ryr1I4895T/WT knock-in mice as a result of reduced ryanodine receptor Ca2+ ion permeation and release from the sarcoplasmic reticulum. *The Journal of General Physiology* 137(1):43.
86. Ludtke SJ, Serysheva II, Hamilton SL, & Chiu W (2005) The pore structure of the closed RyR1 channel. *Structure* 13(8):1203-1211.
87. Lobo PA & Van Petegem F (2009) Crystal structures of the N-terminal domains of cardiac and skeletal muscle ryanodine receptors: insights into disease mutations. *Structure* 17(11):1505-1514.
88. Tung C-C, Lobo PA, Kimlicka L, & Van Petegem F (2010) The amino-terminal disease hotspot of ryanodine receptors forms a cytoplasmic vestibule. *Nature* 468(7323):585-588.
89. Kimlicka L, Lau K, Tung C-C, & Van Petegem F (2013) Disease mutations in the ryanodine receptor N-terminal region couple to a mobile intersubunit interface. *Nature Communications* 4:1506.
90. Tae H, Casarotto MG, & Dulhunty AF (2009) Ubiquitous SPRY domains and their role in the skeletal type ryanodine receptor. *Eur Biophys J* 39:51-59.
91. Bannister Mark L*, et al.* (2007) Malignant hyperthermia mutation sites in the leu(2442)–pro(2477) (dp4) region of RyR1 (ryanodine receptor 1) are clustered in a structurally and functionally definable area. *Biochemical Journal* 401(Pt 1):333-339.
92. Kobayashi S, Yamamoto T, Parsons J, & Ikemoto N (2004) Antibody probe study of Ca2+ channel regulation by interdomain interaction within the ryanodine receptor. *Biochemical Journal* 380:561-569.
93. Yamamoto T, El-Hayek R, & Ikemoto N (2000) Postulated role of interdomain interaction within the ryanodine receptor in Ca2+ channel regulation. *Journal of Biological Chemistry* 275:11618-11625.
94. Sharma P*, et al.* (2012) Structural determination of the phosphorylation domain of the ryanodine receptor. *Federation of European Biochemical Societies Journal* 279(20):3952-3964.
95. Zhiguang Yuchi KL, Filip Van Petegem (2012) Disease mutations in the ryanodine receptor central region: crystal structures of a phosphorylation hot spot domain. *Structure* 20(12):1201–1211.
96. Fiszer D*, et al.* (2015) Next-generation sequencing of RYR1 and CACNA1S in malignant hyperthermia and exertional heat illness. *Anesthesiology* 122 (5):1033-1046.
97. Sambuughin N, McWilliams S, de Bantel A, Sivakumar K, & Nelson TE (2001) Single-amino-acid deletion in the RYR1 gene, associated with malignant hyperthermia susceptibility and unusual contraction phenotype. *The American Journal of Human Genetics* 69(1):204-208.

98. Bradford M (1976) A rapid and sensitive method for teh quantitation of microgram quantities of protein utilizing the priciple of protein-dye binding. *Analytical biochemistry* 72:248-254.
99. Roesl C, Sato K, Schiemann A, Pollock N, & Stowell KM (2014) Functional characterisation of the R2452W ryanodine receptor variant associated with malignant hyperthermia susceptibility. *Cell Calcium* 56(3):195-201.
100. Stephens J*, et al.* (2016) Functional analysis of RYR1 variants linked to malignant hyperthermia. *Temperature*.
101. Haraki T*, et al.* (2011) Mutated p.4894 RyR1 function related to malignant hyperthermia and congenital neuromuscular disease with uniform type 1 fiber (CNMDU1). *Anesthesia & Analgesia* 113(6):1461-1467.
102. Monnier N*, et al.* (2000) An autosomal dominant congenital myopathy with cores and rods is associated with a neomutation in the RYR1 gene encoding the skeletal muscle ryanodine receptor. *Oxford Journals* 9(18):2599-2608.
103. Brini M*, et al.* (2005) Ca2+ signaling in HEK-293 and skeletal muscle cells expressing recombinant ryanodine receptors harboring malignant Hhperthermia and central core disease mutations. *Journal of Biological Chemistry* 280:15380-15389.
104. Isaacs H BM (1993) False-negative results with muscle caffeine halothane contracture testing for malignant hyperthermia. *Anesthesiology* 70(1):5-9.
105. Yan Z*, et al.* (2015) Structure of the rabbit ryanodine receptor RyR1 at near-atomic resolution. *Nature* 517(7532):50-55.
106. Nakano M*, et al.* (2014) Construction and expression of ryanodine receptor mutants relevant to maligant hyperthermia in patients in Japan. *The Showa University Journal of Medical Sciences* 26(2):27-38.
107. Murayama T*, et al.* (2015) Divergent activity profiles of type 1 ryanodine receptor channels carrying malignant hyperthermia and central core disease mutations in the amino-terminal region. *Public Library of Science* 10(6).
108. Samsó M, Feng W, Pessah IN, & Allen PD (2009) Coordinated movement of cytoplasmic and transmembrane domains of ryr1 upon gating. *Public Library of Science* 7(4):e1000085.
109. Zhong X*, et al.* (2013) Conformational dynamics inside amino-terminal disease hotspot of ryanodine receptor. *Structure* 21(11):2051-2060.
110. Amador FJ*, et al.* (2009) Crystal structure of type I ryanodine receptor amino-terminal β-trefoil domain reveals a disease-associated mutation “hot spot” loop. *Proceedings of the National Academy of Sciences* 106(27):11040-11044.
111. Yuchi Z & Van Petegem F (2011) Common allosteric mechanisms between ryanodine and inositol-1,4,5-trisphosphate receptors. *Channels* 5(2):120-123.
112. Ponting CP (2000) Novel repeats in ryanodine and IP3 receptors and protein O-mannosyltransferases. *Trends in Biochemical Sciences* 25(2):47-50.
113. Bosanac I*, et al.* (2002) Structure of the inositol 1,4,5-trisphosphate receptor binding core in complex with its ligand. *Nature* 420:696–700.
114. Bosanac I*, et al.* (2005) Crystal structure of the ligand binding suppressor domain of type 1 inositol 1,4,5-trisphosphate receptor. *Molecular Cell* 17(2):193-203.
115. Chan J*, et al.* (2007) Ligand-induced conformational changes via flexible linkers in the amino-terminal region of the inositol 1,4,5-trisphosphate receptor. *Journal of Molecular Biology* 373(5):1269-1280.
116. Sievers F *, et al.* (2011) Fast, scalable generation of high-quality protein multiple sequence alignments using Clustal Omega. *Molecular Systems Biology* 7(539).
117. Kimlicka L*, et al.* (2013) The cardiac ryanodine receptor N-terminal region contains an anion binding site that Is targeted by disease mutations. *Structure* 21(8):1440-1449.
118. Kelley LA, Mezulis S, Yates CM, Wass MN, & Sternberg MJE (2015) The Phyre2 web portal for protein modeling, prediction and analysis. *Nature Protocols* 10(6):845-858.

119. Gasteiger E*., et al.* (2005) Protein Identification and Analysis Tools on the ExPASy Server;. *The Proteomics Protocols Handbook, Humana Press*:571-607.
120. Jeong H*, et al.* (2009) Genome sequences of Escherichia coli B strains REL606 and BL21(DE3). *Journal of Molecular Biology* 394(4):644-652.
121. SaiSree L, Reddy M, & Gowrishankar J (IS186 insertion at a hot spot in thelon promoter as a basis for lon protease deficiency of Escherichia coli B: identification of a consensus target sequence for IS186 transposition. *Journal of Bateriology* 183(23):6943-6946.
122. Tegel H, Tourle S, Ottosson J, & Persson A (2010) Increased levels of recombinant human proteins with the Escherichia coli strain Rosetta(DE3). *Protein Expression and Purification* 69(2):159-167.
123. Blayney L*, et al.* (2013) ATP interacts with the CPVT mutation-associated central domain of the cardiac ryanodine receptor. *Biochimica et Biophysica Acta (BBA) - General Subjects* 1830(10):4426-4432.
124. Zhang S, Zubaya G, & Goldman E (1991) Low-usage codons in Escherichia coli, yeast, fruit fly and primates. *Gene* 105(1):61-72.
125. Said M*, et al.* (2011) Calcium-calmodulin dependent protein kinase II (CaMKII): A main signal responsible for early reperfusion arrhythmias. *Journal of Molecular and Cellular Cardiology* 51(6):936-944.
126. Yuchi Z, Lau K, & Van Petegem F (2012) Disease mutations in the ryanodine receptor central region: crystal structures of a phosphorylation hot spot domain. *Structure* 20(7):1201-1211.
127. Blayney L*, et al.* (2013) ATP interacts with the CPVT mutation-associated central domain of the cardiac ryanodine receptor. *Biochimica et Biophysica Acta- General Subjects* 1830(10):4426-4432.
128. Van Acker K*, et al.* (2004) The 12 kDa FK506-binding protein, FKBP12, modulates the Ca2 +-flux properties of the type-3 ryanodine receptor. *Journal of Cell Science* 117:1129–1137.
129. Bultynck G*, et al.* (2001) The conserved sites for the FK506-binding proteins in ryanodine receptors and inositol 1,4,5-trisphosphate receptors are structurally and functionally different. *Journal of Biological Chemistry* 276:47715-47724.
130. Leipe DD, Koonin EV, & Aravind L (2003) Evolution and classification of P-loop kinases and related proteins. *Journal of Molecular Biology* 333(4):781-815.
131. Vonrhein C, Bönisch H, Schäfer G, & Schulz GE (1998) The structure of a trimeric archaeal adenylate kinase1. *Journal of Molecular Biology* 282(1):167-179.
132. Lavie A*, et al.* (1998) Crystal structure of yeast thymidylate kinase complexed with the bisubstrate inhibitor P1-(5‘-Adenosyl) P5-(5‘-Thymidyl) pentaphosphate (TP5A) at 2.0 Å resolution: implications for catalysis and AZT activation. *Biochemistry* 37(11):3611-3686.
133. Stehle T & Schulz GE (1992) Refined structure of the complex between guanylate kinase and its substrate GMP at 2·0 Å resolution. *Journal of Molecular Biology* 224(4):1127-1141.
134. Walker JE, Saraste M, Runswick MJ, & Gay NJ (1982) Distantly related sequences in the a- and f-subunits of ATP synthase, myosin,kinases and other ATP-requiring enzymes and a common nucleotide binding fold. *The European Molecular Biology Organization Journal* 1(8):945-951.
135. Weissman JS*, et al.* (1995) Mechanism of GroEL action: Productive release of polypeptide from a sequestered position under groes. *Cell* 83(4):577-587.
136. Rudolph R & Lilie H (1996) In vitro folding of inclusion body proteins. *The Federation of American Sciences* 10(1):49-65.
137. Olsen j, Ong S, & Mann M (2004) Trypsin Cleaves Exclusively C-terminal to Arginine and Lysine Residues. *Molecular and Cellular Proteomics* 3:608-614.
138. Jones P*, et al.* (2008) Localisation of the PKA phosphorylation site, ser 2030, in the three-dimensional structure of the cardiac ryanodine receptor. *Biochemical Journal* 410(2):261-270.

139. Yang T*, et al.* (2007) Elevated resting [Ca2+]i in myotubes expressing malignant hyperthermia RyR1 cDNAs is partially restored by modulation of passive calcium leak from the SR. *American Journal of Physiology* 292(5):1591-1598.
140. Groom LA*, et al.* (2011) Identical de novo mutation in the Type 1 ryanodine receptor gene associated with fatal, stress-induced malignant hyperthermia in two unrelated families. *Anesthesiology* 115(5):938-945.
141. Wagner Ii LE, Groom LA, Dirksen RT, & Yule DI (2014) Characterization of ryanodine receptor type 1 single channel activity using "on-nucleus" patch clamp. *Cell Calcium* 56(2):96-107.
142. Cong L*, et al.* (2013) Multiplex genome engineering using CRISPR/Cas systems. *Science* 339(6121):819-823.
143. Woong Y Hwang YF, Deepak Reyon, Morgan L Maeder, Shengdar Q Tsai, Jeffry D Sander, Randall T Peterson, J-R Joanna Yeh & J Keith Joung (2013) Efficient genome editing in zebrafish using a CRISPR-Cas system. *Nature* 31:227-229.
144. Werner Klingler CB, Michael Georgieff, Frank Lehmann-Horn, Werner Melzer, (2002) Detection of Proton Release from Cultured Human Myotubes to Identify Malignant Hyperthermia Susceptibility. *Anesthesiology* 97:1059-1066.

Appendices

Appendix I

Oligonucleotide primers

Site directed mutagenesis

primer	sequence
c.641C>T forward	GAAGAGGGCTTCGTGATGGGAGGTCACGTCCTC
c.641C>T reverse	GAGGACGTGACCTCCCATCACGAAGCCCTCTTC

N-terminal domain PCR primers

Primer	sequence
Forward primer	GGGGGGATCCATGGGTGACGCAGAAGGCGAA
pGEX6p3/pMALp2g reverse	GCCCGCGGCCGCATTGCCAGACGAGGCCTCCAGCCG
pET32a/pProEXHTb reverse	AAGCTTCGCCAGACGAGGCCTCCAGCCG

Helical domain PCR primers

	Sequence
pET32a forward	CATGCCATGGCGGGCTCCACGCCCCTGGAC
pET32a reverse	CCCAAGCTTGCTTTGGCTGCACCAGAGCC
pProEXHTb forward	CCGGAATCCAAGGCTCCAGCCCCCTGGAC
pProEXHTb/pMALp2g reverse	CCCAAGCTTTTACTTTGGCTGCACCAGAGCC
pGEX6p3 forward	CCGCGGCTCCACGCCCCTGGAC
pGEX6p3 reverse	CCCGCGGCCGCTTACTTTGGCTGCACCAGAGCC
pProEXHTB/pMALp2g forward	CCCGCGGATCCCCCCGGTCCCTGCAGGAGCTG

Appendix II

Vector maps

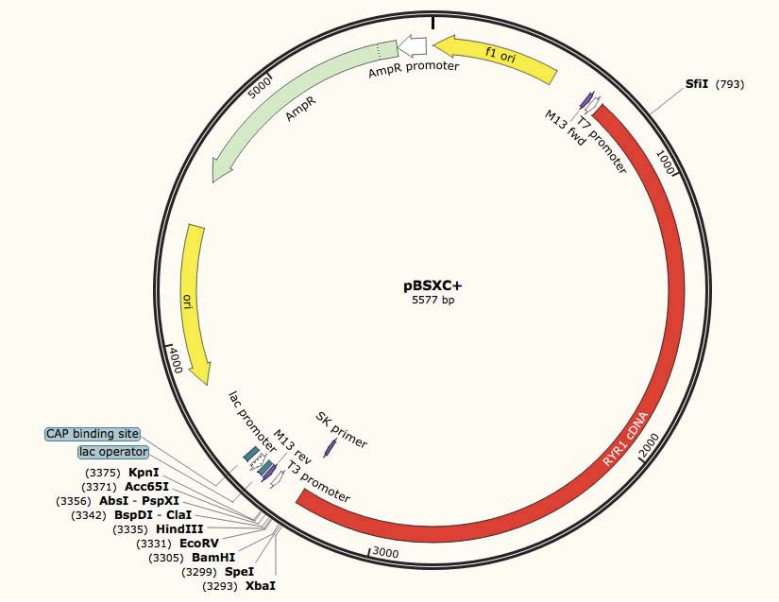

Figure 1 Map of the pBSXC+ vector. The vector map was created using the SnapGene viewer 3.1.2 software.

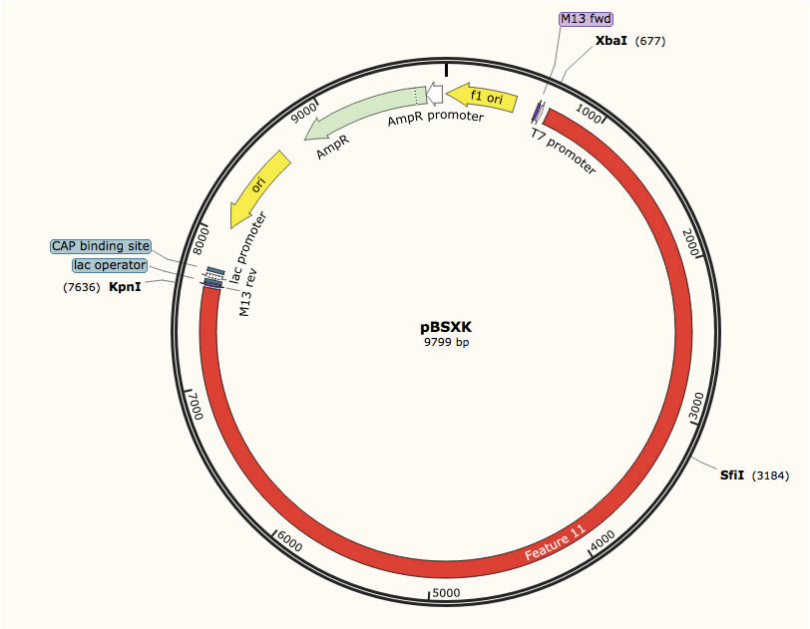

Figure 2 Map of the pBSXK vector. The vector map was created using the SnapGene viewer 3.1.2 software.

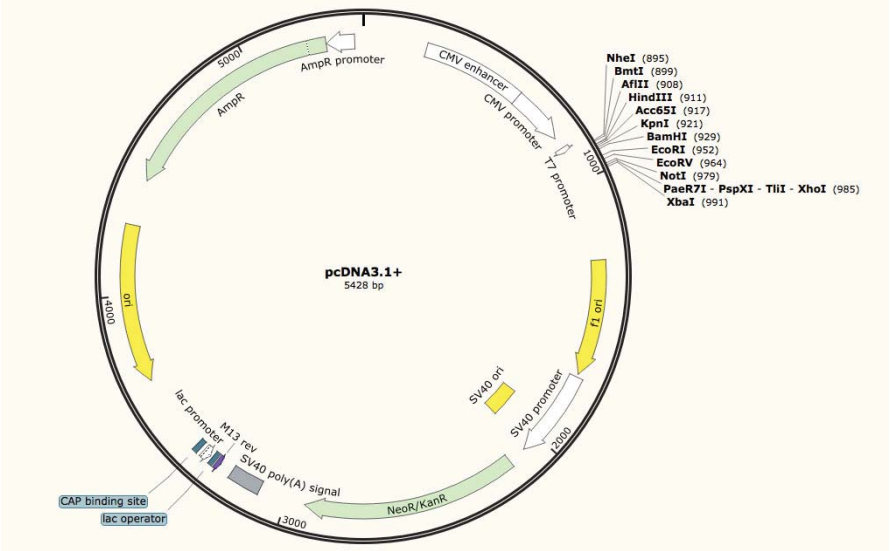

Figure 3 Map of the pcDNA vector. The vector map was created using the SnapGene viewer 3.1.2 software.

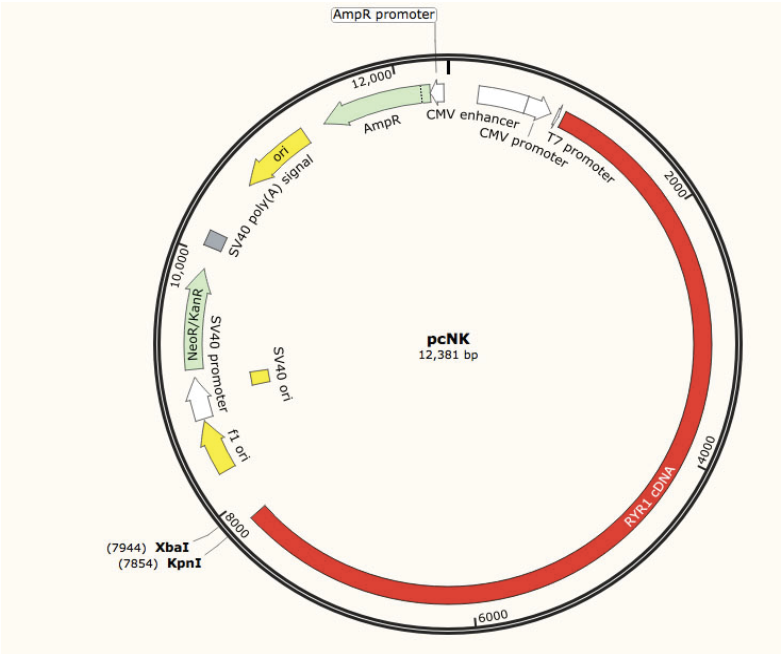

Figure 4 Map of the pcNK vector. The vector map was created using the SnapGene viewer 3.1.2 software.

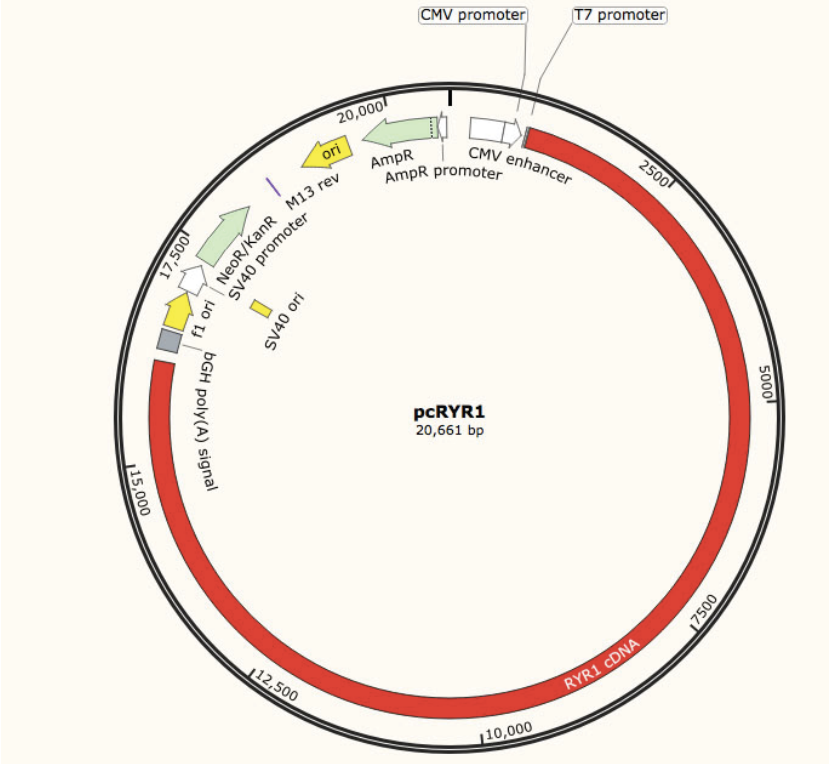

Figure 5 Map of the pc*RYR1* vector. The vector map was created using the SnapGene viewer 3.1.2 software.

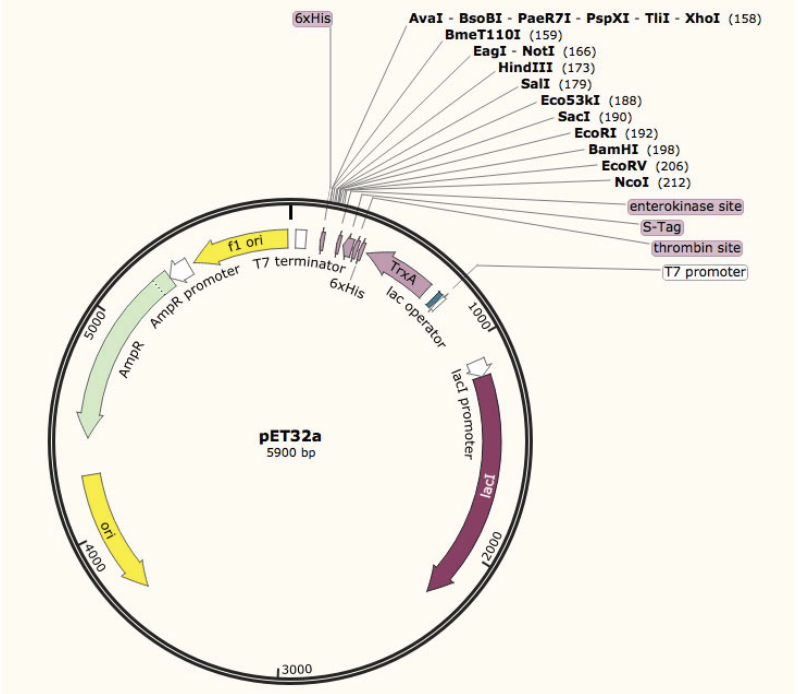

figure 6 Map of the pET32a bacterial expression vector. The vector map was created using the SnapGene viewer 3.1.2 software.

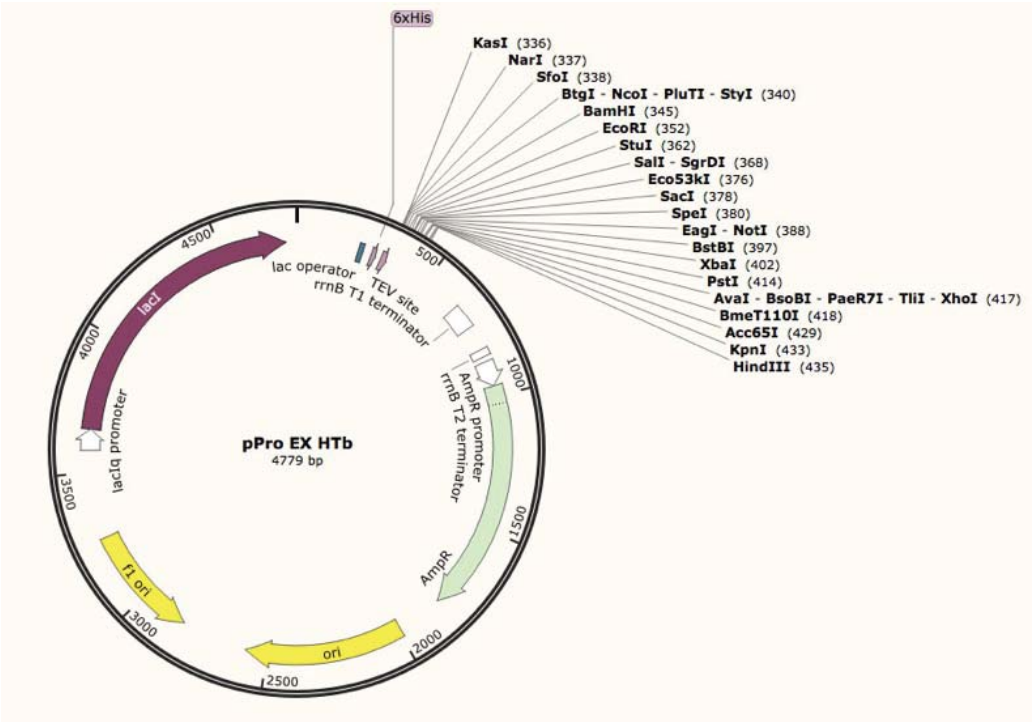

Figure 7 Map of the pProEXHTb vector. The vector map was created using the SnapGene viewer 3.1.2 software.

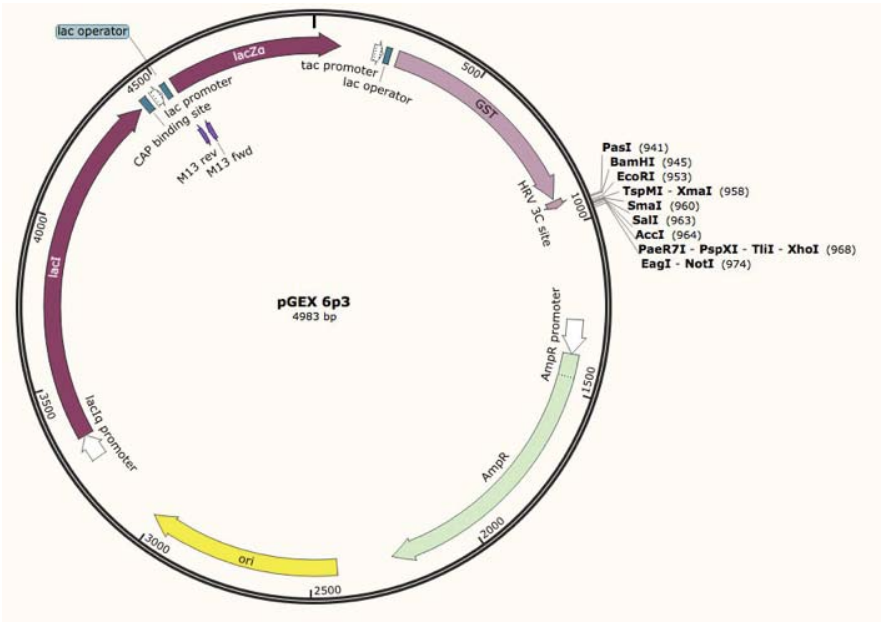

Figure 8 Map of the pGEX6p3 vector. The vector map was created using the SnapGene viewer 3.1.2 software.

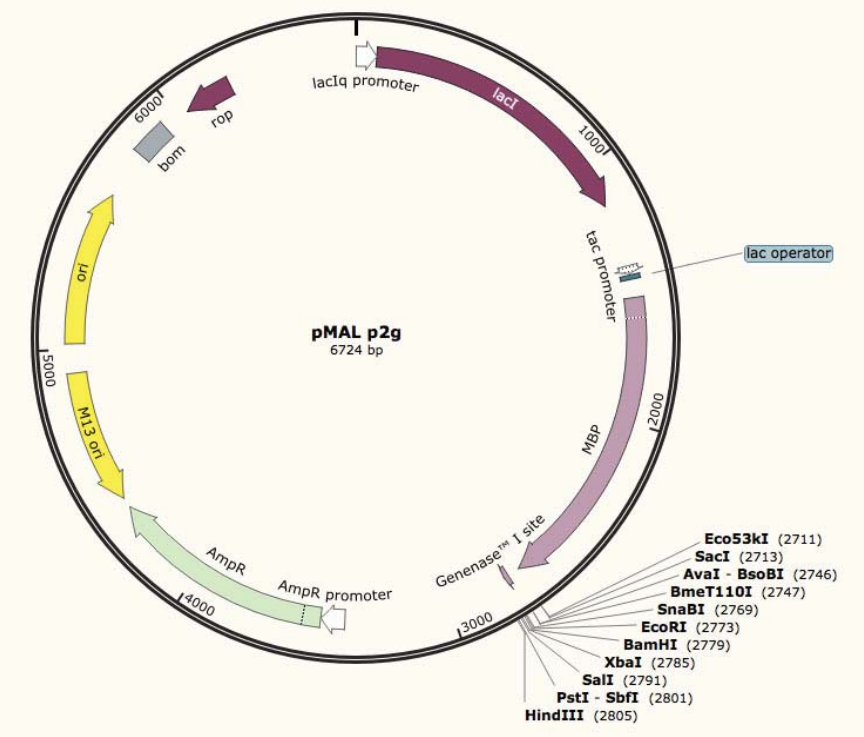

Figure 9 Map of the pMALp2g vector. The vector map was created using the SnapGene viewer 3.1.2 software.

Appendix III

Raw data following Ca^{2+} release assays

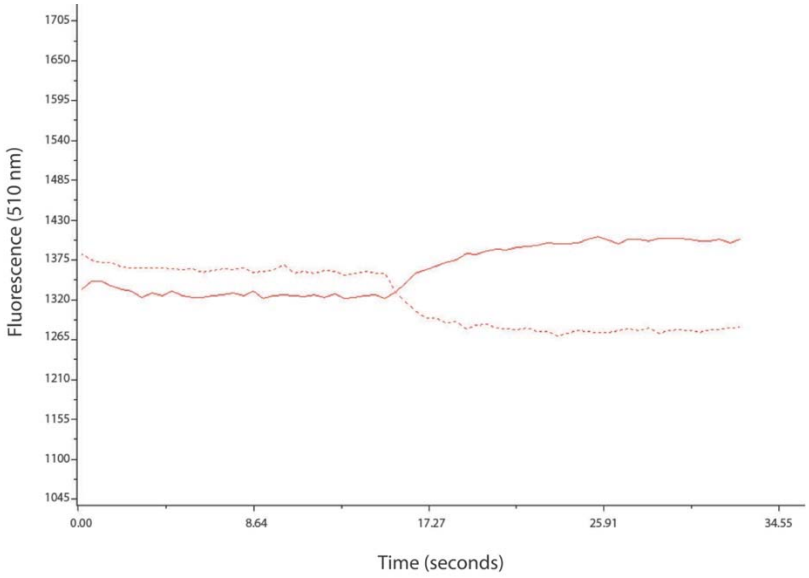

Figure 1 Raw data representative of the Ca^{2+} release assay in HEK293T cells. Fluorescence emission at 510 nm following excitation at 340 (full line) and 380 nm (dashed line). Represented is the raw data following Ca^{2+} release induced in HEK293T cells transiently transfected with pc*RYR1* wild type. A fluorescence base line was established before the addition of 1000 µM 4-C*m*C at roughly 15 seconds.

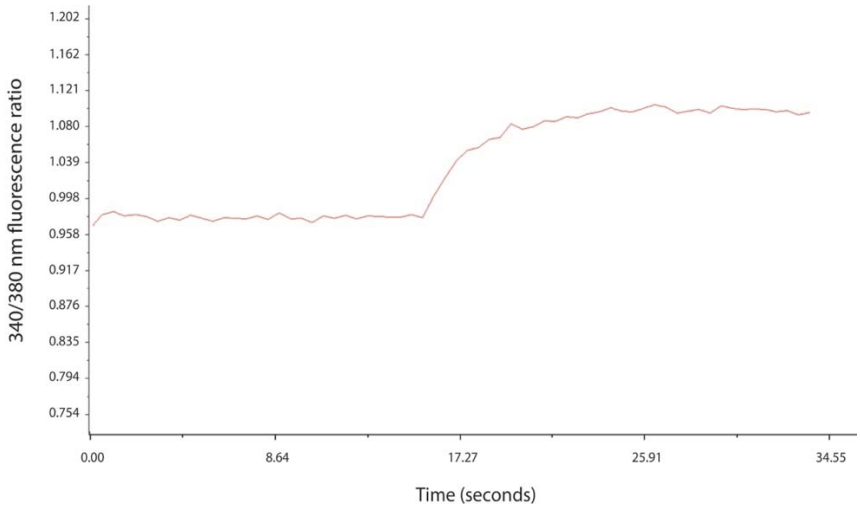

Figure 2 Representative Ca^{2+} release from HEK293T cells transiently transfected with pc*RYR1* wild type. Shown is the change in 340/380 nm fluorescence emission ratio following addition of 1000 µM 4-C*m*C. A fluorescence base line was established before the addition of 4-C*m*C at approximately 15 seconds.

Appendix IV

Confirmation of cloning the *RYR1* nucleotides 1-1674 into a range of bacterial expression vectors

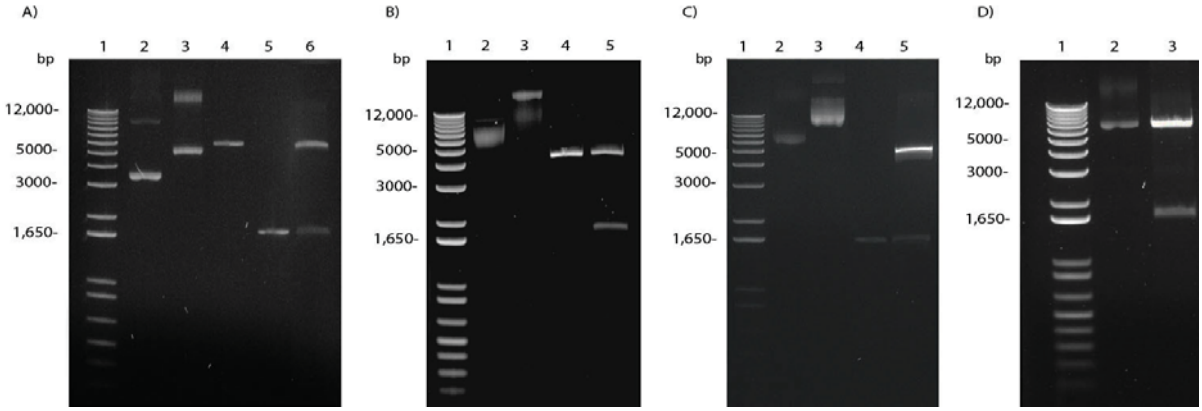

Figure 1 Restriction endonuclease digestion analysis of the *RYR1* N-terminal domain following ligation into a range of expression vectors. DNA was separated on a 1 % (w/v) agarose gel and was separated at 90 mV for one hour DNA was visualised by 0.5 µg/mL ethidium bromide staining using the Image Lab 5.1 software A) Restriction endonuclease digestion of pET32a plus *RYR1* N-terminal domain vector. Lane 1, 1Kb plus DNA size marker. Lane 2, non digested empty pET32a vector. Lane 3, non digested pET32a plus *RYR1* N-terminal domain. Lane 4, Empty pET32a digested with the restriction endonucleases *Bam*HI and *Hind*III. Lane 5, PCR product. Lane 6, pET32a plus *RYR1* N-terminal domain digested with *Bam*HI and *Hind*III. B) Restriction endonuclease digestion of pProEXHTb plus *RYR1* N-terminal domain vector. Lane 1, 1Kb plus DNA size marker. Lane 2, non digested empty pProEXHTb vector. Lane 3, non digested pProEXHTb vector plus *RYR1* N-terminal domain. Lane 4, empty pProEXHTb vector digested with *Bam*HI and *Hind*III. Lane 5, pProEXHTb vector plus *RYR1* N-terminal domain digested with *Bam*HI and *Hind*III C) restriction endonuclease digestion of the pGEX6p3 plus *RYR1* N-terminal domain. Lane 1, 1Kb plus DNA size marker. Lane 2, non digested empty pGEX6p3 vector. Lane 3, non digested pGEX6p3 plus *RYR1* N-terminal domain. Lane 4, PCR product. Lane 5, pGEX6p3 plus *RYR1* N-terminal domain digested with *Bam*HI and *Hind*III. D) restriction endonuclease digestion of the pMALp2g vector. Lane 1, 1Kb plus DNA size marker. Lane 2, non digested pMALp2g vector plus *RYR1* N-terminal domain. Lane 3, pMALp2g vector plus *RYR1* N-terminal domain digested with *Bam*HI and *Hind*III.

Appendix V

Sequence alignment of the human and rabbit *RYR1* cDNA nucleotides

```
Human RYR1      GCTCCAGACCCCAAGGCCCTGCGGCTCGGCGTGCTCAAGAAGAAGGCCATGCTGCACCAG
Rabbit RYR1     GCCCCTGACCCCAAGGCCCTGCGGCTGGGCGTGCTGAAGAAGAAGGCCATTCTGCACCAG
                ** ** ********************* ******** ************** *********

Human RYR1      GAGGGCCACATGGACGACGCACTGTCGCTGACCCGCTGCCAGCAGGAGGAGTCCCAGGCC
Rabbit RYR1     GAGGGCCACATGGACGATGCACTGTTCCTGACCCGCTGCCAGCAGGAGGAGTCCCAGGCT
                ***************** *******  ********************************

Human RYR1      GCCCGCATGATCCACAGCACCAATGGCCTATACAACCAGTTCATCAAGAGCCTGGACAGC
Rabbit RYR1     GCCCGCATGATCCACAGCACTGCCGGCCTGTACAACCAGTTCATCAAGGGCCTGGACAGC
                ********************    ***** ****************** ***********

Human RYR1      TTCAGCGGGAAGCCACGGGGCTCGGGGCCACCCGCTGGCACGGCGCTGCCCATCGAGGGC
Rabbit RYR1     TTCAGCGGGAAGCCCCGGGGCTCAGGGCCGCCGGCTGGCCCTGCGCTGCCCATCGAGGCC
                ************** ******** ***** ** ****** * *************** *

Human RYR1      GTTATCCTGAGCCTGCAGGACCTCATCATCTACTTCGAGCCTCCCTCCGAGGACTTGCAG
Rabbit RYR1     GTCATCCTGAGCCTGCAGGACCTCATTGGCTACTTCGAGCCGCCCTCGGAGGAGCTGCAG
                ** ************************   ************ ***** *****  *****

Human RYR1      CACGAGGAGAAGCAGAGCAAGCTGCGAAGCCTGCGCAACCGCCAGAGCCTCTTCCAGGAG
Rabbit RYR1     CACGAGGAAAAGCAGAGCAAGCTGCGCAGCCTGCGCAACCGCCAGAGCCTCTTCCAGGAG
                ******** ***************** ***********************************

Human RYR1      GAGGGGATGCTCTCCATGGTCCTGAATTGCATAGACCGCCTAAATGTCTACACCACTGCT
Rabbit RYR1     GAGGGGATGCTCTCCCTGGTCCTGAACTGCATCGACCGCCTGAACGTCTACACCACCGCT
                *************** ********** ***** ******** ** *********** ***

Human RYR1      GCCCACTTTGCTGAGTTTGCAGGGGAGGAGGCAGCCGAGTCCTGGAAAGAGATTGTGAAT
Rabbit RYR1     GCCCACTTTGCCGAGTATGCAGGGGAAGAGGCAGCTGAGTCCTGGAAAGAGATTGTTAAC
                *********** **** ********* ******** ******************** **

Human RYR1      CTTCTCTATGAACTCCTAGCTTCTCTAATCCGTGGCAATCGTAGCAACTGTGCCCTCTTC
Rabbit RYR1     CTACTCTACGAACTCCTGGCCTCTCTGATCCGGGGCAATCGTGCCAACTGTGCCCTCTTC
                ** ***** ******** ** ***** ***** *********  ****************
```

Figure 1 Sequence alignment of human *RYR1* cDNA and rabbit *RYR1* cDNA. The alignment was performed by the Clustal omega software (116). * indicates a conserved nucleotide, a blank space represents a non conserved nucleotide.

Appendix VI

Sequence alignment of the of the human *RYR1* cDNA and the *RYR1* cDNA optimised for bacterial expression

```
RYR1 cDNA                1    ATGGGTGACGCAGAAGGCGAAGACGAGGTCCAGTTCCTGCGGACGGACGATGAGGTGGTC
Codon optimised cDNA     1    ATGGGCGATGCCGAAGGCGAAGACGAAGTCCAATTCCTGCGTACCGATGATGAAGTTGTC
                              ***** ** ** ************** ***** ******** ** ** ***** ** ***

RYR1 cDNA               61    CTGCAGTGCAGCGCTACCGTGCTCAAGGAGCAGCTCAAGCTCTGCCTGGCCGCCGAGGGC
Codon optimised cDNA    61    CTGCAATGTAGCGCGACCGTGCTGAAAGAACAGCTGAAACTGTGCCTGGCGGCCGAAGGT
                              ***** ** ***** ******** ** ** ***** ** ** ******** ***** **

RYR1 cDNA              121    TTCGGCAACCGCCTGTGCTTCCTGGAGCCCACTAGCAACGCGCAGAATGTGCCCCCCGAT
Codon optimised cDNA   121    TTTGGCAACCGTCTGTGTTTCCTGGAACCGACCTCTAACGCGCAAAATGTTCCGCCGGAT
                              ** ******** ***** ******** ** **     ******** ***** ** ** ***

RYR1 cDNA              181    CTGGCCATCTGTTGCTTCGTCCTGGAGCAGTCCCTGTCTGTGCGAGCCCTGCAGGAGATG
Codon optimised cDNA   181    CTGGCCATTTGCTGTTTTGTCCTGGAACAGTCACTGTCGGTGCGTGCGCTGCAAGAAATG
                              ******** ** ** ** ******** ***** ***** ***** ** ***** ** ***

RYR1 cDNA              241    CTGGCTAACACGGTGGAGGCTGGCGTGGAGTCATCCCAGGGCGGGGGACACAGGACGCTC
Codon optimised cDNA   241    CTGGCAAATACCGTCGAAGCTGGTGTGGAAAGCAGCCAGGGCGGTGGCCATCGTACCCTG
                              ***** ** ** ** ** ***** *****      ********* ** **  * ** **

RYR1 cDNA              301    CTGTATGGCCATGCCATCCTGCTCCGGCATGCACACAGCCGCATGTATCTGAGCTGCCTC
Codon optimised cDNA   301    CTGTATGGCCACGCAATCCTGCTGCGTCATGCTCACTCCCGCATGTACCTGTCATGCCTG
                              ********** ** ******** ** ***** ***  ********* ***   *****

RYR1 cDNA              361    ACCACCTCCCGCTCCATGACTGACAAGCTGGCCTTCGATGTGGGACTGCAGGAGGACGCA
Codon optimised cDNA   361    ACCACGAGCCGTTCTATGACCGATAAACTGGCATTTGACGTCGGTCTGCAGGAAGATGCG
                              *****   *** ** ***** ** ** ***** ** ** ** ** ******** ** **

RYR1 cDNA              421    ACAGGAGAGGCTTGCTGGTGGACCATGCACCCAGCCTCCAAGCAGAGGTCTGAAGGAGAA
Codon optimised cDNA   421    ACCGGCGAAGCCTGTTGGTGGACGATGCATCCGGCGTCCAAACAACGTTCAGAAGGTGAA
                              ** ** ** ** ** ******** ***** ** ** ***** **  * ** ***** ***

RYR1 cDNA              481    AAGGTCCGCGTTGGGGATGACATCATCCTTGTCAGTGTCTCCTCCGAGCGCTACCTGCAC
Codon optimised cDNA   481    AAAGTGCGCGTTGGCGATGACATTATCCTGGTCAGTGTGAGTTCCGAACGCTATCTGCAC
                              ** ** ******** ******** ***** ********    ***** ***** ******

RYR1 cDNA              541    CTGTCGACCGCCAGTGGGGAGCTCCAGGTTGACGCTTCCTTCATGCAGACACTATGGAAC
Codon optimised cDNA   541    CTGTCTACCGCAAGTGGTGAACTGCAGGTGGACGCTTCTTTCATGCAAACGCTGTGGAAC
                              ***** ***** ***** ** ** ***** ******** ******** ** ** ******

RYR1 cDNA              601    ATGAACCCCATCTGCTCCCGCTGCGAAGAGGGCTTCGTGACGGGAGGTCACGTCCTCCGC
Codon optimised cDNA   601    ATGAATCCGATTTGCAGTCGTTGTGAAGAAGGTTTTGTTACCGGTGGCCATGTCCTGCGC
                              ***** ** ** ***   ** ** ***** ** ** ** ** ** ** ** ***** ***

RYR1 cDNA              661    CTCTTTCATGGACATATGGATGAGTGTCTGACCATTTCCCCTGCTGACAGTGATGACCAG
Codon optimised cDNA   661    CTGTTCCATGGCCACATGGATGAATGCCTGACGATCAGCCCGGCCGACAGCGATGACCAG
                              ** ** ***** ** ******** ** ***** **   *** ** ***** *********

RYR1 cDNA              721    CGCAGACTTGTCTACTATGAGGGGGGAGCTGTGTGCACTCATGCCCGCTCCCTCTGGAGG
Codon optimised cDNA   721    CGTCGCCTGGTTTATTATGAAGGTGGCGCGGTCTGTACCCATGCACGTTCCCTGTGGCGC
                              **  * ** ** ** ***** ** ** ** ** ** ** ***** ** ***** *** *

RYR1 cDNA              781    CTGGAGCCACTGAGAATCAGCTGGAGTGGGAGCCACCTGCGCTGGGGCCAGCCACTCCGA
Codon optimised cDNA   781    CTGGAACCGCTGCGTATTAGTTGGTCCGGTTCACATCTGCGCTGGGGTCAGCCGCTGCGT
                              ***** ** *** * ** ** ***   **    ** ************ ***** ** **

RYR1 cDNA              841    GTCCGGCATGTCACTACCGGGCAGTACCTAGCGCTCACCGAGGACCAGGGCCTGGTGGTG
Codon optimised cDNA   841    GTTCGTCATGTCACCACCGGCCAGTATCTGGCCCTGACGGAAGATCAAGGCCTGGTGGTT
                              ** ** ******** ***** ***** ** ** ** ** ** ** ** ************

RYR1 cDNA              901    GTTGACGCCAGCAAGGCTCACACCAAGGCTACCTCCTTCTGCTTCCGCATCTCCAAGGAG
Codon optimised cDNA   901    GTCGACGCAAGCAAAGCTCATACCAAAGCAACGTCGTTTTGCTTCCGTATTAGCAAAGAA
                              ** ***** ***** ***** ***** ** ** ** ** ******** **   *** **

RYR1 cDNA              961    AAGCTGGATGTGGCCCCCAAGCGGGATGTGGAGGGCATGGGCCCCCCCTGAGATCAAGTAC
Codon optimised cDNA   961    AAACTGGATGTGGCTCCGAAACGCGACGTTGAGGGTATGGGTCCGCCGGAAATCAAATAT
                              ** ************ ** ** ** ** ** ***** ***** ** ** ** ***** **

RYR1 cDNA             1021    GGGGAGTCACTGTGCTTCGTGCAGCATGTGGCCTCAGGACTGTGGCTCACCTATGCTGCT
Codon optimised cDNA  1021    GGTGAATCGCTGTGTTTTGTGCAGCACGTTGCCAGCGGTCTGTGGCTGACCTATGCAGCT
                              ** ** ** ***** ** ******** ** ***   ** ******** ******** ***
```

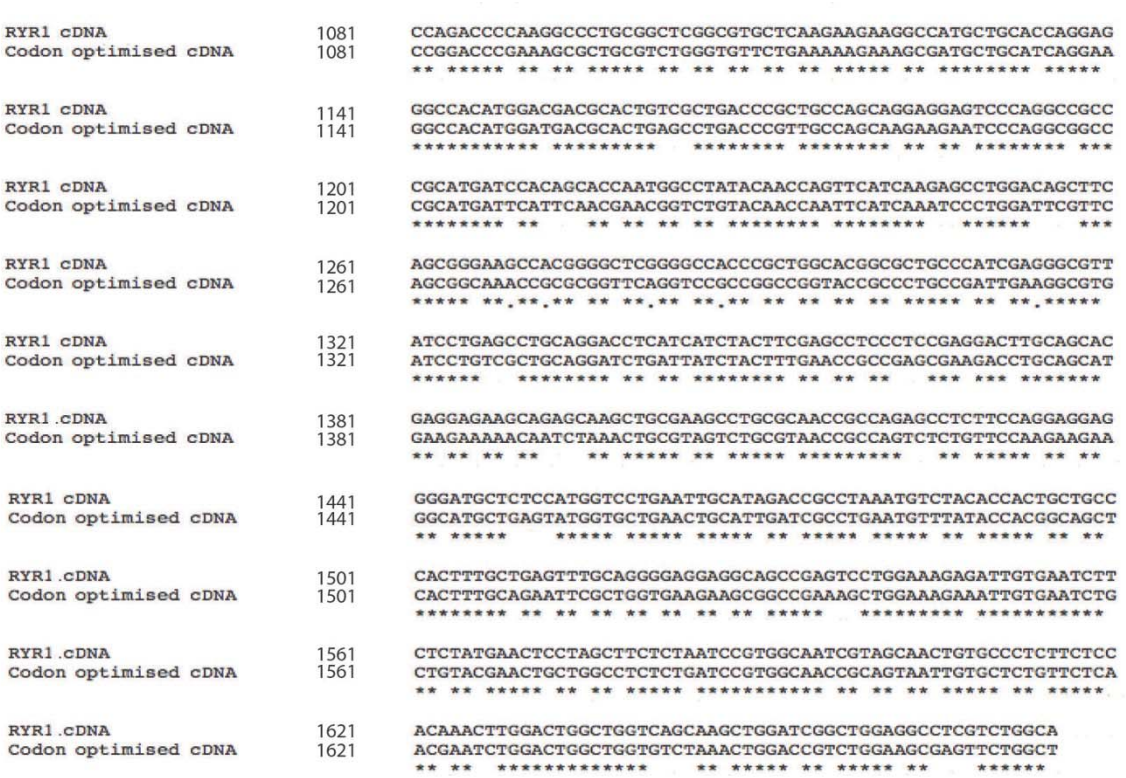

Figure 1 Codon optimised cDNA aligned with the *RYR1* cDNA. The alignment was performed using the clustal omega software. The nucleotide number have been indicated. * a non changed nucleotide, a blank space represents a changed nucleotide.

Appendix VII

Confirmation of cloning the *RYR1* cDNA nucleotides 6,807-7575 into a range of bacterial expression vectors

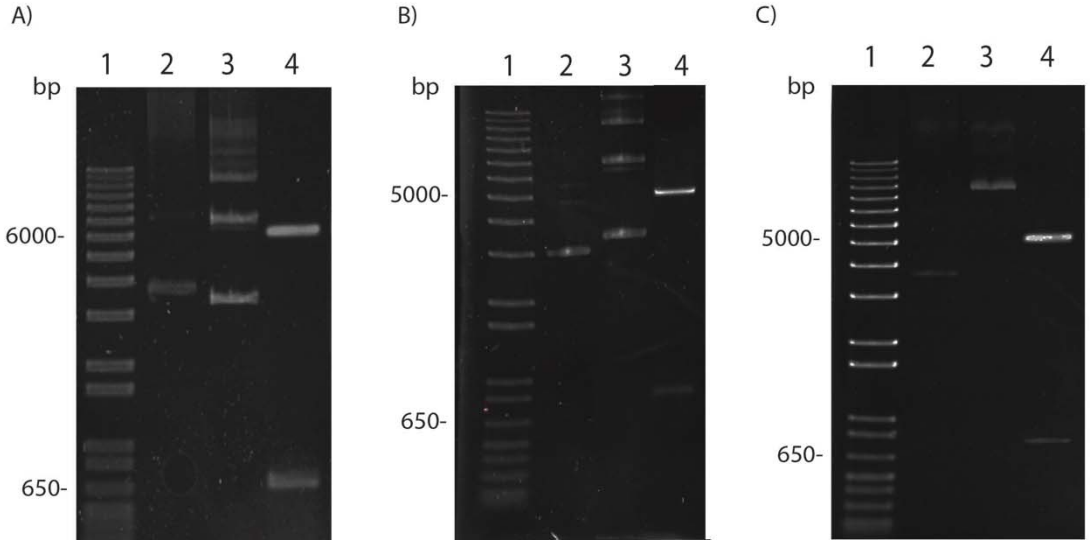

Figure 1 Restriction endonuclease digestion confirming the cloning of *RYR1* nucleotides 6604-7575 into the expression vectors pET32a, pProEXHTb and pGEX6p3. DNA was loaded onto a 1 % (w/v) agarose gel and was separated at 90 mV for one hour DNA was visualised by 0.5 µg/mL ethidium bromide staining using the Image Lab 5.1 software. Lane 1, 1Kb plus size marker. Lane 2, non digested empty vector. Lane 3, non digested vector containing *RYR1* cDNA. Lane, 4 vector containing *RYR1* cDNA following digestion. A) confirmation of cloning into the pET32a vector using the restriction endonuclease *Eco*RI and *Nco*I. B) confirmation of cloning into the pProEXHTb vector using the restriction endonucleases *Eco*RI and *Hind*III. C) Confirmation of cloning into the pGEX6p3 vector using the restriction endonucleases *Eco*RI and *Not*I.

Appendix VIII

PCR amplification of the *RYR1* nucleotides 6,271-7,575 and conformation of cloning into the pProEXHTb and pMALp2g vectors

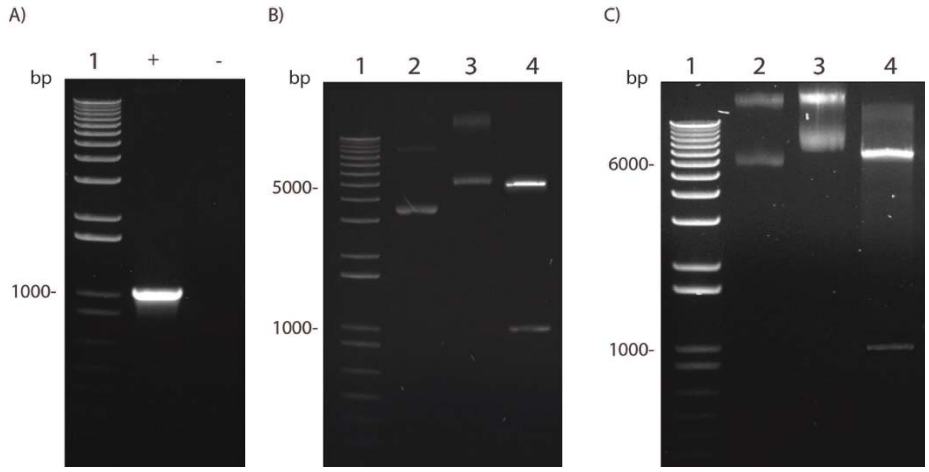

Figure 2 PCR amplification of nucleotides 6,271-7,575 and confirmation of cloning of nucleotides into the pProEXHTb vector and pMALp2g vector. DNA was loaded onto a 1 % (w/v) agarose gel, separated at 90 mV for one hour, DNA and visualised by 0.5 µg/mL ethidium bromide staining using the Image Lab 5.1 software. A) PCR amplification of *RYR1* cDNA. 10 % of the PCR reaction was analysed by gel electrophoresis. Lane 1, 1Kb plus DNA ladder. + indicates the PCR amplification containing template DNA. – indicates negative control for PCR, containing no template DNA. B) Restriction endonuclease digestion analysis of the pProEXHTb plus *RYR1* cDNA. Lane 1, 1 Kb plus size marker. Lane 2, non digested pProEXHTb vector. Lane 3, non digested pProEXHTb plus *RYR1* cDNA. Lane 4, pProEXHTb plus RYR1 cDNA digested with *Bam*HI and *Hind*III C) restriction endonuclease digestion of the pMALp2g vector with RYR1 cDNA. Lane 1, 1Kb plus size marker. Lane 2, non digested pMALp2g vector. Lane 3, non digested pMALp2g vector with *RYR1* cDNA. Lane 4, pMALp2g vector with RYR1 cDNA digested with *Bam*HI and *Hind*III.

Appendix IX

RYR1 cDNA and amino acid sequence

```
   1 ATGGGTGACGCAGAAGGCGAAGACGAGGTCCAGTTCCTGCGGACGGACGATGAGGTGGTC     60
   1 -M--G--D--A--E--G--E--D--E--V--Q--F--L--R--T--D--D--E--V--V-     20

  61 CTGCAGTGCAGCGCTACCGTGCTCAAGGAGCAGCTCAAGCTCTGCCTGGCCGCCGAGGGC    120
  21 -L--Q--C--S--A--T--V--L--K--E--Q--L--K--L--C--L--A--A--E--G-     40

 121 TTCGGCAACCGCCTGTGCTTCCTGGAGCCCACTAGCAACGCGCAGAATGTGCCCCCCGAT    180
  41 -F--G--N--R--L--C--F--L--E--P--T--S--N--A--Q--N--V--P--P--D-     60

 181 CTGGCCATCTGTTGCTTCGTCCTGGAGCAGTCCCTGTCTGTGCGAGCCCTGCAGGAGATG    240
  61 -L--A--I--C--C--F--V--L--E--Q--S--L--S--V--R--A--L--Q--E--M-     80

 241 CTGGCTAACACGGTGGAGGCTGGCGTGGAGTCATCCCAGGGCGGGGGACACAGGACGCTC    300
  81 -L--A--N--T--V--E--A--G--V--E--S--S--Q--G--G--G--H--R--T--L-    100

 301 CTGTATGGCCATGCCATCCTGCTCCGGCATGCACACAGCCGCATGTATCTGAGCTGCCTC    360
 101 -L--Y--G--H--A--I--L--L--R--H--A--H--S--R--M--Y--L--S--C--L-    120

 361 ACCACCTCCCGCTCCATGACTGACAAGCTGGCCTTCGATGTGGGACTGCAGGAGGACGCA    420
 121 -T--T--S--R--S--M--T--D--K--L--A--F--D--V--G--L--Q--E--D--A-    140

 421 ACAGGAGAGGCTTGCTGGTGGACCATGCACCCAGCCTCCAAGCAGAGGTCTGAAGGAGAA    480
 141 -T--G--E--A--C--W--W--T--M--H--P--A--S--K--Q--R--S--E--G--E-    160

 481 AAGGTCCGCGTTGGGGATGACATCATCCTTGTCAGTGTCTCCTCCGAGCGCTACCTGCAC    540
 161 -K--V--R--V--G--D--D--I--I--L--V--S--V--S--S--E--R--Y--L--H-    180

 541 CTGTCGACCGCCAGTGGGGAGCTCCAGGTTGACGCTTCCTTCATGCAGACACTATGGAAC    600
 181 -L--S--T--A--S--G--E--L--Q--V--D--A--S--F--M--Q--T--L--W--N-    200

 601 ATGAACCCCATCTGCTCCCGCTGCGAAGAGGGCTTCGTGACGGGAGGTCACGTCCTCCGC    660
 201 -M--N--P--I--C--S--R--C--E--E--G--F--V--T--G--G--H--V--L--R-    220

 661 CTCTTTCATGGACATATGGATGAGTGTCTGACCATTTCCCCTGCTGACAGTGATGACCAG    720
 221 -L--F--H--G--H--M--D--E--C--L--T--I--S--P--A--D--S--D--D--Q-    240
```

```
 721 CGCAGACTTGTCTACTATGAGGGGGGAGCTGTGTGCACTCATGCCCGCTCCCTCTGGAGG    780
 241 -R--R--L--V--Y--Y--E--G--G--A--V--C--T--H--A--R--S--L--W--R-    260

 781 CTGGAGCCACTGAGAATCAGCTGGAGTGGGAGCCACCTGCGCTGGGGCCAGCCACTCCGA    840
 261 -L--E--P--L--R--I--S--W--S--G--S--H--L--R--W--G--Q--P--L--R-    280

 841 GTCCGGCATGTCACTACCGGGCAGTACCTAGCGCTCACCGAGGACCAGGGCCTGGTGGTG    900
 281 -V--R--H--V--T--T--G--Q--Y--L--A--L--T--E--D--Q--G--L--V--V-    300

 901 GTTGACGCCAGCAAGGCTCACACCAAGGCTACCTCCTTCTGCTTCCGCATCTCCAAGGAG    960
 301 -V--D--A--S--K--A--H--T--K--A--T--S--F--C--F--R--I--S--K--E-    320

 961 AAGCTGGATGTGGCCCCCAAGCGGGATGTGGAGGGCATGGGCCCCCCTGAGATCAAGTAC   1020
 321 -K--L--D--V--A--P--K--R--D--V--E--G--M--G--P--P--E--I--K--Y-    340

1021 GGGGAGTCACTGTGCTTCGTGCAGCATGTGGCCTCAGGACTGTGGCTCACCTATGCTGCT   1080
 341 -G--E--S--L--C--F--V--Q--H--V--A--S--G--L--W--L--T--Y--A--A-    360

1081 CCAGACCCCAAGGCCCTGCGGCTCGGCGTGCTCAAGAAGAAGGCCATGCTGCACCAGGAG   1140
 361 -P--D--P--K--A--L--R--L--G--V--L--K--K--K--A--M--L--H--Q--E-    380

1141 GGCCACATGGACGACGCACTGTCGCTGACCCGCTGCCAGCAGGAGGAGTCCCAGGCCGCC   1200
 381 -G--H--M--D--D--A--L--S--L--T--R--C--Q--Q--E--E--S--Q--A--A-    400

1201 CGCATGATCCACAGCACCAATGGCCTATACAACCAGTTCATCAAGAGCCTGGACAGCTTC   1260
 401 -R--M--I--H--S--T--N--G--L--Y--N--Q--F--I--K--S--L--D--S--F-    420

1261 AGCGGGAAGCCACGGGGCTCGGGGCCACCCGCTGGCACGGCGCTGCCCATCGAGGGCGTT   1320
 421 -S--G--K--P--R--G--S--G--P--P--A--G--T--A--L--P--I--E--G--V-    440

1321 ATCCTGAGCCTGCAGGACCTCATCATCTACTTCGAGCCTCCCTCCGAGGACTTGCAGCAC   1380
 441 -I--L--S--L--Q--D--L--I--I--Y--F--E--P--P--S--E--D--L--Q--H-    460

1381 GAGGAGAAGCAGAGCAAGCTGCGAAGCCTGCGCAACCGCCAGAGCCTCTTCCAGGAGGAG   1440
 461 -E--E--K--Q--S--K--L--R--S--L--R--N--R--Q--S--L--F--Q--E--E-    480

1441 GGGATGCTCTCCATGGTCCTGAATTGCATAGACCGCCTAAATGTCTACACCACTGCTGCC   1500
 481 -G--M--L--S--M--V--L--N--C--I--D--R--L--N--V--Y--T--T--A--A-    500

1501 CACTTTGCTGAGTTTGCAGGGGAGGAGGCAGCCGAGTCCTGGAAAGAGATTGTGAATCTT   1560
 501 -H--F--A--E--F--A--G--E--E--A--A--E--S--W--K--E--I--V--N--L-    520
```

```
1561 CTCTATGAACTCCTAGCTTCTCTAATCCGTGGCAATCGTAGCAACTGTGCCCTCTTCTCC   1620
 521 -L--Y--E--L--L--A--S--L--I--R--G--N--R--S--N--C--A--L--F--S-    540

1621 ACAAACTTGGACTGGCTGGTCAGCAAGCTGGATCGGCTGGAGGCCTCGTCTGGCATCCTG   1680
 541 -T--N--L--D--W--L--V--S--K--L--D--R--L--E--A--S--S--G--I--L-    560

1681 GAGGTCCTGTACTGTGTCCTCATTGAGAGTCCAGAGGTTCTGAACATCATCCAGGAGAAT   1740
 561 -E--V--L--Y--C--V--L--I--E--S--P--E--V--L--N--I--I--Q--E--N-    580

1741 CACATCAAGTCCATCATCTCCCTCCTGGACAAGCATGGGAGGAACCACAAGGTCCTGGAC   1800
 581 -H--I--K--S--I--I--S--L--L--D--K--H--G--R--N--H--K--V--L--D-    600

1801 GTGCTATGCTCCCTGTGTGTGTGTAATGGTGTGGCTGTACGCTCCAACCAAGATCTTATT   1860
 601 -V--L--C--S--L--C--V--C--N--G--V--A--V--R--S--N--Q--D--L--I-    620

1861 ACTGAGAACTTGCTGCCTGGCCGTGAGCTTCTGCTGCAGACAAACCTCATCAACTATGTC   1920
 621 -T--E--N--L--L--P--G--R--E--L--L--L--Q--T--N--L--I--N--Y--V-    640

1921 ACCAGCATCCGCCCCAACATCTTTGTGGGCCGAGCGGAAGGCACCACGCAGTACAGCAAA   1980
 641 -T--S--I--R--P--N--I--F--V--G--R--A--E--G--T--T--Q--Y--S--K-    660

1981 TGGTACTTTGAGGTGATGGTGGACGAGGTGACTCCATTTCTGACAGCTCAGGCCACCCAC   2040
 661 -W--Y--F--E--V--M--V--D--E--V--T--P--F--L--T--A--Q--A--T--H-    680

2041 TTGCGGGTGGGCTGGGCCCTCACCGAGGGCTACACCCCCTACCCTGGGGCCGGCGAGGGC   2100
 681 -L--R--V--G--W--A--L--T--E--G--Y--T--P--Y--P--G--A--G--E--G-    700

2101 TGGGGCGGCAACGGGGTCGGCGATGACCTCTATTCCTACGGCTTTGATGGACTGCATCTC   2160
 701 -W--G--G--N--G--V--G--D--D--L--Y--S--Y--G--F--D--G--L--H--L-    720

2161 TGGACAGGACACGTGGCACGCCCAGTGACTTCCCCAGGGCAGCACCTCCTGGCCCCTGAA   2220
 721 -W--T--G--H--V--A--R--P--V--T--S--P--G--Q--H--L--L--A--P--E-    740

2221 GACGTGATCAGCTGCTGCCTGGACCTCAGCGTGCCGTCCATCTCCTTCCGCATCAACGGC   2280
 741 -D--V--I--S--C--C--L--D--L--S--V--P--S--I--S--F--R--I--N--G-    760

2281 TGCCCCGTGCAGGGTGTCTTTGAGTCCTTCAACCTGGACGGGCTCTTCTTCCCTGTTGTC   2340
 761 -C--P--V--Q--G--V--F--E--S--F--N--L--D--G--L--F--F--P--V--V-    780
```

```
2341 AGCTTCTCGGCTGGTGTCAAGGTGCGGTTCCTCCTTGGTGGCCGCCATGGTGAATTCAAG   2400
 781 -S--F--S--A--G--V--K--V--R--F--L--L--G--G--R--H--G--E--F--K-    800

2401 TTCCTGCCCCCACCTGGCTATGCTCCATGCCATGAGGCTGTGCTCCCTCGAGAGCGACTC   2460
 801 -F--L--P--P--P--G--Y--A--P--C--H--E--A--V--L--P--R--E--R--L-    820

2461 CATCTTGAACCCATCAAGGAGTATCGACGGGAGGGGCCCCGGGGGCCTCACCTGGTGGGC   2520
 821 -H--L--E--P--I--K--E--Y--R--R--E--G--P--R--G--P--H--L--V--G-    840

2521 CCCAGTCGCTGCCTCTCACACACCGACTTCGTGCCCTGCCCTGTGGACACTGTCCAGATT   2580
 841 -P--S--R--C--L--S--H--T--D--F--V--P--C--P--V--D--T--V--Q--I-    860

2581 GTCCTGCCGCCCCATCTGGAGCGCATTCGGGAGAAGCTGGCGGAGAACATCCACGAGCTC   2640
 861 -V--L--P--P--H--L--E--R--I--R--E--K--L--A--E--N--I--H--E--L-    880

2641 TGGGCGCTAACCCGCATCGAGCAGGGCTGGACCTACGGCCCGGTTCGGGATGACAACAAG   2700
 881 -W--A--L--T--R--I--E--Q--G--W--T--Y--G--P--V--R--D--D--N--K-    900

2701 AGGCTGCACCCGTGTCTTGTGGACTTCCACAGCCTTCCAGAGCCTGAGAGGAACTACAAC   2760
 901 -R--L--H--P--C--L--V--D--F--H--S--L--P--E--P--E--R--N--Y--N-    920

2761 CTGCAGATGTCTGGGGAGACGCTCAAGACTCTGCTGGCTCTGGGCTGCCACGTGGGCATG   2820
 921 -L--Q--M--S--G--E--T--L--K--T--L--L--A--L--G--C--H--V--G--M-    940

2821 GCGGATGAGAAGGCGGAGGACAACCTGAAGAAGACAAAACTCCCCAAGACGTATATGATG   2880
 941 -A--D--E--K--A--E--D--N--L--K--K--T--K--L--P--K--T--Y--M--M-    960

2881 AGCAATGGGTACAAGCCGGCTCCGCTGGACCTGAGCCACGTGCGGCTGACGCCGGCGCAG   2940
 961 -S--N--G--Y--K--P--A--P--L--D--L--S--H--V--R--L--T--P--A--Q-    980

2941 ACGACACTGGTGGACCGTCTGGCAGAAAATGGGCACAACGTGTGGGCCCGAGACCGCGTG   3000
 981 -T--T--L--V--D--R--L--A--E--N--G--H--N--V--W--A--R--D--R--V-   1000

3001 GGCCAGGGCTGGAGCTACAGCGCAGTGCAGGACATCCCAGCGCGCCGAAACCCTCGGCTG   3060
1001 -G--Q--G--W--S--Y--S--A--V--Q--D--I--P--A--R--R--N--P--R--L-   1020

3061 GTGCCCTACCGCCTGCTGGATGAAGCCACCAAGCGCAGCAACCGGGACAGCCTCTGCCAG   3120
1021 -V--P--Y--R--L--L--D--E--A--T--K--R--S--N--R--D--S--L--C--Q-   1040

3121 GCCGTGCGCACCCTCCTGGGCTACGGCTACAACATCGAGCCTCCTGACCAGGAGCCCAGT   3180
1041 -A--V--R--T--L--L--G--Y--G--Y--N--I--E--P--P--D--Q--E--P--S-   1060
```

```
3181 CAGGTGGAGAACCAGTCTCGTTGTGACCGGGTGCGCATCTTCCGGGCAGAGAAATCCTAT   3240
1061 -Q--V--E--N--Q--S--R--C--D--R--V--R--I--F--R--A--E--K--S--Y-   1080

3241 ACAGTGCAGAGCGGCCGCTGGTACTTCGAGTTTGAAGCAGTCACCACAGGCGAGATGCGC   3300
1081 -T--V--Q--S--G--R--W--Y--F--E--F--E--A--V--T--T--G--E--M--R-   1100

3301 GTGGGCTGGGCGAGGCCCGAGCTGAGGCCTGATGTAGAGCTGGGAGCTGACGAGCTGGCC   3360
1101 -V--G--W--A--R--P--E--L--R--P--D--V--E--L--G--A--D--E--L--A-   1120

3361 TATGTCTTCAATGGGCACCGCGGCCAGCGCTGGCACTTGGGCAGTGAACCATTTGGGCGC   3420
1121 -Y--V--F--N--G--H--R--G--Q--R--W--H--L--G--S--E--P--F--G--R-   1140

3421 CCCTGGCAGCCGGGCGATGTCGTTGGCTGTATGATCGACCTCACAGAGAACACCATTATC   3480
1141 -P--W--Q--P--G--D--V--V--G--C--M--I--D--L--T--E--N--T--I--I-   1160

3481 TTCACCCTCAATGGCGAGGTCCTCATGTCTGACTCAGGCTCCGAAACAGCCTTCCGGGAG   3540
1161 -F--T--L--N--G--E--V--L--M--S--D--S--G--S--E--T--A--F--R--E-   1180

3541 ATTGAGATTGGGGACGGCTTCCTGCCCGTCTGCAGCTTGGGACCTGGCCAGGTGGGTCAT   3600
1181 -I--E--I--G--D--G--F--L--P--V--C--S--L--G--P--G--Q--V--G--H-   1200

3601 CTGAACCTGGGCCAGGACGTGAGCTCTCTGAGGTTCTTTGCCATCTGTGGCCTCCAGGAA   3660
1201 -L--N--L--G--Q--D--V--S--S--L--R--F--F--A--I--C--G--L--Q--E-   1220

3661 GGCTTCGAGCCATTTGCCATCAACATGCAGCGCCCAGTCACCACCTGGTTCAGCAAAGGC   3720
1221 -G--F--E--P--F--A--I--N--M--Q--R--P--V--T--T--W--F--S--K--G-   1240

3721 CTGCCCCAGTTTGAGCCAGTGCCCCTTGAACACCCTCACTATGAGGTATCCCGAGTGGAC   3780
1241 -L--P--Q--F--E--P--V--P--L--E--H--P--H--Y--E--V--S--R--V--D-   1260

3781 GGCACTGTGGACACGCCCCCCTGCCTGCGCCTGACCCACCGCACCTGGGGCTCCCAGAAC   3840
1261 -G--T--V--D--T--P--P--C--L--R--L--T--H--R--T--W--G--S--Q--N-   1280

3841 AGCCTGGTGGAGATGCTTTTCCTGCGGCTGAGCCTCCCAGTCCAGTTCCACCAGCACTTC   3900
1281 -S--L--V--E--M--L--F--L--R--L--S--L--P--V--Q--F--H--Q--H--F-   1300

3901 CGCTGCACTGCAGGGGCCACCCCGCTGGCACCTCCTGGCCTGCAGCCCCCCGCCGAGGAC   3960
1301 -R--C--T--A--G--A--T--P--L--A--P--P--G--L--Q--P--P--A--E--D-   1320
```

```
3961 GAGGCCCGGGCGGCGGAACCCGACCCTGACTACGAAAACCTGCGCCGCTCAGCTGGGGGC   4020
1321 -E--A--R--A--A--E--P--D--P--D--Y--E--N--L--R--R--S--A--G--G-   1340

4021 TGGAGCGAGGCAGAGAACGGCAAAGAAGGGACTGCGAAGGAGGGCGCCCCCGGGGGCACC   4080
1341 -W--S--E--A--E--N--G--K--E--G--T--A--K--E--G--A--P--G--G--T-   1360

4081 CCGCAGGCGGGGGGAGAGGCGCAGCCCGCCAGGGCGGAGAATGAGAAGGATGCCACCACC   4140
1361 -P--Q--A--G--G--E--A--Q--P--A--R--A--E--N--E--K--D--A--T--T-   1380

4141 GAGAAGAACAAGAAGAGAGGCTTCTTATTCAAGGCCAAGAAGGTCGCCATGATGACCCAG   4200
1381 -E--K--N--K--K--R--G--F--L--F--K--A--K--K--V--A--M--M--T--Q-   1400

4201 CCACCGGCCACCCCCACGCTGCCCCGACTCCCTCACGACGTGGTGCCTGCAGACAACCGC   4260
1401 -P--P--A--T--P--T--L--P--R--L--P--H--D--V--V--P--A--D--N--R-   1420

4261 GATGACCCCGAGATCATCCTCAACACCACCACGTACTATTACTCCGTGAGGGTCTTTGCT   4320
1421 -D--D--P--E--I--I--L--N--T--T--T--Y--Y--Y--S--V--R--V--F--A-   1440

4321 GGACAGGAGCCCAGCTGCGTGTGGGCGGGCTGGGTCACCCCTGACTACCATCAGCACGAC   4380
1441 -G--Q--E--P--S--C--V--W--A--G--W--V--T--P--D--Y--H--Q--H--D-   1460

4381 ATGAGCTTCGACCTCAGCAAGGTCCGGGTCGTGACGGTGACCATGGGGGATGAACAAGGC   4440
1461 -M--S--F--D--L--S--K--V--R--V--V--T--V--T--M--G--D--E--Q--G-   1480

4441 AACGTCCACAGCAGCCTCAAGTGTAGCAACTGCTACATGGTGTGGGGCGGAGACTTTGTG   4500
1481 -N--V--H--S--S--L--K--C--S--N--C--Y--M--V--W--G--G--D--F--V-   1500

4501 AGTCCCGGGCAGCAGGGCCGGATCAGCCACACGGACCTTGTCATTGGGTGCCTGGTGGAC   4560
1501 -S--P--G--Q--Q--G--R--I--S--H--T--D--L--V--I--G--C--L--V--D-   1520

4561 TTGGCCACTGGCTTAATGACCTTTACAGCCAATGGCAAAGAGAGCAACACCTTTTTCCAG   4620
1521 -L--A--T--G--L--M--T--F--T--A--N--G--K--E--S--N--T--F--F--Q-   1540

4621 GTGGAACCCAACACTAAGCTATTTCCTGCCGTCTTCGTCCTGCCCACCCACCAGAACGTC   4680
1541 -V--E--P--N--T--K--L--F--P--A--V--F--V--L--P--T--H--Q--N--V-   1560

4681 ATCCAGTTTGAGCTGGGGAAGCAGAAGAACATCATGCCGTTGTCAGCCGCCATGTTCCAA   4740
1561 -I--Q--F--E--L--G--K--Q--K--N--I--M--P--L--S--A--A--M--F--Q-   1580

4741 AGCGAGCGCAAGAACCCGGCCCCGCAGTGCCCACCGCGGCTGGAGATGCAGATGCTGATG   4800
1581 -S--E--R--K--N--P--A--P--Q--C--P--P--R--L--E--M--Q--M--L--M-   1600
```

```
4801 CCAGTGTCCTGGAGCCGCATGCCCAACCACTTCCTGCAGGTGGAGACGAGGCGTGCCGGC   4860
1601 -P--V--S--W--S--R--M--P--N--H--F--L--Q--V--E--T--R--R--A--G-   1620

4861 GAGCGGCTGGGCTGGGCCGTGCAGTGCCAGGAGCCGCTGACCATGATGGCGCTGCACATC   4920
1621 -E--R--L--G--W--A--V--Q--C--Q--E--P--L--T--M--M--A--L--H--I-   1640

4921 CCCGAGGAGAACCGGTGCATGGACATCCTGGAGCTGTCGGAGCGCCTGGACCTGCAGCGC   4980
1641 -P--E--E--N--R--C--M--D--I--L--E--L--S--E--R--L--D--L--Q--R-   1660

4981 TTCCACTCGCACACCCTGCGCCTCTACCGCGCTGTGTGCGCCCTGGGCAACAATCGCGTG   5040
1661 -F--H--S--H--T--L--R--L--Y--R--A--V--C--A--L--G--N--N--R--V-   1680

5041 GCGCACGCTCTGTGCAGCCACGTAGACCAAGCTCAGCTGCTGCACGCCCTGGAGGACGCG   5100
1681 -A--H--A--L--C--S--H--V--D--Q--A--Q--L--L--H--A--L--E--D--A-   1700

5101 CACCTGCCAGGCCCACTGCGCGCAGGCTACTATGACCTCCTCATCAGCATCCACCTCGAA   5160
1701 -H--L--P--G--P--L--R--A--G--Y--Y--D--L--L--I--S--I--H--L--E-   1720

5161 AGTGCCTGCCGCAGCCGCCGCTCCATGCTCTCTGAATACATCGTGCCCCTCACGCCTGAG   5220
1721 -S--A--C--R--S--R--R--S--M--L--S--E--Y--I--V--P--L--T--P--E-   1740

5221 ACCCGCGCCATCACGCTCTTCCCTCCTGGAAGGAGCACAGAAAATGGTCACCCCCGGCAT   5280
1741 -T--R--A--I--T--L--F--P--P--G--R--S--T--E--N--G--H--P--R--H-   1760

5281 GGCCTGCCGGGAGTTGGAGTCACCACTTCGCTGAGGCCCCCGCATCATTTCTCGCCCCCC   5340
1761 -G--L--P--G--V--G--V--T--T--S--L--R--P--P--H--H--F--S--P--P-   1780

5341 TGTTTCGTGGCCGCTCTGCCAGCTGCTGGGGCAGCAGAGGCCCCGGCCCGCCTCAGCCCT   5400
1781 -C--F--V--A--A--L--P--A--A--G--A--A--E--A--P--A--R--L--S--P-   1800

5401 GCCATCCCGCTGGAGGCCCTGCGGGACAAGGCACTGAGGATGCTGGGGGAGGCGGTGCGC   5460
1801 -A--I--P--L--E--A--L--R--D--K--A--L--R--M--L--G--E--A--V--R-   1820

5461 GACGGTGGGCAGCACGCTCGCGACCCCGTCGGGGGCTCCGTGGAGTTCCAGTTTGTGCCT   5520
1821 -D--G--G--Q--H--A--R--D--P--V--G--G--S--V--E--F--Q--F--V--P-   1840

5521 GTGCTCAAGCTCGTGTCCACCCTGCTGGTGATGGGCATCTTTGGCGATGAGGATGTGAAA   5580
1841 -V--L--K--L--V--S--T--L--L--V--M--G--I--F--G--D--E--D--V--K-   1860
```

```
5581 CAGATCTTGAAGATGATTGAGCCTGAGGTCTTCACTGAGGAAGAAGAGGAGGAGGACGAG   5640
1861 -Q--I--L--K--M--I--E--P--E--V--F--T--E--E--E--E--E--E--D--E-   1880

5641 GAGGAAGAGGGTGAAGAGGAAGATGAGGAGGAGAAGGAGGAGGATGAGGAGGAAACAGCA   5700
1881 -E--E--E--G--E--E--E--D--E--E--E--K--E--E--D--E--E--E--T--A-   1900

5701 CAGGAAAAGGAAGATGAGGAAAAAGAGGAAGAGGAGGCAGCAGAAGGGGAGAAAGAAGAA   5760
1901 -Q--E--K--E--D--E--E--K--E--E--E--E--A--A--E--G--E--K--E--E-   1920

5761 GGCTTGGAGGAAGGGCTGCTCCAGATGAAGTTGCCAGAGTCTGTGAAGTTACAGATGTGC   5820
1921 -G--L--E--E--G--L--L--Q--M--K--L--P--E--S--V--K--L--Q--M--C-   1940

5821 CACCTGCTGGAGTATTTCTGTGACCAAGAGCTGCAGCACCGTGTGGAGTCCCTGGCAGCC   5880
1941 -H--L--L--E--Y--F--C--D--Q--E--L--Q--H--R--V--E--S--L--A--A-   1960

5881 TTTGCGGAGCGCTATGTGGACAAGCTCCAGGCCAACCAGCGGAGCCGCTATGGCCTCCTC   5940
1961 -F--A--E--R--Y--V--D--K--L--Q--A--N--Q--R--S--R--Y--G--L--L-   1980

5941 ATAAAAGCCTTCAGCATGACCGCAGCAGAGACTGCAAGACGTACCCGCGAGTTCCGCTCC   6000
1981 -I--K--A--F--S--M--T--A--A--E--T--A--R--R--T--R--E--F--R--S-   2000

6001 CCACCCCAGGAACAGATCAATATGCTATTGCAATTCAAAGATGGTACAGATGAGGAAGAC   6060
2001 -P--P--Q--E--Q--I--N--M--L--L--Q--F--K--D--G--T--D--E--E--D-   2020

6061 TGTCCTCTCCCTGAAGAGATTCGACAGGATTTGCTTGACTTTCATCAAGACCTGCTGGCA   6120
2021 -C--P--L--P--E--E--I--R--Q--D--L--L--D--F--H--Q--D--L--L--A-   2040

6121 CACTGTGGAATTCAGCTAGATGGAGAGGAGGAGGAACCAGAGGAAGAGACCACCCTGGGC   6180
2041 -H--C--G--I--Q--L--D--G--E--E--E--E--P--E--E--E--T--T--L--G-   2060

6181 AGCCGCCTCATGAGCCTGTTGGAGAAAGTGCGGCTGGTGAAGAAGAAGGAAGAGAAACCT   6240
2061 -S--R--L--M--S--L--L--E--K--V--R--L--V--K--K--K--E--E--K--P-   2080

6241 GAGGAGGAGCGGTCAGCAGAGGAGAGCAAACCCCGGTCCCTGCAGGAGCTGGTGTCCCAC   6300
2081 -E--E--E--R--S--A--E--E--S--K--P--R--S--L--Q--E--L--V--S--H-   2100

6301 ATGGTGGTGCGCTGGGCCCAAGAGGACTTCGTGCAGAGCCCCGAGCTGGTGCGGGCCATG   6360
2101 -M--V--V--R--W--A--Q--E--D--F--V--Q--S--P--E--L--V--R--A--M-   2120

6361 TTCAGCCTCCTGCACCGGCAGTACGACGGGCTGGGTGAGCTGCTGCGTGCCCTGCCGCGG   6420
2121 -F--S--L--L--H--R--Q--Y--D--G--L--G--E--L--L--R--A--L--P--R-   2140
```

```
6421 GCGTACACCATCTCACCGTCCTCCGTGGAAGACACCATGAGCCTGCTCGAGTGCCTCGGC   6480
2141 -A--Y--T--I--S--P--S--S--V--E--D--T--M--S--L--L--E--C--L--G-   2160

6481 CAGATCCGCTCGCTGCTCATCGTGCAGATGGGCCCCCAGGAGGAGAACCTCATGATCCAG   6540
2161 -Q--I--R--S--L--L--I--V--Q--M--G--P--Q--E--E--N--L--M--I--Q-   2180

6541 AGCATCGGGAACATCATGAACAACAAAGTCTTCTACCAACACCCGAACCTGATGAGGGCG   6600
2181 -S--I--G--N--I--M--N--N--K--V--F--Y--Q--H--P--N--L--M--R--A-   2200

6601 CTGGGCATGCACGAGACGGTCATGGAGGTCATGGTCAACGTCCTCGGGGGCGGCGAGTCC   6660
2201 -L--G--M--H--E--T--V--M--E--V--M--V--N--V--L--G--G--G--E--S-   2220

6661 AAGGAGATCCGCTTCCCCAAGATGGTGACAAGCTGCTGCCGCTTCCTCTGCTATTTCTGC   6720
2221 -K--E--I--R--F--P--K--M--V--T--S--C--C--R--F--L--C--Y--F--C-   2240

6721 CGAATCAGCCGGCAGAACCAGCGCTCCATGTTTGACCACCTGAGCTACCTGCTGGAGAAC   6780
2241 -R--I--S--R--Q--N--Q--R--S--M--F--D--H--L--S--Y--L--L--E--N-   2260

6781 AGTGGCATCGGCCTGGGCATGCAGGGCTCCACGCCCCTGGACGTGGCTGCTGCCTCCGTC   6840
2261 -S--G--I--G--L--G--M--Q--G--S--T--P--L--D--V--A--A--A--S--V-   2280

6841 ATTGACAACAATGAGCTGGCCTTGGCATTGCAGGAGCAGGACCTGGAAAAGGTTGTGTCC   6900
2281 -I--D--N--N--E--L--A--L--A--L--Q--E--Q--D--L--E--K--V--V--S-   2300

6901 TACCTGGCAGGCTGTGGCCTCCAGAGCTGCCCCATGCTTGTGGCCAAAGGGTACCCAGAC   6960
2301 -Y--L--A--G--C--G--L--Q--S--C--P--M--L--V--A--K--G--Y--P--D-   2320

6961 ATTGGCTGGAACCCCTGTGGTGGAGAGCGCTACCTGGACTTCCTGCGCTTTGCTGTCTTC   7020
2321 -I--G--W--N--P--C--G--G--E--R--Y--L--D--F--L--R--F--A--V--F-   2340

7021 GTCAACGGCGAGAGCGTGGAGGAGAACGCCAATGTGGTGGTGCGGCTGCTCATCCGGAAG   7080
2341 -V--N--G--E--S--V--E--E--N--A--N--V--V--V--R--L--L--I--R--K-   2360

7081 CCTGAGTGCTTCGGACCCGCCCTGCGGGGTGAGGGTGGCTCAGGGCTGCTGGCTGCCATC   7140
2361 -P--E--C--F--G--P--A--L--R--G--E--G--G--S--G--L--L--A--A--I-   2380

7141 GAAGAGGCCATCCGCATCTCCGAGGACCCTGCGAGGGATGGCCCAGGCATCCGCAGGGAC   7200
2381 -E--E--A--I--R--I--S--E--D--P--A--R--D--G--P--G--I--R--R--D-   2400
```

```
7201 CGGCGGCGCGAGCACTTTGGTGAGGAACCGCCTGAAGAAAACCGGGTGCACCTGGGACAC   7260
2401 -R--R--R--E--H--F--G--E--E--P--P--E--E--N--R--V--H--L--G--H-   2420

7261 GCCATCATGTCCTTCTATGCCGCCTTGATCGACCTGCTCGGACGCTGTGCACCAGAGATG   7320
2421 -A--I--M--S--F--Y--A--A--L--I--D--L--L--G--R--C--A--P--E--M-   2440

7321 CATCTAATCCAAGCCGGCAAGGGTGAGGCCCTGCGGATCCGCGCCATCCTCCGCTCCCTT   7380
2441 -H--L--I--Q--A--G--K--G--E--A--L--R--I--R--A--I--L--R--S--L-   2460

7381 GTGCCCTTGGAGGACCTTGTGGGCATCATCAGCCTCCCACTGCAGATTCCCACCCTGGGC   7440
2461 -V--P--L--E--D--L--V--G--I--I--S--L--P--L--Q--I--P--T--L--G-   2480

7441 AAAGATGGGGCTCTGGTGCAGCCAAAGATGTCAGCATCCTTCGTGCCGGACCACAAGGCG   7500
2481 -K--D--G--A--L--V--Q--P--K--M--S--A--S--F--V--P--D--H--K--A-   2500

7501 TCCATGGTGCTCTTCCTGGACCGTGTGTATGGCATCGAGAACCAGGACTTCTTGCTGCAC   7560
2501 -S--M--V--L--F--L--D--R--V--Y--G--I--E--N--Q--D--F--L--L--H-   2520

7561 GTGCTGGACGTGGGGTTCCTGCCCGACATGAGGGCAGCCGCCTCGCTGGACACGGCCACT   7620
2521 -V--L--D--V--G--F--L--P--D--M--R--A--A--A--S--L--D--T--A--T-   2540

7621 TTCAGCACCACCGAGATGGCGCTGGCGCTGAACCGCTACCTGTGCCTGGCCGTGCTGCCG   7680
2541 -F--S--T--T--E--M--A--L--A--L--N--R--Y--L--C--L--A--V--L--P-   2560

7681 CTCATCACCAAGTGTGCGCCGCTCTTTGCGGGCACAGAACACCGCGCCATCATGGTGGAC   7740
2561 -L--I--T--K--C--A--P--L--F--A--G--T--E--H--R--A--I--M--V--D-   2580

7741 TCTATGCTGCATACCGTGTACCGCCTGTCTCGGGGTCGTTCGCTCACCAAGGCGCAGCGT   7800
2581 -S--M--L--H--T--V--Y--R--L--S--R--G--R--S--L--T--K--A--Q--R-   2600

7801 GACGTCATCGAGGACTGCCTCATGTCGCTCTGCAGGTACATCCGCCCGTCGATGCTGCAG   7860
2601 -D--V--I--E--D--C--L--M--S--L--C--R--Y--I--R--P--S--M--L--Q-   2620

7861 CACCTGTTGCGCCGCCTGGTGTTCGACGTGCCCATCCTCAACGAGTTCGCCAAGATGCCA   7920
2621 -H--L--L--R--R--L--V--F--D--V--P--I--L--N--E--F--A--K--M--P-   2640

7921 CTCAAGCTCCTCACCAACCACTATGAGCGCTGTTGGAAGTACTACTGCCTACCCACGGGC   7980
2641 -L--K--L--L--T--N--H--Y--E--R--C--W--K--Y--Y--C--L--P--T--G-   2660

7981 TGGGCCAACTTCGGGGTCACCTCAGAGGAGGAGCTGCACCTCACACGGAAACTCTTCTGG   8040
2661 -W--A--N--F--G--V--T--S--E--E--E--L--H--L--T--R--K--L--F--W-   2680
```

```
8041 GGCATCTTTGACTCTCTGGCCCATAAGAAATACGACCCGGAGCTGTACCGCATGGCCATG   8100
2681 -G--I--F--D--S--L--A--H--K--K--Y--D--P--E--L--Y--R--M--A--M-   2700

8101 CCTTGTCTGTGCGCCATTGCCGGGGCTCTGCCCCCCGACTATGTGGATGCCTCATACTCA   8160
2701 -P--C--L--C--A--I--A--G--A--L--P--P--D--Y--V--D--A--S--Y--S-   2720

8161 TCTAAGGCAGAGAAAAAGGCCACAGTGGATGCTGAAGGCAACTTTGATCCCCGGCCTGTG   8220
2721 -S--K--A--E--K--K--A--T--V--D--A--E--G--N--F--D--P--R--P--V-   2740

8221 GAGACCCTCAATGTGATCATCCCGGAGAAGCTGGACTCCTTCATTAACAAGTTTGCGGAG   8280
2741 -E--T--L--N--V--I--I--P--E--K--L--D--S--F--I--N--K--F--A--E-   2760

8281 TACACACACGAGAAGTGGGCCTTCGACAAGATCCAGAACAACTGGTCCTATGGAGAGAAC   8340
2761 -Y--T--H--E--K--W--A--F--D--K--I--Q--N--N--W--S--Y--G--E--N-   2780

8341 ATAGACGAGGAGCTGAAGACCCACCCCATGCTGAGGCCCTACAAGACCTTTTCAGAGAAG   8400
2781 -I--D--E--E--L--K--T--H--P--M--L--R--P--Y--K--T--F--S--E--K-   2800

8401 GACAAAGAGATTTACCGCTGGCCCATCAAGGAGTCCCTGAAGGCCATGATTGCCTGGGAA   8460
2801 -D--K--E--I--Y--R--W--P--I--K--E--S--L--K--A--M--I--A--W--E-   2820

8461 TGGACGATAGAGAAGGCCAGGGAGGGTGAGGAGGAGAAGACGGAAAAGAAAAAAACGCGG   8520
2821 -W--T--I--E--K--A--R--E--G--E--E--E--K--T--E--K--K--K--T--R-   2840

8521 AAGATATCACAAAGTGCCCAGACCTATGATCCTCGAGAAGGCTACAACCCTCAGCCCCCC   8580
2841 -K--I--S--Q--S--A--Q--T--Y--D--P--R--E--G--Y--N--P--Q--P--P-   2860

8581 GACCTTAGTGCTGTTACCCTGTCCCGGGAGCTGCAGGCCATGGCAGAACAACTGGCAGAA   8640
2861 -D--L--S--A--V--T--L--S--R--E--L--Q--A--M--A--E--Q--L--A--E-   2880

8641 AATTACCACAACACGTGGGGACGGAAGAAGAAGCAGGAGCTGGAAGCCAAAGGCGGTGGG   8700
2881 -N--Y--H--N--T--W--G--R--K--K--K--Q--E--L--E--A--K--G--G--G-   2900

8701 ACCCACCCCCTGCTGGTCCCCTACGACACGCTCACGGCCAAGGAGAAGGCACGAGATCGA   8760
2901 -T--H--P--L--L--V--P--Y--D--T--L--T--A--K--E--K--A--R--D--R-   2920

8761 GAGAAGGCCCAGGAGCTACTGAAATTCCTGCAGATGAATGGCTACGCGGTTACAAGAGGC   8820
2921 -E--K--A--Q--E--L--L--K--F--L--Q--M--N--G--Y--A--V--T--R--G-   2940
```

```
8821 CTTAAGGACATGGAACTGGACTCGTCTTCCATTGAAAAGCGGTTTGCCTTTGGCTTCCTG   8880
2941 -L--K--D--M--E--L--D--S--S--S--I--E--K--R--F--A--F--G--F--L-   2960

8881 CAGCAGCTGCTGCGCTGGATGGACATTTCTCAGGAGTTCATTGCCCACCTGGAGGCTGTG   8940
2961 -Q--Q--L--L--R--W--M--D--I--S--Q--E--F--I--A--H--L--E--A--V-   2980

8941 GTCAGCAGTGGGCGAGTGGAAAAGTCCCCACATGAACAGGAGATTAAATTCTTTGCCAAG   9000
2981 -V--S--S--G--R--V--E--K--S--P--H--E--Q--E--I--K--F--F--A--K-   3000

9001 ATCCTGCTCCCTTTGATCAACCAGTACTTCACCAACCACTGCCTCTATTTCTTGTCCACT   9060
3001 -I--L--L--P--L--I--N--Q--Y--F--T--N--H--C--L--Y--F--L--S--T-   3020

9061 CCGGCTAAAGTGCTGGGCAGCGGTGGCCACGCCTCTAACAAGGAGAAGGAAATGATCACC   9120
3021 -P--A--K--V--L--G--S--G--G--H--A--S--N--K--E--K--E--M--I--T-   3040

9121 AGCCTCTTCTGCAAACTTGCTGCTCTCGTCCGCCACCGAGTCTCTCTCTTTGGGACAGAC   9180
3041 -S--L--F--C--K--L--A--A--L--V--R--H--R--V--S--L--F--G--T--D-   3060

9181 GCCCCAGCTGTGGTCAACTGTCTTCACATCCTGGCCCGCTCCCTGGATGCCAGGACAGTG   9240
3061 -A--P--A--V--V--N--C--L--H--I--L--A--R--S--L--D--A--R--T--V-   3080

9241 ATGAAGTCAGGCCCTGAGATCGTGAAGGCTGGCCTCCGCTCCTTCTTCGAGAGTGCCTCG   9300
3081 -M--K--S--G--P--E--I--V--K--A--G--L--R--S--F--F--E--S--A--S-   3100

9301 GAGGACATCGAGAAGATGGTGGAGAACCTGCGGCTGGGCAAGGTGTCGCAGGCGCGCACC   9360
3101 -E--D--I--E--K--M--V--E--N--L--R--L--G--K--V--S--Q--A--R--T-   3120

9361 CAGGTGAAAGGCGTGGGCCAGAACCTCACCTACACCACTGTGGCACTGCTGCCGGTCCTC   9420
3121 -Q--V--K--G--V--G--Q--N--L--T--Y--T--T--V--A--L--L--P--V--L-   3140

9421 ACCACCCTCTTCCAGCACATCGCCCAGCACCAGTTCGGAGATGACGTCATCCTGGACGAC   9480
3141 -T--T--L--F--Q--H--I--A--Q--H--Q--F--G--D--D--V--I--L--D--D-   3160

9481 GTCCAGGTCTCTTGCTACCGAACGCTGTGCAGTATCTACTCCCTGGGAACCACCAAGAAC   9540
3161 -V--Q--V--S--C--Y--R--T--L--C--S--I--Y--S--L--G--T--T--K--N-   3180

9541 ACTTATGTGGAAAAGCTTCGGCCAGCCCTCGGGGAGTGCCTGGCCCGTCTGGCAGCAGCC   9600
3181 -T--Y--V--E--K--L--R--P--A--L--G--E--C--L--A--R--L--A--A--A-   3200

9601 ATGCCGGTGGCGTTCCTGGAGCCGCAGCTGAACGAGTACAACGCCTGCTCCGTGTACACC   9660
3201 -M--P--V--A--F--L--E--P--Q--L--N--E--Y--N--A--C--S--V--Y--T-   3220
```

```
9661 ACCAAGTCTCCGCGGGAGCGGGCCATCCTGGGGCTCCCCAACAGTGTGGAGGAGATGTGT   9720
3221 -T--K--S--P--R--E--R--A--I--L--G--L--P--N--S--V--E--E--M--C-   3240

9721 CCCGACATCCCGGTGCTGGAGCGGCTCATGGCAGACATTGGGGGGCTGGCCGAGTCAGGT   9780
3241 -P--D--I--P--V--L--E--R--L--M--A--D--I--G--G--L--A--E--S--G-   3260

9781 GCCCGCTACACAGAGATGCCGCATGTCATCGAGATCACGCTGCCCATGCTATGCAGCTAC   9840
3261 -A--R--Y--T--E--M--P--H--V--I--E--I--T--L--P--M--L--C--S--Y-   3280

9841 CTGCCCCGATGGTGGGAGCGCGGGCCCGAGGCACCCCCTTCCGCCCTGCCCGCCGGCGCC   9900
3281 -L--P--R--W--W--E--R--G--P--E--A--P--P--S--A--L--P--A--G--A-   3300

9901 CCCCCACCCTGCACAGCTGTCACCTCTGACCACCTCAACTCCCTGCTGGGGAATATCCTG   9960
3301 -P--P--P--C--T--A--V--T--S--D--H--L--N--S--L--L--G--N--I--L-   3320

9961 AGAATCATCGTCAACAACCTGGGCATTGACGAGGCCTCCTGGATGAAGCGGCTGGCTGTG  10020
3321 -R--I--I--V--N--N--L--G--I--D--E--A--S--W--M--K--R--L--A--V-   3340

10021 TTCGCACAGCCCATTGTGAGCCGTGCACGGCCGGAGCTCCTGCAGTCCCACTTCATCCCA  10080
 3341 -F--A--Q--P--I--V--S--R--A--R--P--E--L--L--Q--S--H--F--I--P-   3360

10081 ACTATCGGGCGGCTGCGCAAGAGGGCAGGGAAGGTGGTGTCCGAGGAGGAGCAGCTGCGC  10140
 3361 -T--I--G--R--L--R--K--R--A--G--K--V--V--S--E--E--E--Q--L--R-   3380

10141 CTGGAGGCCAAGGCGGAGGCCCAGGAGGGCGAGCTGCTGGTGCGGGACGAGTTCTCTGTG  10200
 3381 -L--E--A--K--A--E--A--Q--E--G--E--L--L--V--R--D--E--F--S--V-   3400

10201 CTCTGCCGGGACCTCTACGCCCTGTATCCGCTGCTCATCCGCTACGTGGACAACAACAGG  10260
 3401 -L--C--R--D--L--Y--A--L--Y--P--L--L--I--R--Y--V--D--N--N--R-   3420

10261 GCGCAGTGGCTGACGGAGCCGAATCCCAGCGCGGAGGAGCTGTTCAGGATGGTGGGCGAG  10320
 3421 -A--Q--W--L--T--E--P--N--P--S--A--E--E--L--F--R--M--V--G--E-   3440

10321 ATCTTCATCTACTGGTCCAAGTCCCACAACTTCAAGCGCGAGGAGCAGAACTTTGTGGTC  10380
 3441 -I--F--I--Y--W--S--K--S--H--N--F--K--R--E--E--Q--N--F--V--V-   3460

10381 CAGAATGAGATCAACAACATGTCCTTCCTGACTGCTGACAACAAAAGCAAAATGGCTAAG  10440
 3461 -Q--N--E--I--N--N--M--S--F--L--T--A--D--N--K--S--K--M--A--K-   3480
```

```
10441 GCGGGAGATATACAGTCCGGTGGCTCGGACCAGGAACGCACCAAGAAGAAGCGCCGGGGG  10500
 3481 -A--G--D--I--Q--S--G--G--S--D--Q--E--R--T--K--K--K--R--R--G-   3500

10501 GACCGGTACTCTGTGCAGACGTCACTGATCGTGGCCACACTGAAGAAGATGCTGCCCATC  10560
 3501 -D--R--Y--S--V--Q--T--S--L--I--V--A--T--L--K--K--M--L--P--I-   3520

10561 GGCCTGAATATGTGTGCGCCCACCGACCAAGACCTCATCACGCTGGCCAAGACCCGTTAC  10620
 3521 -G--L--N--M--C--A--P--T--D--Q--D--L--I--T--L--A--K--T--R--Y-   3540

10621 GCCCTGAAAGACACAGATGAGGAGGTCCGGGAATTTCTGCACAACAACCTTCACCTTCAG  10680
 3541 -A--L--K--D--T--D--E--E--V--R--E--F--L--H--N--N--L--H--L--Q-   3560

10681 GGAAAGGTCGAAGGCTCCCCGTCTCTGCGCTGGCAGATGGCTCTGTACCGGGGCGTCCCG  10740
 3561 -G--K--V--E--G--S--P--S--L--R--W--Q--M--A--L--Y--R--G--V--P-   3580

10741 GGTCGCGAGGAGGACGCCGATGACCCCGAGAAAATCGTGCGCAGAGTCCAGGAAGTGTCA  10800
 3581 -G--R--E--E--D--A--D--D--P--E--K--I--V--R--R--V--Q--E--V--S-   3600

10801 GCCGTGCTCTACTACCTGGACCAGACCGAGCACCCTTACAAGTCTAAGAAGGCCGTGTGG  10860
 3601 -A--V--L--Y--Y--L--D--Q--T--E--H--P--Y--K--S--K--K--A--V--W-   3620

10861 CACAAGCTTTTGTCCAAACAGCGCCGGCGGGCAGTCGTGGCCTGTTTCCGTATGACGCCC  10920
 3621 -H--K--L--L--S--K--Q--R--R--R--A--V--V--A--C--F--R--M--T--P-   3640

10921 CTGTACAACCTGCCCACGCACCGGGCATGTAACATGTTCCTGGAGAGCTACAAGGCTGCA  10980
 3641 -L--Y--N--L--P--T--H--R--A--C--N--M--F--L--E--S--Y--K--A--A-   3660

10981 TGGATCCTGACTGAAGACCACAGTTTTGAGGACCGCATGATAGATGACCTTTCAAAAGCT  11040
 3661 -W--I--L--T--E--D--H--S--F--E--D--R--M--I--D--D--L--S--K--A-   3680

11041 GGGGAGCAGGAGGAGGAGGAGGAAGAGGTGGAAGAGAAGAAGCCAGACCCCCTGCACCAG  11100
 3681 -G--E--Q--E--E--E--E--E--E--V--E--E--K--K--P--D--P--L--H--Q-   3700

11101 TTGGTCCTGCACTTCAGCCGCACTGCCCTGACGGAAAAGAGCAAACTGGATGAGGATTAC  11160
 3701 -L--V--L--H--F--S--R--T--A--L--T--E--K--S--K--L--D--E--D--Y-   3720

11161 CTGTACATGGCCTATGCTGATATCATGGCAAAGAGCTGCCACCTGGAGGAGGGAGGGGAG  11220
 3721 -L--Y--M--A--Y--A--D--I--M--A--K--S--C--H--L--E--E--G--G--E-   3740

11221 AACGGTGAAGCTGAAGAGGAGGTTGAGGTCTCCTTTGAGGAGAAACAGATGGAGAAGCAG  11280
 3741 -N--G--E--A--E--E--E--V--E--V--S--F--E--E--K--Q--M--E--K--Q-   3760
```

```
11281 AGGCTCTTGTACCAGCAAGCACGGCTGCACACCCGGGGGGCGGCCGAGATGGTGCTGCAG  11340
 3761 -R--L--L--Y--Q--Q--A--R--L--H--T--R--G--A--A--E--M--V--L--Q-   3780

11341 ATGATCAGTGCCTGCAAAGGAGAGACAGGTGCCATGGTGTCCTCCACCCTGAAGCTGGGC  11400
 3781 -M--I--S--A--C--K--G--E--T--G--A--M--V--S--S--T--L--K--L--G-   3800

11401 ATCTCCATCCTCAATGGAGGCAATGCTGAGGTCCAGCAGAAAATGCTGGATTATCTTAAG  11460
 3801 -I--S--I--L--N--G--G--N--A--E--V--Q--Q--K--M--L--D--Y--L--K-   3820

11461 GACAAGAAGGAAGTTGGCTTCTTCCAGAGTATCCAGGCACTGATGCAAACATGCAGCGTC  11520
 3821 -D--K--K--E--V--G--F--F--Q--S--I--Q--A--L--M--Q--T--C--S--V-   3840

11521 CTGGATCTCAATGCCTTTGAGAGACAGAACAAGGCCGAGGGGCTGGGCATGGTGAATGAG  11580
 3841 -L--D--L--N--A--F--E--R--Q--N--K--A--E--G--L--G--M--V--N--E-   3860

11581 GATGGCACTGTCATCAATCGCCAGAACGGAGAGAAGGTCATGGCGGATGATGAATTCACA  11640
 3861 -D--G--T--V--I--N--R--Q--N--G--E--K--V--M--A--D--D--E--F--T-   3880

11641 CAAGACCTGTTCCGATTCCTACAATTGCTCTGTGAGGGGCACAATAATGATTTCCAGAAC  11700
 3881 -Q--D--L--F--R--F--L--Q--L--L--C--E--G--H--N--N--D--F--Q--N-   3900

11701 TACCTACGGACACAGACAGGGAACACGACCACTATTAACATCATCATTTGCACTGTGGAC  11760
 3901 -Y--L--R--T--Q--T--G--N--T--T--T--I--N--I--I--I--C--T--V--D-   3920

11761 TACCTCCTGCGGCTGCAGGAATCCATCAGCGACTTCTACTGGTACTACTCGGGCAAGGAT  11820
 3921 -Y--L--L--R--L--Q--E--S--I--S--D--F--Y--W--Y--Y--S--G--K--D-   3940

11821 GTCATTGAAGAGCAGGGCAAGAGGAACTTCTCCAAAGCCATGTCGGTGGCTAAGCAGGTG  11880
 3941 -V--I--E--E--Q--G--K--R--N--F--S--K--A--M--S--V--A--K--Q--V-   3960

11881 TTCAACAGCCTCACTGAGTACATCCAGGGTCCCTGCACCGGGAACCAGCAGAGCCTGGCG  11940
 3961 -F--N--S--L--T--E--Y--I--Q--G--P--C--T--G--N--Q--Q--S--L--A-   3980

11941 CACAGTCGCCTATGGGACGCAGTGGTGGGATTCCTGCACGTGTTCGCCCACATGATGATG  12000
 3981 -H--S--R--L--W--D--A--V--V--G--F--L--H--V--F--A--H--M--M--M-   4000

12001 AAGCTCGCTCAGGACTCAAGCCAGATCGAGCTGCTGAAGGAGCTGCTGGATCTGCAGAAG  12060
 4001 -K--L--A--Q--D--S--S--Q--I--E--L--L--K--E--L--L--D--L--Q--K-   4020
```

```
12061 GACATGGTGGTGATGTTGCTGTCGCTACTAGAAGGGAACGTGGTGAACGGCATGATCGCC  12120
 4021 -D--M--V--V--M--L--L--S--L--L--E--G--N--V--V--N--G--M--I--A-   4040

12121 CGGCAGATGGTGGACATGCTCGTGGAATCCTCATCCAATGTGGAGATGATCCTCAAGTTC  12180
 4041 -R--Q--M--V--D--M--L--V--E--S--S--S--N--V--E--M--I--L--K--F-   4060

12181 TTCGACATGTTCCTGAAACTCAAGGACATTGTGGGCTCTGAAGCCTTCCAGGACTACGTA  12240
 4061 -F--D--M--F--L--K--L--K--D--I--V--G--S--E--A--F--Q--D--Y--V-   4080

12241 ACGGATCCCCGTGGCCTCATCTCCAAGAAGGACTTCCAGAAGGCCATGGACAGCCAGAAG  12300
 4081 -T--D--P--R--G--L--I--S--K--K--D--F--Q--K--A--M--D--S--Q--K-   4100

12301 CAGTTCAGCGGTCCAGAAATCCAGTTCCTGCTTTCGTGCTCCGAAGCGGATGAGAACGAA  12360
 4101 -Q--F--S--G--P--E--I--Q--F--L--L--S--C--S--E--A--D--E--N--E-   4120

12361 ATGATCAACTGCGAAGAGTTCGCCAACCGCTTCCAGGAGCCAGCACGCGACATCGGCTTC  12420
 4121 -M--I--N--C--E--E--F--A--N--R--F--Q--E--P--A--R--D--I--G--F-   4140

12421 AACGTGGCGGTGCTGCTGACCAACCTGTCGGAGCATGTGCCGCATGACCCTCGCCTGCAC  12480
 4141 -N--V--A--V--L--L--T--N--L--S--E--H--V--P--H--D--P--R--L--H-   4160

12481 AACTTCCTGGAGCTGGCCGAGAGCATCCTTGAGTACTTCCGCCCCTACCTGGGCCGCATC  12540
 4161 -N--F--L--E--L--A--E--S--I--L--E--Y--F--R--P--Y--L--G--R--I-   4180

12541 GAGATCATGGGCGCGTCACGCCGCATCGAGCGCATCTACTTCGAGATCTCAGAGACCAAC  12600
 4181 -E--I--M--G--A--S--R--R--I--E--R--I--Y--F--E--I--S--E--T--N-   4200

12601 CGCGCCCAGTGGGAGATGCCCCAGGTGAAGGAGTCCAAGCGCCAGTTCATCTTCGACGTG  12660
 4201 -R--A--Q--W--E--M--P--Q--V--K--E--S--K--R--Q--F--I--F--D--V-   4220

12661 GTGAACGAGGGCGGCGAGGCTGAGAAGATGGAGCTCTTCGTGAGTTTCTGCGAGGACACC  12720
 4221 -V--N--E--G--G--E--A--E--K--M--E--L--F--V--S--F--C--E--D--T-   4240

12721 ATCTTCGAGATGCAGATCGCCGCGCAGATCTCGGAGCCCGAGGGCGAGCCGGAGACCGAC  12780
 4241 -I--F--E--M--Q--I--A--A--Q--I--S--E--P--E--G--E--P--E--T--D-   4260

12781 GAGGACGAGGGCGCGGGCGCGGCGGAGGCGGGCGCGGAAGGCGCGGAGGAGGGCGCGGCG  12840
 4261 -E--D--E--G--A--G--A--A--E--A--G--A--E--G--A--E--E--G--A--A-   4280

12841 GGGCTCGAGGGCACGGCGGCCACGGCGGCGGCGGGGGCGACGGCGCGGGTTGTGGCGGCC  12900
 4281 -G--L--E--G--T--A--A--T--A--A--A--G--A--T--A--R--V--V--A--A-   4300
```

```
12901 GCAGGCCGGGCCCTGCGAGGCCTCAGCTACCGCAGCCTGCGGCGGCGCGTGCGGCGGCTG  12960
 4301 -A--G--R--A--L--R--G--L--S--Y--R--S--L--R--R--R--V--R--R--L-   4320

12961 CGGCGGCTTACGGCCCGCGAGGCGGCCACCGCAGTGGCGGCGCTGCTCTGGGCAGCAGTG  13020
 4321 -R--R--L--T--A--R--E--A--A--T--A--V--A--A--L--L--W--A--A--V-   4340

13021 ACGCGCGCTGGGGCCGCTGGCGCGGGGGCGGCGGCGGGCGCGCTGGGCCTGCTCTGGGGC  13080
 4341 -T--R--A--G--A--A--G--A--G--A--A--A--G--A--L--G--L--L--W--G-   4360

13081 TCGCTGTTCGGCGGCGGCCTGGTGGAGGGCGCCAAGAAGGTGACGGTGACCGAGCTCCTG  13140
 4361 -S--L--F--G--G--G--L--V--E--G--A--K--K--V--T--V--T--E--L--L-   4380

13141 GCAGGCATGCCCGACCCCACCAGCGACGAGGTGCACGGCGAGCAGCCGGCCGGGCCGGGC  13200
 4381 -A--G--M--P--D--P--T--S--D--E--V--H--G--E--Q--P--A--G--P--G-   4400

13201 GGAGACGCAGACGGCGAGGGTGCCAGCGAGGGCGCTGGAGACGCCGCGGAGGGCGCTGGA  13260
 4401 -G--D--A--D--G--E--G--A--S--E--G--A--G--D--A--A--E--G--A--G-   4420

13261 GACGAGGAGGAGGCGGTGCACGAGGCCGGGCCGGGCGGTGCCGACGGGGCGGTGGCCGTG  13320
 4421 -D--E--E--E--A--V--H--E--A--G--P--G--G--A--D--G--A--V--A--V-   4440

13321 ACCGATGGGGGCCCCTTCCGGCCCGAAGGGGCTGGCGGTCTCGGGGACATGGGGGACACG  13380
 4441 -T--D--G--G--P--F--R--P--E--G--A--G--G--L--G--D--M--G--D--T-   4460

13381 ACGCCTGCGGAACCGCCCACACCCGAGGGCTCTCCCATCCTCAAGAGGAAATTGGGGGTG  13440
 4461 -T--P--A--E--P--P--T--P--E--G--S--P--I--L--K--R--K--L--G--V-   4480

13441 GATGGAGTGGAGGAGGAGCTCCCGCCAGAGCCAGAGCCCGAGCCGGAACCAGAGCTGGAG  13500
 4481 -D--G--V--E--E--E--L--P--P--E--P--E--P--E--P--E--P--E--L--E-   4500

13501 CCGGAGAAAGCCGATGCCGAGAATGGGGAGAAGGAAGAAGTTCCCGAGCCCACACCAGAG  13560
 4501 -P--E--K--A--D--A--E--N--G--E--K--E--E--V--P--E--P--T--P--E-   4520

13561 CCCCCCAAGAAGCAAGCACCTCCCTCACCCCCTCCAAAGAAGGAGGAAGCTGGAGGCGAA  13620
 4521 -P--P--K--K--Q--A--P--P--S--P--P--P--K--K--E--E--A--G--G--E-   4540

13621 TTCTGGGGAGAACTGGAGGTGCAGAGGGTGAAGTTCCTGAACTACCTGTCCCGGAACTTT  13680
 4541 -F--W--G--E--L--E--V--Q--R--V--K--F--L--N--Y--L--S--R--N--F-   4560
```

```
13681 TACACCCTGCGGTTCCTTGCCCTCTTCTTGGCATTTGCCATCAACTTCATCTTGCTGTTT  13740
 4561 -Y--T--L--R--F--L--A--L--F--L--A--F--A--I--N--F--I--L--L--F-   4580

13741 TATAAGGTCTCAGACTCTCCACCAGGGGAGGACGACATGGAAGGCTCAGCTGCTGGGGAT  13800
 4581 -Y--K--V--S--D--S--P--P--G--E--D--D--M--E--G--S--A--A--G--D-   4600

13801 GTGTCAGGTGCAGGCTCTGGTGGCAGCTCTGGCTGGGGCTTGGGGGCCGGAGAGGAGGCA  13860
 4601 -V--S--G--A--G--S--G--G--S--S--G--W--G--L--G--A--G--E--E--A-   4620

13861 GAGGGCGATGAGGATGAGAACATGGTGTACTACTTCCTGGAGGAAAGCACAGGCTACATG  13920
 4621 -E--G--D--E--D--E--N--M--V--Y--Y--F--L--E--E--S--T--G--Y--M-   4640

13921 GAACCCGCCCTGCGGTGTCTGAGCCTCCTGCATACACTGGTGGCCTTTCTCTGCATCATT  13980
 4641 -E--P--A--L--R--C--L--S--L--L--H--T--L--V--A--F--L--C--I--I-   4660

13981 GGCTATAATTGTCTCAAGGTGCCCCTGGTAATCTTTAAGCGGGAGAAGGAGCTGGCCCGG  14040
 4661 -G--Y--N--C--L--K--V--P--L--V--I--F--K--R--E--K--E--L--A--R-   4680

14041 AAGCTGGAGTTTGATGGCCTGTACATCACGGAGCAGCCTGAGGACGATGACGTGAAGGGG  14100
 4681 -K--L--E--F--D--G--L--Y--I--T--E--Q--P--E--D--D--D--V--K--G-   4700

14101 CAGTGGGACCGACTGGTGCTCAACACGCCGTCTTTCCCTAGCAACTACTGGGACAAGTTT  14160
 4701 -Q--W--D--R--L--V--L--N--T--P--S--F--P--S--N--Y--W--D--K--F-   4720

14161 GTCAAGCGCAAGGTCCTGGACAAACATGGGGACATCTACGGGCGGGAGCGGATTGCTGAG  14220
 4721 -V--K--R--K--V--L--D--K--H--G--D--I--Y--G--R--E--R--I--A--E-   4740

14221 CTACTGGGCATGGACCTGGCCACACTAGAGATCACAGCCCACAATGAGCGCAAGCCCAAC  14280
 4741 -L--L--G--M--D--L--A--T--L--E--I--T--A--H--N--E--R--K--P--N-   4760

14281 CCGCCGCCAGGGCTGCTGACCTGGCTCATGTCCATCGATGTCAAGTACCAGATCTGGAAG  14340
 4761 -P--P--P--G--L--L--T--W--L--M--S--I--D--V--K--Y--Q--I--W--K-   4780

14341 TTCGGGGTCATCTTCACAGACAACTCCTTCCTGTACCTGGGCTGGTATATGGTGATGTCC  14400
 4781 -F--G--V--I--F--T--D--N--S--F--L--Y--L--G--W--Y--M--V--M--S-   4800

14401 CTCTTGGGACACTACAACAACTTCTTCTTTGCTGCCCATCTCCTGGACATCGCCATGGGG  14460
 4801 -L--L--G--H--Y--N--N--F--F--F--A--A--H--L--L--D--I--A--M--G-   4820

14461 GTCAAGACGCTGCGCACCATCCTGTCCTCTGTCACCCACAATGGGAAACAGCTGGTGATG  14520
 4821 -V--K--T--L--R--T--I--L--S--S--V--T--H--N--G--K--Q--L--V--M-   4840
```

```
14521 ACCGTGGGCCTTCTGGCGGTGGTCGTCTACCTGTACACCGTGGTGGCCTTCAACTTCTTC  14580
 4841 -T--V--G--L--L--A--V--V--V--Y--L--Y--T--V--V--A--F--N--F--F-   4860

14581 CGCAAGTTCTACAACAAGAGCGAGGATGAGGATGAACCTGACATGAAGTGTGATGACATG  14640
 4861 -R--K--F--Y--N--K--S--E--D--E--D--E--P--D--M--K--C--D--D--M-   4880

14641 ATGACGTGTTACCTGTTTCACATGTACGTGGGTGTCCGGGCTGGCGGAGGCATTGGGGAC  14700
 4881 -M--T--C--Y--L--F--H--M--Y--V--G--V--R--A--G--G--G--I--G--D-   4900

14701 GAGATCGAGGACCCCGCGGGTGACGAATACGAGCTCTACAGGGTGGTCTTCGACATCACC  14760
 4901 -E--I--E--D--P--A--G--D--E--Y--E--L--Y--R--V--V--F--D--I--T-   4920

14761 TTCTTCTTCTTCGTCATCGTCATCCTGTTGGCCATCATCCAGGGTCTGATCATCGACGCT  14820
 4921 -F--F--F--F--V--I--V--I--L--L--A--I--I--Q--G--L--I--I--D--A-   4940

14821 TTTGGTGAGCTCCGAGACCAACAAGAGCAAGTGAAGGAGGATATGGAGACCAAGTGCTTC  14880
 4941 -F--G--E--L--R--D--Q--Q--E--Q--V--K--E--D--M--E--T--K--C--F-   4960

14881 ATCTGTGGAATCGGCAGTGACTACTTTGATACGACACCGCATGGCTTCGAGACTCACACG  14940
 4961 -I--C--G--I--G--S--D--Y--F--D--T--T--P--H--G--F--E--T--H--T-   4980

14941 CTGGAGGAGCACAACCTGGCCAATTACATGTTTTTCCTGATGTATTTGATAAACAAGGAT  15000
 4981 -L--E--E--H--N--L--A--N--Y--M--F--F--L--M--Y--L--I--N--K--D-   5000

15001 GAGACAGAACACACGGGTCAGGAGTCTTATGTCTGGAAGATGTACCAAGAGAGATGTTGG  15060
 5001 -E--T--E--H--T--G--Q--E--S--Y--V--W--K--M--Y--Q--E--R--C--W-   5020

15061 GATTTCTTCCCAGCTGGTGATTGTTTCCGTAAGCAGTATGAGGACCAGCTTAGCTGA     15117
 5021 -D--F--F--P--A--G--D--C--F--R--K--Q--Y--E--D--Q--L--S--*-
```

Figure 1 *RYR1* cDNA and RyR1 amino acid sequence. The sequence was taken from ensemble (Transcript ID: ENST00000359596).